library Copy
Corrected
21/10/96

J.B. KEENE
Head
Department of Geology & Geophysics

The Petrology, Petrophysics, Structure, Geophysics, Geotechnical and Geological Aspects of the Koongarra Uranium Ore Body, as part of the Alligator Rivers Analogue Project.

MICHAEL S.C. HALLETT

Being a dissertation submitted as fulfilment
of requirements for the degree of Master of Science.

Department of Geology and Geophysics
The University of Sydney

February 1996

Declaration

This thesis contains work that is entirely that of the author except where duly acknowledged.

29.2.1996.

Abstract

The exposed Koongarra uranium orebody provides a model or analogue of a leaking man-made nuclear waste repository, which may be characterised to ascertain the paths of movement of radionuclides away from the primary orebody (repository) into the environment. Considering the present and future accumulation of radioactive waste created by nuclear powered electricity generation, characterisation of Koongarra as a natural analogue to such a site is rationalised.

The Koongarra uranium deposits are located in the Alligator Rivers Uranium Province of the Northern Territory of Australia, approximately 200 km east of Darwin. The orebodies occur within steeply dipping Cahill Formation schists of early Proterozoic age, southeast of a prominent escarpment of Kombolgie Formation sandstones, separated from the latter by a reverse fault zone - the Koongarra Fault. Geology, structure and weathering of the region and local vicinity define the macroscale framework for the uranium orebody and the subsequent dispersion fan. The uranium dispersion fan is located in a 25 - 30 m deep zone of weathered schists and clays, over which lie Quaternary sands and minor ferricrete lenses.

Borehole studies and Borehole Television investigations elucidate a major fold structure in the lithologies of the site, the nose of which is fractured. An examination of the amphibolitic units and their notional role as hydrologic

barriers indicates that these units have little influence on movement of groundwater at the site.

The weathered zone is variable in character and shows deeply weathered regolithic terrain characteristics. Little development of laterite in the aluminium-rich clays is found at the site. Development of the weathered profile is dominated by oxidising groundwaters and is most intense within metres of the base of weathering, where the great majority of matrix flow and fracture flow groundwater movement occurs. It is surmised that this zone is also where the major movement of radionuclides occurs, particularly along schistose foliation or fractures.

A characterisation of the site utilising petrophysical and geophysical techniques determined the major regions of groundwater flow at the site. Petrophysical studies included dry bulk density, apparent porosity, intrinsic permeability, galvanic (water saturated) resistivity, ultrasonic compressional wave velocity and magnetic susceptibility. The lithologies exhibited distinct characteristics, especially the contrasts between the weathered schists, unweathered schists and the Kombolgie Sandstone. The unweathered schists exhibited mass properties typical for unweathered metasedimentary units; moderate density, low porosity and very low permeability. The lower weathered zone schists exhibited low density, high porosity and moderate matrix permeability.. The upper weathered zone materials exhibited very low density, very high porosity and very low permeability.

All units displayed low magnetic susceptibility excepting the amphibolitic units which displayed moderate magnetic susceptibility. Contrasts in compressional wave velocity and electrical resistivity showed that the weathered material has less strength and lower resistivity than the unweathered schists. The partly weathered material near the base of weathering demonstrated the highest water permeability and is likely to be the zone of greatest groundwater movement, most intense weathering and the region of highest radionuclide movement.

Geophysical surveys of the site comprised magnetic, electromagnetic, self-potential, electrical resistivity, radiometric and gravity. These delineated structural and lithological characteristics of the site, which can be compared to the petrophysical studies. Image processing of the data reveals significant additional information from the data about the character of the site than has been seen in previous studies. The magnetic data elucidate structural features and lithologies at the site not seen in geological studies. The electromagnetic and SP surveys indicate the regions at the site of enhanced water saturation and drainage, which correspond strongly to the geological studies and the petrophysical data.

Electrical resistivity profiling shows the horizontally layered nature of the site, especially in the weathered zone, corresponding to the petrophysical data. Radiometric surveys indicate movement of radionuclides in the very shallow subsurface. The geophysical surveys indicate an inferred drainage of

groundwaters at the site to the south and south-southeast, corresponding to groundwater chemistry and pumping test results.

This documentation of the Koongarra site provides a valuable site characterisation. The information presented within identifies the dynamics of the weathered zone of the site and will be useful for studies of possible nuclear waste repositories. Additionally, the studies of the weathered zone provides useful information for other weathered site hydrological investigations, and for regolith studies in northern Australia, particularly in argillaceous terrains.

Acknowledgments

I would like to gratefully acknowledge those organisations involved in the Alligator Rivers Analogue Project (ARAP), being : The Australian Nuclear Science and Technology Organisation (ANSTO) ; The Swedish Nuclear Fuel Inspectorate (SKI) ; The UK Department of the Environment (UKDoE) ; the US Nuclear Regulatory Commission (USNRC) ; the US Department of Energy (USCoE) ; The Japan Atomic Energy Research Institute (JAERI) ; The Central Research Institute for Electric Power Industry (CRIEPI) and The Power Reactor and Nuclear Fuel Development Corporation of Japan (PNC). Thanks to Denison Australia for access to and use of facilities and scientific data.

My personal thanks go to my supervisors Dr D W Emerson and Dr K J Mills for their continuing support, guidance and invaluable assistance and to Mr Peter Duerden, the ARAP Project Manager, for his enthusiasm and clear thinking competence in the face of the mountainous job of coordinating the ARAP. Many thanks also to Mr Phil Manning and Mr L Q Cao for their roles in field and laboratory work. Thanks variously to D Garton, R Lowerson, R Edis, T Payne, A Snelling, P Jolly and K Martin.

Grateful thanks to Geoterrex Pty Ltd for support, encouragement and use of software and hardware, especially to Dave Daggar, for his immeasurable help in the production of the geophysical images. Final thanks to Marcela for her help and support.

TABLE OF CONTENTS

LIST OF TABLES

LIST OF FIGURES

CHAPTER ONE :

INTRODUCTION

The Koongarra Uranium Orebody as a Natural Analogue

ān'alogue, n. Analogous, parallel ; process of reasoning from parallel cases.

The Koongarra uranium orebody (Snelling 1990) is being studied as a natural analogue for the modelling of proposed High Level Nuclear Waste (HLNW) repositories, as part of the Alligator Rivers Analogue Project (ARAP). The project was managed by the Australian Nuclear Science and Technology Organisation (ANSTO), sponsored by the OECD Nuclear Energy Agency (NEA), with funding from a number of organisations worldwide, including The Swedish Nuclear Fuel Inspectorate (SKI) ; The UK Department of the Environment (UKDoE) ; the US Nuclear Regulatory Commission (USNRC) ; the US Department of Energy (USDoE) ; The Japan Atomic Energy Research Institute (JAERI) ; The Central Research Institute for Electric Power Industry (CRIEPI) and The Power Reactor and Nuclear Fuel Development Corporation of Japan (PNC).

In the context of the HLNW repository study, a natural analogue is a naturally occurring geologic system that reasonably represents expected processes and behaviours of proposed nuclear waste repositories in one or many aspects, including geological framework, hydrology, geochemistry and climate, as well as numerous other possible contributing factors.

This thesis is directed toward providing a geological, geophysical, geotechnical and structural framework for a specific natural site within which the migration of radionuclides and processes affecting radionuclide migration can be modelled and understood, particularly within the relatively porous, weathered zone of rock extending up to thirty or so metres below the ground surface. It is only within such a framework that geochemical and hydrological modelling of the site can become meaningful.

The Study of Natural Analogues

To understand the need for the study of natural analogues, we must appreciate that repositories are required for the (effective) permanent storage of HLNW. HLNW is the inevitable by-product of the generation of electricity by nuclear means, as well as from nuclear weapons programs and to a smaller extent, research and medical uses of radioisotopes. There is a pressing need to consider the past, present and future generation of HLNW and its consequent storage.

There are currently significant amounts of HLNW in temporary storage. Over 10 years ago (1984), there was already 11 700 tonnes of spent nuclear fuel and 370 000m^3 of "reprocessing" waste in temporary storage (Krauskopf 1988). Realistically speaking, there will be an increase in production of HLNW at least in the immediate future. Therefore appropriate and effective methods of storage must be considered. A plausible answer for the more permanent storage of HLNW is within geologically mined repositories.

Natural analogues reflect many aspects the expected behaviour of nuclear waste repositories and the study of these analogous sites can assist in assessing the feasibility of using mined repositories for the permanent storage of nuclear waste.

Nuclear and other methods of Power Generation

In 1987, nuclear power provided 16% of the world's electricity. The countries currently using nuclear power to generate electricity include France, Belgium, Sweden, Finland, the UK, The US, Japan and Eastern Europe (Blix, 1987). As demands for electricity increase, so too the need for further electricity generation will increase. To satisfy these demands, there are a number of methods available for the generation of electrical power, including nuclear power. These include fossil fuels, hydroelectricity, solar, windpower, tidal power and biomass generated power. The possibility of hydrogen as an energy source has also been suggested as a serious alternative (Bockris 1980).

However, there are only two realistic, practical and large-scale providers of electricity today - coal and nuclear energy. Both means of power generation need to be considered in terms of expense, feasibility, environmental and human cost. In recent years, it has become obvious that there is a greater and greater need for cleaner production of energy and more effective disposal of the waste produced by energy generation.

In view of the likely continued and increasing use of nuclear power in the generation of electricity, it is necessary to underline the pressing need for the safe disposal of nuclear waste currently being generated, that which is already existent in "temporary storage" and that which will be generated in the future. The vital lesson to be gained from analogue studies on a site such as Koongarra is that it can be seen as an integral and essential part in the planning of the disposal of high level nuclear waste. Fluid movement in the Koongarra subsurface augments scientific knowledge of repository behaviour in other natural environments.

Disposal of HLNW

The time required for high level nuclear waste products to decay to low levels of toxicity varies from a few hundred years (^{129}I and ^{99}Tc) up to more than ten million years (^{210}Pb and ^{226}Ra)(Krauskopf 1988). The time required for HLNW products to decay to a level approximately equivalent in radiation levels to the original uranium used to produce nuclear fuel is over one million years (Ringwood 1978). This timescale is of course inconceivable.

High level nuclear waste contains numerous radioactive elements which decay at highly variable rates and generate further radioactive daughter products which are also highly radioactive and may have long half-lives. Examples of this are ^{210}Pb and ^{226}Ra, generated by the decay of actinide elements present in HLNW, which may remain at toxic levels for up to 100 million years (Krauskopf 1988).

Regulations regarding accepted levels of toxicity and slow release of radioactive elements into the environment vary from nation to nation. The accepted time for which the radioactive waste must be completely contained by engineering means and not escape into the surrounding environment also varies from country to country (for example, 300 - 1000 yrs in the U.S.). It can be seen then that measures to contain HLNW must not only be assured of being effective in the short term, but must also conform to varying guidelines of containment over extremely long periods of time. Therefore, we need to consider what options are available for the disposal or containment of the toxic by-products of our nuclear power generation.

A number of techniques for the disposal of HLNW have been proposed. These are discussed briefly in order to put the study of mined geologic repositories in context.

The simplest of these is to store the waste at only a shallow depth in arid regions. This method would require great shielding from any natural or human disturbances, either in the form of huge protective structures or within a mountain (Krauskopf 1988). One advantage of this method is that the waste is easily monitored and retrieved if necessary or desirable for further reprocessing and use. Nevertheless, risks are greater and this method is not presently a serious consideration.

Disposal of HLNW by injection in very deep boreholes into the earth's crust has been proposed. This would involve drilling holes up to 5km deep and emplacing waste canisters within (Milnes 1985). A difficulty with this method is that

radionuclides would gradually leach from the borosilicate glass used to immobilise the waste. A variation on this technique proposes injecting HLNW into deep boreholes and allowing the natural heat that the waste generates to melt the surrounding rock and then allow it to recrystallise and solidify, thus diluting and immobilising the waste. Problems associated with this method include the potential danger of the molten, radioactive rock remobilising and moving upward, carrying highly mobile, concentrated radioactive fluids with it into the biosphere.

Emplacement of HLNW deep under ice sheets in the polar regions is another method that has been suggested. However, prediction of stability for a body such as ice is not possible for the far distant future. Additionally, political and environmental arguments against this method are very strong.

Disposal on the ocean floor, either in a subduction zone or in clays on a very stable oceanic plate is another technique for disposal that has been considered. However, on the grounds of our lack of knowledge of the behaviour of subduction zones, the first of these methods can be discounted. The second method offers a seemingly stable and isolated environment, but if the canisters were to decay or become ruptured, how quickly would the radionuclides disperse into the environment and pose a hazard?

Another method suggested in the past is that of dispatching HLNW into space, assuring that its isolation from terrestrial environments is complete. The immediate objection to this method is the disastrous effects that could occur if the craft

carrying the waste into space explodes in the earth's atmosphere. Additional to this argument would be the great expense of carrying out this method of disposal.

However, it is necessary to dispose of HLNW, and in doing so, the safest and most permanent solution must be selected. Perhaps the most favoured option is that of a mined geologic repository. This method of disposal allows advanced and comprehensive knowledge of the site of disposal, continued monitoring of waste and possible retrieval of waste if mitigating circumstances require it. Additionally, the geological framework parameters, geochemical parameters and the areal extent of the repository can be well known allowing for future reprocessing of the waste if necessary. Mined geologic disposal also has the advantage that it can be achieved at a reasonable cost and the techniques involved in creating the repository are already well established, unlike most of the other methods.

It can be seen from the number of international nuclear authorities involved directly or indirectly with the ARAP, a project primarily concerned with studying an analogue of a nuclear waste repository, that there is considerable interest and research occurring toward the option of a geological, mined repository for the disposal of high level nuclear waste (see also Lemons *et al* (1989)).

Selection of a Repository Site

There are many factors to be considered carefully in the design of a geologic mined repository. These include the geology, geochemistry, hydrology, geomorphology

and stucture of the site. Is the region stable in the long term, what is the country rock and how would it react to the presence of high concentrations of radionuclides? Is the rock fractured or porous to a significant degree, is the geochemistry of the rock type and groundwater conducive for a repository? The hydrology of the site needs to be carefully considered and tied in to the geology - what is the present state of the groundwater and the water table? What is the future state of the hydrology of the site likely to be? What are the groundwater flowpaths at the site, and what is the timescale of groundwater flowpaths from the site of HLNW storage to the earth's surface or to the biosphere?

The circumstances and location for a prospective repository site need to be considered. If the most conducive parameters for determining the location can be defined, then a suitable site for a repository can be chosen. If the geological, hydrological, geomorphological and geochemical characteristics of a prospective site, both now and in the past, are understood, then modelling and predicting the expected behaviour of such a system in the future can be made far more plausible.

To complement laboratory and theoretical studies of the migration of radionuclides into the environment from a repository over long periods of time, we can study natural analogues. These natural systems have been active over large timescales and may be scrutinised in an effort to define effectively the natural parameters that influence radionuclide migration in the subsurface. The results from these studies may be compared and correlated with the laboratory and theoretical evidence in an effort to form valid conclusions.

Ideally, a number of different natural analogues showing similar characteristics to a proposed repository site in one or several properties, such as rock type, degree of fracturing, tectonic setting and geochemical character should be studied. Understandably, no single analogue will match the proposed repository site identically, however by modelling and understanding a number of analogues with particular aspects relevant to a repository and most importantly, understanding the past behaviour of the analogue over geological time, scientists may be able to designate and design sites for HLNW repositories that may be considered acceptable to the scientific community and the public.

This thesis is not aimed at assessing the processes and problems that may arise in a repository as a function of geological time. However, Koongarra, the analogue under study, has been subject to the variations in natural conditions imposed over long periods of time and these factors are considered in the process of analysing the site. The implications of variation of natural conditions over time are important in the study of both the analogue (the past) and the repository site (the future). Changes in climate, topography and even atmospheric variations all need to be considered with regard to radionuclide behaviour and migration.

An ideal analogue would have a concentration of radionuclides within a geological framework that has been subject to a variety of geological stresses, geomorphological and geochemical variation, climatic changes and hydrological constraints over a long period of time.

The Koongarra uranium orebody is such a site, albeit at a shallow depth. The Koongarra uranium orebody has been exposed to a significant amount of weathering and shows considerable migration of radionuclides through highly weathered rock in near surface groundwater and as such could be considered as an analogue for the worst-case scenario of a HLNW repository, or a near surface repository for low level or intermediate nuclear waste.

The ARAP role in analogue study is aimed at understanding the mobilisation of radionuclides from the discrete zone of the orebody, transport in the groundwater, the redeposition of the radionuclides in the form of a dispersion fan and the further migration of particular radioelements into the local environment.

The Koongarra site has been scrutinised as a natural analogue since 1981, when the Australian Atomic Energy Commission first considered the feasibility of Koongarra as a natural analogue. Since 1988, the site has been under the study of a growing number of scientists from a number of international organisations. This study has been pursuing the quantitative modelling of the processes involved in the migration of the primary uranium away from the orebody in an effort to make comparisons and correlations with studies of other natural analogue systems.

This thesis contributes to the analogue study in attempting to improve understanding of the physical character of the site which then provides constraints on hydrological and geochemical modelling of the site. The migration and redeposition of radionuclides (the "dispersion fan") at the Koongarra site has

proved to be primarily in the shallow weathered zone of rock, clay, regolith and sands (down to about 30 m deep or so) that intersect the upper sections of the primary orebody.

Field geophysical, geological, structural data and laboratory petrophysical data have been considered separately and then in a complementary sense, in order to gain confidence of both methods of inquiry. This method ensures that the laboratory data is meaningful and practical, rather than simply abstract data that are not tied to actual, large-scale physical conditions. The data obtained were also closely studied with reference to concurrent work conducted by other scientists studying the Koongarra site.

In this manner, a framework has been constructed which reflects as accurately as possible, given time and budgetary confines, the constraints imposed upon uranium migration at Koongarra in physical terms. This framework should provide a solid basis on which to build a useful 4-dimensional quantitative model, or analogue, which may be used as a reference when scientists consider the many factors involved in selecting and modelling a site to act as a HLNW repository.

The History of the Site

The uranium deposits at Koongarra were discovered in July 1970 by Noranda Australia Ltd. The discovery was made during ground exploration following the discovery of anomalies on an airborne spectrometer survey of the area. By 1978,

an environmental impact statement for an open cut mine at Koongarra had been put forward by Noranda.

Two employees of Noranda, M.Foy and C Pederson made an early study of the geology of the site (Foy and Pederson, 1975), using information gleaned by field geologists from a drilling program conducted at the site. This was followed by a further study by Pederson (Pederson, 1978).

The ownership of the Koongarra site was transferred to Denison Mines Ltd in March 1980. A study initiated by the Australian Atomic Energy Commission (the precursor to ANSTO) in 1981, sponsored by the US Nuclear Regulatory Commission to determine the suitability of a site within the Alligator Rivers Uranium Field as a potential natural analogue, pronounced the Koongarra Uranium ore bodies as the most suitable site (Payne, 1991).

The Alligator Rivers Analogue Project was begun in 1988, following study between the years 1981 and 1988 by a range of scientists on radionuclide migration at Koongarra and the suitability of the site as a natural analogue of a nuclear waste repository. This thesis is part of, and also complements the work of the ARAP. By the time of presentation of this thesis, the final reports of the ARAP will be concluded. This thesis contributes significantly to one of these final reports (Geophysics, Petrophysics and Structure). It also contributes additional studies and more detailed analysis of and conclusions to pertinent sections of work undertaken that were not able to be made previously due to the time constraints of the project.

Site Location and Description

Koongarra is located about 225km east of the city of Darwin, in the Northern Territory of Australia, latitude 12°52'S, longitude 132°50'E. The uranium deposits are within the Alligator Rivers Province of the Pine Creek Geosyncline, and are part of the Alligator Rivers Uranium Field, which also includes the Jabiluka, Ranger and Narbalek uranium deposits.

The site is surrounded by the Kakadu National Park on all sides, lying on a gently sloping eastern flank of the Mt Brockman massif, an outlier of sandstone separated from the the Arnhem Land Plateau by the Koongarra Valley. This site is drained by Koongarra Creek, which runs into Nourlangie Creek, eventually to join the South Alligator River. The topography of the site is dominated by the strongly outcropping sandstone plateau of the Mt Brockman massif which stands up to 90m high near the site and up to 200m near Nourlangie Rock. The surrounding valley is relatively flat and deeply weathered to the point where outcrop of the country rock is very rare. The area is vegetated by dry sclerophyll forest and scrub.

Climate

The climate of the site is a tropical monsoonal system dominated by a seasonal wet and dry cycle. The wet season extends from about November to the following April and is characterised by consistent soaking rain and storms, during which local roads may become impassable and low areas become flooded wetlands. The dry

season is essentially dry and hot with little or no rain. These factors are significant as they alter the local water table and hence the weathering system and also may restrict field access. Temperatures remain high year round and may reach above 35° celsius at any time of year.

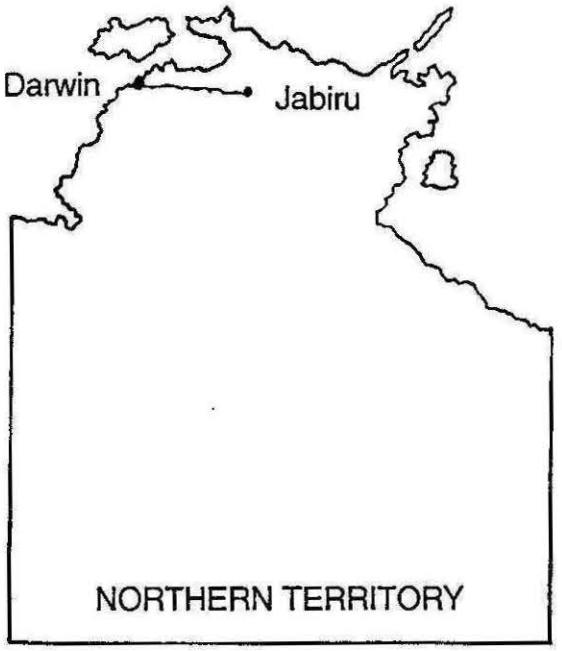

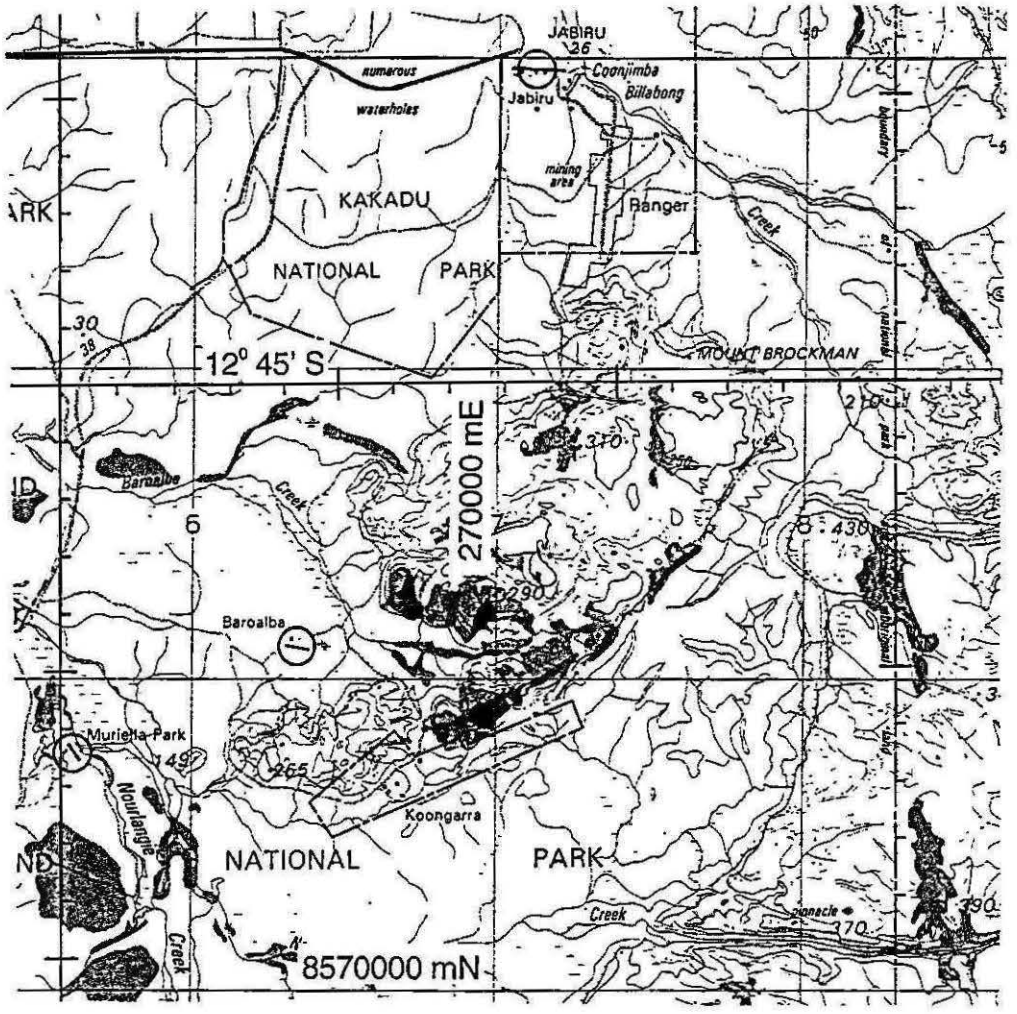

Figure 1.1: Location of the Koongarra Site.

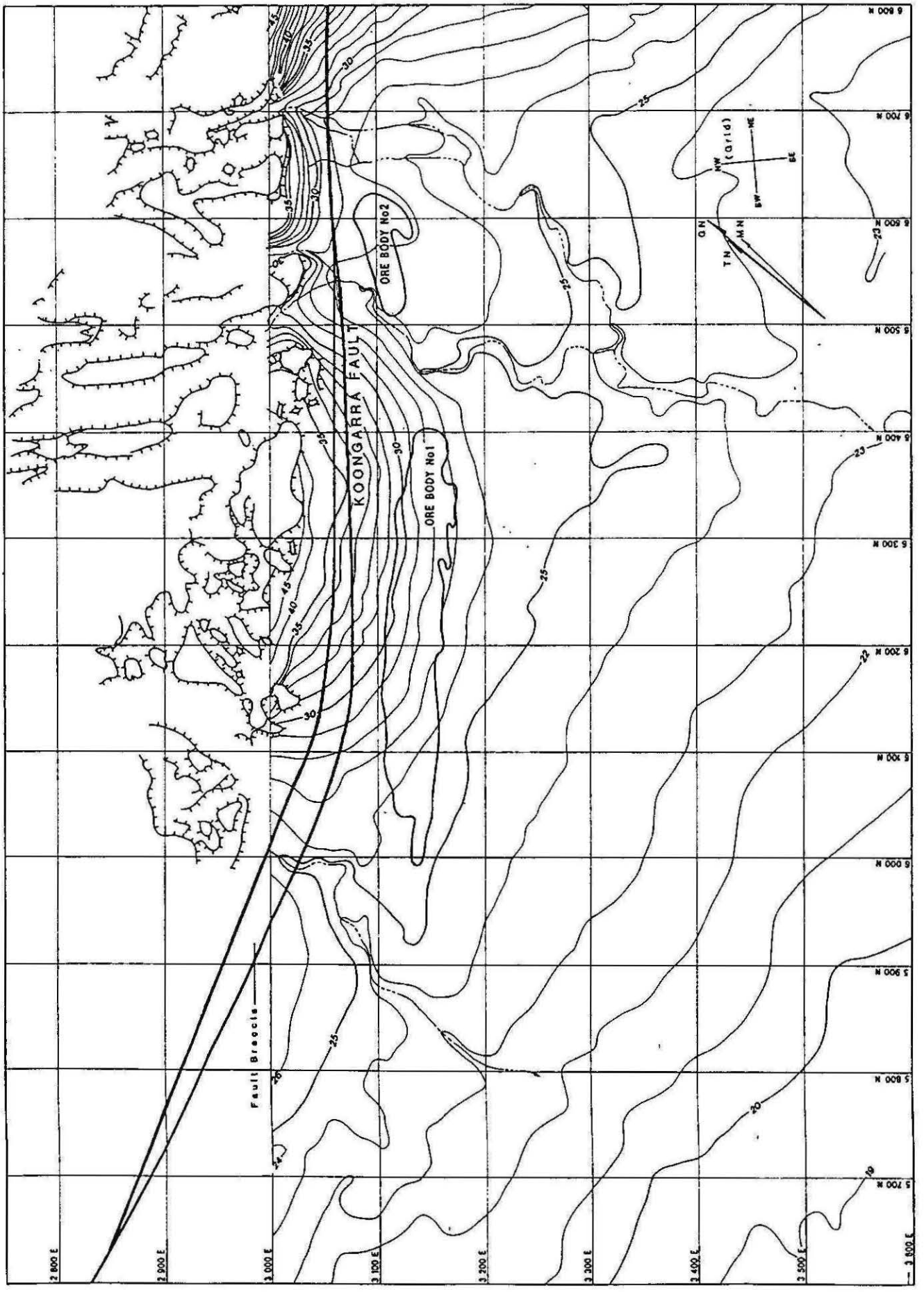

Figure 1.2: Koongarra Uranium Orebody Site Plan.

Summary and Discussion of Rationale and Aims

It has been seen that there is a clear need for effective disposal of the present stocks of HLNW. The use of nuclear means of electricity generation has been considered with regard to other means of electricity generation. Although nuclear energy can be expensive, quite dangerous and the generator of undesirable wastes, it will inevitably act as source of electric energy for the foreseeable future, even if only as an interim energy solution. Blix (1987) indicated that not only will the generation of electricity by nuclear means continue, it will increase to keep up with demand, despite the numerous alternative energy generating technologies that are currently being developed. Therefore, the generation of further HLNW is likely to continue.

Therefore, the problem of effectively permanent disposal must be addressed. Milnes (1985), Krauskopf (1988) and Ringwood (1978) have documented the variety of options that have been suggested for the disposal of HLNW in the past twenty years and it is with reference to the most favoured of these options - that of mined geologic disposal - that this thesis and its mother project the ARAP are directed.

The study of analogues and the relevance of such study to the design of high level nuclear waste repositories has been discussed. Through the study of Koongarra as an analogue of a mined waste repository, the processes affecting radionuclide

migration from a geological environment into the biosphere may be better understood and provide solutions to one of the dilemnas of the industrial world.

CHAPTER TWO :

THE REGIONAL PERSPECTIVE

Lithologies

The rocks that surround and incorporate the Koongarra uranium orebodies are located in the northeastern section of the Pine Creek Geosyncline and have been outlined regionally by Needham (1982, 1988) and Prowse (1990). In the local region they are comprised of an Archaean basement, Lower Proterozoic metasediments and Middle Proterozoic sandstones, conglomerates, volcanics and intrusives. Reported dates of sedimentary deposition and volcanic intrusion vary between workers. Dates presented here represent this author's interpretation of the timing of geological events with regard to the proposals of previous workers.

Archaean (>2500Ma)

The Nanambu Complex (2500 - 2200Ma)

The basement rocks in the area are Archaean to Lower Proterozoic in age (Pederson 1978) and are referred to as the Nanambu Complex. This complex comprises leucocratic garnetiferous granites and gneissic granites which were affected by metamorphism during the early Proterozoic. They may be found 5km to the north of Koongarra occurring as the Magela Mass, a gneissic dome.

Lower Proterozoic (2500 - 1600Ma)

The Kakadu Group

The Archaean granites were overlain by the Kakadu Group, Lower Proterozoic quartz rich sediments that became fused with the Nanambu Complex granites and gneisses.

The Cahill Formation (2200 - 1900Ma)

Overlying the Nanambu Complex unconformably is the Cahill Formation, a sequence of Lower Proterozoic regionally metamorphosed and deformed metasediments including carbonaceous schists, garnetiferous schists, quartz-chlorite schists and quartzofeldspathic schists as well as some dolomitic, magnesitic and amphibolitic units. It is within the Cahill Formation schists that the Koongarra Uranium Ore bodies are found.

The Nourlangie Schist

The Cahill Formation is overlain apparently conformably or with a slight unconformity by the Nourlangie Schist, psammitic to pelitic metasediments that have undergone varying degrees of metamorphism. Sedimentation in the region then came to a close around 1900Ma.

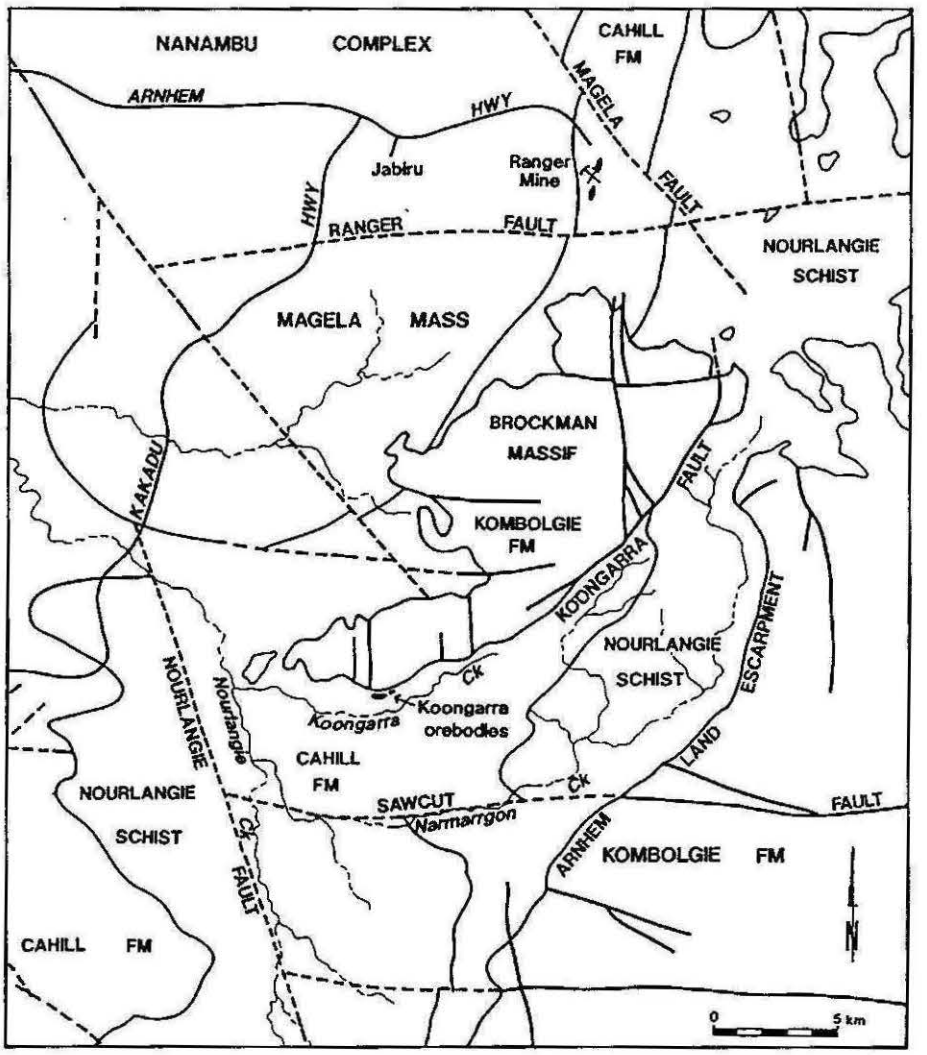

Figure 2.1: Lithology and Structure in the Koongarra Region (From Emerson *et al* 1992).

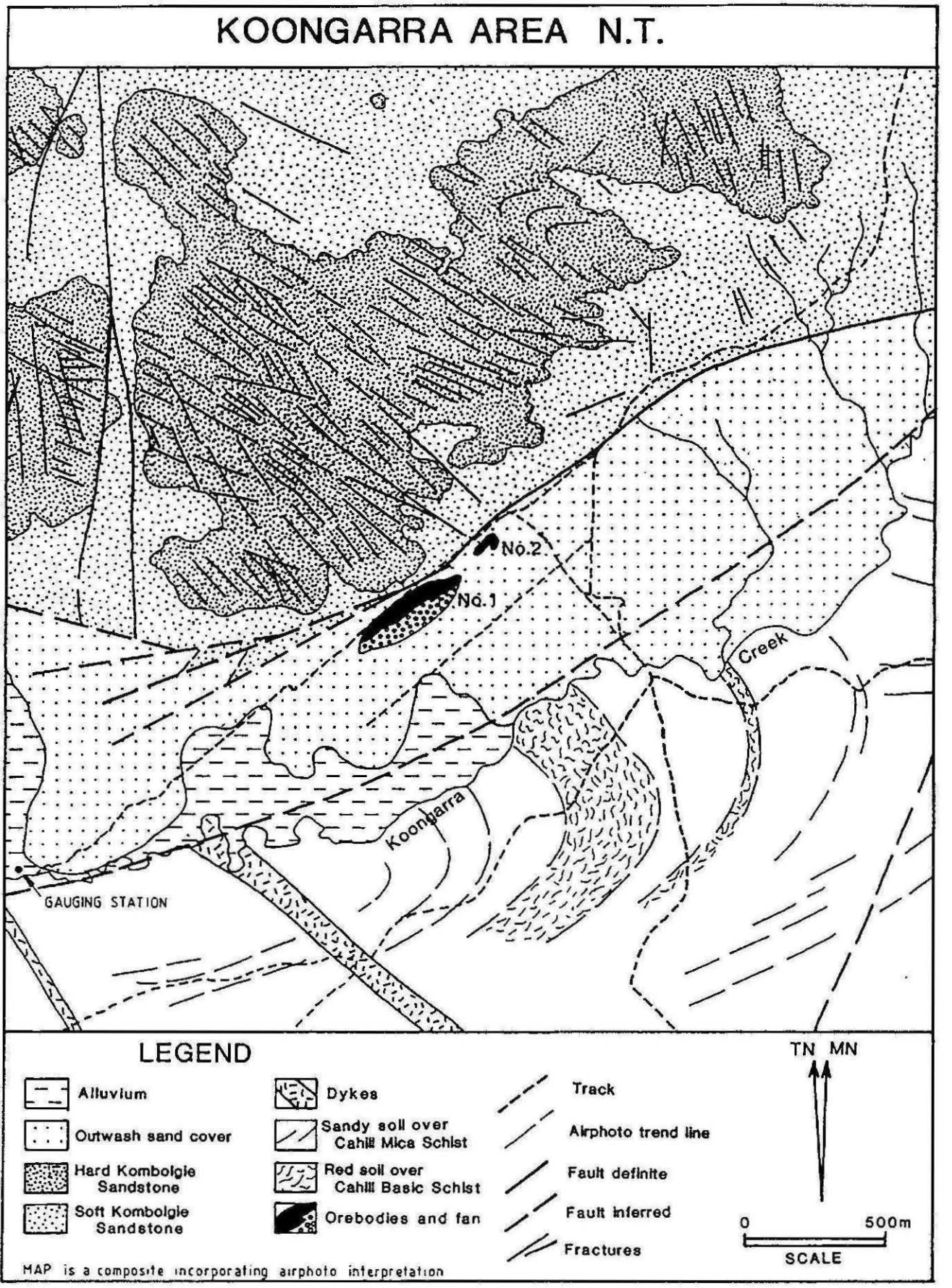

Figure 2.2: Local lithology and structure based on aerial photography (from Emerson *et al* 1992).

The Zamu Dolerite (about 1900Ma)

Intruding into the Cahill Formation in places is the Zamu Dolerite. This has a continental tholeiite basalt composition and forms sills within the host rock. The Zamu Dolerite has been locally altered to amphibolites and in some places partial or total replacement by chlorite has occurred (Ferguson and Needham 1978). It is possible that amphibolitic units found at Koongarra may have originally been Zamu Dolerite. This unit was emplaced at or near the end of sedimentation. Page *et al* (1980) indicate the period of intrusion was 1940 Ma. Snelling (1992) suggests a date of between 1900 Ma and 1885 Ma.

Carpentarian

The Kombolgie Formation (1790 - 1710 Ma)

The sediments of the Kombolgie Formation unconformably overlie the older units. The Kombolgie Formation comprises mature quartz and quartzite pebble conglomerates and quartz sandstones. Also included in this group are some volcanic members of basaltic composition through to rhyodacitic flows, ignimbrites and tuffaceous sandstones. The volcanic units are not exposed near the Koongarra site, but are found to the east of the site at the Arnhem Land escarpment. The sandstone of the Kombolgie Formation, which forms the distinctive escarpments adjacent to the site and characteristic of the region, as well as the quartz pebble conglomerates may be found at Nourlangie Rock a few kilometres southwest of Koongarra.

More recent studies by the Australian Geological Survey Organisation in the Northern Territory have led to the conclusion that the Kombolgie Formation is

significantly older than 1648 Ma (Page *et al* 1980), between 1790 to 1710 Ma. Kombolgie Formation sandstones have been found in contact with the Oenpelli Dolerite and have been hornfelsed.

Geological History

The geological history of the region surrounding Koongarra is relatively complex. The influence of numerous events that have occurred during the geological development of the local area can be seen at Koongarra and are expressed in the character of the distribution of primary uranium ore and the subsequently formed dispersion fan. A summary of the timing of geological events is presented on Table 2.1.

Archaean to Lower Proterozoic (2500 - 2200 Ma)

The underlying basement of the region is comprised of the Nanambu Complex (2500-2200 Ma) granitoids and granitic gneisses. This group of rocks was exposed around 2200Ma and eroded to form the fluvial sands of the Kakadu Group that were laid over, and later fused with, the Nanambu Complex during amphibolite grade regional metamorphism in the period from 1870 to 1800 Ma.

Lower Proterozoic (2200-1870 Ma)

Laid down unconformably on the Archaean basement and the Kakadu Group is the Cahill Formation. The lower member of the Cahill Formation contains micaceous and quartzofeldspathic schists and includes dolomitic and carbonaceous

metasediments suggesting a facies change from the fluvial system of the Kakadu Group to an evaporative facies. The Upper member of the Cahill Formation is more dominantly quartzitic and quartzofeldspathic suggesting parents rocks of silt, sand and mud. The Nourlangie Schist was then deposited on top of the Cahill Formation. Evidence of an unconformity between the Nourlangie Schist and the underlying Cahill Formation is inconclusive. The parent sediments of these schists were psammitic to pelitic sands and muds.

At about the same time as the deposition of these Early Proterozoic sediments or just after, was the intrusion along bedding of the Zamu Dolerite to form sills. Some of the amphibolitic units found within the Cahill Formation at Koongarra may represent altered equivalents of these dolerites, or may be tuffaceous layers of basaltic composition.

Orogenesis (1870 - 1800 Ma)

During this period the Pine Creek Sequence was subject to powerful orogenic processes including folding, metamorphosis and faulting. It was at this time that the sediments of the Kakadu Group and the overlying Cahill and Nourlangie Formations were deformed and metamorphosed and the underlying granites were reworked to form gneisses. Burial pressures and temperatures confining the Cahill Formation resulted in a peak prograde metamorphism in the Koongarra region of amphibolite facies.

Figure 2.1 indicates the major fault trends in the region near Koongarra. Northwest trending faults such as the Nourlangie Fault and the fault trend northwest of the Mt

Brockman massif most probably pre-date deposition and upfaulting of the Kombolgie Formation. Significant jointing seen on airphotos of the region in The Kombolgie Formation may represent reactivation of fault movement in this direction. East - west trending faults can be seen to penetrate both the basement metamorphic units and the Kombolgie Formation in the centre of the Mt Brockman massif.

Four major folding episodes, F1 to F4 (Needham 1988) have been identified and occurred as part of this orogeny. A deformation at the peak of metamorphism (F2) resulted in the easily recognisable schistosity in the Cahill Formation schists. The last folding episode occurred during retrograde metamorphosis at the end of the orogeny. Following the final phase of folding, more granite was intruded into these rocks.

Post-Orogenic Period (1800 - 1650 Ma)

The period after the orogeny up to the beginning of deposition of the Kombolgie Formation (1800 Ma to 1650) was essentially one of erosion of the metamorphic groups, interspersed with periods of deposition of airfall tuffs from the Edith River Group. Intrusions of Oenpelli Dolerite as large lopoliths also occurred during this period, up to 1690 Ma (Snelling 1992).

Uranium Mineralisation

Exact relationships of the primary uraninite deposition within the host and associated units is not entirely clear and opinions of timing and method of emplacement vary. Debate continues as to whether the primary mineralisation

occurred before or after the deposition of the Kombolgie Formation or even after the formation of the Koongarra Fault. Ferguson, Ewers and Donnelly (1980) proposed that the uranium was deposited in dolines following the 1870-1800 Ma regional metamorphic period and later remobilised by igneous heat prior to deposition of the Kombolgie Formation. Hills and Richards (1976) reported the presence of radiogenic lead derived from uranium mineralisation from Pb-Pb isotopic data of between 1800 and 1700 Ma as well as possible further uranium recrystallisation from U-Pb data at 870 Ma. Maas (1987, 1989) reported Sm-Nd isotopic dates of uraninites from 1650-1550 Ma and suggested ore genesis after Kombolgie Formation deposition and the later faulting.

Snelling (1992) suggests that since mineralisation is found in the breccia zones of the Koongarra Fault, primary mineralisation was introduced by circulating fluids from the Kombolgie Formation above. However, the extensive retrogressive alteration seen in the Cahill schists containing the orebodies, which most probably occurred at the time of primary ore genesis, is absent from the Kombolgie sandstones across the fault. This factor would suggest that the mineralisation is pre-Kombolgie. Snelling (1992) suggests a three stage process for the development of the primary ore, citing as the second and third steps, Hills and Richards (1976) U-Pb data which he suggests indicate a date of crystallisation of uranium at 870 Ma and Maas' (1987, 1989) indicating further redistribution at 870 Ma. This does appear somewhat contradictory to the earlier cited age of the ore by Hills and Richards (1976) at 1700 - 1800 Ma. Considering that the most probable time of emplacement of primary ore was concurrent with the pervasive retrogressive alteration associated with the quartz-chlorite schists, perhaps the

most reasonable assumption is that primary ore genesis occurred within the schists prior to deposition of the Kombolgie Formation, then three episodes of redistribution at varying temperatures occurred later, followed finally by formation of the secondary dispersion fan in the past 3 Ma (Airey, Golian and Lever, 1986). The proposed episodes of uranium mineralisation are indicated on Table 2.1.

Deposition of the Kombolgie Formation (1790 - 1710Ma)

This formation contains three main units; a lower coarse grained sandstone and sandstone conglomerate unit; a unit of siltstones and tuffaceous siltstones; and an upper unit of sandstones and conglomerates indicating a braided alluvial fan environment.

Faulting Episodes (1600 - 1500Ma)

Following shortly after the deposition of the Kombolgie Formation (1600 Ma), were a number of faulting episodes. These resulted in significant faults such as the Koongarra Fault, the Sawcut Fault and the Nourlangie Fault and an uplifted horst block in the area of and probably a causative factor in the formation of the present Koongarra Valley (Figure 2.3).

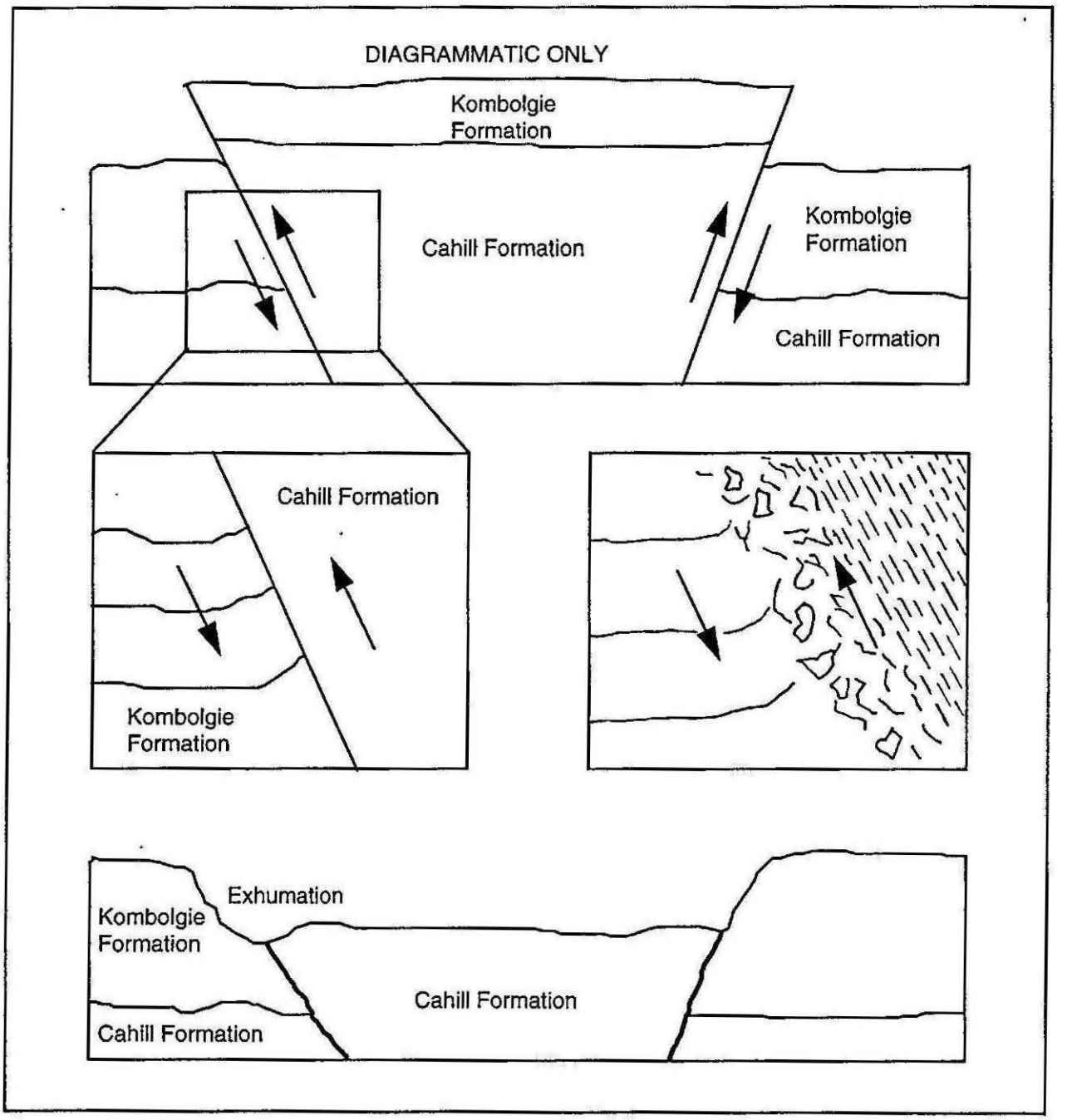

Figure 2.3: Koongarra Valley Fault Block Development.

Erosion (1500Ma to the present)

The period from 1500 Ma to the present comprised a time of relative geological inactivity and erosion with a few minor volcanic intrusive events. This period of erosion resulted in the topography as it is recognised today. The Kombolgie Sandstone overlying the uplifted horst block of the Koongarra Valley was removed by erosion to expose the more readily weathered Cahill Formation and the Nourlangie schists below. The margins of the Koongarra Valley today are essentially controlled by the boundary faults of this horst block. The scalloped western margin of the Mt Brockman Massif is the natural erosional margin of a gently east dipping sheet of weather-resistant Kombolgie sandstone.

It has been suggested that coastal erosion resulted in the formation of the Koongarra Valley and the Arnhem Land Escarpment during periods of high sea-level such as during the Cretaceous. There are no clearly established marine deposits in support of this and the present day topography can be adequately explained in terms of the present day wet season erosion affecting a block faulted terrain.

Overlain on the present geomorphological conditions are more detailed features pertaining to the weathering process, such as weathering horizons, lateritic ferricrete crusts and sand deposits. The development of these features was critical in the formation of the dispersion fan and is discussed in further detail in Chapter 4.

AGE	DATE (Ma B.P.)	EVENTS			LITHOLOGIES
Archaean	2500	Intrusion of the Magela Mass			Nanambu Complex Granitoids
			Uplift and exposure		
	2200	Fluvial deposition	Erosion UNCONFORMITY		Kakadu Group
Early Proterozoic		Evaporative sedimentary facies			Cahill Formation
	1970			MAJOR OROGENIC CYCLE, F1 to F4 FOLDING	Nourlangie Schist
	1940	Intrusion of dolerite sills (Needham)			Zamu Dolerite
	1900 1885	Intrusion of dolerites (Snelling)			
	1870	REGIONAL PROGRADE METAMORPHOSISM : The Top End Orogeny	U mineralisation (Ferguson, Ewers and Donnolley)		Myra Falls Metamorphics
	1820	Retrogressive			
Middle Proterozoic	1803	metamorphism			Edith River Volcanics
(Carpentarian)	1800	Faulting and erosion	U mineralisation (Hills and Richards)	POST OROGENIC PERIOD	Oenpelli Dolerite (Snelling)
			U mineralisation (Emerson et al)		Kombolgie Formation
	1700				
	1688				Oenpelli Dolerite (Page, Compston and Needham)
	1650 1610		U mineralisation (Maas)		
	1600		U mineralisation (Snelling)	Faulting; Koongarra, Sawcut, Nourlangie	
	1550				
	1500	Localised faulting, uplifting and jointing			
	870		U redistribution		

Table 2.1: Geological events in the Koongarra Region.

CHAPTER THREE :

SITE STRUCTURE AND GEOLOGY

Structure

The primary structural features at the Koongarra site include the Koongarra Fault, F1 to F4 folds formed during the 1870 Ma orogenesis, an apparent fault along the Koongarra Creek (Emerson *et al* (1992, ARAP Final Report Vol.4)) and localised minor faulting and jointing that occurred after 1500 Ma. A mine geology plan for Noranda (Pederson 1978) suggested two significant cross-faults nearly perpendicular to the Koongarra Fault, one to the south of the orebodies and another to the north of the orebodies. This study has found no evidence to corroborate these faults and it is possible that they may have been interpreted to account for the apparently displaced schist and dolomitic units in the southwest of the site.

The Koongarra Fault

The Koongarra Fault shows an apparent curvature in plan and cross-section. There are a number of possibilities that may account for the curved appearance, the most likely of which, this author suggests, is that the fault is composed of numerous, fractured fault blocks that were first moved in a dip-slip direction and then cross-faulted and fractured roughly perpendicular to the original fault in many places at a later stage, giving rise to a curved shape.

Field observations of the Kombolgie Sandstone by this author, near the location of the fault indicate an upward tilting of the beds nearest to the fault, corroborating a predominant dip-slip movement of the Koongarra Fault. Further to this, Emerson *et al* (1992) determined that the sandstone is upended and folded about a cylindrical axis within the fault surface.

The positions of the fault and the fault breccia both at the surface and at depth are debatable and this study concludes that the location of the fault is in fact different to that interpreted previously. The fault is largely eroded away and not exposed at the ground surface, contrary to earlier suggestions.

If the Koongarra Fault was formed by a dip-slip movement followed by cross-faulting, it is reasonable to suggest that the very nature of the faulting may have a major influence on the flow of groundwater from the Kombolgie Sandstone across to the Cahill Formation schists. It has been proposed in earlier ARAP reports that groundwaters are flowing across the Koongarra Fault breccia into the schists at depth. This infers groundwater movement into the Kombolgie Sandstone on the escarpment and downward to depth into the sandstone, giving the fault a major role in the down-gradient movement of groundwater at the site (Snelling 1990, ARAP 1st Annual Report).

It is suggested that the springs sometimes found at the base of the Kombolgie Sandstone near the fault zone are evidence that the fault is relatively impermeable and not presently acting as a groundwater conduit. Petrophysical studies by this

author and Emerson *et al* (1990) show that the Kombolgie Sandstone has low matrix permeability and petrophysical and drill hole studies of the Kombolgie sandstone indicate that the open fractures and joints seen at the surface are closed at depths below the zone of predominant weathering (30m depth or so), ipso facto any groundwater presently moving through the Kombolgie Formation and into the schists would be at shallow depths. Any other groundwater movement through the sandstones would have to be dominantly via undetected macrofractures. Supposing that cross faults do exist and validate the curvature of the Koongarra Fault, it must be postulated whether they are directly or indirectly related to the fracture zones seen at the surface in the sandstone and whether they had any previous role in the channelling of groundwater through the Koongarra Fault zone.

It can be seen that the joints in the Kombolgie Sandstone at or near the surface must have once acted as water conduits, since silica can be found lining the joint surfaces (Wyroll 1992, ARAP Final Report Volume 3). This author has seen extensive fracture zone channelways on the escarpment, which are frequently filled with well developed quartz crystal veins, featuring in some localities exposures of large, open veins filled with milky and amethystine quartz crystal prisms. These fracture zones obviously once acted as significant fluid conduits and may have even crossed the Koongarra Fault. If this is the case, at what stage were the joints filled in and what role did they play in groundwater movement before infilling?
Wyroll (1992) suggests the Kombolgie Formation sandstone cliffs at Koongarra represent a "relaxed" escarpment, meaning that at the surface, fracture zones are opening up through the process of geomorphological development. It seems

plausible to this author that a large proportion of the joints seen at the surface in the Kombolgie Sandstone therefore may be merely surficial or related to the geomorphological opening of the escarpment and not be related to the inferred cross-Koongarra Fault faulting and fracturing.

This study does not interpret the Koongarra Fault as a conduit for groundwater movement at present, excepting a minor role in the weathered zone. Petrophysical studies outlined later in this thesis determined that the Kombolgie Sandstone is relatively more permeable at the surface where it has been weathered along fractures and through pore channels. Unless localised zones of micro and macrofaulting undetected in petrophysical sampling are widespread within the sandstone, significant fluid movement below the relatively shallow weathered zone should not be expected. In any case, the influence of such unquantifiable features cannot be determined by laboratory petrophysical techniques.

Folding Episodes in the Cahill Formation

The various effects of the regional folding episodes F1 to F4 proposed by Needham (1988) can be directly related to the lithologies at Koongarra which show dominant schistosity near parallel to bedding and can be summarised as follows : the F1 and F2 folds are isoclinal and developed the axial plane schistosity nearly parallel to bedding. The F2 folds occurred at about the peak of the prograde metamorphosis that occurred at around 1870 - 1800 Ma and resulted in the dominant schistosity of the metamorphic units at Koongarra and in the region. This

schistosity has previously been inferred to have had an influence on the preferred direction of groundwater movement at the site and is further investigated in Chapter 5. The schistosity presumed to have developed during the F1 and F2 events has been further examined through the use of the borehole television logs of a number of boreholes at the site (see Figure 3.2). The variations and orientations in direction of the schistosity have indicated a large fold structure to the southwest of the No. 1 orebody (Figures 3.4 and 3.7) and are discussed in more detail later in this chapter. The suggestion of such a structure in the southwest section of the site assisted in solving the puzzle of apparently out of place units in this part of the site and led to re-interpretation of the geological plan of the Koongarra site (Figure 3.8). This fold is interpreted to have occurred during the F3 folding event as the schistosity is folded around in the shape of the fold. The F4 folding episode occurred during the retrograde metamorphosis at about 1800 Ma and resulted in smaller kink-fold structures.

A fault running parallel to the Koongarra Creek has been proposed (Emerson *et al* 1992), following study of airphotos of the region and site. A large fold structure to the south of the creek can be derived from the variations in colour and vegetation of the ground surface. Field observations by this author also indicate that the lithologies in this area are of a different nature to those found surrounding the orebodies.

Borehole Studies

Borehole studies at Koongarra have been the principal method of investigation of the lithological, structural and petrophysical characteristics of the site. For this reason, it is essential to have an accurate gauge on the locations of the boreholes yielding those data. This study has had the advantage of hindsight in the initiation of borehole investigations, especially when there have been specific aims to the study, for instance in the study of the location and effects of the amphibolites at the site. The addition of the Borehole Television technique has made inferences regarding lithology and structure possible where data available previously left a puzzle from which only surmises of the geological structure could be made.

Borehole Map

A map of the boreholes at Koongarra is presented in Figure 3.1. This borehole plan was constructed solely by this author. Considerable effort and investigation was made to ascertain the correct location of the boreholes. The location of boreholes and plotting onto the borehole plan to construct a reliable site plan was considered by this author to be the first step in the borehole studies, so that deductions regarding petrophysical results, geological data, the BTV data and other borehole studies with regard to geochemical and hydrological studies could be made with confidence. This author solely constructed this new and accurate borehole plan for use by all other authors in the final reports of the Alligator Rivers Analogue Project.

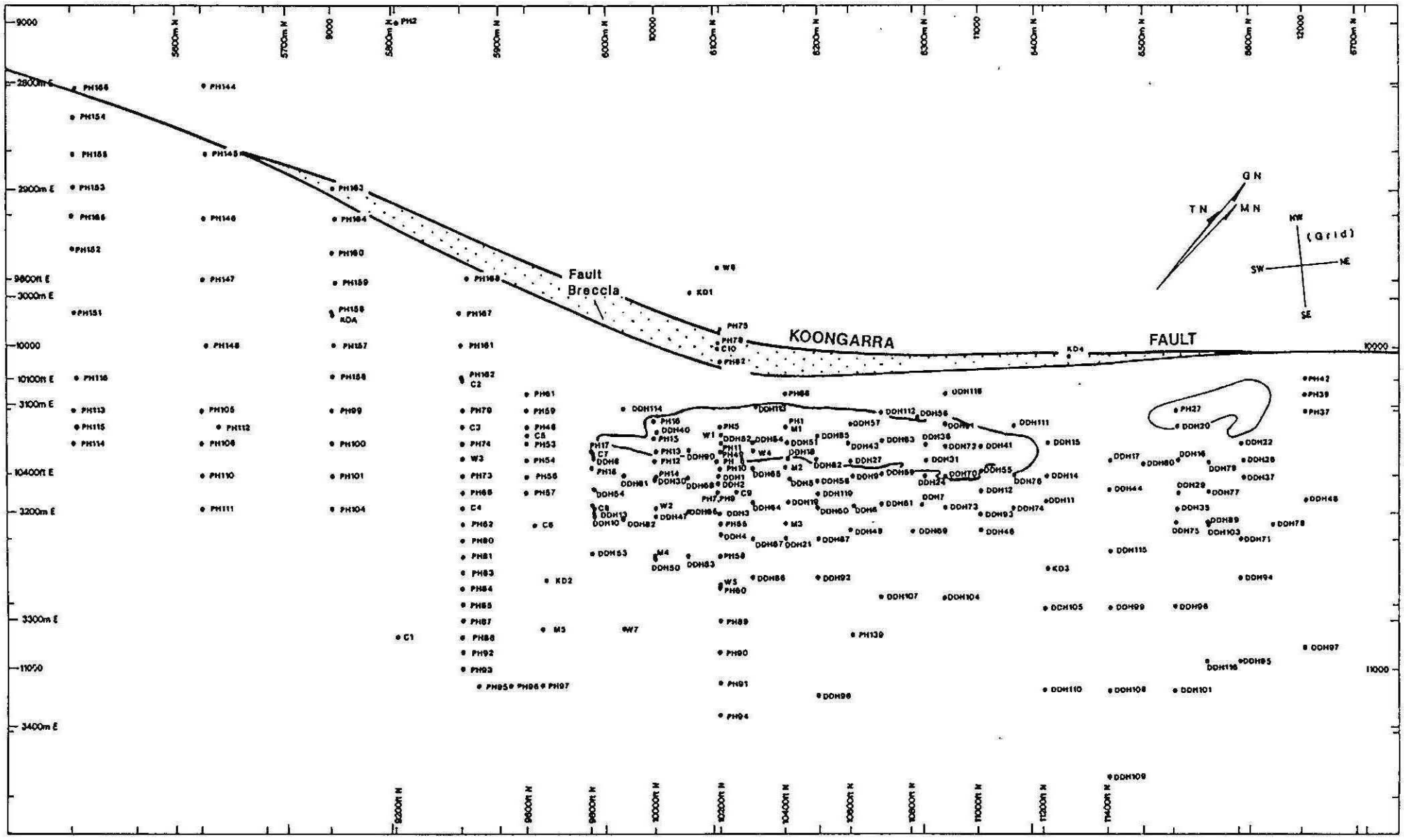

Figure 3.1: Plan of Boreholes at Koongarra.

The X and Y location of each borehole was obtained from the borehole log and compiled in a data file which was then plotted using the Golden Software "SURFER" program. These data are presented in Appendix I. It was found that drafting and redrafting of the site borehole locations in numerous previous presentations had resulted in the inaccurate location of many of the boreholes.

Occasionally, the effects of these incorrect locations were significant and could have affected the interpretation of lithological boundaries. This borehole plan was accepted as the "base-map" of the site for use by all volumes of the Alligator Rivers Analogue Project.

Borehole Television Studies

Considerable study of the structure of Koongarra through the use of the Borehole Television (BTV) was made by Emerson *et al* (1992, ARAP Final Report Vol.4). This study presents only a summary of the conclusions from that presentation and instead focusses on the relevance of the BTV studies to the conclusions of this thesis. The BTV studies were carried out concurrently with the studies of the site geology and structure by this author and others as part of this thesis and as part of the ARAP. The results of the BTV studies were instrumental in the definition of the geological map of the site presented by this author and also by Emerson *et al* (1992).

The BTV comprises a well logging probe with a miniature camera which views the entire inside wall of the borehole via a conical mirror. The probe relays data to the RAAX BIPS 300 (Borehole Image Processing System 300) which converts the digital image into a "flat" image of the borehole wall on a videocassette. The system of conversion of the image from a circular to a planar one is depicted in Figure 3.3. The graphical resolution of the processed image from the BTV system is 0.5mm.

The BTV system is able to give information about fracture size, spacing, density, direction and a little lithological information. The interactions and combinations of the data reveal numerous features of the character of the structure at Koongarra, far more than is available from either field observations or drillcore, because data from the BTV is recorded *in-situ.* For a site such as Koongarra where outcrop is poor and very weathered when exposed, the BTV method is an invaluable aid. Inferences may be made regarding the position and orientation of zones of greater fracturing and thus zones of enhanced permeability. The orientation of the fracturing and schistosity can be gauged and pertains directly to the structure of the site, particularly the existence, position and shape of the F3 fold in the lithologies to the southwest of the orebodies.

Data were obtained from 20 boreholes at Koongarra. These boreholes are indicated in Figure 3.2. The boreholes sampled were of the C, PH and M, percussion holes that lie in the southern half of the site. No boreholes near the Number 2 orebody were sampled using the BTV. It must be stressed that the great

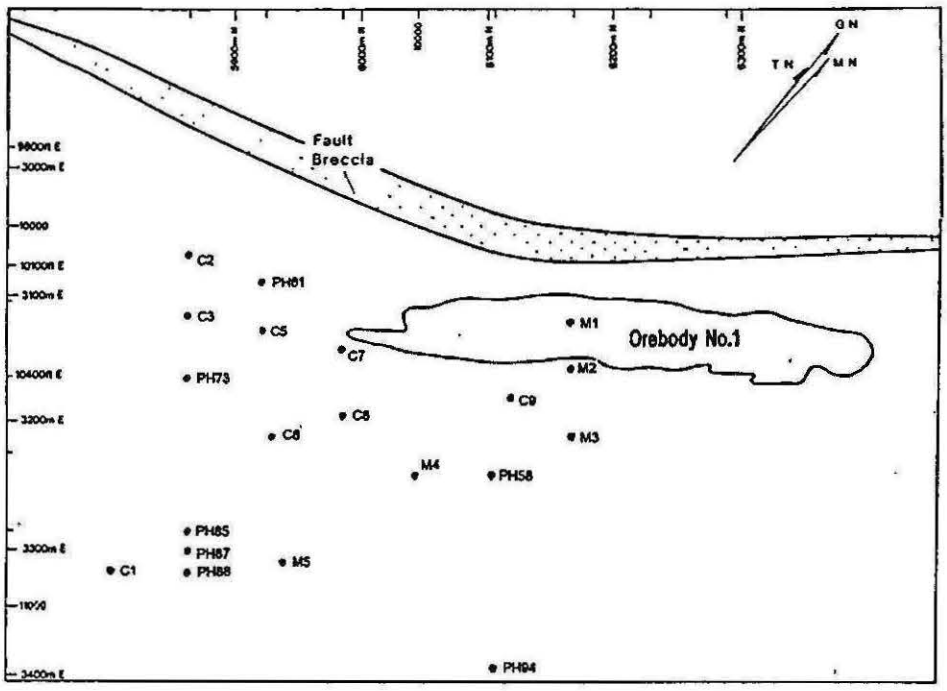

Figure 3.2: Map of boreholes examined with the BTV technique.

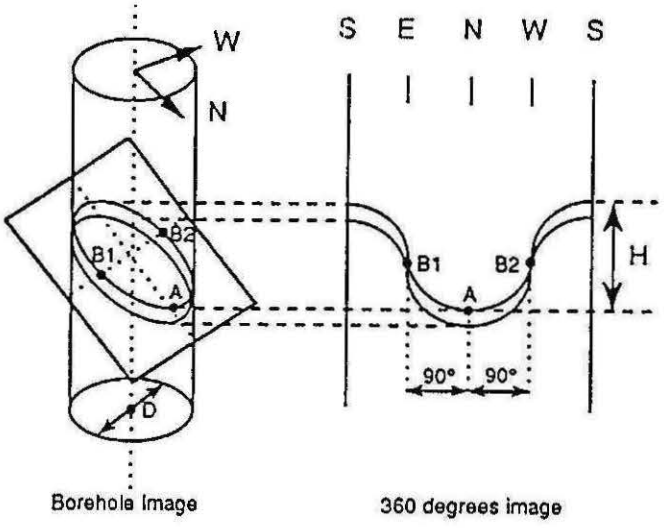

DIP DIRECTION : A, angle from North clockwise, direction of down dip azimuth (DDA) ; in this case, DDA is 000°
STRIKE : ±90°, in this instance, is 090°or 180°
DIP : $\tan^{-1}$ H/D , in this instance, dip is 45°
DIAMETER : D, distance B1 to B2, minimum width
±90° from point A
Note that the "borehole image" is NOT the camera image, but an image of the outside view of the borehole.

Figure 3.3: Schematic diagram of the method of the BTV camera prepared by this author both for the ARAP and this thesis.

majority of BTV observations are from below the weathered zone. Borehole casings in all but one case - borehole M3 - prevented the lithologies from being observed in the upper zones of rock.

Results from the BTV Studies

Fractures

Correlation between the intensity of fracturing (fracture density) recorded for the graphitic schists and the Rock Quality Designation factor (RQD) analysis (given as a percent) presented in Volume 4 of the ARAP final reports (Emerson *et al* 1992) can be made. Although the BTV technique was not employed in any of the diamond drill holes such as DDH53 in which the RQD analysis was made and only a small section of percussion hole C9 was recorded, a tentative positive correlation between the characteristics of the lithologies from the various techniques can be made.

The graphite-muscovite-chlorite schists had a fracture density of 4.0/m, 2.0/m greater than the average for all lithologies (2.0/m) and far greater than the other lithologies which range in fracture density from 1.0 - 2.5/m. In comparison, the RQD recorded for the graphitic schists in DDH53 was the lowest of all the unweathered Cahill formation rocks. Graphitic intercalations in the quartz-chlorite schists gave "poor" rock quality results of 34%, and graphite-quartz-chlorite schists gave a lower result of 27%. The highest RQD measured was the Kombolgie Sandstone (77%), followed by the mica-garnet-pyrite-quartz-chlorite schists (50%).

The lowest fracture density recorded for any of the Cahill Formation schists was 0.99/m for the muscovite-quartz-feldspar schist which was either not observed in the RQD analysis or not differentiated from the bulk of the schists as a distinct unit. Curiously, although the graphite-mica-quartz schists recorded the most fractures per metre from the BTV, the graphite-quartz-chlorite schists showed the lowest fractures per metre of all the Cahill Formation units (Table 3.1). The garnet-mica-quartz schists showed the highest RQD values of the schists (strongest) but recorded only a moderately low fracture density per metre from the BTV. This could be due either to the variation in the methods used to gain the data or to the RQD examination which only examined lithologies from one borehole. It must also be mentioned that the results from the RQD analysis are susceptible to error due to the drilling process and handling after drilling which may damage core specimens.

Data gathered from petrophysical studies can also be compared against the BTV results. The unweathered graphitic schists show higher average water permeabilities (0.9md) than the other unweathered Cahill Formation lithologies (0.2 - 0.3md), which correlates with both the BTV results and the RQD fracture analysis. This author suggest the true permeabilities of the graphitic units may even be higher, as the method used for testing of water permeabilities required sound cores, which may not necessarily accurately represent the graphitic units, given that they are generally more fractured. Thus the petrophysical results may be biased toward the stronger cores available for testing.

Generally speaking, the three techniques agreed with regard to the relative strength of the unweathered schists and the Kombolgie Sandstone (except for the permeabilities) and the weakness of the graphitic units. However, with some units, the difficulty of classification of a generally gradational schist regime becomes evident, as virtually identical lithologies are given different names in the different examinations.

Table 3.1: Relative Lithological strengths. A comparison between BTV, RQD and water permeability results. (M = Mica, Q = quartz, F = Feldspar, KS = Kombolgie sandstone, Gr = Graphitic, Amph = Amphibolite).

Method	Lithology						
	Stronger				Weaker		
BTV (Fractures/m)	MQFS 0.99	KS 1.51	GrQChS 1.96	GMQS 2.17	Amph 2.18	QChS 2.31	GrMQS 4.00
RQD (%)			KS 77	GMQChS 50	QChS 38	GrQChS 34,27	
Permeability (md)	Amph 0.2	QChMS 0.3	GrS 0.6	KS 0.9			

It is interesting to note the contradictions in the results for equivalent lithologies from techniques that are analysing very similar and related characteristics (Note that Graphitic Quartz Chlorite Schist and Quartz Chlorite Schist are transposed in order of relative strength for the BTV fracture analysis and the RQD and so are Mica Quartz Feldspar Schist and Garnet Mica Quartz Chlorite Schist, which are virtually equivalent lithologies).

Concentrations of fractures and zones of fractures of similar orientation observed in some holes may occasionally be correlated between holes. However no conclusions can be drawn from the data whether they are indicative of large, distinct fracture zones or faults.

Fracture orientations were seen to vary in a consistent manner, which is echoed in the schistosity trends observed by the BTV technique. Fracture orientations in the BTV tested holes in the centre of the No. 1 orebody trend in a southwesterly direction. The boreholes on the nose of the fold, to the western end of the No. 1 orebody show variable fracture orientations, which could be expected given the position on the fold. Boreholes to the south of the No. 1 orebody and on the southern limb of the fold show a prominent north-south fracture trend.

Schistosity

Fracture and schistosity orientations determined by the BTV were found to be particularly uniform in each separate hole and orientations of schistosity were found to vary in a systematic way. The schistosity developed during the first two folding episodes (Needham 1988) during orogenesis, which is observed to run parallel to bedding, was used as a guide when interpreting the structure of the Koongarra site through the use of the BTV.

The orientations of the schistosities observed in the BTV logs were plotted on stereoplots, in plan view and in section. The results of some of the plan and

section views of the BTV observed schistosities and fractures can be seen in Figures 3.4 and 3.5. The trends of the schistosities indicate a large F3 fold with a mean axis plunging 12^{0} to 73^{0} (true). The presence of such a structure immediately clarifies the position of the apparently displaced dolomitic units southwest of the orebodies. Previous workers have interpreted major cross-faults in this area to account for the position of these lithologies (Pederson 1978). Geological studies of the site from borehole logs by this author corroborate the proposed BTV fold, showing the dolomitic unit plunging to the east under the younger units. The position of graphitic units found to the south of the orebodies is also explained by the curvature of the graphitic unit around the BTV interpreted fold.

Flattening of the steeply dipping schistosity can be observed in boreholes C6 and M1 and may be the indicator of drag effects from the reverse fault, mirroring the effects of the Koongarra Fault on the Kombolgie Sandstone outcrop observed on the escarpment near to the fault breccia.

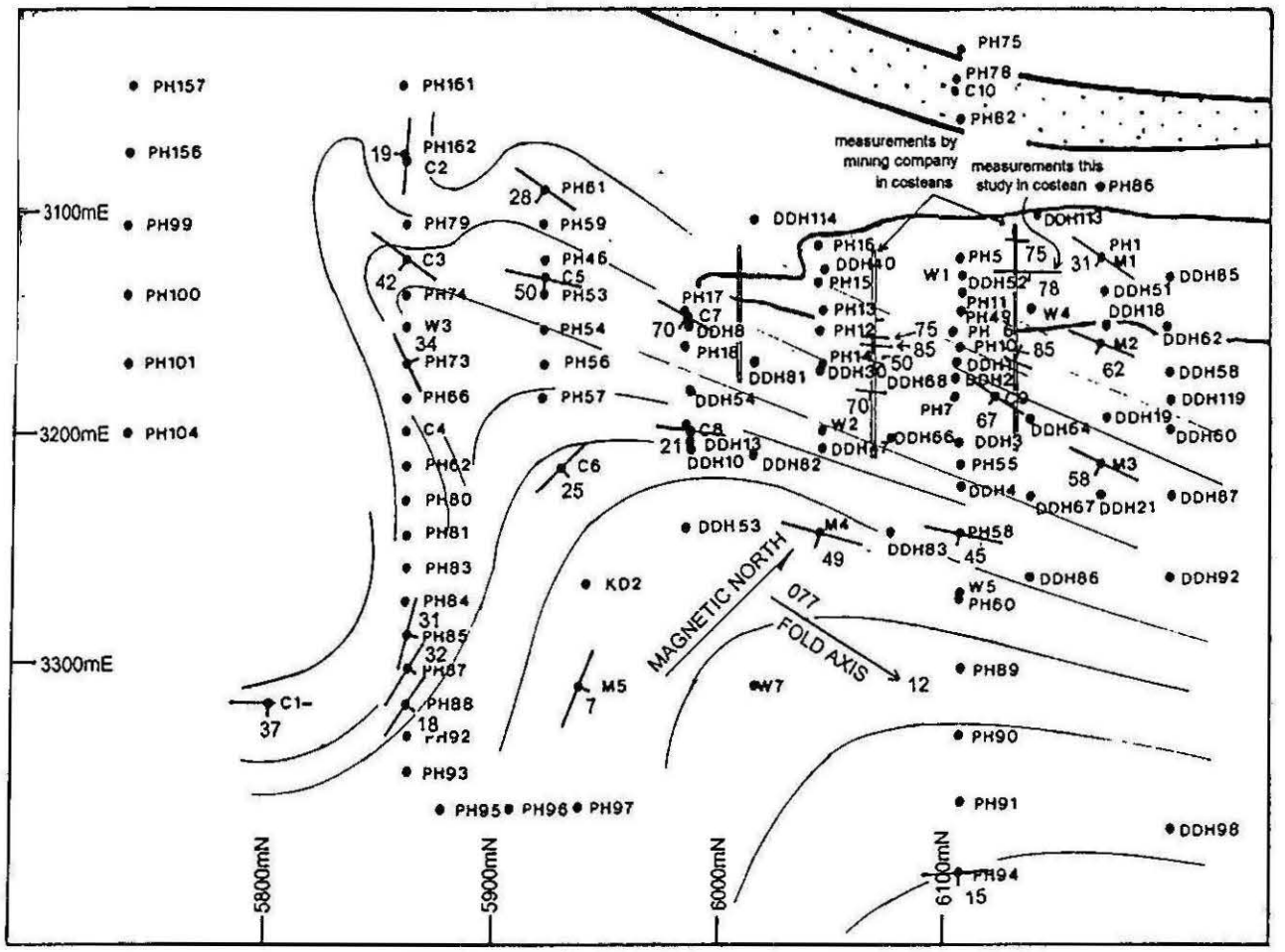

Figure 3.4: Site structure revealed by the BTV studies of schistosity and foliation.

Figure 3.5: Cross Section of Schistosity trends through PH 61, C5 and C6.

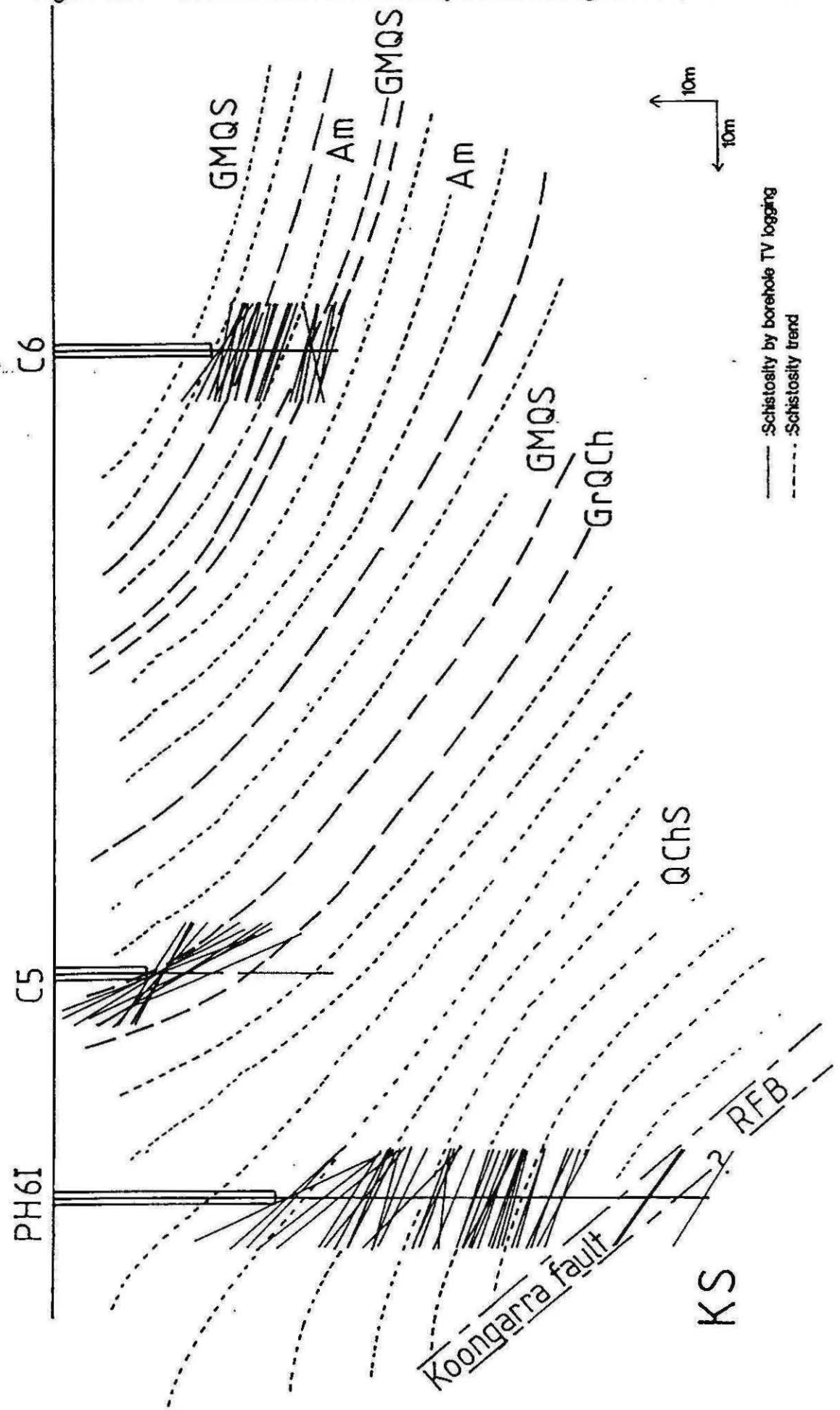

The Weathered Zone

Percussion hole M3 is the only hole from which BTV data were obtained for the upper weathered and transition zones. In the weathered zone of rock, banded clay materials obscure any visible fractures. This may be due to complete weathering of the schists and infilling of fractures or may represent smearing of the clays due to the effects of the drilling. It is not possible to deduce from the scarce data whether this indicates that the majority of groundwater movement in this zone is matrix flow, but this is inferred from the data in this single borehole.

In the lower parts of the weathered zone, discontinuous and continuous fractures are evident and filled with clays. As the boundary between weathered rock and unweathered rock is approached, the continuous fractures predominate. It is possible that this zone may therefore have the highest groundwater conductivities. This is to some degree reflected in the petrophysical data collected from these zones. The weathered and lower weathered or transition zone can be seen to have by far the highest water permeabilities and the highest porosities, excluding the very porous but relatively impermeable upper weathered zone.

Conclusions on the Borehole Television Studies

The BTV studies at the Koongarra site have revealed numerous features of the structure of the site that were not discernible previously. These features have implications for both the structural and lithological studies of the site. In eliciting

data leading to the delineation of the large F3 fold in the schistosity and the units at Koongarra, the BTV technique has been instrumental in a re-appraisal of the Koongarra site structure and thus the preferred direction of groundwater flow and its relationship to schistosity direction.

The *in situ* observations of fracture distribution and orientation in the unweathered rock and in the lower weathered zone allow certain inferences to be made regarding the method of flow, whether fracture or matrix dominated. The scarce data gathered from the weathered zone of rock suggests that flow is matrix dominated. Correlations between the BTV observations and the petrophysical and fracture analysis data have been useful in both confirming the validity of the BTV data and the results from these other techniques. The BTV technique is obviously a useful tool for analysing site geology and structure even after comprehensive borehole studies.

Used in combination with other site structural and permeability data, the main implication for the flow of groundwater at the site given by the BTV data is that the schistosity direction may introduce a bias toward a southwest to southerly direction, following the main trends in the distribution of fracture and schistosity orientations.

Although no continuous fracture zones could be correlated over large areas of the site from hole to hole using the BTV and no conclusive evidence of previously documented cross-faults was found by this author, the presence of these fracture zones or faults cannot be disproved. Additionally, the RQD analysis of DDH53 and

the BTV studies indicate that major fracture zones other than the Koongarra Fault do exist in the schists. However, the presence of the large fold structure would appear to effectively negate the need for the previously surmised cross-faults to explain either the position of the dolomitic units to the south of the western end of the No. 1 orebody or the general groundwater flow directions.

The distribution of fracture density across the southern end of the site does not indicate significantly higher fracture densities in the boreholes over the nose of the fold structure or along the fold axis as may have been anticipated. Therefore, a preferred flow in this direction (striking 250°, virtually WSW) is not anticipated and agrees with conclusions drawn regarding flow direction from the BTV studies.

It can be seen that the technique of Borehole Television at Koongarra has been an invaluable aid in delineating structural features not evident from other techniques. Schistosity direction, fracture density and alignment which pertain directly to permeability and groundwater movement are determined *in situ*, a feature which has been seen to have certain advantages over other studies such as borehole specimen analysis. The BTV system has proved to function as a useful secondary technique for making comparisons with lithological and fracture studies of borehole core and petrophysical data.

Lithologies

The Cahill Formation

Distinct lithological qualifications and boundaries in the amphibolite grade metamorphic Cahill Formation equivalent schists at Koongarra are rare due to the nature of the depositional facies of the sediments and the subsequent numerous metamorphic and alteration events that have occurred since diagenesis. The sedimentary facies responsible for the Cahill Formation is interpreted by this author to be a gradational, possibly regressive shallow shelf environment. Considering the nature of this environment and the considerable deformation since deposition, it would be optimistic to overqualify or too readily classify the lithologies at Koongarra as discrete units or distinct entities.

A comprehensive study of the borehole logs of the site has been carried out in order to more clearly understand the site geology. Unfortunately, only one borehole core tray (DDH53) was available for sampling and physical examination. Ambiguities in the borehole log were revealed by comparison of the core specimens and the borehole log (for example, core logged as fault breccia).

This study of the geology of the Cahill Formation at the Koongarra site indicates that the lithologies are divided into six very broad categories within a quartz-chlorite schist regime:

Unit H. The lowest unit in the sequence is an interlaminated dolomite, schist and silicified dolomitic marble group and is at least 60m thick.

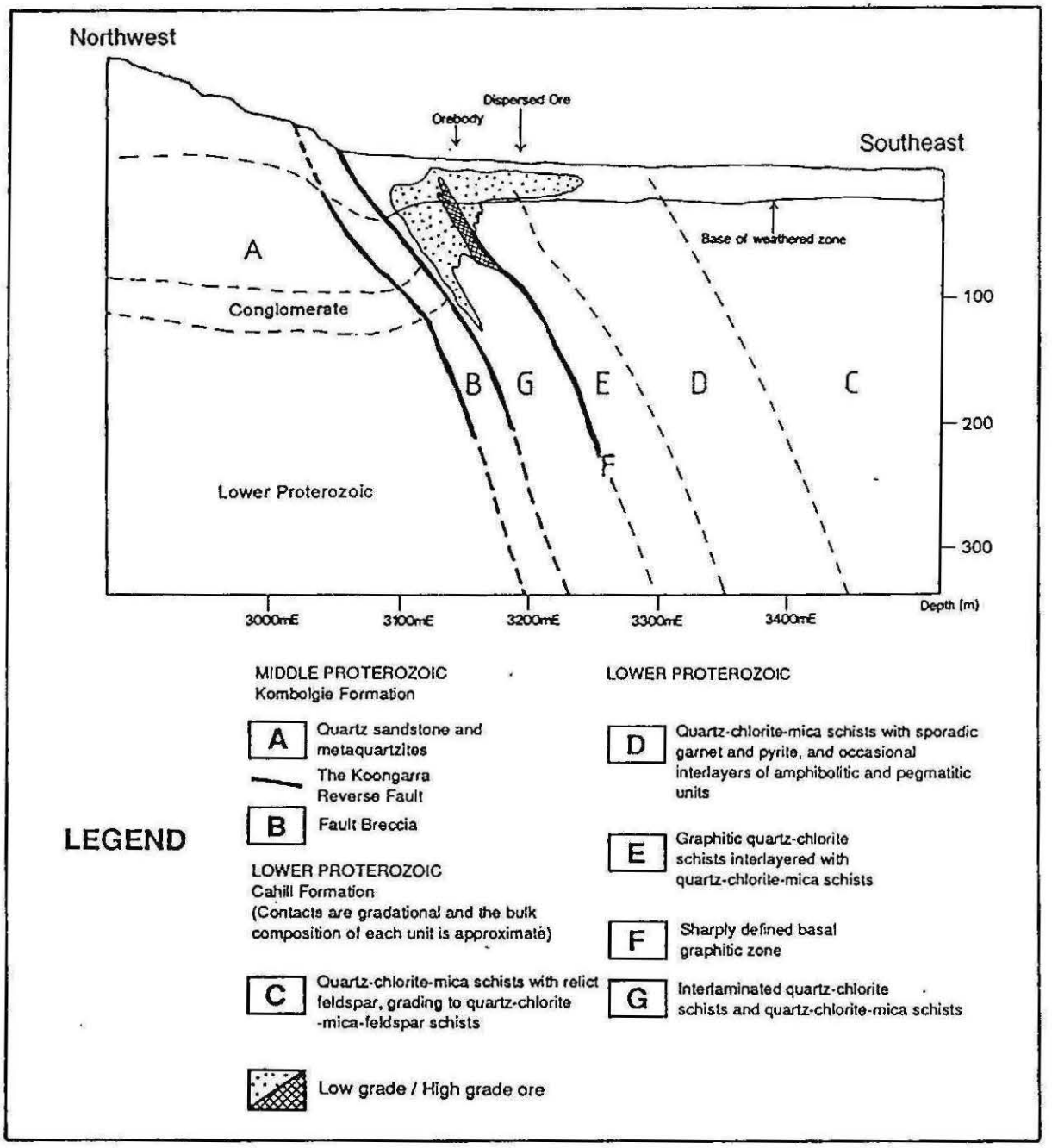

Figure 3.6 : Geological Cross-Section. This cross-section indicates the lithology and structure delineated through borehole studies carried out by this author and represents a significant revisal of earlier presented geological plans. The Proterozoic sequence, Koongarra Fault, uranium ore and the weathered zone are represented. The Koongarra Fault lies between units B and G. Units A and B contain the Kombolgie Sandstone which forms the escarpment at the site. Evident at the site is the upper Sandstone unit of the Kombolgie Formation, dipping gently southeast, and dragged upward close to the Koongarra Fault Zone. The conglomeratic lower member of this formation can be seen at Nourlangie Rock, south of the site. Units C to G are subdivisions of the Proterozoic Cahill Formation schists, described in the text of this thesis. A dolomitic unit (H) underlies these units but is not evident on this orebody cross-section.

Unit G. The next unit is a group of quartz-chlorite and quartz-mica schists, the footwall rocks to the uranium mineralisation and is approximately 60m thick.

Unit F. A distinct graphitic band overlies these units and acts as a marker unit in the sequence. The graphitic band varies in composition, from lenses of pure graphite to graphitic quartz-chlorite schist and varies in thickness from generally 1 to 10 m.

Unit E. Overlying the graphitic band is a graphitic quartz-chlorite and graphitic quartz-chlorite-mica schist sequence. The carbonaceous content of these schists is believed to be an influencing factor in the location of the primary ore mineralisation (30 - 40m thick).

Unit D. Next in this sequence is a quartz-mica schist unit in which aluminium garnet porphyroblasts are common. This unit is largely affected by retrogressive alteration, the garnets commonly altered to chlorite. This unit is up to 80m thick.

Unit C. The uppermost unit encountered at Koongarra is a quartz-mica-feldspar and quartz-chlorite schist. Within this unit can be found occasional interlayers of amphibolitic units and some pegmatitic units. The amphibolites are discussed in more detail later in this chapter. This unit is at least 100m thick.

The Depositional Environment of The Cahill Formation

This study concludes that the sedimentary facies responsible for the deposition of the Cahill Formation at Koongarra was most likely a shallow marine environment which gradually altered to an environment of largely terrigenous sediments, either by infilling by terrigenous material or from a minor regressive event. The initial

sediments were probably very shallow limey muds or possibly even evaporitic deposits. These sediments resulted in dolomitic marbles which are more than 60m thick at Koongarra. As the environment changed, an increased quantity of aluminium rich sediments were deposited, possibly from extrusive basaltic materials or from a change in composition of the muds from carbonate, magnesium rich to aluminium, iron and magnesium rich, giving rise to the greenshist layers common within the dolomite.

Further increase in aluminium rich sedimentation then occurred, the dolomite grading into quartz-chlorite schists (Unit G). After this was a slowing of deposition, a period of terrigenous deposition and the possible development of organic algal muds which may have been the source of the distinct graphitic layer above the quartz chlorite and quartz mica schists. The distinct lower boundary to the graphite layer (Unit F) may be the result of a cessation in volcanic activity which may have been responsible for the increased aluminium content of the schists above the dolomites. Increasing terrigenous deposition after this stage with concurrent contribution of organic matter resulted in the garnet rich quartz-chlorite-mica schists above, which appear to be derived from aluminous muds and silts. Within this unit are layers of amphibolite which represent either metamorphosed extrusive basalts or shallow intrusives emplaced along bedding during or shortly after deposition of these sediments.

The upper unit encountered at the site is a series of quartz-chlorite-mica and quartz-chlorite-mica-feldspar schists indicative of a further increase of terrigenous sands and silts of higher feldspathic content.

The Kombolgie Sandstone

The Kombolgie Sandstone is the youngest unit encountered at Koongarra. During the period of faulting that occurred around 1600 Ma, the younger Kombolgie Formation sediments were thrust up by a reverse fault against the older, previously deformed Cahill Formation schists.

The Kombolgie Formation is made up of three main members; a lower conglomeratic unit that outcrops 3km southwest of Koongarra at Nourlangie Rock, a middle member which is a thin layer of silts and an upper layer which is a medium to coarse grained well sorted quartz sandstone most probably deposited in a fluvial or shallow tidal environment which shows prominent ripple mark and cross-bedding structures. It is this upper unit that makes up the escarpment west of the orebodies at Koongarra.

Examination of borehole DDH 53 indicated that the lower conglomeratic Kombolgie unit appears to have been mistaken for fault breccia in at least this borehole. Drillcore described in the borehole logs as "quartz-augen mylonite " examined by this author was clearly rounded quartz pebble conglomerate, which poses a problem of interpretation for the other borehole logs. If this particular interpretation of the Kombolgie conglomerate as breccia or mylonite is consistent

throughout the other borehole logs, then a shallower depth to the unconformity should be considered.

Geological Map of the Site

The structure and lithologies of the site have been examined by Pederson (1978) and Snelling (1990) and various geological plans of the Koongarra site have been presented. The present study included a thorough re-examination of the borehole logs with reference to previous studies, an examination of borehole DDH 53, BTV studies and recent reviews of the site structure (Emerson *et al* 1992). Natural outcrops of the lithologies other than the Kombolgie Sandstones are very scarce in the area of the Koongarra site and are limited to highly weathered metamorphics on the banks of the Koongarra Creek, in eroding gutters and at one location on the track in to the site to the northeast of the No. 1 orebody.

A revised plan of the geology of the site considering the new conclusions is presented in Figures 3.7 and 3.8. It can be clearly seen that the geological map (Figure 3.8) presented by this author is markedly different to that interpreted by Pederson (1978) from the initial studies of the site geology, and also from the local geology map of the site presented in ARAP Final Report Volume 2: Geologic Setting, which presents Pederson's original map. These earlier studies were based on structural information in the area of the orebodies and did not have the advantage of *in situ* observations provided by the BTV.

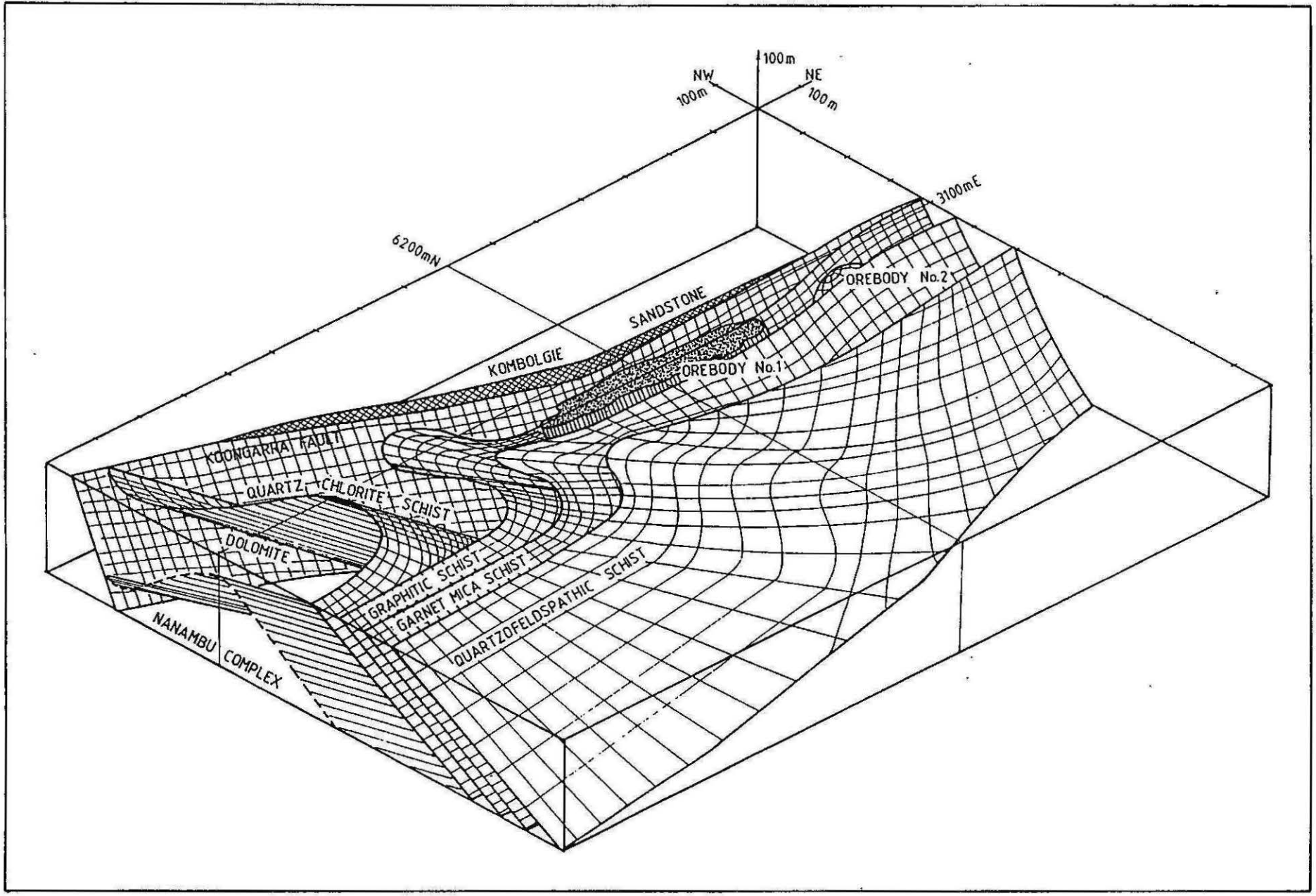

Figure 3.7: Three-dimensional plan of the site structure and lithology incorporating borehole geology and BTV structural studies (From Emerson *et al* 1992).

The structural interpretation of the site by this study and Emerson *et al* (1992) detects a broad F3 fold in the sequence at Koongarra. The presence of this structure clarified the distribution of lithologies at the site and explained the apparently ambiguous positions of the dolomites and graphitic units southwest of the orebodies previously thought to be along strike of the lithologies in the vicinity of the orebodies. The implications of the BTV studies were combined with studies of the geology of the site and led to a three dimensional depiction of the site, presented in Figure 3.7. Study of the borehole logs and the construction of geological cross-sections, especially to the southwest of the main orebodies confirms both the presence of dolomites and quartz-chlorite schists in the south of the site, and the large fold structure.

Dolomitic units at Koongarra

It could be postulated that the fractured, karstified dolomites found to the south of the main orebody may be more permeable than the surrounding units due to increased fracture flow and may have acted, or be acting as an hydrologic "drain" for the site, affecting the direction of groundwater flow in the weathered and transition zones in the vicinity of the orebodies. The borehole logs show that dolomites south of the orebodies exhibit significant karst features such as the development of caves and significant brittle fracturing which may be considered significant in analysis of the hydrology of the site.

Ferguson, Ewers and Donnelley (1980) proposed that karstification of limestones and formation of dolines occurred in the region following the 1870 to 1800 Ma metamorphic period and suggested that they were responsible for the concentration of uranium at the site.

It is plausible that the fractured dolomite may be more permeable in the transition/lower weathered zone than the other Cahill Formation lithologies. Petrophysical studies have shown that the highest permeabilities in the other units are found in this lower weathered zone of rock. The presence and location of the dolomitic units in the weathered zone should therefore be considered as they may be directly relevant to the overall groundwater movement at the site.

This study found that only 24 of the 301 boreholes at the site intersect the dolomitic units. DDH53 did not intersect the dolomitic units, nor did any of the boreholes examined with the BTV, so direct observations on the character of the dolomites were not possible in this study. The carbonate units are found in some drillholes to the north of the orebodies, but are well below the weathered zone and would not be expected to play a major role in determining groundwater flow direction. To the south of the orebodies, the dolomites are shallower and are recorded at depths shallow enough to be considered in the weathered zone (PH105 and PH103) and weather readily to clays. Partially silicified dolomite can be found outcropping 650m south of the southwest tip of the No.1 orebody in Koongarra Creek. Discharge of the groundwater, either into the local groundwater scheme or into the

Koongarra Creek, via the fractured dolomites could conceivably occur to the southwest of the site.

The influence of the increased permeabilities along fractures resulting from the effects of the F3 folding of the schistose rocks and the bias of increased permeability (and thus groundwater flow) along schistosity indicated by the petrophysical data is probably sufficient to preferentially channel water from a southeasterly direction to a south to south-southwesterly direction without any possible effects from a fractured dolomite in the south.

It is interesting to note that as early as the ARAP First Annual Report, January 1990, Payne suggested the delineation of seven distinct zones of groundwater at the Koongarra site (See Figure 4.5) and indicated two zones of most similar character. Zone V shows a close similarity in groundwater chemistry character to Zone II. Zone V is to the to the south and south-southeast of the southern end of the No.1 orebody. At this early stage of the ARAP, it was still postulated that the main flow of groundwater at the site was in a southeasterly direction as inferred (indirectly) by depictions of the "dispersion fan" on early maps representing the site.

Considering the structure and location of lithologies at the site, this author concludes that the dolomites are too distant from the main area of investigation to have any major effects on the direction of groundwater flow in the area of the dispersion fan.

Amphibolites at Koongarra

The amphibolitic units at Koongarra warrant further investigation. Previous mine geology plans of the Koongarra site (Pederson 1978 and Snelling 1990) have depicted numerous amphibolite bands along strike of the other lithologies as discrete entities. During the course of the ARAP, the Northern Territory Power and Water Authority declared that amphibolites and their weathered products could play a major role in determining the direction and relative mobility of groundwaters at the site, following observations on the character of amphibolitic and doleritic units in the region.

In an effort to test the validity of these claims and the possible significant influence they may have on groundwater flow direction, a study of the amphibolites was carried out by this author with the gratefully acknowledged assistance of Dr. K.J. Mills. This investigation was both for the purposes of the ARAP and this thesis and was published as a complete paper in the ARAP Progress Report 1 March 1991 - 31 August 1991 and as well in the ARAP Final Report Volume 4.

Amphibolitic units in the Jabiru area have been described by Ferguson and Needham (1978) and were considered to be the metamorphosed equivalents of the Zamu Dolerite. The Zamu Dolerite is a suite of lower Proterozoic, preorogenic continental tholeiitic intrusives. These dolerites were injected into the rocks of the local region at various stratigraphic levels as conformable sills between 1 and 300m thick and then folded and metamorphosed during the regional

metamorphism between 1870 and 1800 Ma. This period of metamorphosis resulted in the alteration of many of the dolerites in the region to amphibolites. The degree of metamorphosis increases from the southwest to the northeast, from areas where the dolerites remain unaltered (Zamu Creek where the type specimen of Zamu Dolerite can be found), to the Jabiru area where medium grade amphibolitic alteration can be seen, to high amphibolitic facies in the northeast near Oenpelli.

The amphibolitic units at the Koongarra site can be compared directly with the lithologies described by Ferguson and Needham (1978). The amphibolites in the region were shown to have a similar initial composition to the least altered dolerites of the region, that of a hypersthene-normative continental tholeiitic basalt. Retrogressive, low temperature alteration to quartz-chlorite rocks with an accompanying loss of calcium, sodium, potassium, barium and strontium in areas near to uranium mineralisation was also reported by Ferguson and Needham, a feature observed at Koongarra.

The amphibolitic units at the site were examined with a view to making comparisons with the lithologies described by Ferguson and Needham (1978). Five core specimens from DDH98 were examined petrologically and petrophysically, particularly with reference to density and magnetic susceptibility, which are useful indicators of their parentage and composition. The results of these examinations are presented in Table 3.2.

The specimens show compositional and textural similarities. The degree of alteration varies between specimens, but all specimens indicate a medium grained (0.2 - 2.0mm) middle amphibolite facies ancestry. Only the specimens from 108.2m and 137.8m still possess textural and mineralogical features of middle amphibolite facies. Deep green strongly pleochroic hornblende, plagioclase, smaller amounts of quartz and pleochroic brown to pale yellow biotite and minor proportions of ilmenite and apatite are found. The ilmenite is found as string-like aggregates up to 4mm in length and concurs with descriptions of ilmenite in amphibolites in the region given by Ferguson and Needham (1978). In sections cut parallel to these strings, they are observed as oval shaped rings which may be a textural artefact of the previous igneous parent rock. The degree of alteration of these more amphibolitic rocks preserves little of the original texture and leaves little evidence of the nature of the original lithology. Garnet was observed in the specimen from 137.8m. Ferguson and Needham only mentioned observing garnets in amphibolites near Oenpelli.

The three other specimens observed show some textural features of the higher grade metamorphism but they have been strongly altered compositionally by the extensive and pervasive low grade greenschist facies retrogressive alteration that affected the site. Only relic xenoblastic metamorphic quartz from the earlier metamorphosis remains. The hornblende found in the less altered specimens is pseudomorphed by pale green chlorite and the biotite pseudomorphed by pleochroic bright green to pale yellow chlorite. Plagioclase is clouded or totally replaced by fine grained sericite. Some of the hornblende in the specimen from

120.4m is preserved in an advanced stage of conversion to chlorite. Such features suggest that these lithologies were initially amphibolites.

Inclined Depth (m)	Description	Dry Bulk Density (g/cc)	Magnetic Volume Susceptibility cgsx10^{-6} (≈SIx10^{-5})
108.2	Foliated amphibolite (hornblende-plagioclase-quartz rock)	3.06 3.06	112 121
115.5	Altered amphibolite (chlorite-plagioclase-quartz rock)	2.81 2.81	59 67
120.4	Altered amphibolite (chlorite-sericite-quartz rock)	2.77 2.79	68 64
137.8	Foliated amphibolite (hornblende-garnet-plagioclase rock)	2.92 2.92	96 387
143.6	Altered amphibolite (chlorite-sericite-quartz rock)	2.78 2.73	69 69

Table 3.2 Petrology and petrophysics of DDH98 samples.

The alteration of the lithologies to low grade greenschist facies is crucial to the definition of the lithologies at the site and it is seen that lithologies named amphibolites are likely in places to be quartz-chlorite schists. The amphibolites and quartz-chlorite schists are very closely related and the distribution of lesser or greater alteration from amphibolite to quartz-chlorite schist is erratic. True amphibolitic rocks at the site are only remnant lenses that were not affected as strongly by the retrogressive low grade metamorphic events around 1800Ma.

In consideration that the amphibolites at the site are regional equivalents of those lithologies described by Ferguson and Needham (1978) and further studied by the Northern Territory Power and Water Authority (Peter Jolly in particular), the distribution of amphibolites across the site was closely scrutinised. Earlier site plans by Pederson (1978) and Snelling (1990) show amphibolites occurring in thick, widespread bands across the site. Considering the variance between the site plans of Emerson *et al* (1990)(and this thesis) and these earlier representations, a thorough investigation of the presence and location of amphibolites at the site was carried out.

The entire suite of borehole logs from Noranda Pty Ltd was examined and compared with available core of known composition and the complete core of DDH53. Core described in the logs closely concurred with inspections by this author. Of the 120 inclined diamond drill holes and 181 vertical percussion holes, only 15 holes showed amphibolitic units near the No.1 orebody. Given the postulated site structure, the conjectural up-dip locations of these amphibolites in the transitional and weathered zones were plotted on a site plan and are presented in Figure 3.9. Continuity of lithologies up-dip from known drillhole occurrences is dubious and actual occurrences in the weathered zone may be greater or lesser given the nature of the low grade alteration at the site.

It can be seen from Figure 3.9 that there are sporadic occurrences of amphibolite to the southeast and southwest of the No.1 orebody and massive occurrences to the east of the northeastern end of the No.1 orebody. Previous presentations of

site geology and the dispersion fan showed a coincidental correlation of the location of the amphibolites and the furthest extent of the dispersion fan (which may have led to the assumption that the amphibolites were acting as a hydrologic barrier). It can be seen from Figure 3.9 that the amphibolites at the site are far less extensive than has been presented previously and that the actual projected intersections of the transition zone and the weathered zone and amphibolitic units in DDH50 and DDH98 actually lie within the dispersion fan. Depictions of the dispersion fan as a simple two-dimensional line on a site plan must be treated with extreme caution as the reality is that the dispersion fan is in fact highly variable laterally and vertically as well as in concentration of uranium.

Given the close association of amphibolitic units and quartz-chlorite schists and the lesser occurrences of amphibolites in the area of the No.1 orebody and its dispersion fan than previously thought, this author considers that the amphibolitic units and their weathered products at the site do not constitute a significant hydrologic barrier and therefore do not have any significant effects on southerly trending groundwater flow directions at the site, particularly near the No.1 orebody.

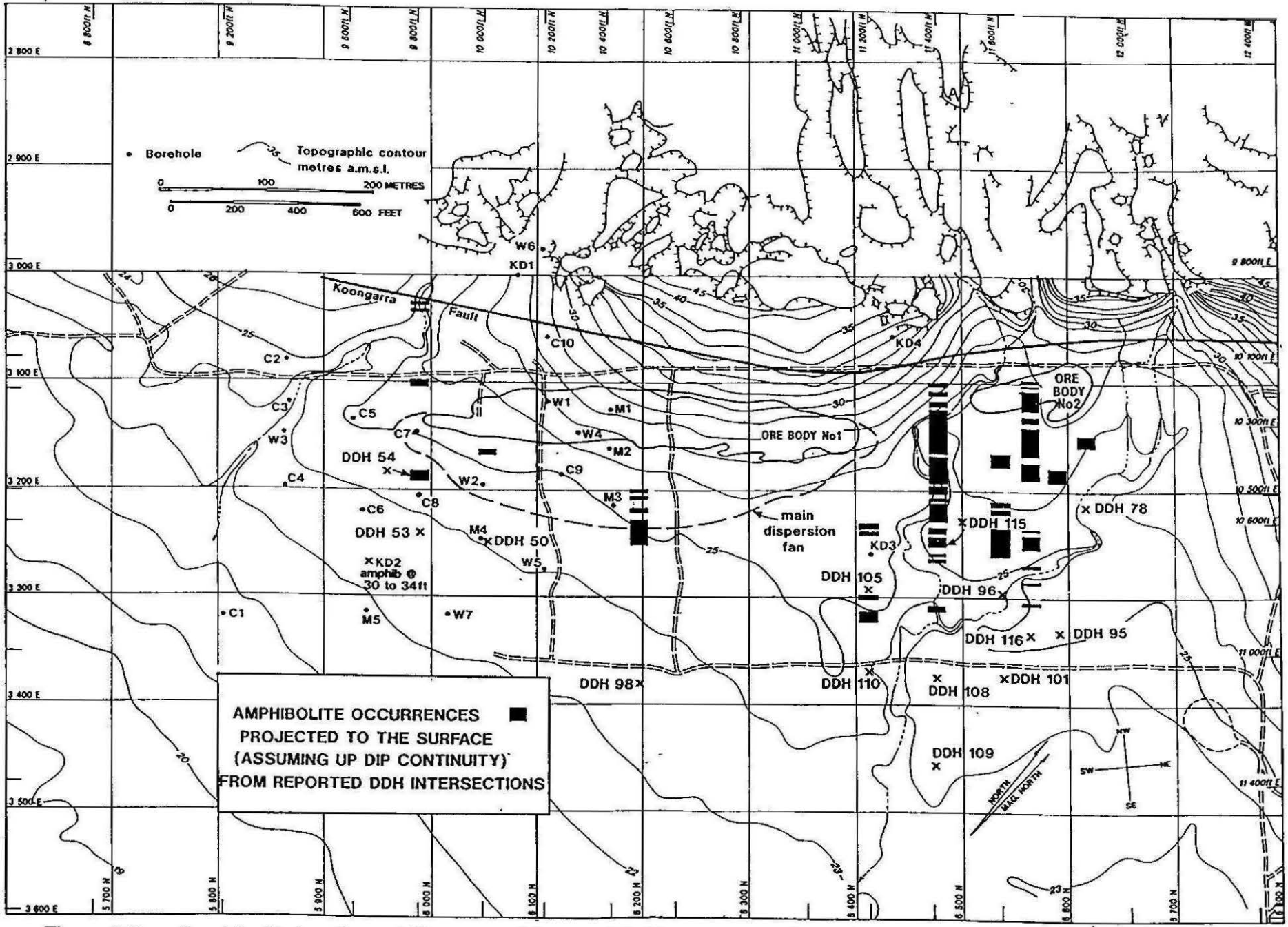

Figure 3.9: Amphibolite locations at Koongarra. The amphibolites were considered to act as possible barriers to groundwater at Koongarra.

DISCUSSION OF SITE GEOLOGY AND STRUCTURE

The geology of the site is dominated by a sequence of schists of generally pelitic composition which has been folded, metamorphosed to amphibolite grade and largely retrogressed to chlorite. These schists have then been thrust in a reverse fault against the younger Kombolgie Formation sediments.

New information and further analysis from extensive study of borehole logs by this author, (including compilation of an accurate borehole map of the site) and BTV studies unavailable to previous workers has redefined the site geology and structure. A broad fold to the south of the main orebodies in the Cahill Formation schists, is interpreted as an F3 event and a fault or discontinuity of some sort occurs to the southeast of the orebodies in vicinity of and paralleling the Koongarra Creek. The two economic orebodies lie within quartz-chlorite schists and graphitic quartz-mica garnet schists on the northern limb of this fold. The roles of the amphibolitic and dolomitic units at the site have been examined with reference to groundwater flow directions (restricting or assisting flow respectively) and it is considered that these units have relatively little influence on the preferred direction of groundwater movement in the direct vicinity of the No.1 orebody although their effects are not entirely discounted.

The constraints on the movement of groundwater in the weathered and lower weathered zones of rock suggest that there is a structural and lithological bias in the vicinity of the No.1 orebody for groundwater to flow in a south to south-

southwesterly direction although gravity alone would dictate flow in a southeasterly direction. The primary motion of groundwater at the site appears to be dominated by flow along fractures in the lower weathered zone of rock and by a matrix flow through the weathered zone.

Comparisons between RQD fracture analysis and BTV fracture density studies have proved to be valuable in checking both techniques. Both techniques reasonably agreed to the relative strength and degree of fracturing of the various lithologies. The weathering and direction of groundwater flow have resulted in the erratic dispersion fan of economic grade which is present in the weathered and transition zone of rock.

The proposed structure and lithological sequence herein can be viewed with considerable confidence and is invaluable in any studies of the site which consider the groundwater movement or chemistry and the distribution of radionuclides through the various weathered lithologies.

The depositional environment of the lithologies has been examined and is considered to be a shallow marine environment with increasing terrigenous input. The schists were metamorphosed to amphibolite facies and later, with the introduction of hydrothermal fluids retrogressed almost completely to lower temperature greenschist facies. It would appear that this extensive alteration is not evident in the Kombolgie Formation.

CHAPTER FOUR :

WEATHERING AT KOONGARRA

The processes and events pertaining to the development of the regional and local environment from the Proterozoic to the present are directly relevant to the formation of the weathering profile and the radionuclide dispersion fan at Koongarra, the main subject of investigation of the ARAP. These events include the geomorphological development of the region around Koongarra, the opening of the Koongarra Valley, the consequent and subsequent removal by erosion of the Cahill Formation above the orebodies, and the time of the initial exposure of the No.1 orebody to oxidising conditions.

The climatic and weathering conditions of the region from the time of orebody exposure to the present, which have resulted in the more recent weathering of the country rock around the orebody, must be considered. The effects of these conditions on the development of the various weathering horizons within the regolith and the radionuclide dispersion fan then need to be assessed.

The development of the regolith at Koongarra is considered with regard to the recently proposed models of regolith development of Ollier (1994) and Butt and Anand (1994), and regolith-facies landform models proposed by Ollier (1994). The roles of the retreating escarpment and the "lateritic" horizons at Koongarra and their proposed effect on the development of the dispersion fan and the downward

weathering of the Cahill Formation schists during the course of the ARAP (Snelling (1990) and Prowse (1990)) are considered.

Since the weathered zone is the dominant area of groundwater movement and uranium migration away from the discrete zone of the orebody, a physical and mineralogical examination of the regolith at Koongarra was undertaken as part of this thesis so that events pertaining to the uranium mobilisation could be understood in the context of the framework in which they developed.

Geomorphological Events

The geomorphological development of the Koongarra Valley can be viewed as a two stage process. The first, the weathering down of the horst block of upthrust sandstone and metamorphics, resulted in the Koongarra Valley. This process was probably dominated by denudation along the well established fault and joint patterns (for example the Koongarra Fault and the Sawcut Fault) in the central part of the horst beginning about 1500 Ma. Once the Kombolgie Formation overlying the Cahill Formation had been removed, the second stage in the development of the Koongarra Valley occurred, the formation of an escarpment similar to that presently existing, and the "opening" of the Koongarra Valley (from about the Late Miocene) through lowering of the more easily weathered Cahill Formation.

It is evident that the escarpment at Koongarra has formed through exhumation of the fault zone breccia (Wyroll 1992). Suggestions have been made during the ARAP that the Kombolgie Sandstone escarpment may have acted as a protective cover over the orebodies, gradually retreating into the Mt Brockman Massif exposing the schists and the No.1 orebody to weathering. Retreat of the escarpment cannot realistically be said to have any direct bearing on development of the secondary dispersion fan, considering the more likely development of the Koongarra Valley through fault exhumation which is predominantly vertical rather than horizontal. The escarpment at Koongarra is not structurally like the other Arnhem Land escarpments in which sandstone unconformably overlies older schists, and cannot be viewed as having the same geomorphological development.

The rates of weathering of the various formations at Koongarra would only allow exhumation as a possible escarpment development process given the geologic and structural conditions. Additionally, the deeper weathering evident in the zone of fault breccia compared to either the Kombolgie Sandstone or the Cahill Formation schists makes the exhumation explanation of valley development more feasible.

The outwash of quartz sands from the Kombolgie Sandstone escarpment would have formed an apron over the Cahill Formation Schists during this period of valley opening and Cahill Formation weathering and can still be seen today. This fan may lower rates of weathering currently and may have inhibited the onset of oxidising conditions to the No.1 orebody. However it must be noted that the depth and extent of the fan is variable at present and no doubt varied laterally and vertically

throughout the development of the dispersion fan. With this in mind it is very difficult to place quantitative estimates on the degree of inhibition of weathering it may have caused. It must be realised also that sand - saprolite boundaries in weathering profiles result in iron enrichment and ferricrete development, which may influence later weathering rates. This author considers that, for instance the simplistic view that a single layer within the regolithic profile inhibits downward weathering and denudation and thus may cause slower development of the dispersion fan should be discarded in favour of an holistic view that takes into account the numerous processes involved in the development of the regolith and their effects on one another. Wyroll (1992) suggests it is not clear how laterite origin and development relates to general erosional and geomorphological controls.

Wyroll (1992) suggested that escarpment retreat at Koongarra was likely to be site specific and quite low, citing a possible maximum of 2.2mm/Ka, based on 10Be ages obtained from joint planes at the escarpment behind the orebodies. Anything in excess of this is considered unlikely simply considering the degree of preservation of the aboriginal rock art on the escarpment behind the site.

Needham (1988) proposed that deep weathering marked by a palaeosaprolitic profile developed in the Cahill Formation during the Proterozoic, was overlain by the Kombolgie Formation. This previously weathered surface would presumably weather more readily when exposed after removal of the Kombolgie Formation and have implications on the rate of surface denudation of the Cahill Formation at Koongarra. Wyroll (1992) investigated the unconformity between the Cahill and

Kombolgie Formation exposed 4km north of Koongarra and found no indication of a weathered profile in the schists at that site. Nor did the Nanambu Complex rocks at Granite Hill, have the characteristics of intense chemical weathering that Needham proposed.

It has been suggested that a significant regional lateritic profile developed at Koongarra (Williams (1969), Needham (1982), Snelling (1990), Prowse (1990)) which may have acted to "seal" the Koolpinyah surface and inhibit the onset of recent oxidising conditions. Examination of these deposits (Wyroll 1992) has revealed that the concretions found in the Koongarra Valley represent only well developed ferruginous duricrusts of recent origin, possibly even as recent as the Quaternary and concurrent with present day weathering events, rather than as a laterite crust associated with earlier deep chemical weathering. The development of the ferricretes and their part in regolith development are discussed in further detail later in this chapter. This study concludes that there is insufficient evidence to support claims of a palaeosaprolitic profile or of a well developed laterite crust at Koongarra.

Rates of denudation of the Cahill and Kombolgie Formations have been discussed in detail by Wyroll (1992) as part of the ARAP and will not be further analysed in this thesis. Contemporary denudation rates estimated from rates of stream solute and suspended load transport in the region are approx $30m^3/km^2/yr$ or 30m/Ma, although these represent total catchment rates. Wyroll (1992) suggested that lower rates than this are probable for the Koongarra site, suggesting that a rate of

between 5m/Ma and 30m/Ma is a plausible range for the denudation of the Cahill Formation in the Koongarra region. Regional denudation rates generally concur with these values, but these need to be corrected for climatic variations of the Late Pliocene - Quaternary. Rates of denudation are likely to be highly site specific due to the largely unknown palaeoclimatic variations and their lengths and effects, although some guidance may be given by the Late Quaternary glacial and interglacial periods.

In the area surrounding Koongarra, it appears that the Koolpinyah surface must have been lowered by at least 100m since the Kombolgie Formation overlying the schists had been removed, given the topographic position of the unconformity north of Koongarra. This would place the time of initiation of weathering of the Cahill at the site at about 3 - 18 Ma, the Pliocene to Early Miocene. From this we can deduce that even deep weathering from this period would not be seen in the present weathering profile since the current weathering profile is far below the depth to where a weathered profile developed during the Pliocene would have extended. Following the removal of sufficient overlying rock to place the No.1 orebody at less than 30m depth, by about the Late Miocene, the formation of the dispersion fan would have begun.

Wyroll (1992) tentatively placed the onset of the development of the dispersion fan, given the rate of denudation and the time at which the opening of the Koongarra Valley began, at between 1 and 6 Ma. Considering the regional rates of denudation and the proposed amounts of Cahill Formation schists removed from over the No.1

orebody, this would seem a reasonable assumption. Further to this, Wyroll (1992) suggests that the dispersion fan could only have formed within the last 1 - 2 Ma. This calculation probably includes the time for the weathered front to reach the No.1 orebody added to the time involved in the creation of the dispersion fan at its current limits.

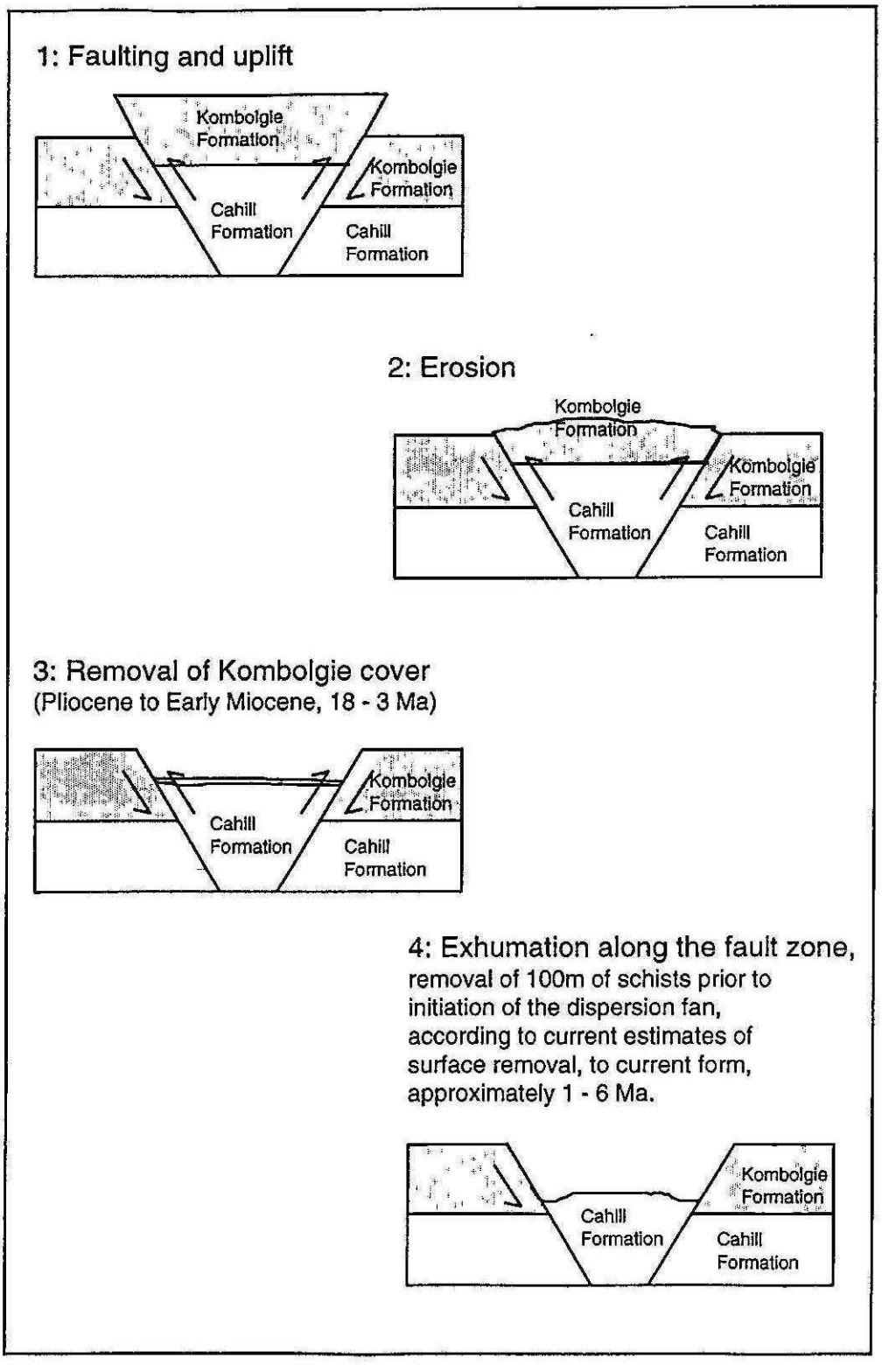

Figure 4.1: Erosional and scarp development in the Koongarra Valley.

Landform Facies Models

A comparison can be made between the landform and regolith at Koongarra and three Landform Facies Models presented by Ollier (1994, See Figure 4.2). Ollier cites three distinct environments for the formation of the regolith although undoubtedly there is a continuum of transitions between the three nominal landform facies models he presented.

The regolith profile at Koongarra most resembles something between the Erosional regime (Model 2) and the Residual regime (Model 1)(see also Figure 4.7), although the depth of lateritic residuum at Koongarra is much less than represented in Model 1 and is often entirely absent. The depth of weathering at Koongarra is greater than indicated in Model 2, and often has a sand layer of some depth at the surface. However, the profile at Koongarra does possess the simplicity of Ollier's Model 2. Massive iron segregations as indicated in Model 1 are not found at Koongarra although the initial stages of these are evident (mottles). In some ways, such as the content (including significant depths of gravels and sands), the profile at Koongarra is consistent with Model 3 - the Depositional regime, which, however, shows a depth to the base of sands and gravels far deeper than Koongarra and an overall depth far greater.

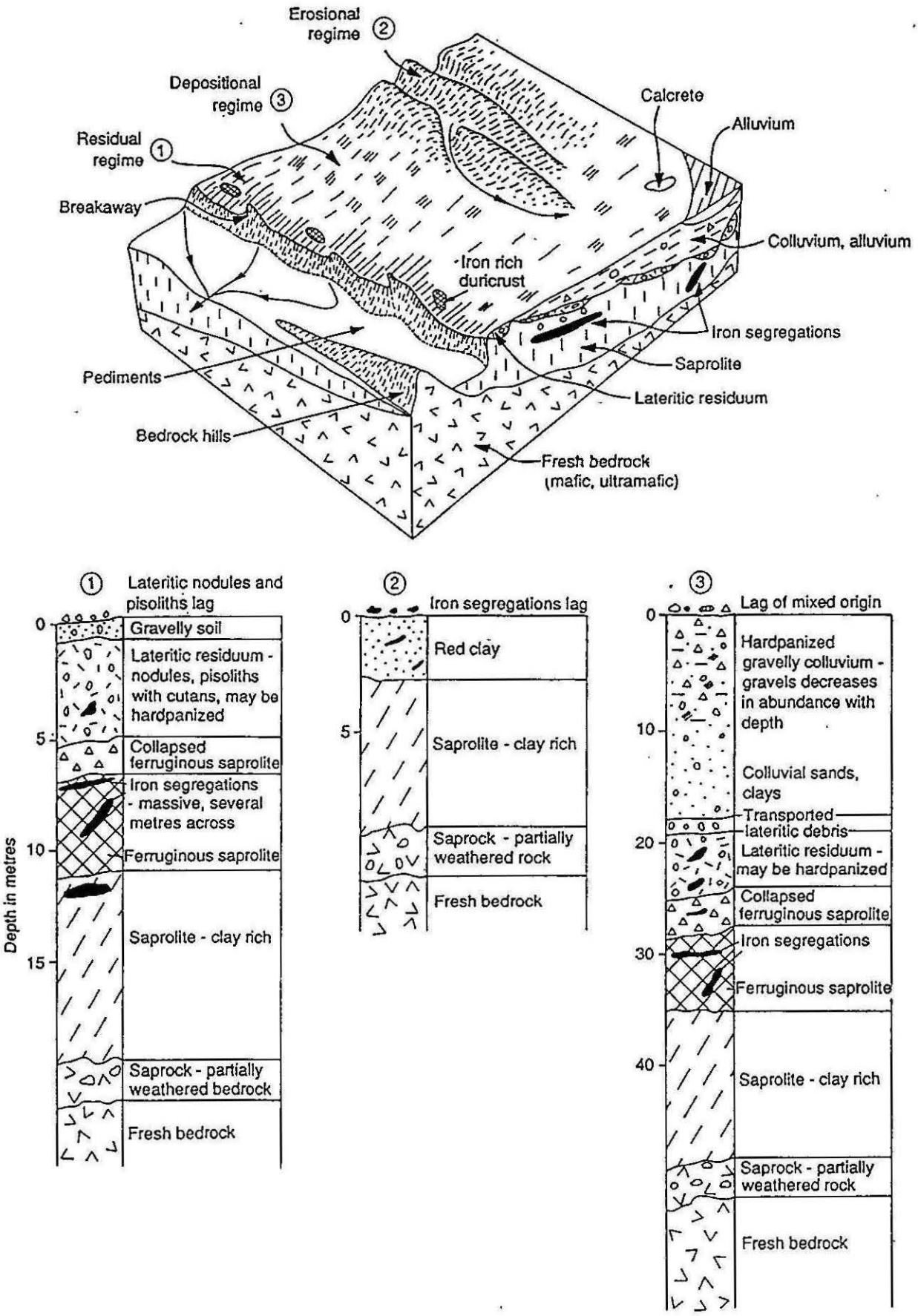

Figure 4.2: Generalized landform-facies models (from Ollier 1994).

There is little recorded evidence of a layer of transported lateritic debris at the erosional unconformity between saprolite and pedolith at Koongarra. This is no doubt due to the position of Koongarra immediately adjacent to the Kombolgie Sandstone escarpment, which shows no laterite profile development. However, gravels at Koongarra are sometimes hardpanized and include transported lateritic debris. Wyroll notes that the age of the ferricretes at Koongarra is diachronous, suggesting perhaps that the material found marking the base of the sand apron may have been transported and then further indurated by fluids entering from the saprolite. At places where the ferricretes are exposed, it could be presumed that they are the remnants of the same layer after the sand apron has been eroded away. There appears to be no clear distinction between the saprolite and the transported gravels above the saprolite in the core logs at Koongarra.

Given the location of Koongarra at a significant change of slope, but on a relatively flat-lying area, it is quite reasonable to consider it as somewhere between a depositional and a residual regime. The models presented by Ollier are located in a mafic terrain and Koongarra is a fractured aluminium-rich schistose terrain, quite different in its characteristics. Koongarra is also dominated by the sudden change in lithology across the Koongarra Fault which has bearing on the process of development of the regolith.

Clearly the regolith profile at Koongarra cannot be compared directly to Ollier's proposed Landform Facies Models. The geomorphological characteristics at

Koongarra are quite different to the area modelled by Ollier, although the principles are the same and still applicable.

Palaeoclimatic History of the Region

The most relevant period of weathering for the purposes of the ARAP is the time immediately preceding (and leading to) the initiation of the dispersion fan. Earlier climatic events that may have influenced the rate of weathering and thus the formation and timing of the dispersion fan also need to be considered. These include the onset of conditions similar to those of the present day and middle to late Tertiary deep weathering events that may have affected the region and have been considered responsible for lateritic crusts in the Koongarra area.

Studies in other areas in Northern Australia indicate that the Late Cretaceous to Tertiary was a period of an intense monsoonal climate, conducive to deep weathering and lateritisation. An example of this is the Weipa bauxite deposit. However, it may be over-extrapolation to extend the same conditions to the location of Koongarra at this time. This is the time at which Needham (1982) and Snelling (1990) proposed deep weathering of the Koolpinyah Surface resulting in the formation of thick laterites that inhibited the rates of denudation in the Late Cenozoic.

Wyroll (1992) suggested that the onset of conditions similar to those at present may have begun in the late Tertiary to early Pleistocene, which roughly concurs

with the time of exposure of the No.1 orebody to weathering conditions. Prior to this time, evidence suggests a wetter climate and more intense monsoonal conditions, through the late Cretaceous to Tertiary. At this time, there is evidence of wetter conditions than at present both in the Weipa bauxite beds and there are localities in the Kimberley in Western Australia, that suggest widespread Miocene rainforests.

Wyroll (1992) suggested that since the onset of near-present climatic conditions, in the middle Pleistocene through the Holocene, the pattern of conditions has been dominated by global glacial and interglacial periods, characterised by long (100 Ka) glacial conditions resulting in dry to arid conditions in northern Australia, separated by shorter (10 Ka) interglacial periods with similar levels of precipitation to that of today.

There is much postulation about palaeoclimates in northern Australia during the Cenozoic, however the timing and duration of the various events is clearly not well understood. A more complete discussion of these events can be found in Wyroll (1992). The quantitative effects of these events on rates of denudation in the region can only be surmised. Whether rates of denudation during dryer periods or wetter periods were higher or lower respectively and by how much could, with present knowledge, be only erudite guesswork. Even if quantitative estimates could be obtained, it is most likely that weathering rates would be very site specific.

Pain and Ollier (1994) suggest that deeper weathering processes (below a few tens of metres) are largely unaffected by climatic conditions due to the effects of

geothermal heat. Climate, it is suggested, is only relevant to the kind of weathering. At greater depths, they suggest that climate affects only the rate of weathering but this factor becomes unimportant with increasing depth due to the primary influence of geothermal heat. Nevertheless, the geomorphological development and palaeoclimatic effects on the environment are relevant and must be considered when examining the development of the regolith.

Table 4.1 Geological Time Scale Summarising Cenozoic events at Koongarra

Time M.Y.	ERA	PERIOD	EPOCH	EVENT
	Cenozoic	Quaternary	Holocene	
1.8			Pleistocene	Initiation of the dispersion fan
			Pliocene	Kombolgie Formation cover removed from Cahill schists
23.5		Tertiary	Miocene	Onset of near-present climatic conditions
38.5			Oligocene	
53.5			Eocene	
65			Palaeocene	

The Regolith at Koongarra

The weathered zone of rock at Koongarra has not been previously evaluated with regard to current regolith terminology and the only attempt to classify the weathered material into sub-categories to date can be found in Emerson *et al*

(1992)(to which this author contributed). Certainly at Koongarra, no definitive model of the regolith and its formation has been suggested or agreed upon in the ARAP. This study aims to address a regolith model and assess the roles of the various zones in the weathered material in the evolution of regolith. The regolith is a zone of complex, varied and numerous interactions and it is unwise to oversimplify the history of its formation.

Regolith studies by Ollier (1994), Anand *et al* (1994), Butt and Anand (1994), Bourman (1994) and Pain and Ollier (1994) elucidate a discussion on the process of regolith formation, its relevance in determining age relationships and the evolution of the regolith with regard to the surrounding environment. These studies are considered with regard to the regolith at Koongarra, the processes concerned, the mineralogical features elicited by the ARAP study and conclusions by this author.

If the most recent concepts in regolith formation are applied to the model at Koongarra, the development of the regolith at Koongarra can be better clarified and may shed light on recent discussions of the regolith in Northern Australia by other authors. The regolith material at Koongarra is considered in this thesis at hand specimen scale, petrophysically, through study of borehole logs and mineralogical examination.

Mineralogy of Koongarra

Murakami *et al* (1992) (ARAP Volume 9) and Edis *et al* (1992) (ARAP Volume 8) defined the chemistry and mineralogies at Koongarra and their weathered products. The mineralogies at Koongarra are presented in this chapter and are valuable in the discussion of the regolith.

The major minerals of the Cahill Formation schists at Koongarra are quartz, chlorite and muscovite with smaller amounts of graphite, sulfide, garnet, feldspar and remnant biotite (Edis *et al* 1992). The chlorite varies between magnesium-rich within the primary ore zone and iron-rich outside this zone. Clay minerals from the weathering of these schists are primarily kaolinite, vermiculite, illite (in the transition zone, or saprock) and smectite (outside the zone of hydrothermal alteration). Iron oxides present are goethite, haematite and ferrihydrite which occur as "fissure and remnant schistosity coatings, dispersed clay coatings, and nodules" (Edis *et al* (1992)). Manganese is represented as lithiophorite. The daughter products of biotite and chlorite weathering, are manganese-rich kaolinite within the alteration halo and iron-rich smectite outside it.

The process of weathering at Koongarra begins with a quartz-chlorite assemblage. The chlorite weathers first to vermiculite which then weathers to kaolinite. At each stage of this weathering process, iron is released and the assemblage of weathered materials comprises vermiculite, kaolinite, smectite, ferrihydrite, goethite and haematite in varying quantities according to both depth and degree of

weathering. The zone directly above the primary ore zone shows no clay minerals other than kaolinite (Edis *et al* 1992).

Edis *et al* (1992) suggests "Manganese, and to a lesser extent amorphous iron phases (for example ferrihydrite), appear to have been leached from the weathered primary ore zone, and deposited down-gradient". (Ferrihydrite being "amorphous" iron oxide and trivalent, as opposed to ferrous or bivalent iron oxide). This point is interesting in the discussion of the relative importance of lateral and vertical migration processes in the formation of regolith. Groundwater zones delineated by Payne (1991) (see Figure 4.10) also suggest lateral movements of material ("weathered products") in the weathered zone). The presence of iron in the fractures is closely tied to the presence of uranium.

Edis *et al* (1992) also reported that occasional bands of bleached clay (2% Fe) are juxtaposed with iron-rich crystalline phases (20% Fe) (presumably in the upper saprolite or the pedolith). This point is relevant in the discussion of the migration of Fe in the regolith detailed later in this chapter.

The process of incipient weathering includes the weathering of biotite which absorbs water as it alters to vermiculite and expands in the process. This author considers that this process is probably a likely cause of the later inhibition of groundwater movement through fractures in the weathered zone. Perhaps it is possible the clays are generally immobile and reflect the country rock but the

soluble iron phases are very mobile over time and migrate extensively laterally and vertically.

A Generalised Lateritic Weathering Profile

There appears to be some confusion in both the ARAP and in recent regolith debate regarding the meaning of laterite and its various incarnations within regolithic profiles (see discussion later this chapter). The representation, development and type of ferruginous material at Koongarra becomes clear through proper study of the regolith. Whether materials are *in-situ*, transported, recent or ancient, rapidly becomes apparent. Through this study, a model or conception of the regolith can be created. It is worth noting at this point that the term "laterite" is nebulous and that reference to laterite in this section is generally to hard, iron-rich crusts.

In an effort to translate the results of the Koongarra study into current regolith terminology, recent regolith discussions have been consulted. This author found that these discussions were in places contradictory and there appears to be no complete scheme through which to describe the regolith. An attempt was made by this author to construct a working scheme to apply at Koongarra, using common elements of the various schemes proposed by other authors, most notably Ollier, Pain, Butt and Anand.

A "typical" lateritic profile consists of parent rock underlying weathered regolithic stratigraphy (see Figure 4.3). The character of the weathered zone at Koongarra can be compared to such a profile. At the base of the regolith is a clearly distinguishable weathering front (immediately above unweathered rock). Above this front is weathered lithic material termed Saprolith. The saprolith is defined as all weathered material retaining lithic fabric and is generally divided into two zones, Saprock and Saprolite. Saprock is rock representative of the earliest stages of weathering. Trescases (1992) suggests saprock has an upper limit of 20% of weatherable minerals altered. Above this lies saprolite, which is rock material with greater than 20% of weatherable materials altered.

The upper weathered material is divided into a lower Pallid Zone, an upper Mottled Zone, a pedoplasmation or pedoturbation front, a ferruginous zone and a soil layer. Recent discussions of the regolith are in discordance with regard to terminology and division of this zone, particularly the position and significance of the pedoplasmation front and the extents of the saprolith and pedolith.

Butt and Anand (1994) describe saprolith as all weathered materials having a lithic fabric i.e. saprock and saprolite, separated from the pedolith by the pedoplasmation front. However, in the same paper they state that in the pedolith, the lithic fabric is only "largely" destroyed. Butt and Anand (1994) also state that the mottled zone is part of the pedolith, above the pedoplasmation front and presumably does not exhibit remnant lithic fabric. Lawrance (1994) also shows the mottled zone above a pedoturbation front, but below the erosional unconformity.

Ollier (1994) suggests the saprolite includes the mottled zone, implying that original rock fabric can be found in the mottled zone. However, he suggests that the pedoplasmation front is above the mottled zone, separating it from a ferricrete crust, and is often an unconformity.

The mottled zone describes material that is clayey or sandy, exhibits iron-enrichment in variably sized "mottles" and in which the original lithic fabric is mostly or completely destroyed by soil formation processes. Clay-rich and sand-rich zones are referred to as plasmic and arenose respectively. In discussing formation and types of laterites, Anand et al, (1994) refer to "ferruginous saprolite" and "lithic nodules" in ferruginous horizons. They obviously consider that the saprolite extends up to the base of the ferruginous/ferricrete zone and beyond the pedoplasmation front.

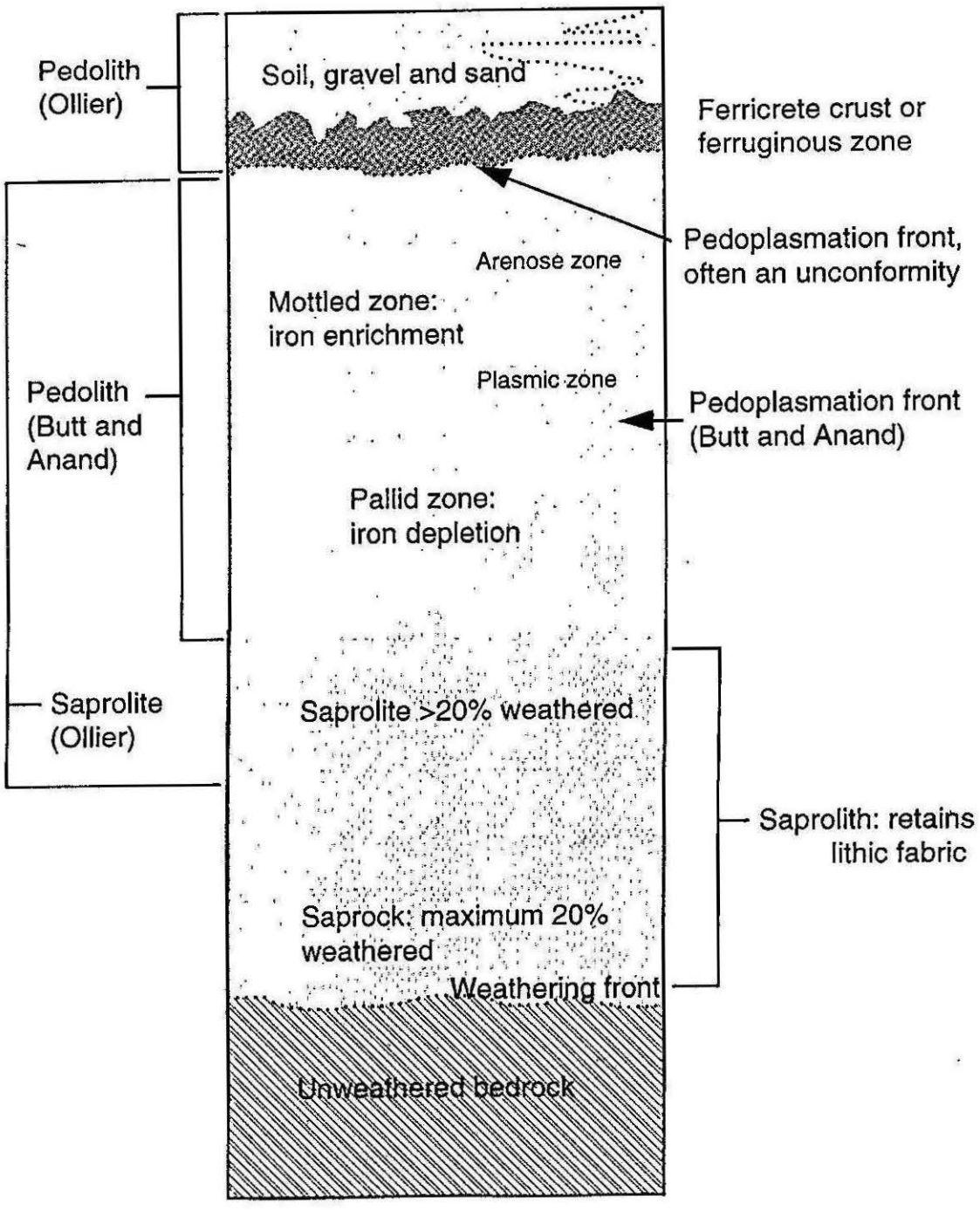

Figure 4.3: A generalised regolithic profile.

For the purposes of this study, the saprolite is considered to include the mottled zone. The boundary between saprolite and pedolith, where lithic fabric is completely destroyed is obviously subjective. In the case suggested by Ollier (1994), the definition of the pedoplasmation front is clearer as he suggests it is often an unconformity above the mottled zone. This author favours this description.

The upper section of the mottled zone exhibits iron-enrichment and according to Ollier (1994) shows vesicular, vermiform or tubular ferricrete characteristics. CSIRO workers (Butt and Anand, Anand *et al*) make no clear distinction in this zone between pisolitic or vermiform (worm-like) laterite although both sides appear to agree on the possible presence of a gravelly lateritic layer at the upper limit.

The uppermost zone, the pedolith, comprises all weathered and transported materials from above the top of the pedoplasmation front to the ground surface. Within the pedolith lies a laterite/ferricrete crust or ferruginous zone and a layer of transported and sometimes lateritised soils and gravels. The resorted earth layer may show pisolitic or nodular iron-oxide deposits.

The Lateritic Profile at Koongarra

Some studies of the regolith have been made previously at Koongarra. These have generally referred to the upper 25m of rock as "The Weathered Zone". McMahon, Burgess and Yeates (1981) briefly described the regolith. Summaries of these were presented by Wyroll (1992) and are shown in Figure 4.4. Emerson *et al* (1992)(and

this author therein) used a petrophysical and visual basis for the characterisation of the weathered zone and divided the weathered zone into three sub-zones; Lower weathered or Transitional (Zone B); relatively sandy highly weathered Cahill Formation (Zone A2); and relatively clayey highly weathered Cahill Formation (Zone A1). Sands and transported gravels above this were not examined petrophysically.

The weathered material at Koongarra exhibits a "classic" lateritic profile and can be readily related to current regolith terminology; the transitional zone analogous to saprock; Zone A2 to a pallid zone of iron depletion and; Zone A1, an upper zone of iron-enrichment, a mottled zone. Above this is a soil profile.

This regolith profile analogy can be compared to presentations by McMahon, Burgess and Yeates (1981) and Emerson *et al* (1992) (Figure 4.4). Studies of both diamond drill hole core and percussion hole samples by this author were used to elaborate on the distinctions drawn by previous authors.

The well documented "Transitional Zone" in the ARAP is considered to be saprock and at Koongarra is characterised by strong original schistose fabric with iron-oxide lined fractures. Above the transitional zone saprock lies Zone A2; sandy extremely weathered Cahill Formation (arenose but within the pallid zone) and; A1, clayey, extremely weathered Cahill Formation (plasmic mottled zone), analogous to saprolite. Emerson *et al* (1992) noted that there is a general increase in clay content toward the surface and attribute the sandiness of Zone A2 to

disaggregated quartz and mica from the schists prior to the weathering of chlorite to clay. The arenose material clearly exhibits lithic fabric.

The sandy part of the weathered zone can be considered as the saprolith, rock material with >20% weatherable minerals altered but retaining lithic fabric. The schistose fabric of the parent rocks at Koongarra is a good indicator of degrees of weathering. Lithic fabric is probably more evident and better preserved in the schists in hand specimen analysis at Koongarra than in laterite profiles described by Ollier where the parent rock is mafic.

The saprolith grades into pedolith through a mottled zone and at Koongarra this distinction is very rarely clear and this author suggests that the placement of the pedoplasmation front at the top of the pallid zone (rather than at the top of the mottled zone) is subjective and open to error.

A study of percussion holes, in particular W7, reveals that degrees of weathering vary down the lateritic profile and are not always directly associated with depth. For instance, at a depth of 11.3m in W7, rock that is clearly saprolith at 13.0m becomes extremely weathered to clays with no relict lithic fabric except for the presence of micas and could be classified as pedolith. Above this zone however, the degree of weathering is lower again, grading into saprolith. Above 7.1m, the degree of weathering becomes extreme, schistose fabric is obliterated and clays predominate.

The degree of weathering from place to place in the profile is determined primarily by access of oxidising groundwaters to weatherable minerals through fractures and fracture zones. Edis *et al* (1992) noted that enriched and depleted clays occurred within centimetres of one another in the upper weathered zone. Petrophysical studies of this zone indicate very low matrix permeabilities.

Laterites (as described by Ollier (1994)) develop in the mottled zone and duricrusts develop as part of the soil. A mottled zone at Koongarra can be distinguished and has been documented by McMahon, Burgess and Yeates (1981). The development of pisolitic rinds around mica grains was noted. The upper section of the mottled zone exhibits iron enrichment and according to Ollier (1994) is characterised by vesicular, vermiform or tubular ferricrete, which compares favourably with the weathered zone section presented by McMahon, Burgess and Yeates (1981), whereas the resorted earth usually has pisolitic or nodular iron oxide deposits.

The upper zone of the regolith at Koongarra is a soil profile of variable thickness consisting of gravelly sands, soils and "ferricrete" layers. Most of the cemented laterite that has been held responsible in some discussions for the inhibition of weathering of the Cahill Formation schists at Koongarra lies within the upper soil profile, above a weathering unconformity.

The iron indurated crusts found at Koongarra are developed as a function of the hydrologic contrast between the upper parts of the mottled zone and the more

permeable overlying sands and gravels. Within this soil zone, iron enriched fluids precipitate in the soils through chelating compounds and result in lateritised sediments. The mode of development of the crusts is through chelation of iron rich fluids in the upper two or three metres of resorted and transported earth and gravel. This process leads to the formation of nodular laterite, which may become cemented into hardened masses. These may overlie residual laterite profiles and have no genetic relationship with the underlying materials (Anand *et al* 1994). Given the position of the ferricretes either at the surface or at the base of the sand apron and within the soil layers, the ferricretes are obviously part of a presently developing profile and are quite distinct from those developed through Tertiary deep weathering events in other areas and are not conidered to be a significant factor in inhibiting deeper weathering processes in the saprock.

Wyroll (1992) alludes to the presence of iron concretions and crusts at Koongarra, developed in "young" alluvial deposits which he terms "iron indurated crust - ferricrete". This term is analogous with descriptions of lateritised sediments given by Anand *et al* (1994) which are defined as iron impregnated and indurated sediments.

Distinctions in recent literature between laterite, iron indurated duricrusts and ferricretes are vague. The meaning of the term laterite according to Ollier (1994) originally represented the mottled zone in saprolite. In general regolith discussions however, laterite has come to mean merely hard, iron-rich material in the mottled zone and the ferruginous zone above. The development of laterite is not

necessarily related to deep and extreme conditions of weathering responsible for the formation of great depths of ferruginous oxyhydroxides. This will be referred to later in this chapter.

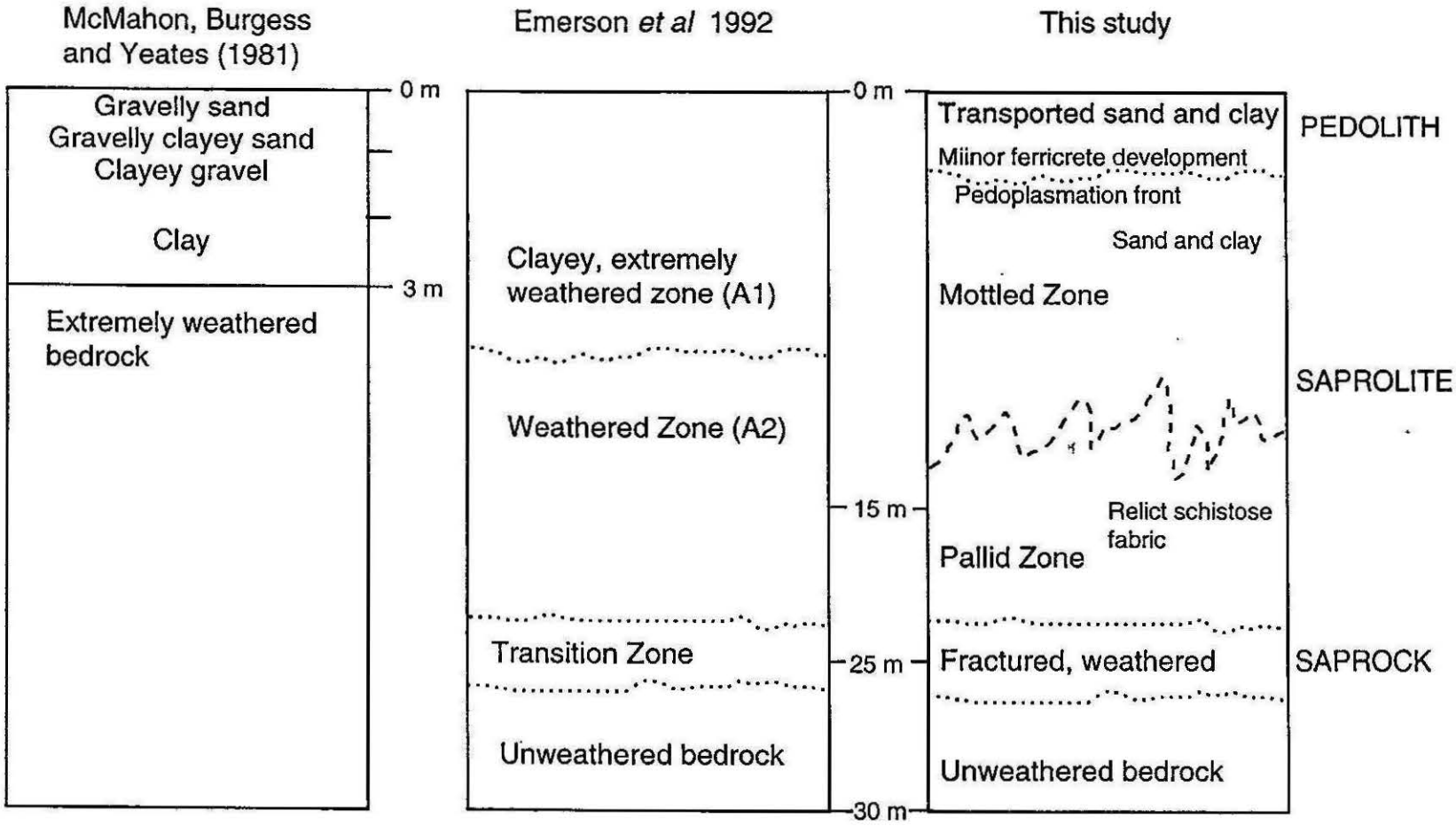

Figure 4.4: A comparison of regolith examinations at Koongarra

Significantly, the Koongarra regolith exhibits features very close in character to the "typical" laterite profile presented by Ollier (1994) and exhibits development of laterite both within the mottled zone and within transported sediments above an erosional unconformity at the top of the saprolite.

Evidence of the early stages of laterite development in the mottled zone are present at Koongarra. In the upper 3m of the regolith, but beneath the pedoplasmation front, the presence of laterite pisoliths, mottled clay and laterised mica fragments was noted by McMahon, Burgess and Yeates (1981). These are clearly within *in-situ* material. At other locations, particularly at the base of the sand apron or at surface, the "laterite" (iron concretion) development is associated with transported sediments. Ollier (1994) notes that the nature of lateritic material above the erosional unconformity is usually pisolitic or nodular. The crusts referred to by Wyroll as ferricrete and by Snelling (1990) as laterite are clearly nodular and developed by lateral iron enrichment. "Laterite" development at Koongarra occurs predominantly within transported sediments. Lateritic profile development within shallow *in-situ* material at Koongarra results only in mottles, not hard iron-rich crusts, a feature that may be related to the aluminium-rich composition of the original rock, contrasting with mafic, more iron-rich terrains.

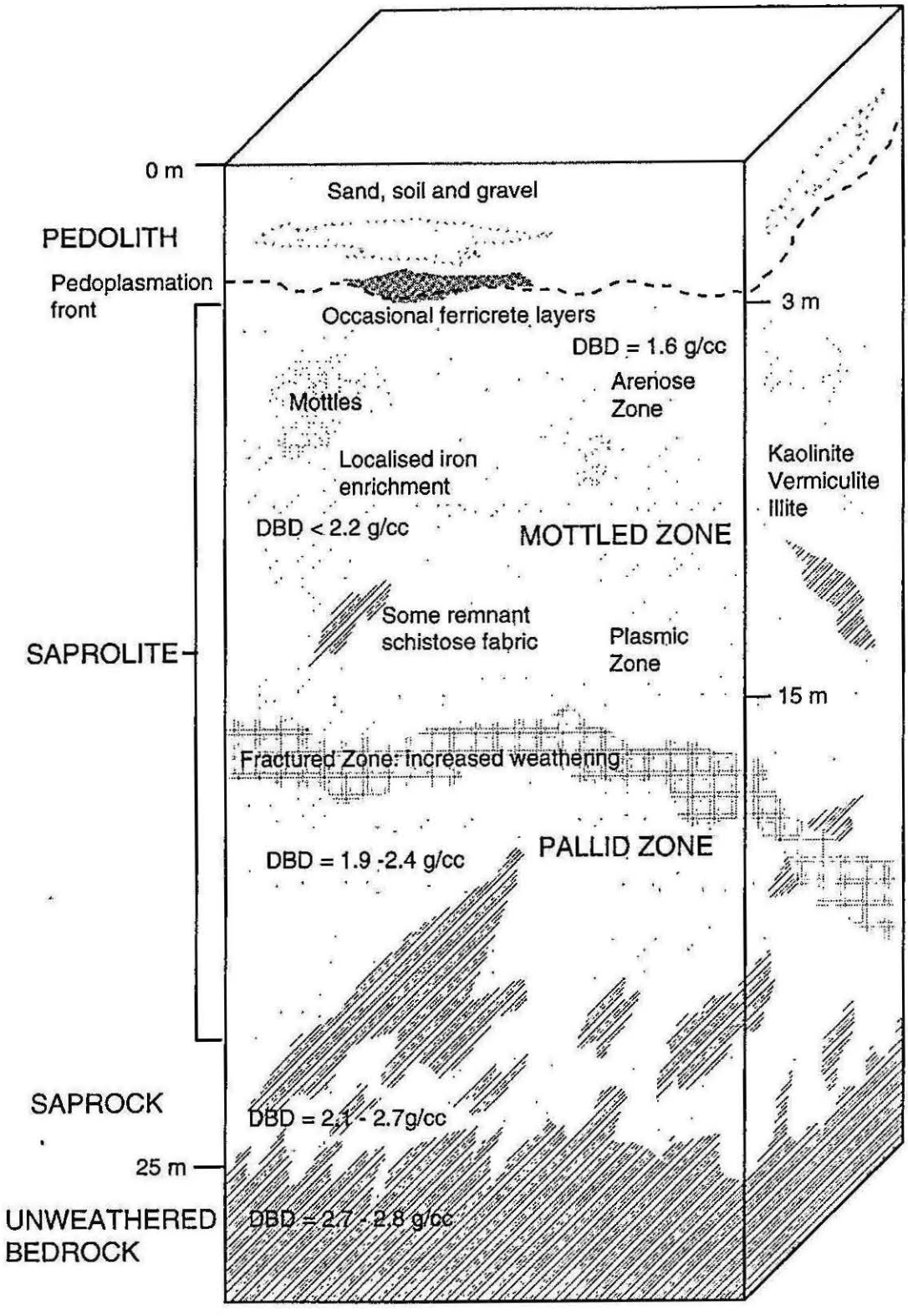

Figure 4.5: Diagrammatic representation of the regolith at Koongarra

Lateral (transported / absolute) vs Vertical (*in-situ* / relative) Laterite Formation (or: A discussion of recent literature on regolith character in Northern Australia)

References to recent discussions in Australian regolith studies (as mentioned at the beginning of this chapter) are directly relevant to the study of the regolith at Koongarra. There appears to be a polarisation in this debate of the importance of the predominant mode of iron-enrichment in the upper regolith, whether it occurs laterally, through transported groundwaters, or vertically, through translocation of iron from underlying parent rock.

On examination of the two sides of this debate, it appears that the main discordance is not which processes are most important, nor whether lateral or vertical processes predominate, but that adequate definitions of the various zones of the regolith have not been universally agreed upon. Butt and Anand (1994) affirm this point: "There is, unfortunately, no universally agreed system for the terminology of deeply weathered regoliths".

The two sides in this debate are defined by Ollier and Pain of Australian Geological Survey Organisation (AGSO) and Anand and Butt of The Commonwealth Scientific and Industrial Research Organisation (CSIRO). Pain and Ollier present a predominantly lateral interpretation of laterite formation whilst Butt and Anand favour a vertical mode. Comments from the contrasting sides are quoted to illustrate inconsistencies in the current debate.

Anand *et al* (1994) state that "*Geochemical signatures in lateritic materials generally reflect the underlying bedrock mineralisation. These findings contrast those of Ollier (1994) who implies that laterites generally form in sediments that unconformably overlie either bedrock or saprolite and do not show lithodependence*". In this statement they imply that laterites are lithodependent. They also suggest that a statement by Ollier, that laterites could be separated from saprolite by an unconformity (thus **independent** of lithology), is incorrect. What Ollier actually says in the article referred to, is that a break between saprolite and resorted material above is a **significant feature** in many laterite profiles. Nowhere in the paper referred to does Ollier say laterites are independent of underlying lithology. The suggestion that an erosional unconformity may often separate the saprolite from an overlying ferricrete crust does not directly imply that iron deposited there is lithodependent, nor that laterite beneath the pedoplasmation front is lithodependent.

The disparity between lateral and vertical formation of the deeper "lateritic" profile and the shallower, iron-enriched surficial materials is elaborated throughout the papers cited here. However, there is a lack of clarity in the terminology of these "iron-rich regolith materials" (ie those currently grouped together under the term laterite). It appears that regolith studies are still at a rudimentary stage and workers are still seeking adequate definitions and nomenclature.

Ollier (1994) suggests that the word "laterite" was originally used to describe the mottled zone, but goes on to state that "laterite" now generally means the hard,

nodular crust at the top of the profile. It appears that Ollier considers all iron-enriched materials within a lateritic profile to be "laterite". If he believes otherwise, it is certainly not stated.

Ollier (1994) alludes to Butt and Zeegers (1992) in suggesting that the present debate is polarised between vertical and lateral modes of laterite formation. Further, Pain and Ollier (1994) reiterate that "*Regolith profiles are often treated as if they are the result of vertical differentiation processes*", making clear their lateral interpretation, but do not announce to whom or what they are referring in such a statement. In studying the literature it appears that Pain and Ollier (1994) refer to Butt and Anand (1994) and Anand *et al* (1994).

Discussion

The problem of the current regolith debate lies in the definition of the term "laterite" -what is it and where does it occur? Ollier (1994) describes the original meaning of the word "laterite" but now regards it as "*the hard, iron-rich material at or near the top of a lateritic profile*".

Anand *et al* (1994) interpret laterite as an iron-rich material derived from a particular process of formation which they do not elaborate on, although they readily refer to "*lateritised material* " and "*laterite crusts*". They make a clear distinction between what they call non-lateritic iron segregations and gossans, laterite from the upper part of the mottled zone and lateritised sediments. Given

that the noun "laterite" is so poorly defined, conjugating a verb "to lateritise" to create "lateritised" is considered by this author to be over-reaching.

Table 4.2: Literal meanings and definitions of regolith terminology.

Name / Term	Derivations
Laterite	Red friable ferruginous surface clay much used for roadmaking in the tropics (f. L: *later* - brick + ite).(Note also - L: *lateralis, latus, -eris*: side)
Ferricrete	ferri: used to indicate presence of iron in ferric (trivalent) forms crete: presumably derivative of *concretus*, past participle of CON (*crescere, cret* - grow)
Indurate	Make, become hard; make callous or unfeeling. L: *durare* f *durus* - hard
Ferruginous	Of, containing iron-rust or iron as a chemical constituent; rust coloured, reddish brown. L: *ferrugo - ginis* rust. Ferrum (bivalent) + OUS.
Pedoplasmic	*pedo*: foot, *plasma*: gas
Duricrust	*durus*; hard +crust
Pedolith	*pedo*: foot. *lithic*; of rock
Plasmic	*plasma*; gas

The term "laterite" could also be seen to imply lateral processes, however the literal meaning is quite different (See Table 4.2). It is perhaps curious that the discussion of the importance of **lateral** processes involved in the formation of **laterite** should occur. The similarity of these two words may have added to the confusion (See Table 4.2). In any case, scientific method dictates that if a theory or an observation can be improved, it should be. To assimilate this approach into this study, our conclusion could be that the original definition of "laterite" was unclear or ambiguous.

This author suggests new terms such as "mottled saprolite" and "pallid saprolite" should be used to describe deeper material. Surficial iron concretions formed by lateral processes could then be more clearly termed "laterites". Perhaps because the term "laterite" and "lateritic profile" have become so ingrained in modern discussions, there is a general unwillingness to alter the definitive name and instead a myriad of materials derived from different processes are given the same name. The entire regolith is often referred to as a "laterite profile" even if iron concretions are absent.

The result of this poor nomenclature, and the mixing of descriptive and generic concepts, is utter confusion. For instance, Ollier (1994) states *"in general laterite discussions, the hard, iron-rich material at the top of a weathering profile is termed laterite"*. Why not refer to this material as "hard, iron-rich concretions in the mottled saprolite"? There could be no misunderstanding either the mode of formation nor the location of the material and its relationship to the surrounding weathered

material. (And this description could be used whether or not the material was used for road-building in the tropics!).

It is evident that the intended meaning of "laterite" varies greatly and it is this lack of adequate definition that is the sole cause of the current debate. A clear definition is necessary. The meaning at present is vague and thus the discussion regarding this subject is indeterminate, diffuse, subjective, emotive and thus lacking scientific procedure or depth. The various authors are not referring to the same material when they use the word "laterite", rather, a group of things. Instead of arguing the merits of lateral or vertical processes, a better approach would be to create a useful descriptive nomenclature and classify sub-groups within that structure according to mineralogy and mode of formation.

This author suggests removal or better definition of the term "laterite profile" and to refer to this iron-depletion / enrichment profile as "hydrated iron oxide-rich regolith". The iron-enriched material at the ground surface derived from lateral migration processes could be named according to its mode of formation. The underlying mottled zone and pallid zones now called "the laterite profile" could be classified within iron-enriched regolith profile nomenclature and the name "laterite" could be avoided.

A descriptive nomenclature (based on the type and mode of formation of material) could be created in contrast to the earlier efforts which attempted to pigeonhole all varieties of ferricrete crusts into one mode of formation or the other. Clear distinctions could then be drawn between iron enriched material below a

weathering unconformity and that above it, thus the predominant mode of formation for any given ferruginous material could be addressed.

It is obvious for instance that "lateritised sediments" are formed predominantly by lateral processes, since the shallow zone of soils, sands and gravels is a highly permeable, oxidising environment. There appears to be no argument in present discussions regarding the various incarnations of these iron-rich materials and how they are formed.

Beneath the weathering unconformity at Koongarra, parent rock is weathered to clays and in petrophysical studies, exhibits extremely low permeability. Lateral movement of iron-enriched groundwaters in this zone would generally be very low and it could be suggested that vertical processes would play a far more important role in this zone than in the unconsolidated material. Perhaps studies of the time necessary for the formation of iron nodules in the mottled zone could be compared with the rate of movement of groundwater and the diffusion and vertical translocation of ions through this zone.

The issue of lateral and vertical differentiation should be addressed with regard to the parent rocks concerned. In the current regolith debate, "lateral" and "vertical" processes are constantly referred to. However, it is never stated how far groundwater must travel before it can be considered to have moved "laterally". Groundwater compositions are affected by the material through which they travel.

Water can move quickly in unconsolidated sediments and a region with no lateral movement would be rare.

In deeper weathered material, especially if clay-rich, lateral or vertical water movement is likely to be extremely slow and significant changes in the groundwater chemistry would probably occur before waters had migrated far from source rocks of another type in a laterally different position. The role of physical erosion of the ground surface and the removal of weathered clays with it need to be considered in this instance, since this will alter the environment at depth and allow oxidising conditions to penetrate deeper.

Movement of "materials" or "the products of weathering", constantly referred to in the recent discussions (ie groundwater and ions) is probably mostly lateral in the soil layers with a greater component of vertical movement in the saprolite. The vertical component of weathering in the saprolite may be imposed by the gradual erosion of surface material and thus exposure of deeper materials to oxidising conditions. At Koongarra, observation of the composition of the kaolinite derived from weathering of chlorite and biotite indicates that the composition of the clay in the saprolite strongly reflects the composition of the unweathered material in the parent rock beneath (for instance Fe and Mg-rich).

In conclusion, the mode of formation of ferruginous material is likely to depend on the position of this material in the profile. The predominant mode of formation, whether lateral or vertical is certainly very site-specific. Better definition of

terminology would avoid confusion in discussions of the regolith and result in clearer understanding of the ferruginous material involved. A working model of the regolith has been derived from the various studies presented by other authors. This model has been applied to the weathered zone at Koongarra and compared to other models.

The importance of lateral or vertical processes clearly depends on the location of weathered material that is being discussed. The present "polarisation" in the debate of the regolith and the formation of iron-rich and iron-depleted zones in the saprolith and the transported material above appears to be mainly caused by poor terminology used to describe the regolith and its components.

Physical Factors in the Formation of the Weathered Zone at Koongarra

This section discusses the physical modes of the formation of the weathered profile at Koongarra. The main parameters of this process are groundwater, oxidation, fractures and the various interactions of these.

In both in the unweathered and weathered material (excepting the saprock), matrix permeability has been shown to be very low (See Chapter 5). The main study of the migration of radionuclides in the weathered zone at Koongarra (virtually absent in the unweathered material) has focussed on the movement of materials and subsequent deposition (adsorption) through, and in, the fractures.

Borehole TV studies of the structure and fracturing of the site have provided very adequate controls on fracture density, location, distribution and orientation (discussed in Chapter 3). Pumping tests and the resultant studies of drawdown cones linking zones of fracturing have delineated valuable information pertaining directly to groundwater movement. These studies have led to the derivation of flow directions through fractures. Petrophysical and groundwater chemistry studies of the weathered zone have corroborated these studies (see Chapter 5).

A physical model of groundwater flow direction and the mode of movement of weathered products at Koongarra has developed and been largely substantiated through these structural studies which, although indirect, are convincing.

To better define this model we must consider the main role of oxidising groundwater in the weathering of the parent rock, the channels facilitating it and the constraints affecting it:

* The main modes through which groundwater may access parent rock and cause weathering: Fractures, their presence, intensity, size, orientation and distribution; including geological and structural constraints (for example anisotropy of permeability in the schists along foliation and the preference for fractures to develop along schistosity)

* The major processes inhibiting movement of groundwater and weathered materials; Fracture infilling by weathered products; and permeability and porosity constraints (requiring assimilation of the petrophysical database).

Broader scale studies must be included in the development of the model, including:

* The areal and vertical extents of the weathered zone.

* Hand specimen studies of the percussion hole samples of the upper weathered zone (note erratic development of weathering)

* Landscape evolution (discussed in Chapter 2).

* **Fracturing**

The weathered Zone at Koongarra is variably fractured along the predominant F2 imposed schistosity, which generally follows or is subparallel to bedding. The structure of the schistosity at the site is presented in Figure 3.3. Fracture analyses by Emerson *et al* (1992) indicated that cross fracturing normal or subnormal to bedding and foliation is present but minor. Microfracture studies indicated that crack widths in unweathered rock are commonly >20 - 30 microns, exceeding the nominal flow-threshold crack-width of 10 microns. The lithologies exhibiting the highest fracture intensities were fault zone material and graphitic units. Unfortunately, the weathered material could not be treated for enhancement and study of fractures, however, the results from these studies from unweathered rock can reasonably be extrapolated to the point of incipient weathering. The dominant schistosity directions (determined by the BTV technique) in individual boreholes can be seen on Figure 3.4 (from Emerson *et al* 1994).

Petrophysical data presented in Chapter 5 indicate lowest matrix permeabilities in the rocks at Koongarra are in the upper weathered zone and the unweathered rock. Anisotropy of permeability was marked, with along foliation permeabilities

significantly greater than cross-foliation (4:1 to 5:1 in unweathered material and about 2:1 in weathered material). Emerson *et al* (1992) noted that "As water movement has occurred and does still occur in the weathered zone presumably this takes place largely through matrix flow". This is corroborated by the absence of visible open fractures in much of the weathered materials studied, however given the character of the lower weathered zone or and transition zone (where incipient weathering occurs), it is thought that when fracture flow does occur, it dominates flow in the weathered zone.

It can be surmised that the greatest flow of groundwater at the site occurs at the base of the weathered material, where permeabilities are highest and weathering is incipient. The fracture / schistosity orientation significantly influences permeability and so could be considered to have an effect on the direction of groundwater flow. The appearance of fractures in the upper weathered zone is low, presumably because infilling by clays has made the fractures invisible. In the unweathered material, although fractures are quite evident, it is possible that these may be largely closed due to burial pressure. At this point, reference needs to be made to Chapter 5, Petrophysics.

Fracture intensity and direction can be considered to be perhaps the primary determining feature of access of groundwater to weatherable material and thus the direction of groundwater flow.

* **Inhibiting Factors**

The two channels for groundwater flow through rock are matrix flow and fracture flow. Petrophysical results have indicated greater flow along microfractures than matrix flow at. This bias will strongly affect groundwater flow directions at the site. Foliation and microfracturing have been observed to be commonly parallel. Foliation at Koongarra is subparallel to bedding and parallel to the topographic contours in the vicinity of the No. 1 orebody (approximately SW - NE).

Low matrix permeability and high foliation permeability probably inhibit flow along the line of gravity (NW - SE), groundwater instead moving preferentially along the direction of schistosity / foliation / microfracturing. In the area of the No. 1 orebody, foliation is approximately SW - NE. The petrophysical results indicate that the transition zone and lower weathered zones show a 4:1 or 5:1 ratio of fracture:matrix flow. It can be surmised that the direction of flow of waters moving through the weathered rock at Koongarra would be some combination of the line of gravity and the predominant direction of foliation and microfracturing.

Earlier maps of the site have shown groundwater flowing normal to topography, but these ignore the constraints of fracturing and schistosity in the weathered rock. A combination of gravitational and schistosity-imposed constraints suggest that flow direction would be a WSW direction. Earlier studies suggest that groundwater flow at Koongarra is in a NNE to SSW direction, closer to the line of gravity.

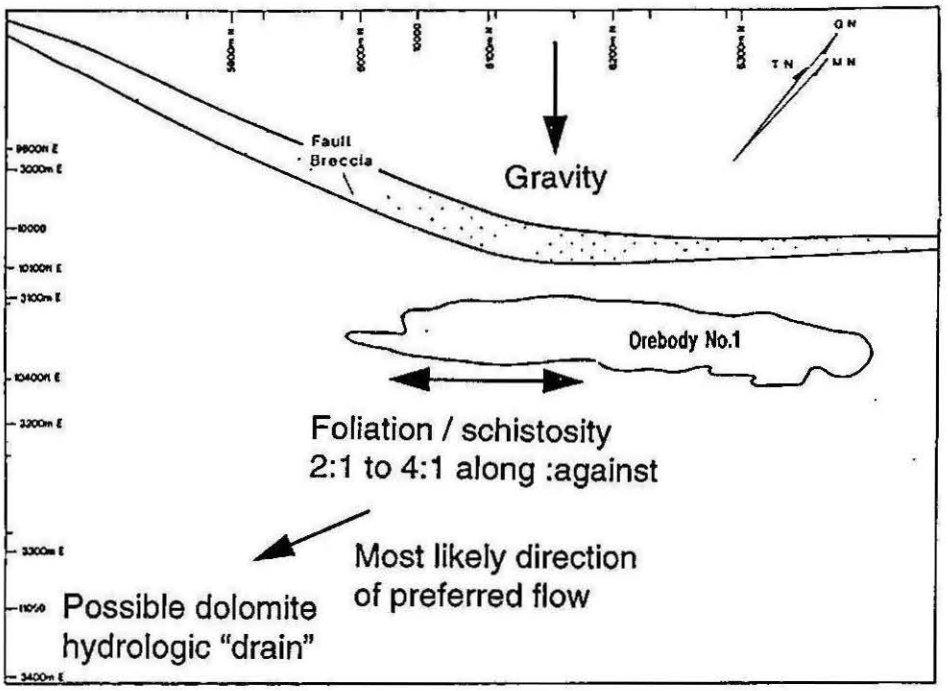

Figure 4.6: Preferential flow directions at Koongarra.

The factors inhibiting fracture flow include constriction of fractures through deep burial, inaccessibility of fractures to weathering / oxidising groundwaters at depth, and at shallow depths, infilling of fractures by weathered products. Since the migration of radionuclides in the weathered zone is the focus of the Koongarra study, inhibition of fracture flow in this zone is of primary importance.

The primary weatherable minerals at Koongarra are chlorite and micas (as earlier this chapter). These minerals oxidise and absorb H_2O at a molecular level, to form vermiculite and kaolinite (See Figure 4.8, from Murakami *et al* 1992), which results in expansion. The chlorite and biotite first accessed through fractures and foliation weather and expand, gradually filling the fractures and foliation water pathways

with extremely low permeability clays. It may be that expansion of clays in the initial stages of weathering wedges fractures open and facilitates groundwater movement prior to infilling of the fractures by clays. As the ground surface is removed by erosion, the oxidising front of incipient weathering gradually moves downward. Concurrent with this process is the infilling of fractures with clays.

A relative increase in quantities of clay in the weathered profile can be seen in Figure 4.9 (from Koppi *et al* (1990). As one proceeds upward from the base of weathering, clays gradually increase in proportion. Through the same process, groundwater movement would shift from fracture flow to matrix flow (and possibly also from lateral to vertical).

The infilling of fractures and foliation has significant implications for the movement and subsequent inhibition of radionuclides in the weathered zone. The speed of development of clays from chlorite and micas is therefore a determining feature governing the distance uranium radionuclides can travel downgradient through the fractures until severely constrained in movement by extremely low matrix permeabilities. Secondary uranium minerals primarily occur in fractures, associated with Fe coatings (Fe is one of the most mobile phases in the Koongarra mineralogy and is released at each stage in the weathering process).

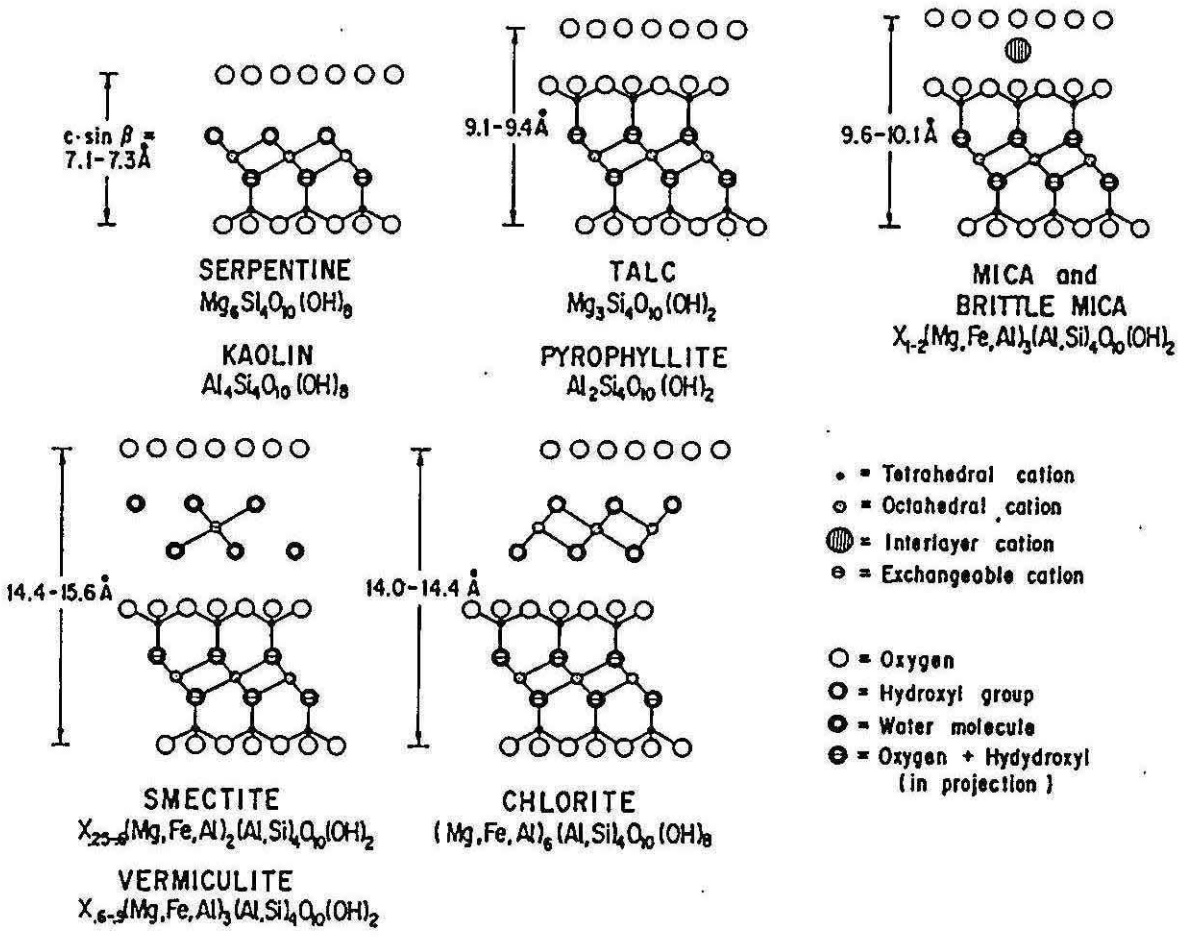

Figure 4.7: Crystal structures of major clay minerals (from Murakami *et al* 1992).

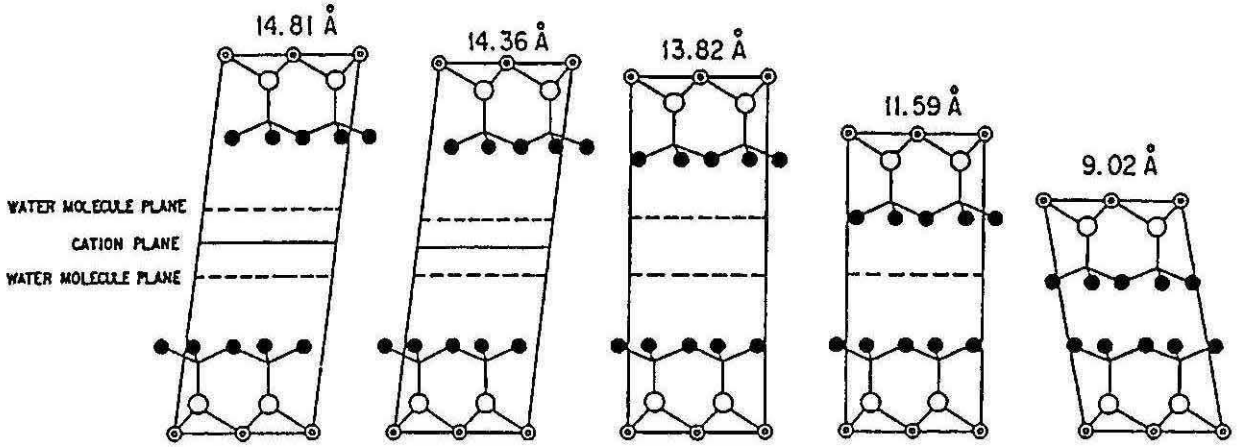

Figure 4.8: Hydration stages of vemiculite (from Murakami *et al* 1992).

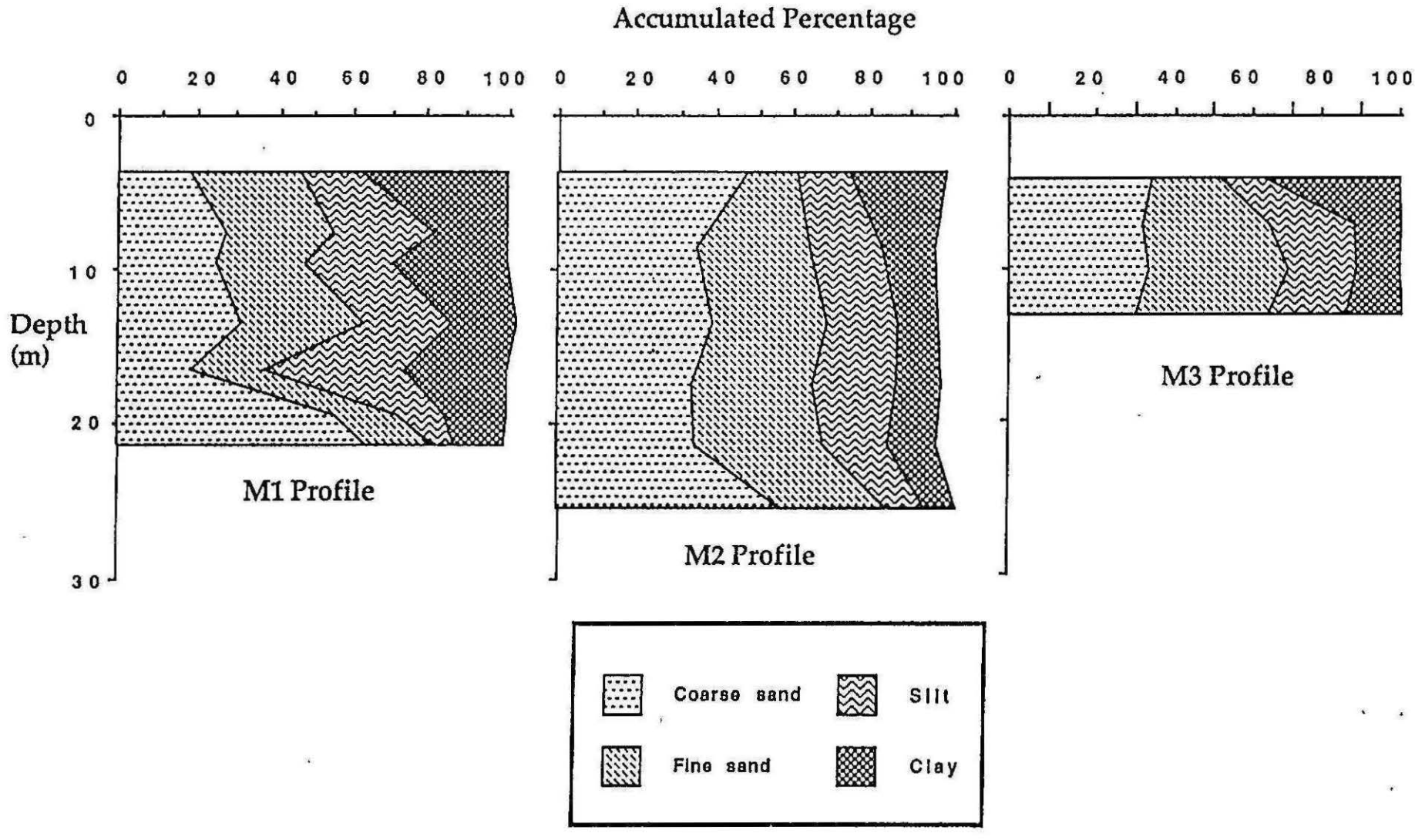

Figure 4.9: Particle size analysis of M1, M2 and M3 percussion hole profiles (from Koppi *et al* 1991). Note the increase in clay content closer to the ground surface.

Figure 4.10: Groundwater chemistry variations delineated through sampling of boreholes (from Payne 1991). The two zones showing closest similaritiy in groundwater geochemistry are Zones II and V.

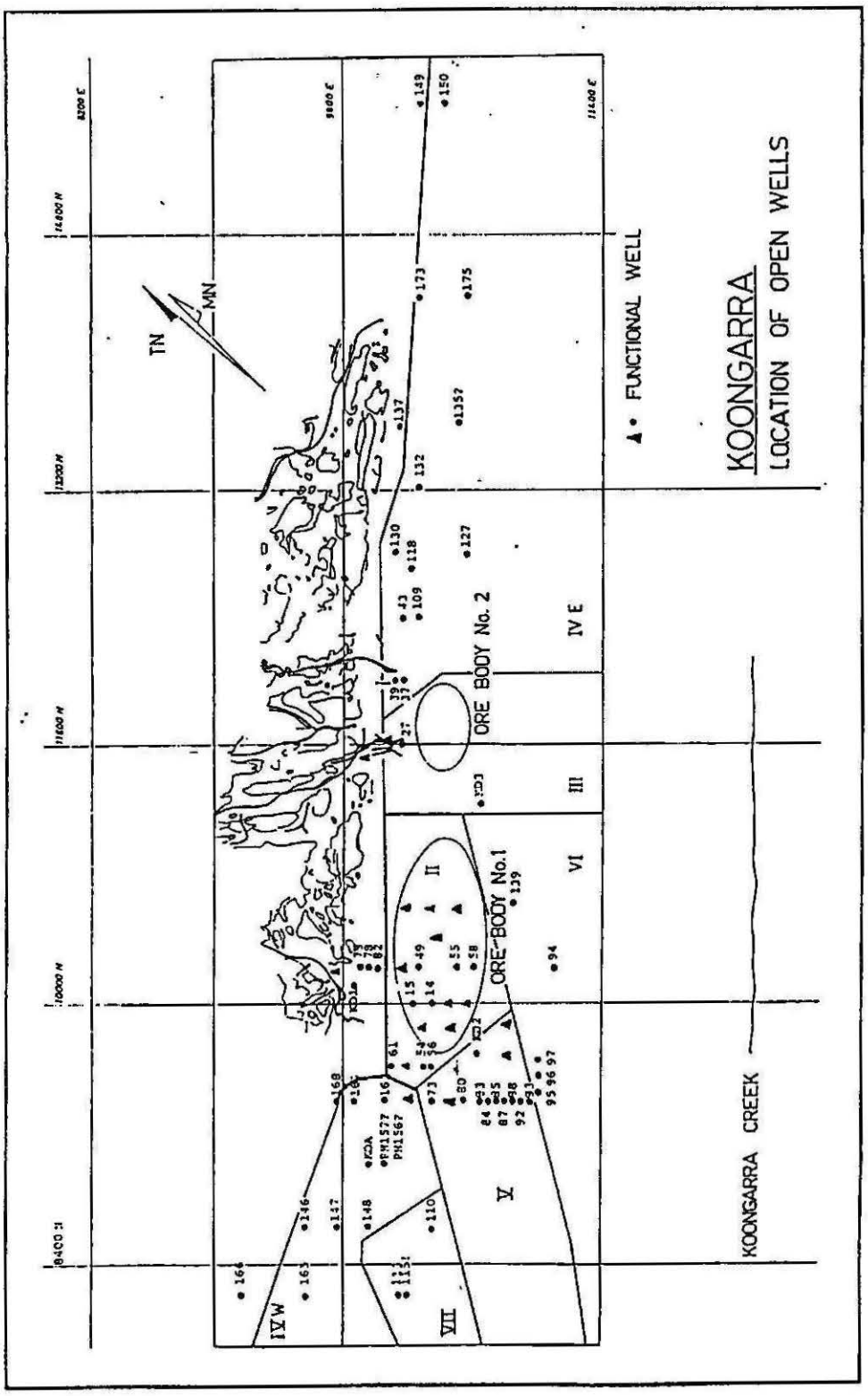

* **Physical Extents of Weathering**

A contour map of the base of the weathered zone has been created through study of all available borehole logs (DDH and PH : 300 in total). This author prepared this map both for the ARAP and for the purposes of this thesis. The map was made using the SURFER gridding and contouring package by GOLDEN SOFTWARE. A grid was created which covered the area of all of the boreholes, with a density of 100 x 100 divisions / pixels. The minimum curvature grid interpolation method was used for the plots presented. Other gridding methods were tested and considered successful (such as Kriging) but the cubic spline method was considered to best represent the data. The interpolation for the grid was made through a weighted averaging of the closest 10 data points to each grid cross-point.

The minimum curvature method has a tendency to smooth the data somewhat. Given the highly irregular nature of the parameter studied (ie the base of weathering) and the irregular distribution of the boreholes, this method may not faithfully represent every data point. Also, since the depth to the base of weathering is highly irregular, this method was chosen to illustrate the broad features of the base of weathering.

The depths to the base of weathering were gathered through painstaking study of each borehole log to ascertain independently from the logs, where this author considered the true base of weathering to be (in some boreholes quite a difficult task). The dip of each borehole was noted when examined for the depth to the base of weathering. The displacement the base of weathering due to the dip of the

borehole was calculated and thus the correct x and y locations were determined. additionally, the difference between depth down the borehole (inclined) and the true vertical depth of the base of weathering was determined. These calculated true x, y and z data were used to create the weathered zone map.

Errors in the data:

Judgement of the base of weathering in borehole logs is subjective. Borehole logging was carried out by two different loggers. Presumably a study of the base of weathering was not the prime motivation of these loggers. The base of weathering can be seen to be gauged inconsistent internally (within logs by the same logger) and the difference in assessment of the base of weathering by the two loggers was also quite evident. Wherever it was possible, each borehole log was studied by this author and a consistent definition of the base of weathering was sought to determine a more accurate result.

Davis (1992) mentioned difficulties in his interpretation of the upper parts of the geologic logs due to the nonstandard descriptions used for weathered material. Most percussion holes were logged on the basis of composite samples taken every 5 ft. Davis actually devised his own methodology to interpret from the logs whether clays were residual or in-situ. He considered the base of significant weathering to be the depth of the casing or the depth at which the drill bits were changed from one type to another. However this scheme would only reflect the condition of the material being drilled. A definition of the base of the weathered zone based on

geologic observations from the borehole logs is considered by this author to be the most reliable method of acquiring accurate data.

One error in the geologic logs was illustrated through this author's study of the core trays of DDH 53. Descriptions given in the geologic logs, and the samples actually observed (by the author) in the core trays were often different. The most striking example of this was the classification of rounded quartz pebble conglomerate (observed by this author at Nourlangie Rock 3 km south of Koongarra) as "fault breccia", which it clearly was not. If this case is repeated in all or many of the boreholes, then it is suggested that the Koongarra Fault Breccia zone is actually shallower than has been previously represented in cross-sections through the site. Given these significant inadequacies in the borehole logs, the weathered zone map needs to viewed cautiously.

In compiling the data from the geologic logs, significant other anomalies were also found. In boreholes only metres apart (the x,y,z location of the recorded base of the weathered zone), depth to the base of weathering varied by up to 10 m. The base of weathering is no doubt erratic, however it is thought that this kind of inconsistency is probably likely to be the result of those logging the core.

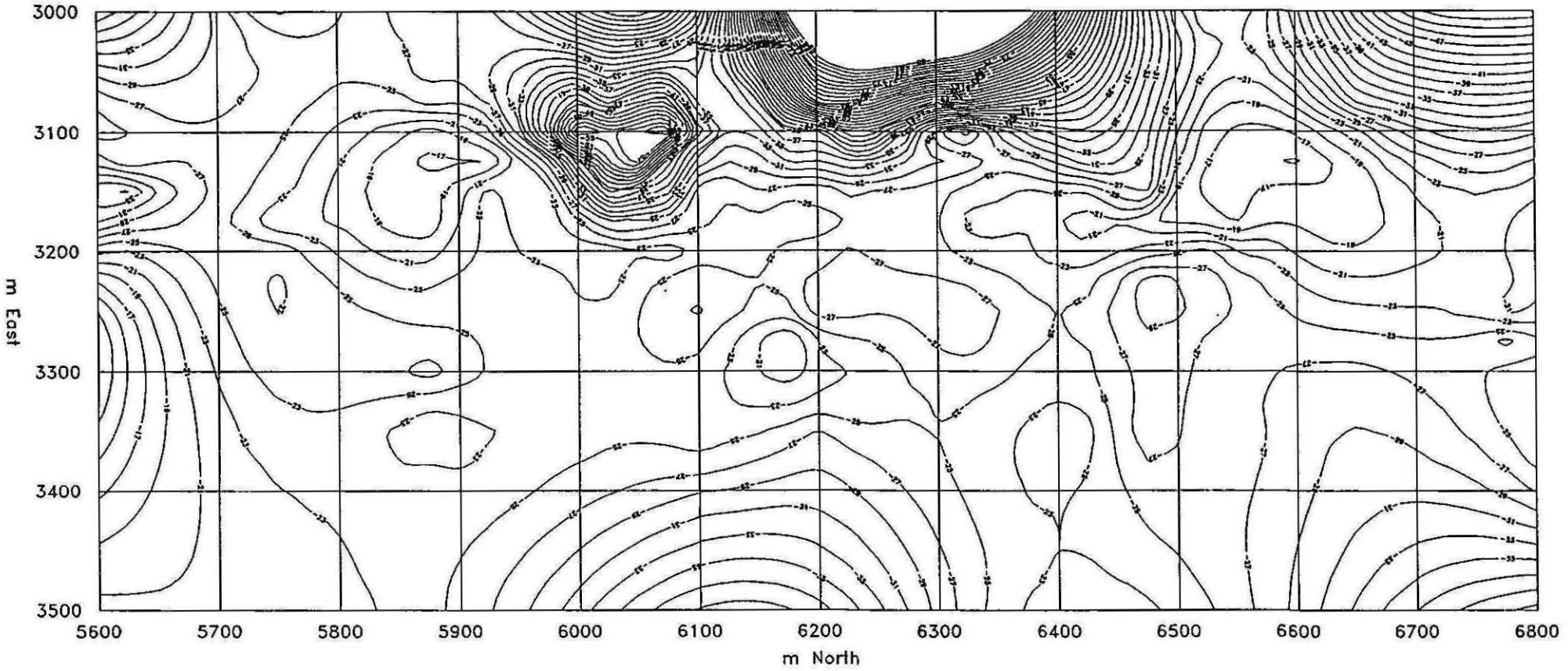

Figure 4.11: Contour map of the base of weathering

* **Hand specimen analysis of Weathered Material**

Studies of weathered material from a number of percussion holes were made to better understand the variation in intensity of the weathering patterns of the regolith. These were made with reference to and in a similar mode to a physical study of Borehole W7 presented in Emerson *et al* (1994). Physical property results are presented in Chapter 5: Petrophysics. Boreholes studied by this author included: M1, M2, M3, W1, W2, W5 and W7.

The broad trend observed in the weathered material is the gradual degradation of lithic fabric and schistosity and replacement by clays. An interesting feature to emerge from these studies was the variability of weathering at shallow depths, between about 18 m to 6 m. Zones of intense weathering could be seen at depths of up to 18m, interspersed with predominantly moderately weathered material still exhibiting obvious schistose fabric. Within shallower material, up to 6 m depth, small zones (15 cm across) showing strong lithic fabric could be found among material which was predominantly clay and disaggregated quartz. These results are depicted in Figure 4.5.

The implication from this study is that degrees of weathering are strongly affected by some factor beyond matrix flow (which would weather rock more uniformly). Presumably the aberrant sections of greater or lesser weathered material (in the deeper and shallower sections of the boreholes respectively) could be more or less fractured zones which have been subject to greater or lesser access of groundwater through fractures. This study therefore lends support to the notion that

weathering is strongly affected by the presence or absence of fractures, and also that weathering patterns may be dictated by fracture zones which have not been fully quantified in the ARAP.

Petrophysical studies of the percussion hole material observed in this section are essential to the illustration of the physical basis of the study and can be found in the Appendix of petrophysical data.

A Developmental Model for the Formation of the Regolith and Dispersion Fan at Koongarra

A model for the development of the regolith and the dispersion fan at Koongarra can be created by assimilating the physical characteristics of the material in conjunction with studies of the extent, nature and distribution of weathered materials and the structural and geomorphological development of the site.

This model is illustrated in Figure 4.12 (i). At this stage, the base of weathering has not yet reached the top of the No.1 orebody. Groundwater flow at the base of the weathered zone is controlled and directed in the direction of schistosity and existent zones of increased fracturing (as previously indicated, on Figures 4.5 and 4.6). Zones of highest lateral flow are the surficial sands and gravels and the base of weathering (saprock). Lateral groundwater movement in the pallid and mottled zones is restricted due to infilling of fracture zones. Iron migrates laterally as ionic products both in the saprock, where incipient weathering is occurring and in the

surficial materials. Zones of less fracturing are weathered less and survive as regions of less weathered rock in the upper pallid zone and lower mottled zone, exhibiting stronger relict lithic (schistose) fabric.

Figure 4.12: The development of the weathered profile and dispersion fan.

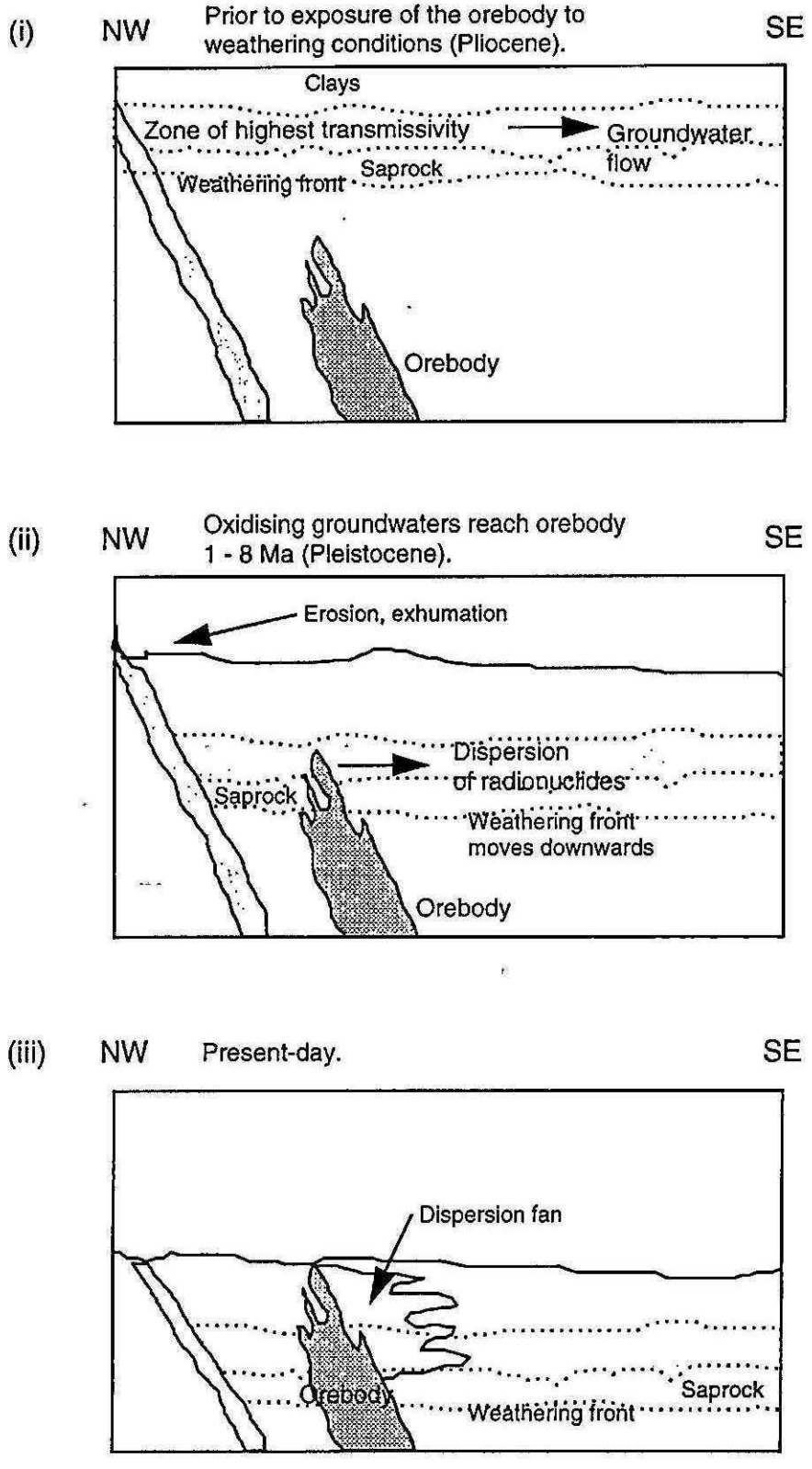

The second figure, 4.12 (ii) illustrates a later stage when the weathering front has reached the top of the No.1 orebody. Of course the process is gradual and there are innumerable intermediate phases between the two figures. At the stage illustrated in Fig 4.12 (ii), mobilisation of uranium radionuclides has begun and lateral movement is occurring. Direction and movement of these nuclides is strongly influenced by schistose anisotropy and presence or absence of fracture zones. In fact, the distance the radionuclides may move before being inhibited in mobility by fracture and schistosity filling clays is no doubt also determined primarily by the presence of fracture zones through which they can migrate, and the intensity of fracturing in these zones.

As time proceeds, the weathering front migrates vertically as the upper levels of the regolith are removed by erosion, and oxidising conditions are able to access fresh rock. In Figure 4.12 (iii), the first radionuclides to migrate in part (ii) are already within the pallid zone where permeability is significantly lower. Matrix flow dominates in this zone and groundwater flow is restricted. Within this zone, previously highly fractured zones have been weathered mostly to clays and previously less weathered and fractured material remain as less weathered, schistose zones. As these zones "migrate" upwards, they are further weathered and disaggregated until close to the top of the mottled zone where virtually all original rock fabric is destroyed and the only original materials to be found are quartz and occasional mica. Migration of Fe in this zone, particularly close to the surface and greater oxidation potentials, results in zones of Fe-enrichment and occasional mottles.

At the upper extent of the mottled zone is a region of greatest oxidation potential contrast and occasionally ferricretes or hardened iron-rich concretions occur. The depth of the pedolith (sands and gravels) is highly variable, especially in the context of Koongarra, where seasonal climatic variations can be great and large amounts of water movement can occur during the wet season. For this reason and also as mentioned by previous authors, the surficial zone is considered to be "fluid" in its distribution and depth. These transported materials are less consolidated than the materials below them and are more prone to movement by water and even wind. There are examples at Koongarra where almost all the sands and gravels have been removed by erosion and the harder ferricretes at the top of the mottled zones are exposed. Other areas show great depths of sands weathered from the quartz-rich Kombolgie Sandstone. Significant variations in the depth of these sand aprons has been noted (especially near the creek) even during the 10 years of study of the ARAP.

The mode of lateral movement of radionuclides through the weathered zone has been likened to the "sweeping" effect of a broom. Although a simple analogy, it is effective in illustrating the migration of radionuclides away from the primary orebody. The broom can be compared to the oxidising groundwaters in the "transition zone". The broom gradually sweeps the top of the primary ore away from the orebody, each "sweep" taking another layer from the top of the primary orebody. The implication from this model is that the dispersion fan is built up by additions at the bottom and that the youngest dispersed radionuclides in the dispersion fan can be found near its base. Further from the location of this broom,

its effect is lessened, in this case by the inhibiting effect of the clays in the fractures and the uranium radionuclides cease moving.

Petrophysical data corroborate that the zone of highest matrix transmissivity is found not at the very base of weathering, but a few metres above this incipient weathering zone, perhaps due to the gradual opening of fractures and foliation through clay mineral expansion.

Conclusions

Through an understanding of the myriad processes influencing the weathered profile at Koongarra and assimilation of the physical observations made on the weathered materials as part of this study, a model of the development of the weathered zone and dispersion fan at Koongarra has been made. The processes leading to the formation of the weathered profile have been related to recent discussions of the regolith in northern Australia. A construction of a typical regolith profile for Koongarra was sought through these studies in concert with knowledge of the materials and products of weathering at Koongarra.

The regolith or "lateritic profile" at Koongarra is only partially developed in the sense of a classical "laterite" profile, given the absence of a thick surface layer of hard, iron-rich "laterite". The upper part of the regolith at Koongarra develops iron-rich mottles but little more.

The weathered profile at Koongarra has been observed to be complex and the entire mechanism for its formation, variations and continuing development could scarcely be expected to be fully quantified. However, an appreciation of the major contributing features has been gained and this appreciation enables a more realistic picture of the mechanisms involved.

In unravelling the analysis of the regolith in recent discussions, it is revealed that lateral groundwater movement dominates within the surficial materials and vertical processes become more evident in deeper material (although it is still unclear whether it predominates). This scheme can be adequately applied for the Koongarra weathered zone. The question of migration of materials upward still remains: What physical parameter facilitates this upward motion? Seasonal water variations below the ground? Perhaps the downward motion of the weathered profile merely makes the movement of Fe appear upwardly mobile.

The likely movement of groundwater in the regolith at Koongarra and its mode, whether predominantly lateral or vertical has been considered. Lateral movement of water certainly occurs in the surficial sands and has also been demonstrated in the deeper weathered material, particularly within the most transmissive zone; The Transition Zone or saprolite. Lateral movement of materials (Fe) over significant distances (more than a few mm) appears to be somewhat restricted, given the composition of clays in the alteration halo and those outside it. It may be that Fe is mobile at the incipient stage but doesn't absorb into clays, rather it adsorbs onto fracture coatings.

It appears that lateral movement of weathered materials is ironically restricted by the very process of weathering that frees them to migrate in the first place. During incipient weathering, when the fractures first open up to allow water movement, chlorite and biotite expand, absorbing water (and other materials) to form impermeable clays vermiculite and kaolinite which fill the fractures through which the oxidising waters flowed.

The ARAP has covered in detail many of the parameters necessary to properly understand a comprehensive model of the weathered zone at Koongarra. This thesis has provided information on many of the other parameters. A comprehensive physical characterisation was carried out to determine the probable interactions between these zones and groundwater movement is the basis for the analysis of the weathered zone presented in this thesis and is presented in Chapter 5. The study of the weathering horizons and the petrophysical characterisation of the weathered lithologies are complementary and although presented in separate chapters are closely associated.

Suggestions for Further Study

This study has delineated a working model through which to understand the mobilisation and subsequent immobilisation of radionuclides at Koongarra. The weathered material has been presented using contemporary regolith terminology and current regolith definitions.

However, there are many issues that could have been better resolved given more time. The borehole TV data holds a wealth of information that could not be completely represented within the time frame of the ARAP. Further drilling and application of the BTV could delineate connected zones of fracturing which could not be physically proved in this study. Further pumping tests could target theorised interconnected fracture zones to verify that significantly greater water movement occurs in these zones compared to unfractured rock, which has been delineated up to this point largely through inference. Further studies of the petrophysical data could be made to better correlate fractured zones delineated by additional BTV studies and high permeability zones shown by the petrophysical data.

CHAPTER FIVE :

PETROPHYSICS

A comprehensive study of the petrophysical properties of the Koongarra site has been carried out in order to best define those physical properties of the rock (at drillhole scale and by lab analysis), that effectively control the movement of groundwater, and thus radionuclides, at Koongarra. Of particular interest are the results gathered from the weathered zone samples.

306 drillcore samples were subject to petrophysical analysis. These samples were obtained from 28 boreholes (20 diamond drill holes and 8 cable tool drillholes) which are indicated on Figure 5.1. Some surficial ferricretes were obtained by hand specimen collection.

The boreholes sampled for petrophysical testing were from the central part of the Number 1 orebody and to the southeast. No boreholes from the direct proximity of the No. 2 orebody were sampled for petrophysical testing. Petrophysical tests carried out included mass properties (density, porosity and permeability), compressional wave velocity, magnetic susceptibility and electrical resistivity. The petrophysical testing programme was carried out using procedures documented by Emerson (1991).

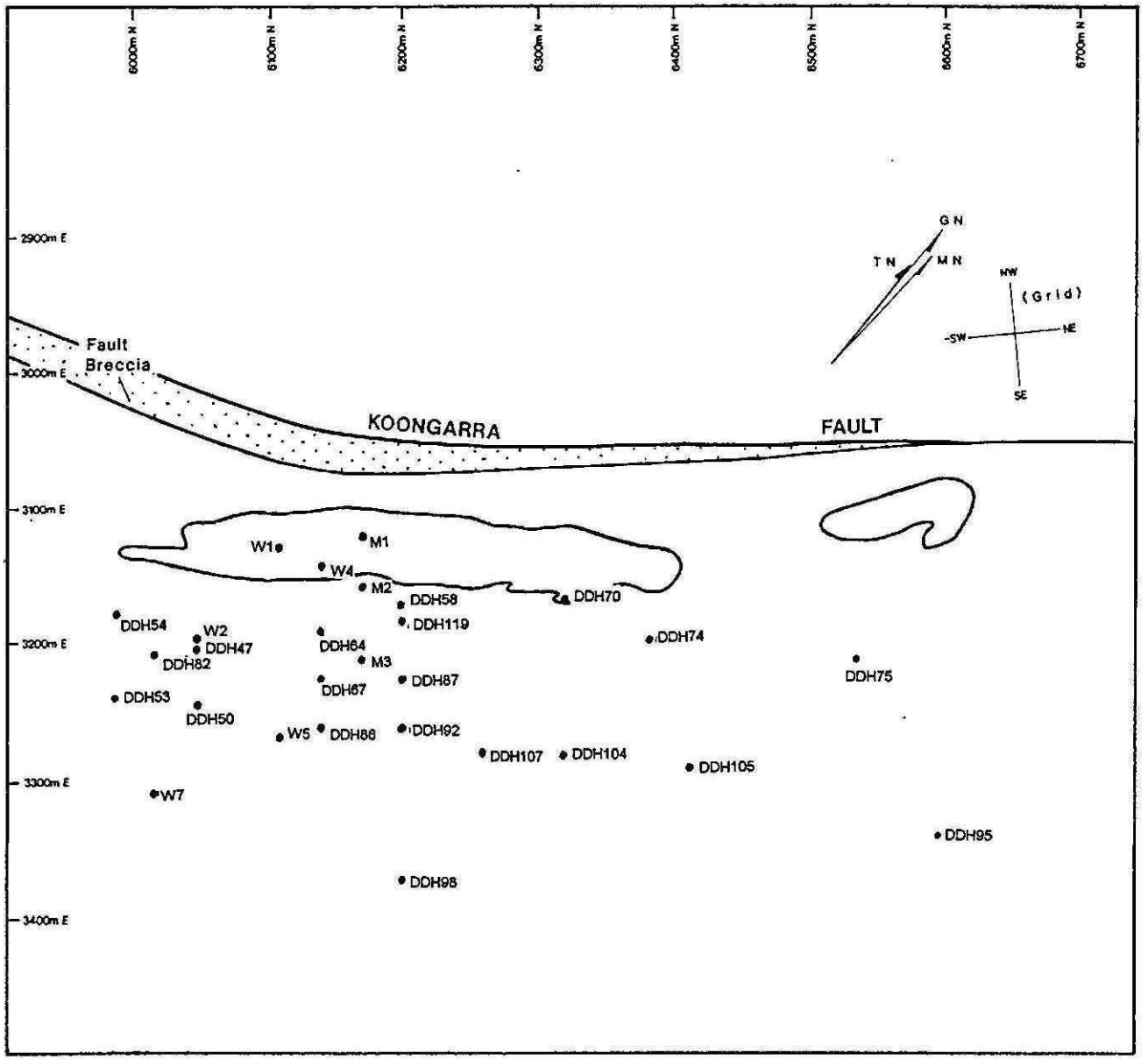

Figure 5.1: Boreholes sampled for petrophysical testing.

The rationale behind the petrophysical testing was to provide quantitative information about the character of the rock "framework" in which the ARAP modelling exercise is set, such as relative rock strength, amount of porous (void) space, mineralogy, degree of weathering and ability of the material to conduct water. Density can indicate relative rock strength, degree of weathering and mineralogy. Porosity and permeability reveal information pertaining to the ability of water to flow through the rock. Acoustic measurements relate directly to rock strength and degree of fracturing. The magnetic properties and sample resistivity measurements relate to the field geophysical surveys and indirectly to geological and hydrological properties. These results can be correlated to the geotechnical properties and, although not a direct measurement of hydrological properties, they can provide useful data from which to draw inferences respecting numerous other studies. With these considerations, the petrophysical study was carried out.

The lateral and vertical variations in petrophysical character serves as a useful counterpoint for comparison and correlation to the geochemical, hydrological and geophysical databases. In addition, the petrophysical database provides quantitative values for the various zones of the regolith (as detailed in Chapter 4) which may be invaluable for future workers studying regolithic materials.

The samples were classified into five petrophysical categories: The Weathered Zone (A), The Transition Zone (B), Unweathered Cahill Formation schists (C), Kombolgie Sandstone (D) and Quaternary ferricretes (E) based on lithology, degree of visible weathering and means of collection. The number of samples from each zone is indicated in Table 5.1. Further qualification of the petrophysical

sampling zones has been made in Chapter 4 and the petrophysical data have served to substantiate regolith classifications of the weathered materials made therein.

Zone A samples comprise the highly weathered schists of the M and W series cable tool drillholes and some of the upper sections of the diamond drill holes. Approximately half of these samples were obtained from cable tool drillholes, the others from diamond drill core.

Zone B samples are of an intermediate nature between Zone A and the unweathered schists. These samples showed some weathering and fracturing but not the mineral dissociation nor high clay content of the highly weathered material. Zone B samples were found to correlate closely with the saprolith zone in regolith nomenclature.

Zone C comprises unweathered schists and is subdivided into Zone C1: Quartz-chlorite schists, C1a: silicified schists, Zone C2: graphitic schists and Zone C3: amphibolites.

Zone D constitutes Kombolgie Sandstone samples with varying degrees of weathering.

Table 5.1: Petrophysical Sampling Zones

ZONE	Lithology	Number of Samples
A	highly weathered schists of the Lower Proterozoic Cahill Formation	(116)
	A1* M and W series holes, tube samples	64
	A2** diamond drill hole samples	52
B	lower weathered 'transitional' zone of Cahill Formation	16
C	unweathered schists of the Cahill Formation	(129)
	C1 quartz-mica-chlorite schists	111
	C1a silicified schists	4
	C2 graphitic schists	6
	C3 amphibolites	8
D	Middle Proterozoic Kombolgie Sandstone (and some reverse fault breccia samples)	42
E	Quaternary ferricretes (magnetic tests only)	3
* Zone A1 sampling was carried out by cable tool drilling in 1988, and the relatively fresh material is more argillaceous than the Zone A2 DDH materials from the 1970's drilling program, which also provided the Zone B, C, D materials. **Zone A2 sampling favoured the more cohesive, consolidated materials ; the sampled materials may not be as representative as A1.		Total : 306

The great majority of the petrophysical testing was carried out by this author in the University of Sydney Department of Geology and Geophysics Petrophysical Laboratory. This testing included porosity, permeability, density, compressional wave velocity, magnetic susceptibility and electrical resistivity. From these data, this author compiled the petrophysical database, created data histograms, scatter plots and the petrophysics vs depth diagram of W7 and DDH 50 as well as classification tables (see Tables 5.2 to 5.4 which were used in the ARAP Final Report). These figures and tables were presented as part of a paper presented at the 9th ASEG Conference (Hallett *et al* 1992). The complete petrophysical database is included as Appendix 2. Mercury injection porosimetry was carried out at the ANSTO Advanced Materials Laboratory at Lucas Heights.

Methods

Mass Properties: Density, Porosity and Permeability.

Sample masses were determined using electronic balances which were accurate to 0.01 g. Samples were vacuum saturated and following this, sample volume, dry bulk density and water accessible porosity were calculated using Archimedes Principle. Density quoted is in grams/cubic centimetre, and porosity as a percentage. Porosity of some samples was determined using Helium injection at 100 psi (6895 kPa). Total porosity values of the clayey materials was calculated by determining volumes after heating the samples to 110°C in order to release water from the molecular structure. Mercury injection porosimetry determines pore space in the samples (in the range 0.01 to 360 µm) by injecting mercury into the sample at increasing pressures, up to 60 000 psi.

Permeability measurements were carried out on cohesive core samples obtained from drilling either the 2" diamond drillhole material or the 5" cable tool material. Permeabilities were obtained by placing the cores in a device which exerted 100 psi pressure on the sides of the core. Air pressure at 20 psi was exerted at one end of the specimen. The quantity and rate of air passing through the core was used to calculate permeability. In the case of the less permeable, clay-rich specimens, water was used to calculate permeability rather than air. Permeability measurements are presented in millidarcys.

Acoustic Velocity

The relative conductance of the samples to Compressional waves (P-Waves) was determined using a number of different core samples. Some cores tested were the small 25 mm and 37 mm samples, some were larger cores cut directly from the 2" and 5" drillhole material. Equipment used included OYO 200 kHz transducers, a pulse generator transmitter and an oscilloscope receiver. P-Wave velocity was calculated considering the length of the core and the time in μs (microseconds) for the signal to arrive at the receiver. A 5 kN force was applied while the cores were tested to simulate confining pressures underground (0.025 Mpa/m) and also to close any fractures that may have been induced in the drilling and sampling procedures.

Ideal testing conditions for compressional wave velocity are that the diameter of the core is greater than the length and that the wavelength of the compressional wave is greater than the length of the sample tested. In some of the smaller (25 mm and

37 mm) samples, this was not possible, however, comparisons of these results with the larger cores tested indicated that the results gathered under non-ideal conditions were still very accurate. Compressional wave velocities are given in metres/second.

Magnetic Susceptibility

The petrophysical samples were tested for magnetic volume susceptibility using a Bartington Susceptibility Bridge (Model MS2). The results presented are in cgs x 10^{-6} (approximately SI x 10^{-5}). The specimens were tested at two frequencies (430 Hz and 4300 Hz), however the variation of magnetic susceptibility due to frequency was very low, so those data presented here are the low frequency results. The results from the Bartington susceptibility bridge are considered to be extremely accurate. Some measurements of the remanent magnetic field were made on weathered zone samples, however the results were inconsistent largely because the orientation of the cores tested could not be accurately determined from the borehole logs.

Electrical Resistivity

Complex resisitivity measurements were carried out at frequencies from 0.1 Hz to 10 MHz, using core vacuum saturated with 63 ohm m $Mg(HCO_3)_2$ solution. Resistivity was calculated in ohm m. The solution was used to mimic the prevailing conditions of conductivity of the groundwater at Koongarra. The cores were placed inside a piece of perpex tube filled with silicone gel. This "potting" of the specimens was done to negate conduction of current along the surface of the cores between the two ends via the saturating solution. The potted tube was placed between two

waterbaths and two and four electrode resistivity measurements were made. Equipment used was a Solartron 1250 Frequency Response Analyser, using low current densities (2×10^{-3} amp/m^2) with very high input impedance amplifiers (109 ohm m). Measurements of resistivity between 0.1 Hz and 1000 Hz were made using the Solartron Frequency Response Analyser. Higher frequency results were gathered using Hewlett Packard 4274A and 4275A Meters for frequencies up to 100 kHz and 10 MHz respectively. Resistivity values quoted in the petrophysical database are the 1 kHz results from the Solartron Frequency Response Analyser.

Methods of Testing: Biases and Error

The location of the boreholes from which samples were obtained introduces biases and not all of the lithologies at Koongarra could be tested petrophysically. However, the distribution of samples is considered by this author to be quite broad and representative of the great majority of material at the Koongarra site.

Generally speaking, the samples collected for petrophysical testing were biased towards the stronger specimens, as the samples first had to survive the cable tool or diamond drilling, and then further drilling in the laboratory to obtain samples that could be effectively tested. Samples that were high in clay or very fractured often did not survive the drilling procedure and this factor may have strongly biased the outcome of some measurements.

The necessity of using cohesive samples in the petrophysical testing influenced permeability tests strongly. Certain samples within the zones A and B were strongly fractured and it was not possible to make a core from them of a

satisfactory state to withstand the testing procedure without sample failure and meaningless results. Also, some samples (for example the Koongarra Fault breccia) had such large open fractures that it was not possible to obtain a meaningful permeability result. There is a bias in some fractured specimens such that the permeabilities obtained are effectively fracture permeabilities rather than matrix permeabilities. Similarly, fractured material from the Koongarra Fault breccia was often broken into pieces and could not be tested for permeability due to its physical condition. This illustrates a limitation of laboratory petrophysical examination: that the results gathered in a laboratory do not properly reflect so-called "real" conditions. However, the petrophysical data yield quantitative information regarding the matrix properties of the rock, which other techniques can only suggest through inference. Obviously, we need to take into consideration that laboratory testing (especially of permeability) cannot completely reflect existent broad-scale features such as macrofracturing.

Acoustic velocity results were also biased toward the more cohesive specimens, because highly weathered or fractured materials could not withstand the testing procedure. Efforts were made to test all available material for acoustic velocity and great care was taken in order to maintain the integrity of the material being tested, especially with strongly weathered samples.

Errors in the mass properties and magnetic susceptibilities are considered to be negligible.

Errors and bias in the resistivity measurements is also considered to be very low. Sample strength is not as critical in the electrical tests since the samples are almost completely encased in supportive silicone gel. There was some variability in the resistivity values and phase angles, which manifest as different resistivity values in duplicate tests. However, these were less than 10% for the low frequency measurements and less than 5% for the higher frequency measurements.

Results

The results of the petrophysical testing program are documented in Tables 5.2 to 5.4, in Figures 5.2 to 5.23 and in the Petrophysical Database which is included in complete form as Appendix 2. This thesis is the first publication of the Petrophysical Database compiled by this author for the ARAP and it is considered that a considerable amount of further work could be carried out using the database to yield further valuable information about the Koongarra site.

Mass Properties:

Density

The results of the density measurements can be seen in Table 5.2. The average density of all rock tested shows an increasing trend with depth. For Zone A1, wet bulk density is cited. Unweathered samples shows densities generally reflecting their mineralogy: the quartz-chlorite mica schists show an average density of 2.72 g/cc. The variation in densities reflects both the porosity and the mineral grain densities. Zone C3, the amphibolites, show the highest dry bulk density, 2.97 g/cc, reflecting the presence of a primary constituent mineral, hornblende which has a

TABLE 5.2
SUMMARY OF PHYSICAL PROPERTY RESULTS

ZONE		Bulk Density g/cc *	Porosity % **	Permeability md ***	Resistivity Ωm	Velocity m/s	Mag k 10^-6 cgs ≈ SI 10^-5
A1	av	1.95	34.0	1147	53	1582	21
	r	1.60 - 2.43	16.4 - 40.5	1 - 8708 (µd)	14 - 177	779 - 2202	12 - 62
(Weath.	n	56	6	40	16	23	33
M, W)	s	0.21		1785	42	425	14
A2	av	2.21	16.1	61.2	127	2283	30
	r	1.62 - 2.55	4.4 - 38.4	2.0 - 536.8	16 - 719	1163 - 3433	13 - 50
(Weath.	n	44	33	35	19	19	33
DDH)	s	0.20	4.1	98.3	156	699	6
B	av	2.48	7.7	5.2	112	2963	47
	r	2.14 - 2.79	0.4 - 16.3	0.8 - 39.9	46 - 208	1838 - 5105	23 - 63
(Lower	n	15	12	10	6	7	11
Weath.)	s	0.21	5.6	12.2			12
C1	av	2.72	1.8	0.3	5943	4894	47
	r	2.07 - 2.98	<0.1 - 7.8	<0.1 - 2.0	50 - 122370	2895 - 6125	11 - 104
(Qtz - chl	n	105	103	95	57	32	76
mica sch.)	s	0.09	1.5	0.4	17624	1088	20
C1(a)	av	2.63	0.6	0.2	32391	5726	4
	r	2.60 - 2.64	0.3 - 1.1	<0.1 - 0.3	4020 - 99060		<1 - 7
(silic.)	n	4	4	4	4	1	4
C2	av	2.70	0.8	0.6	736	4660	36
	r	2.65 - 2.76	0.2 - 1.1	0.5 - 0.7	31 - 3230	3947 - 5079	33 - 39
(Graphitic	n	6	6	2	6	3	2
sch.)							
C3	av	2.97	0.7	0.2	117887	5444	145
	r	2.88 - 3.06	0.1 - 2.2	<0.1 - 0.5	8333 - 517503	4921 - 6554	76 - 387
(Amphib.)	n	8	8	8	7	4	7
D	av	2.61	2.1	0.9	6823	4466	3
	r	2.40 - 2.69	0.1 - 8.2	<0.1 - 12.2	252 - 75834	2516 - 6105	<1 - 12
(Komb. Ss.)	n	39	39	38	30	15	28
	s	0.06	2.0	1.0	14992	966	3

* For A1 wet bulk densities are cited; all other densities are dry bulk.
** Porosities are apparent except for A1, where total porosities are cited.
*** A1 water permeabilities are in microdarcys, all others are air permeabilities in millidarcys.
av : mean value ; r : range ; n : number of samples ; s : standard deviation.
Resistivities measured galvanically at 1 kHz on saturated specimens.
P-wave velocities measured at 500 kHz under uniaxial load

grain density of 3.08 g/cc. The silicified schists and the Kombolgie Sandstone show much lower density, 2.63 g/cc and 2.61 g/cc respectively, reflecting the presence of quartz which has a grain density of 2.65 g/cc. The relatively high densities of the graphitic schists indicates only minor proportions of graphite in these rocks (graphite having a density of 2.2 g/cc).

As minerals such as amphibole, chlorite and mica are weathered to clays, causing expansion of the lithic fabric, the overall density decreases. Additionally the bulk density of these weathered minerals (such as kaolinite) are generally lower than unweathered minerals. This is illustrated in the plot of parameters of W7 and DDH 50 (Figure 5.23), from which it can be discerned that the relationship of density to depth is not strictly linear. This illustrates that the degree or intensity of weathering may be sporadic and variable and may depend on factors other than depth.

The density histogram indicates a few features of the rock at Koongarra: Firstly that the range of densities for the A1, A2 and B zones is very broad, secondly that the unweathered material shows a narrow distribution of densities, irrespective of lithology. Interestingly, the samples of Zone B, the Transitional Zone (or Saprock), shows the most even distribution of densities without a concentration of densities around a certain value.

The Density vs Depth scatter plot shows similar results. Once the unweathered material is encountered (Zone C1), densities do not increase greatly with increasing depth, as the porosity has become very low and bulk rock densities are dictated by mineral grain density.

Figure 5.2:

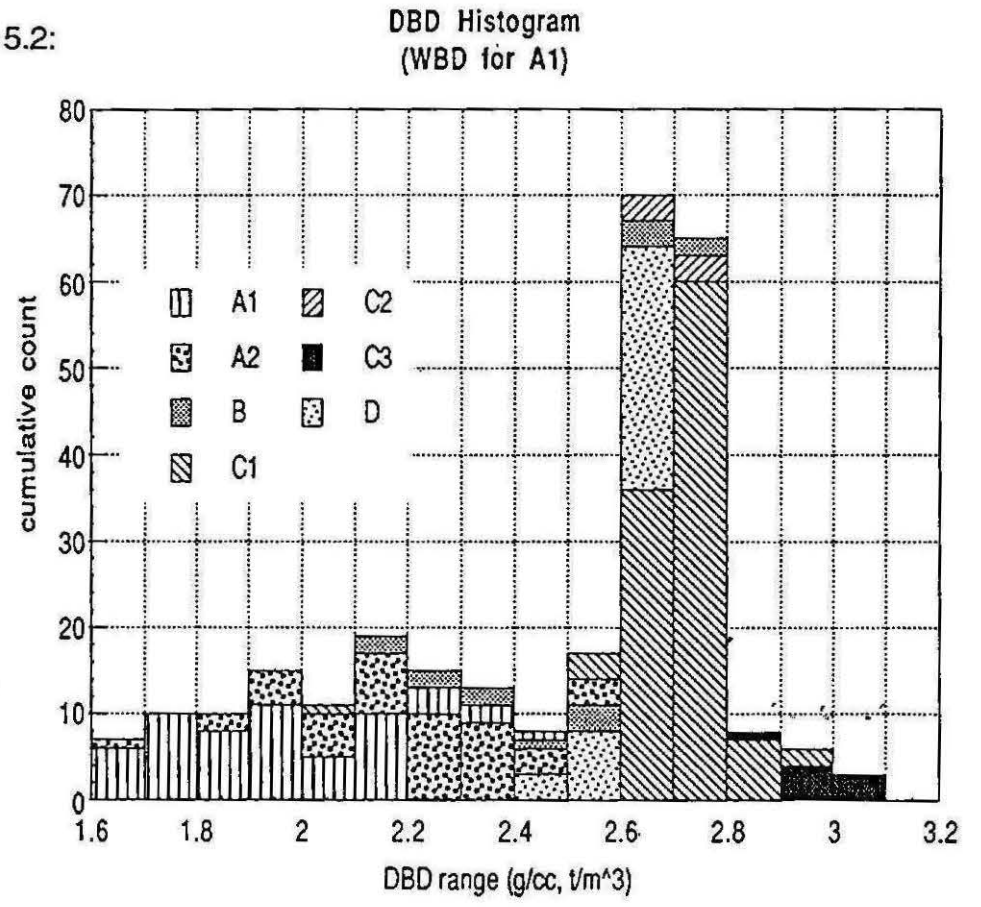

Figure 5.3:

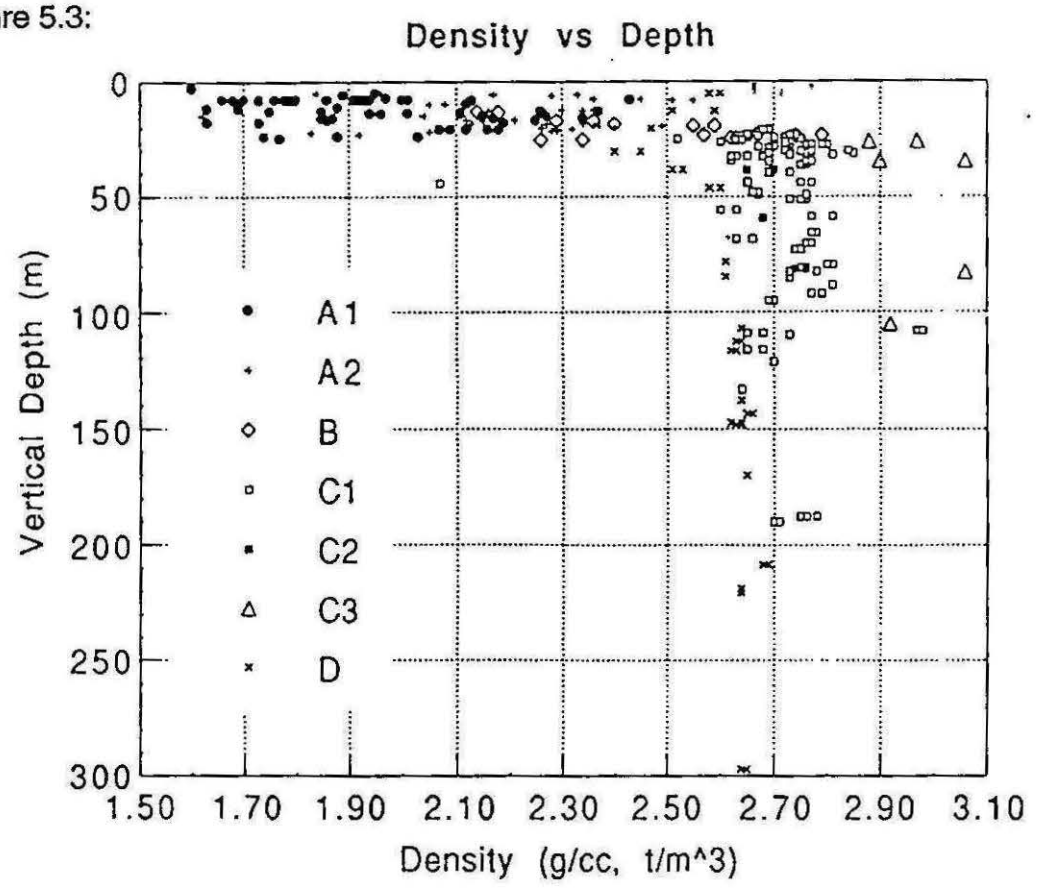

Porosity

Logically and conversely to the density results, the porosity of all samples can be seen to decrease with depth. This is accountable both to decreasing amounts of weathering and greater confining pressures with increasing depth, which causes the closure of voids.

For Zone A1, the total porosity rather than the apparent porosity is cited. The apparent porosity of these materials is expected to be about a third of the total porosity (or about 11%). Generally, the weathered samples of the Cahill Formation schists show a very high average porosity and a large range of porosities. In contrast, the unweathered materials have average porosities under two percent, independent of lithology. The relatively large range of porosity values for the Kombolgie Sandstone reflects variations in weathering from shallow samples to deeper samples. It is interesting to note the marked contrast that the effects of weathering have on the Kombolgie Sandstone compared to the Cahill Formation schists. The mercury injection porosimetry results lie within the same ranges as the porosities determined at the Petrophysical Laboratory at Sydney University by this author (excepting only the amphibolites) and serve to verify those results.

From the porosity histogram it can be seen that the porosities of all the samples of the unweathered material are grouped together in one region of the histogram.

The Porosity vs Depth scatter plot shows all the weathered materials collected in the top centre and top right hand corner of the plot, with only a few zone B samples having relatively low porosity. The horizontal scale has been plotted as a

Figure 5.4:

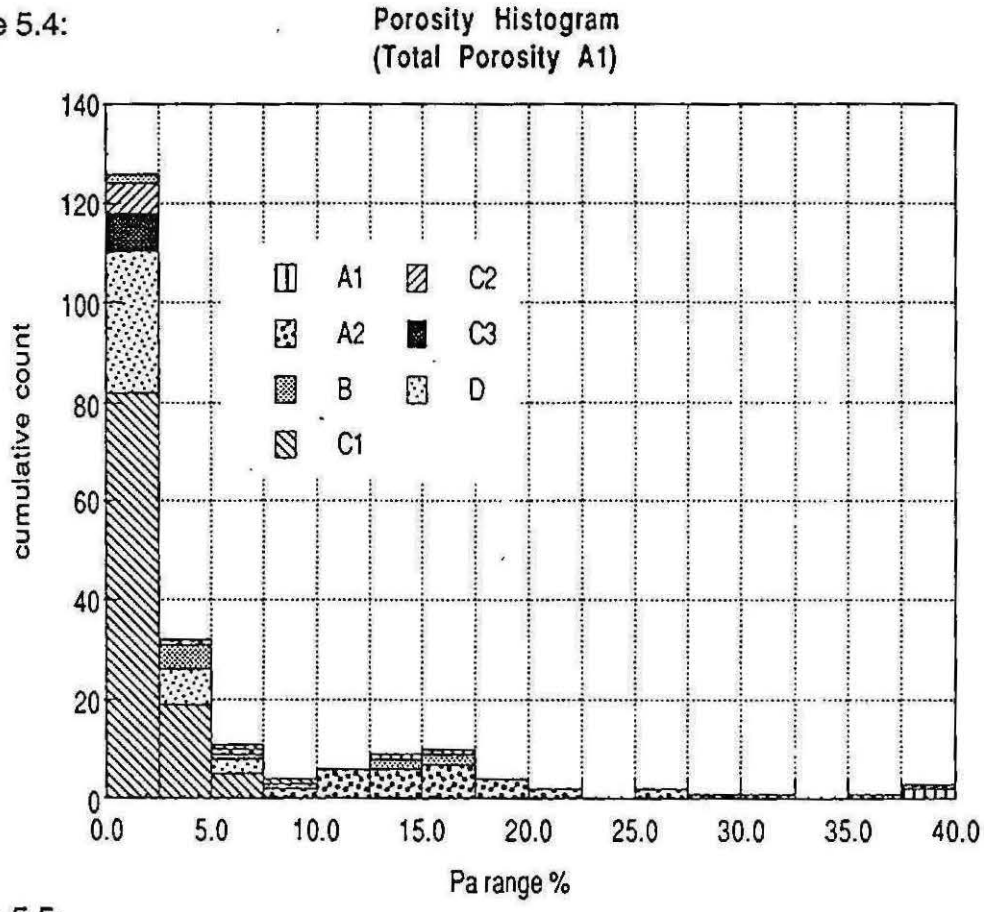

Figure 5.5:

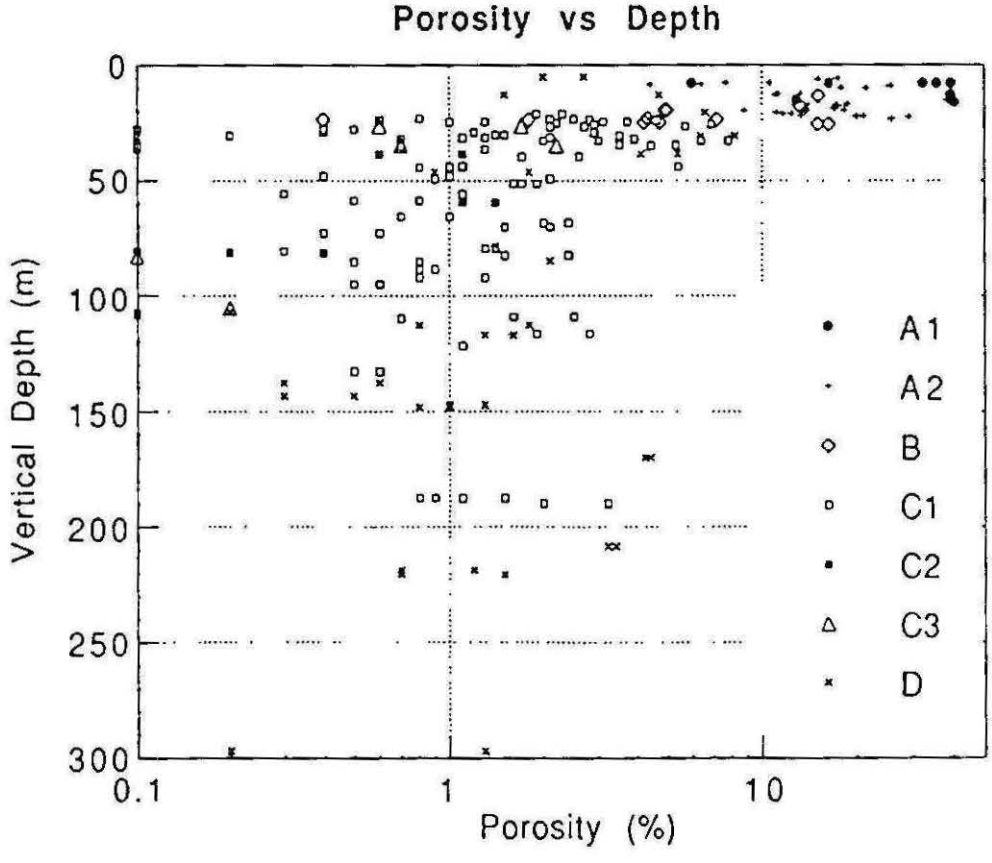

logarithmic scale to illustrate the distribution of the unweathered samples within the porosity range 0.1 - 10 %.

TABLE 5.3
MERCURY INJECTION POROSIMETRY RESULTS

ZONE	Drillhole	Vertical Depth m	Median pore diameter µm	Pore area sq m/g	Porosity (Hg) %	Dry Bulk Density g/cc
A1	M1	8	19.41	4.62	6.0	1.57
	M3	15	101.25	4.02	12.9	1.76
A2	53	6	1.27	7.21	12.7	2.40
	107	23	1.27	7.94	29.6	1.83
	119	22	0.31	8.41	16.7	2.31
B	74	20	0.42	7.84	11.3	2.41
C	50	51	0.02	2.30	1.7	2.64
	50	109	0.06	3.03	2.7	2.64
D	117	61	0.11	2.58	3.7	2.57

Permeability

The permeability data gathered are interesting. The trend for permeabilities is similar for the porosity in that permeability decreases with increasing depth and with lesser weathering. Generally however the permeabilities are quite low, all zones have permeabilities in millidarcies. Results for Zone A1 are quoted in microdarcies, and it can be seen that the permeability of this zone is relatively low, averaging 1.1 md, compared to the lower weathered zone materials of Zones A2 and B, which have average permeabilities of 61.2 and 5.2 md respectively. Examination of the petrophysical database reveals that except for one sample, Zone B samples have low permeabilities, between about 1 and 2 md. The distribution of highest permeabilities is not static and high permeabilities can be found at many depths in Zone A2, however, studying the petrophysical database one can see that there is a preference for higher permeabilities around a depth of 20 m. Some samples had visible open fractures and display quite high permeabilities. These results could reflect similar fluid pathways in the in-situ material and may be indicative of the major mode of fluid movement in this zone.

Average permeabilities of unweathered rock are all low, less than 1 md. For all sample of the Cahill Formation schists, cores were intentionally cut parallel and perpendicular to the direction of foliation. In the Zone B and unweathered materials, a marked anisotropy of permeability can be seen (the samples have been marked // or _|_ in the petrophysical database) between samples cut perpendicular to schistosity or foliation to those drilled parallel to foliation. The anisotropy was often a factor of 4 or 5 times more flow in cores cut parallel to schistosity compared to core cut perpendicular to foliation.

Figure 5.6:

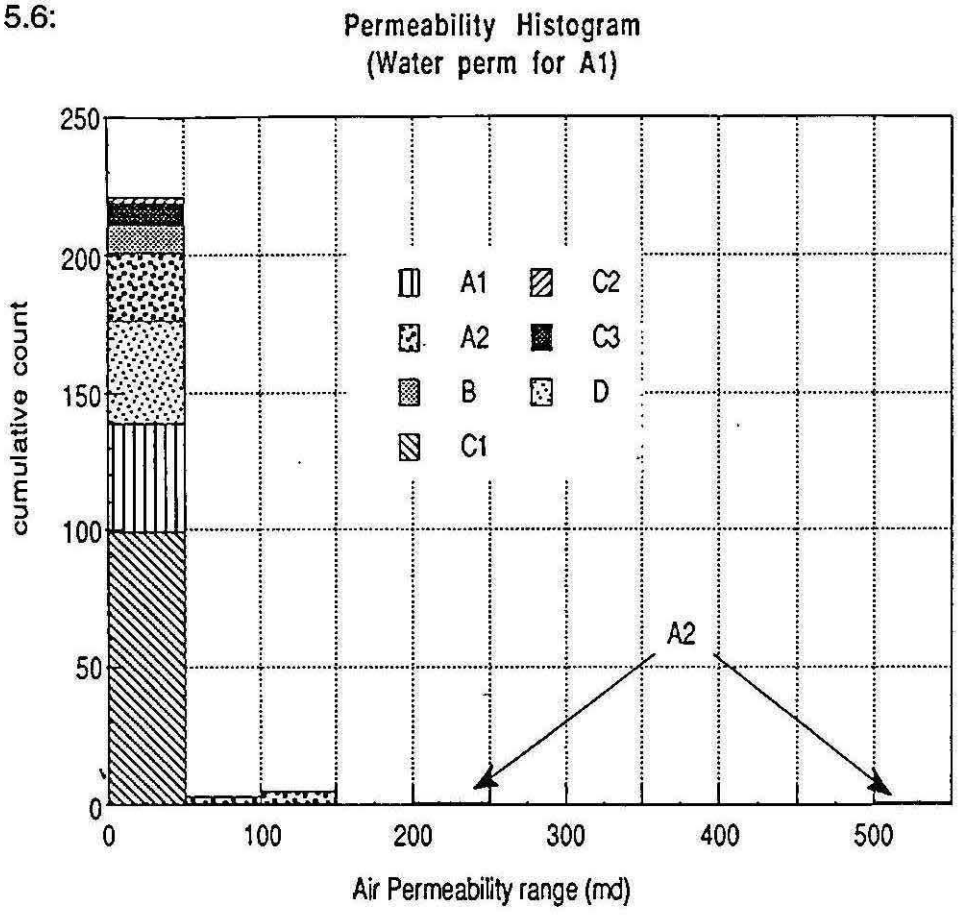

Figure 5.7:

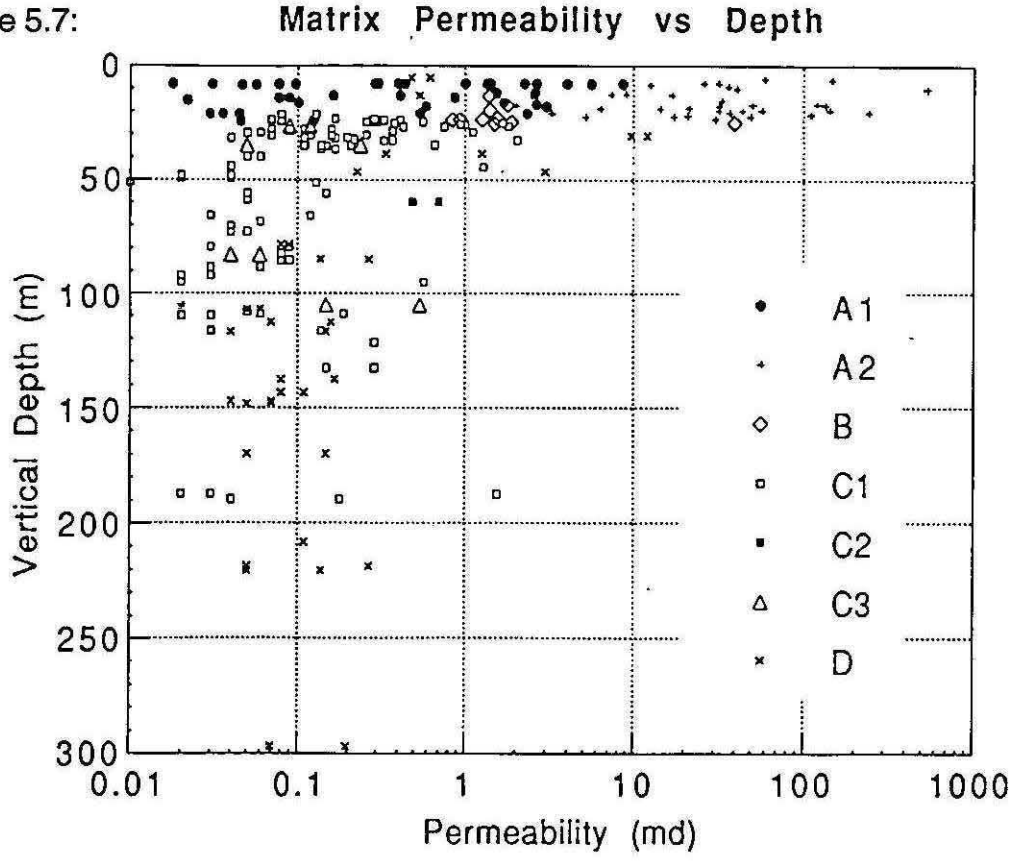

The permeability histogram indicates a clumping of permeability values of all zones in the low range, with only Zone A2 showing high permeabilities.

Two plots of matrix permeability vs depth have been created. The first shows data of all zones and illustrates the higher permeabilities of the weathered materials compared to the unweathered samples. The uniform distribution of permeability (under 1 md) for zones C1, C2, C3 and D can be easily recognised. The second plot shows only the weathered materials. Firstly, the variation in depth of the transitional zone can be appreciated. Secondly, the broad spread of permeability with depth can be recognised. Thirdly, the generally high permeability of Zone A2 can be observed, particularly the vague gathering of high permeability data about the 20 m depth line.

Figure 5.8:

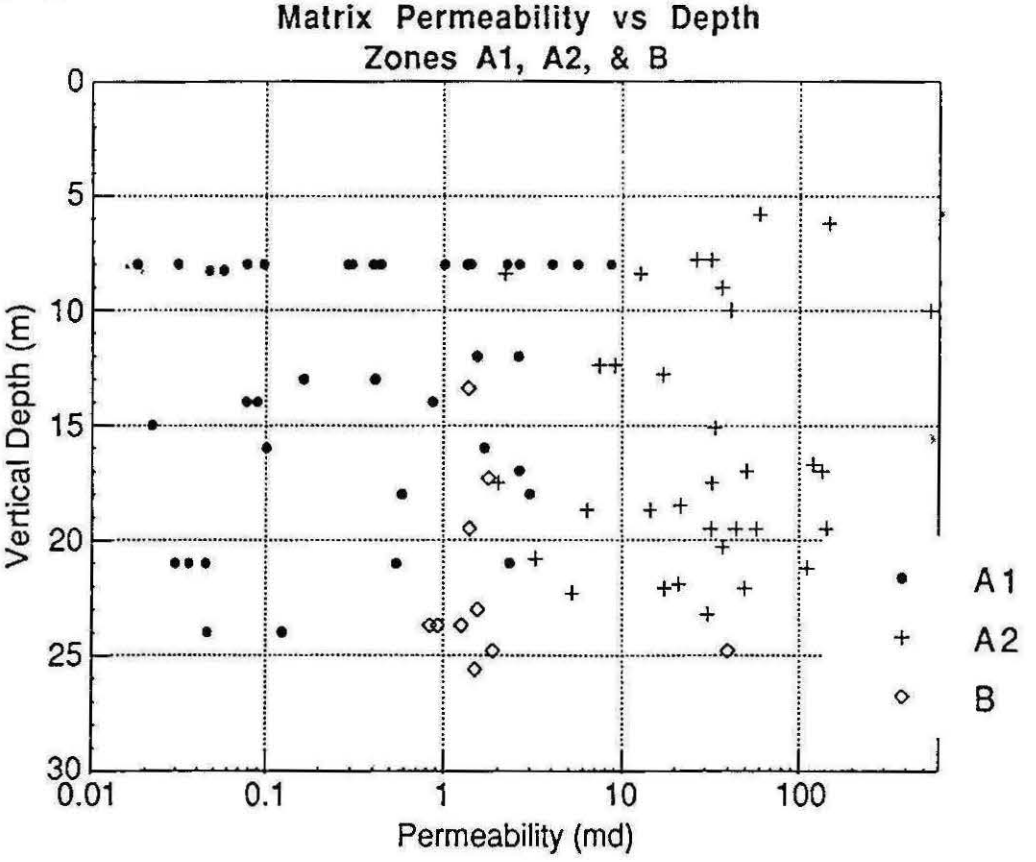

Acoustic Velocity

Acoustic velocities in the materials at Koongarra increase with depth and this is a reflection of the relative strength of the rocks tested. The lowest velocities recorded are from Zone A1, averaging 1582 m/s. Zone A2 and Zone B average 2283 and 2963 m/s respectively. Average acoustic velocities for the unweathered materials are relatively higher; 4894, 4660, 5444 and 4466 m/s for Zones C1, C2, C3 and D respectively. The lower average acoustic velocity of the Kombolgie Formation indicates a greater variation in weathering of the materials sampled.

The P-Wave velocity histogram shows a marked distinction between the velocities of the weathered materials and the unweathered materials, with only a few of the unweathered materials exhibiting velocities lower than 4000 m/s.

The P-Wave velocity vs Depth scatter plot shows very similar characteristics to the Density vs Depth scatter plot, indicating the close relationship between higher density (low porosity) and higher P-Wave velocity. However, in contrast to the density results, the P-Wave velocities do not readily identify lithological differences, particularly between the unweathered schists and the Kombolgie Sandstone.

Further to this, the relationship between P-Wave velocity, density and porosity is readily illustrated by Figures 5.21 and 5.22, Porosity vs P-Wave Velocity and Density vs P-Wave Velocity. In these figures clear correlations can be recognised between increasing porosity and decreasing P-Wave velocity, or increasing density and increasing P-Wave velocity respectively.

Figure 5.9:

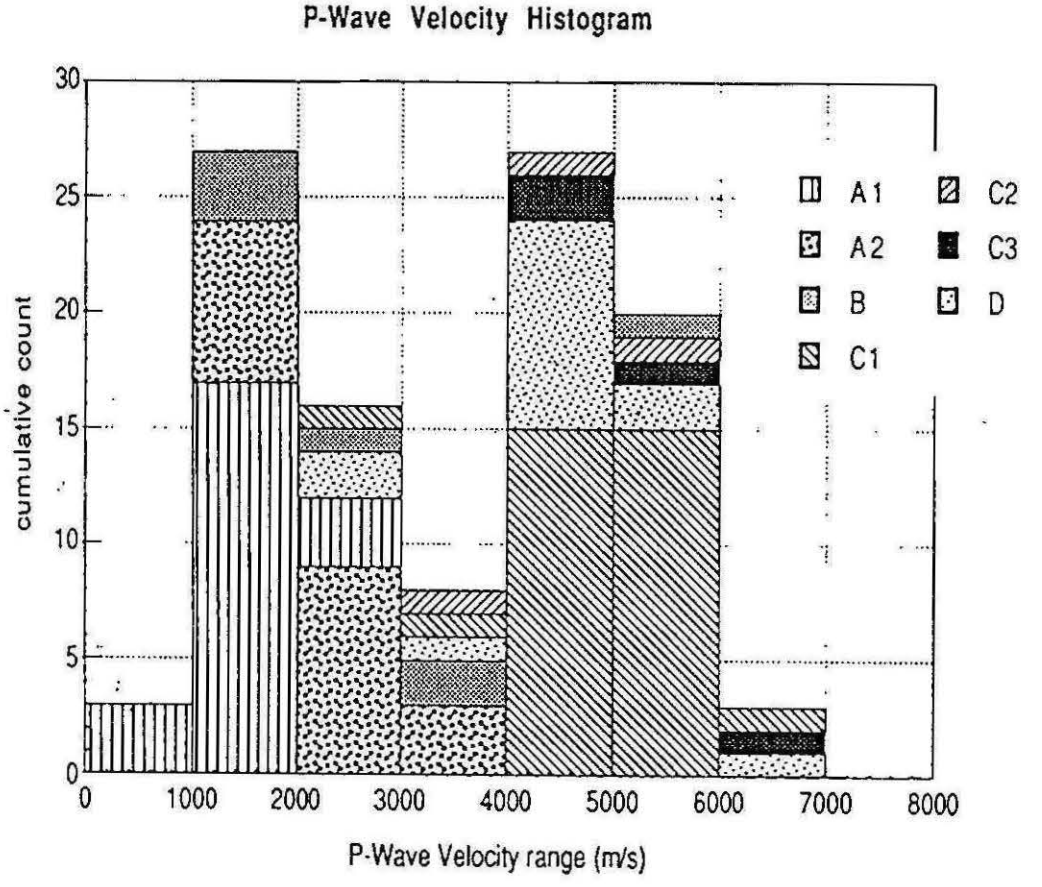

Figure 5.10:

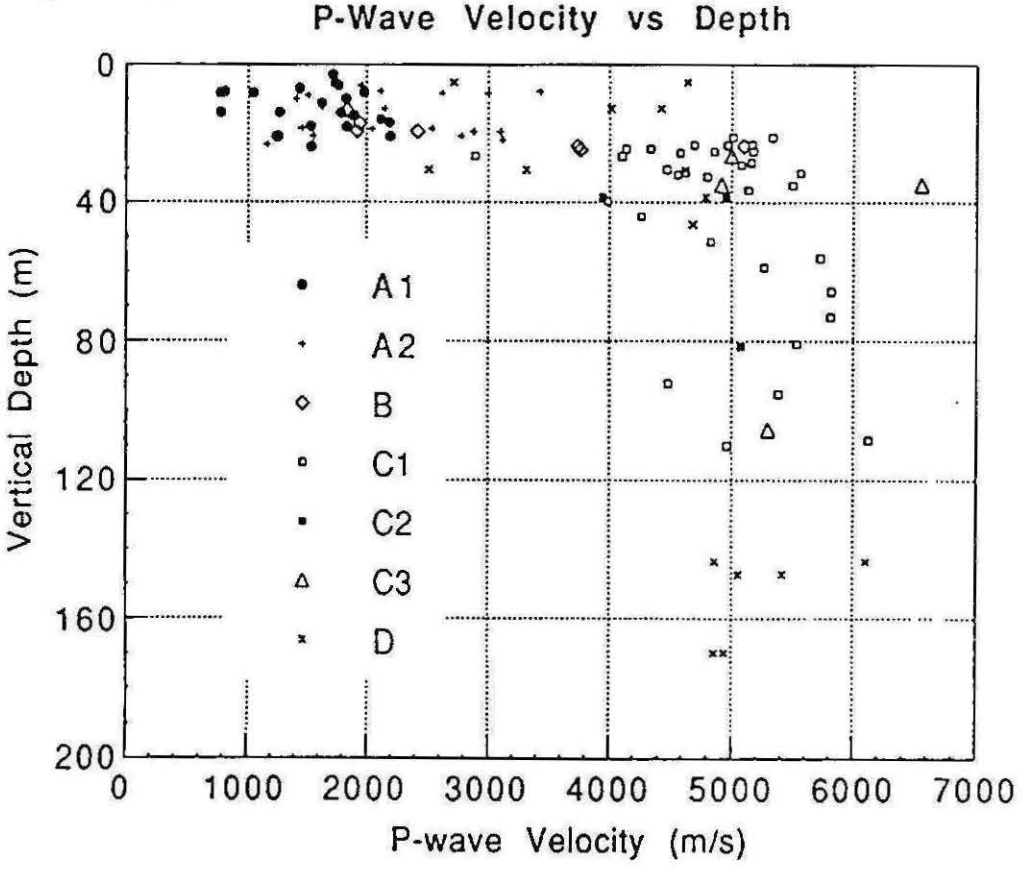

Magnetic Susceptibility

The magnetic suceptibilities distinguished primarily the Kombolgie Sandstone and the amphibolitic units. All lithologies present at Koongarra showed low susceptibilities in general geological terms, the Kombolgie Sandstone showing extremely low susceptibilities (a distinguishing feature) and the amphibolites showing the highest susceptibilities of all lithologies at the site. The three ferricretes tested showed similar magnetic susceptibility to the amphibolites. The Cahill Formation schists exhibited susceptibilities intermediate between these distinctive units. The unweathered Cahill Formation schists displayed a greater range of susceptibilities than the weathered schists and a higher average than Zones A1 and A2. The unweathered schists and the transitional Zone B showed the same average magnetic susceptibility. Clear distinctions between susceptibility ranges of the weathered schists and the unweathered schists are difficult to recognise on the Magnetic Susceptibility vs Depth scatter plot.

Figure 5.11:

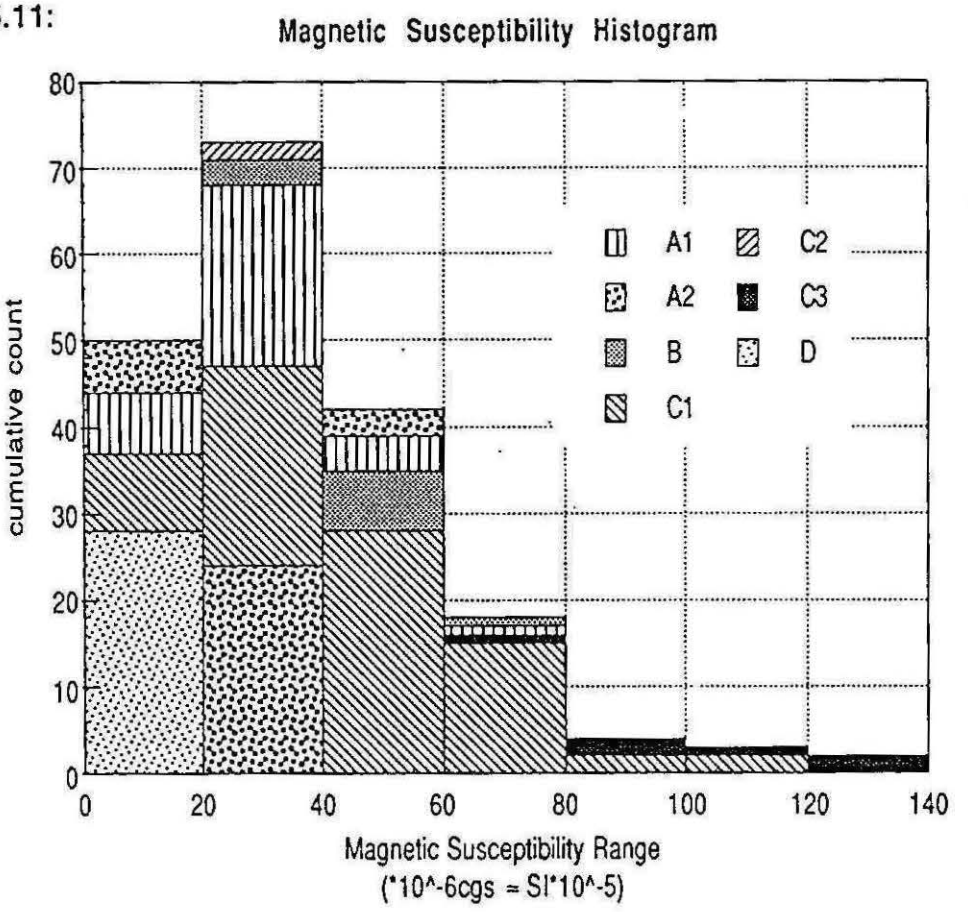

Figure 5.12:

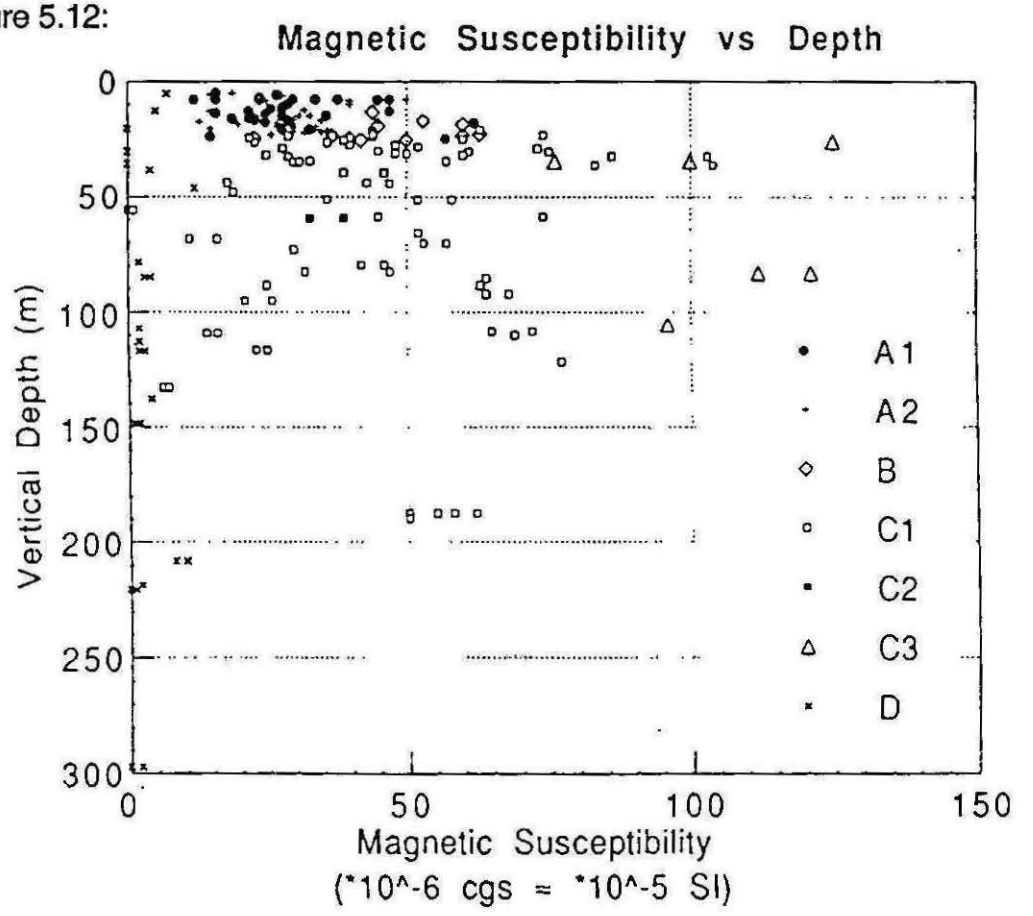

Electrical Resistivity

The resistivity of the rocks at Koongarra reflects a number of different features. Electrical resistivity of a rock is dependent on the degree of saturation of the rock, the salinity of the saturating solution, the porosity distribution, interconnected porosity, temperature, mineral constituents of the rock and the conductive mineral content. In the petrophysical testing program, saturation, water salinity and temperature are known. Thus, the results largely reflect the porosity distribution and interconnected-ness, mineral type and conductive mineral content. If the mineral type is known, particularly in this case the graphitic schists, then the electrical resistivity will be dependent on the type and amount of porosity. These considerations are valuable when considering the resistivity ranges of the various lithologies at Koongarra.

The resistivity results characterise the lithologies at Koongarra well. There is a general increase in the resitivities of the Cahill Formation with depth, excepting of course the graphitic schists. Generally, the range of resistivities for all lithologies at Koongarra is moderate compared to geologic materials (Emerson 1969). The resistivities of the weathered zone materials are relatively low and reflect the higher porosity of this zone. Existent macrofractures or fracture zones within **in-situ** material would result in lower resistivities which cannot be determined by laboratory testing. The increase in resistivity values with depth also correlates with the decrease in both porosities and permeabilities with depth.

Figure 5.13:

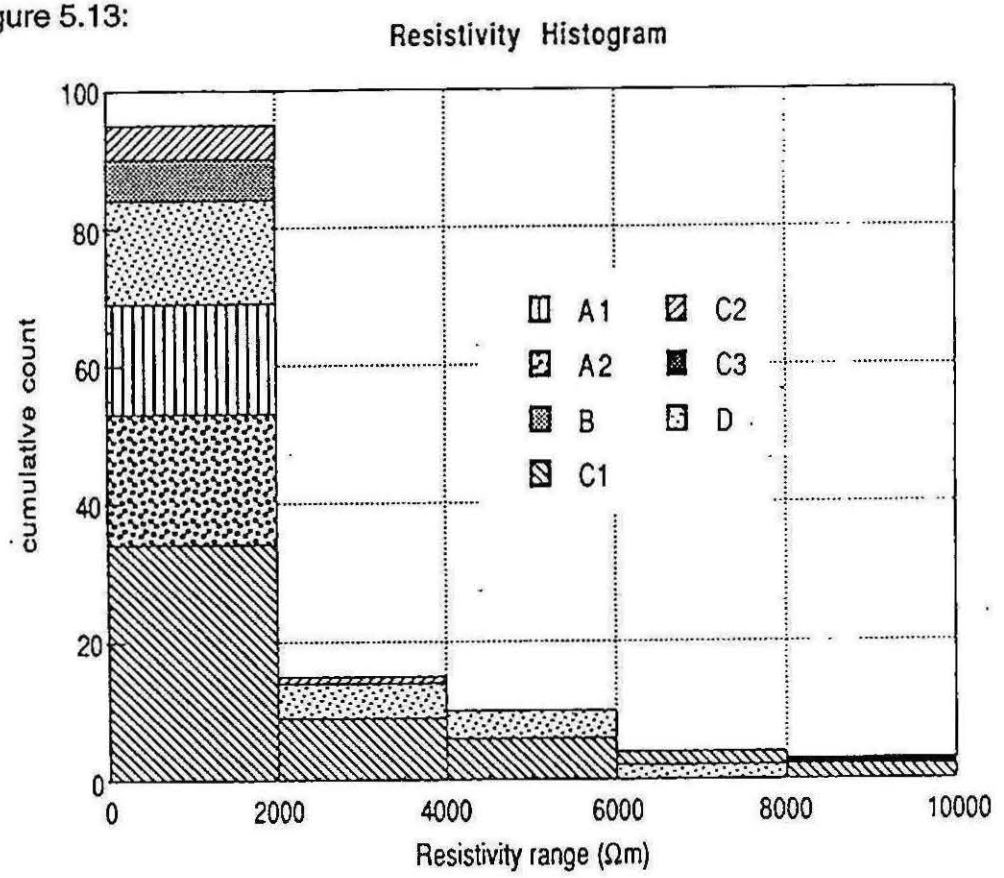

Figure 5.14:

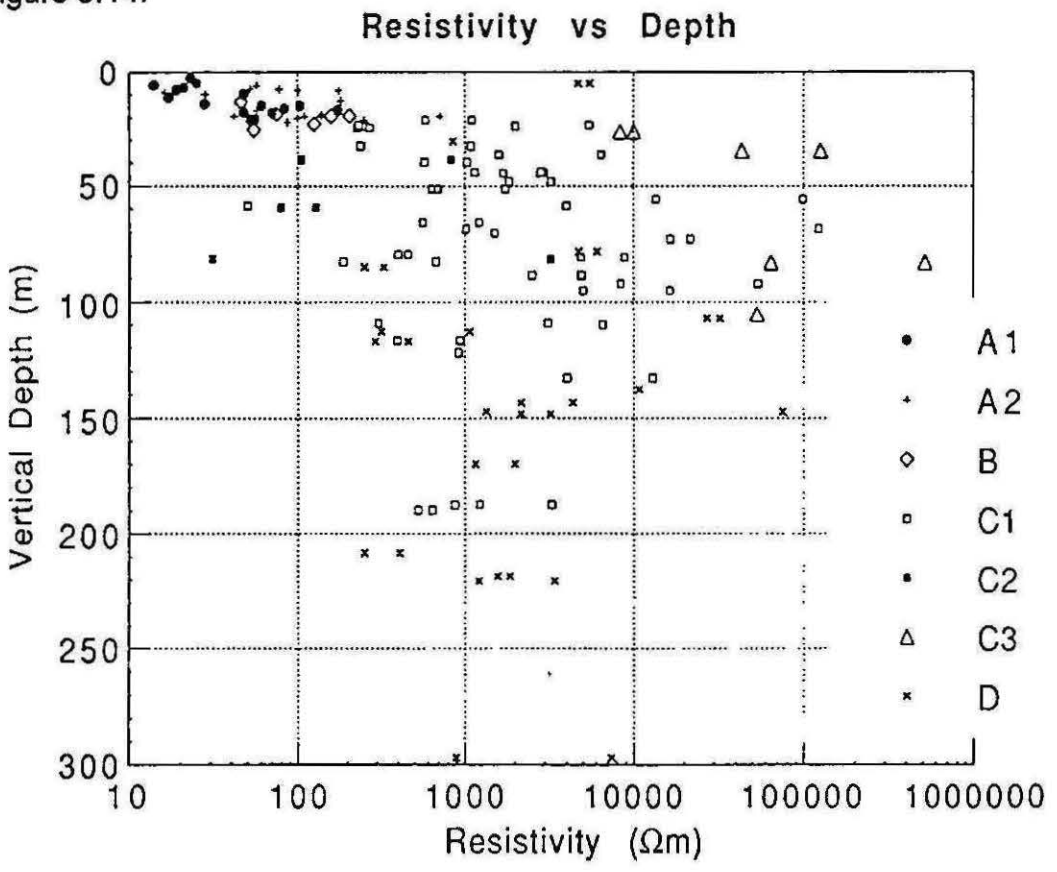

The graphitic schists are generally more conductive than the other Cahill Formation schists. The anisotropy of resistivity along foliation compared to across permeability is marked and corroborates the relationship between resistivity and conductive mineral content. The non-graphitic schists also show a marked anisotropy of resistivity in samples tested in different orientations of foliation, but not as extreme as the graphitic schists.

The resistivity histogram indicates the main features of the resistivity distribution in the lithologies at Koongarra. The weathered zone materials show low resistivities. The unweathered Cahill Formation schists show the highest resistivities, the most resistive being the amphibolites, the least resistive being the graphitic schists. The C1 zone of the unweathered Cahill Formation schists shows the greatest resistivity range, followed by the Kombolgie Sandstone.

The Resistivity vs Depth scatter plot indicates the paucity of high resistivity values at shallow depths, but a broader distribution of resistivities at greater depths, with a bias toward higher resistivity.

Other Cross Plots

A number of comparisons between various petrophysical properties are presented in Figures 5.15 to 5.22.

Figure 5.15: Density vs Magnetic Susceptibility:

This crossplot serves mainly to reflect the lower magnetic susceptibilities of the weathered zone samples which possess lower densities and the higher density and magnetic susceptibilities of the amphibolites. The low density Kombolgie

Sandstone samples are observed to have low magnetic susceptibilities and low densities. The unweathered Cahill Formation Schists show the most broad range of susceptibilities and there is no strong correlation between density and magnetic susceptibility.

Figure 5.16: Density vs Porosity:

A strong inverse relationship can be seen between density and porosity. A particular relationship can be discerned in the samples from Zone A1, all samples possessing low densities and high porosities.

Figure 5.17: Porosity vs Matrix Permeability:

A broad correlation can be seen between the porosity and permeability results, particularly notable are the Zone A2 samples which show corresponding high permeability and porosity. The Zone A1 samples were not plotted as the density results were wet bulk densities. Zone B samples show porosity and permeability ranges which in places correspond with Zone C samples, indicating that this is a region of incipient weathering and that the more profound effects of weathering have mostly not affected the porosity and permeability characteristics of this zone. Generally, however, the distribution of these samples on the scatter plot is in the upper ranges of all samples presented. Zone C samples and the Kombolgie Sandstone show a broad range of porosity values but a relatively restricted range of permeabilities.

Figure 5.18: Porosity vs Resistivity:

A clear inverse relationship can be seen between these properties in the rocks tested at Koongarra, with the exception of the graphitic schists and one C1 zone sample. The highest resistivity and lowest porosity correlation is found in the amphibolitic units.

Figure 5.15:

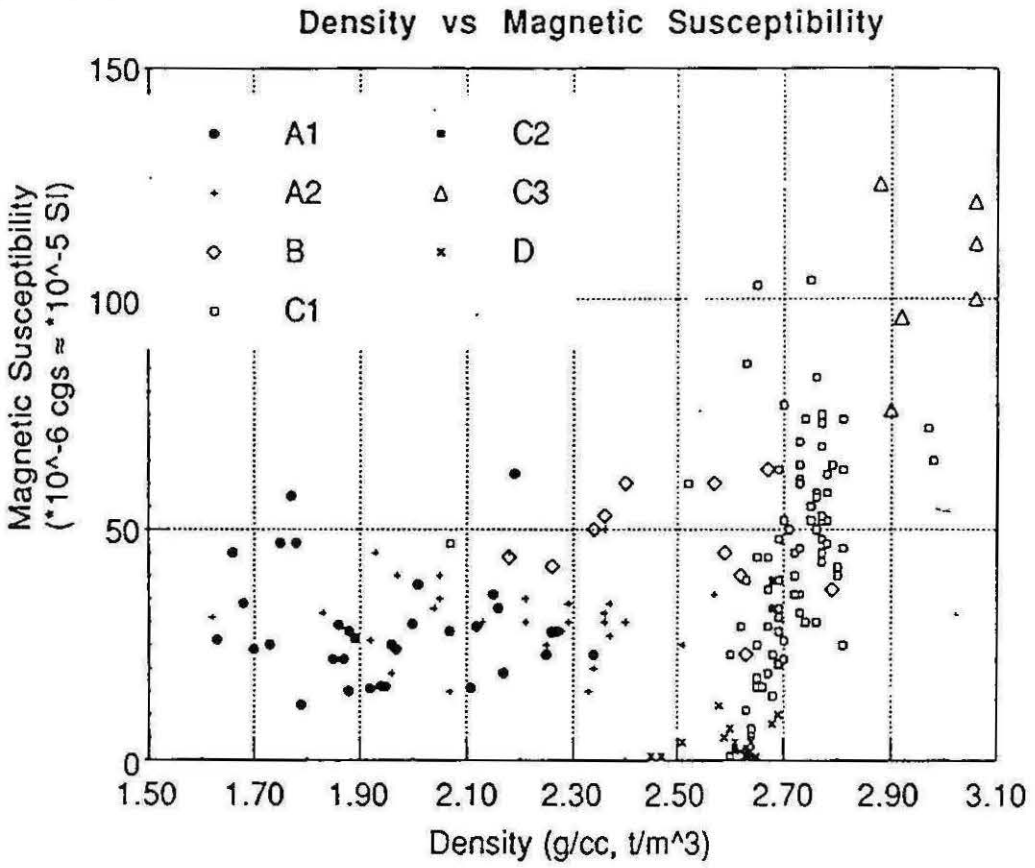

Figure 5.16:

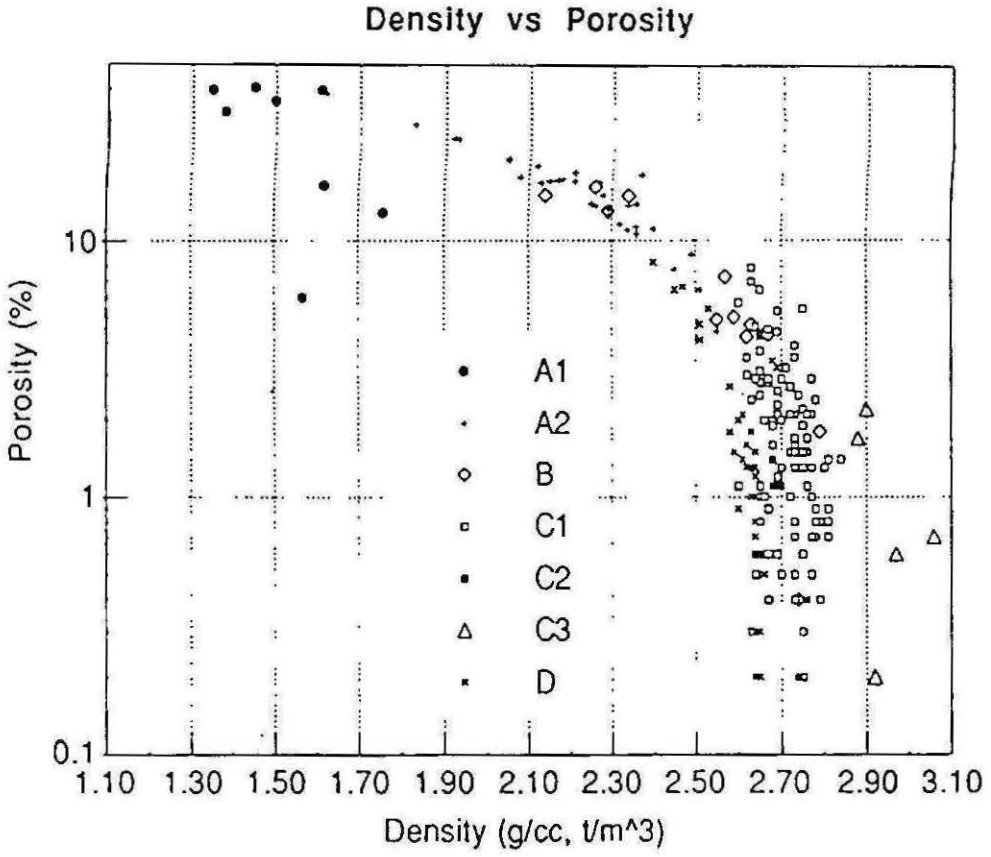

Figure 5.17:

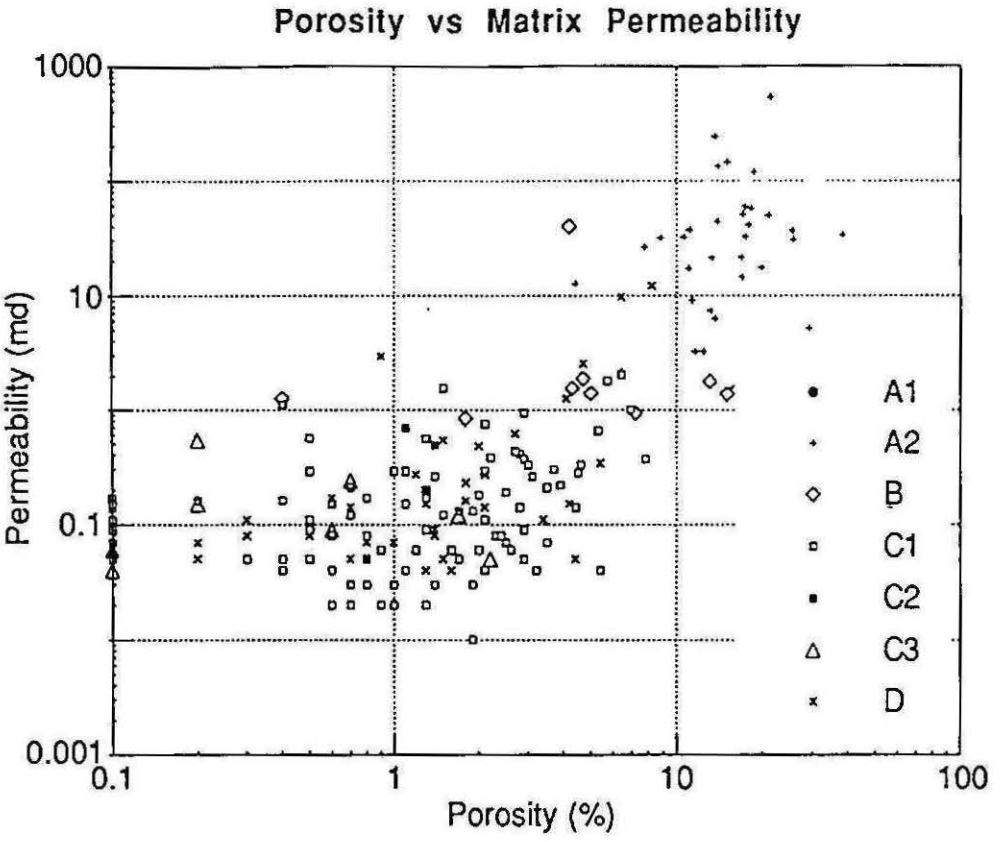

Figure 5.18:

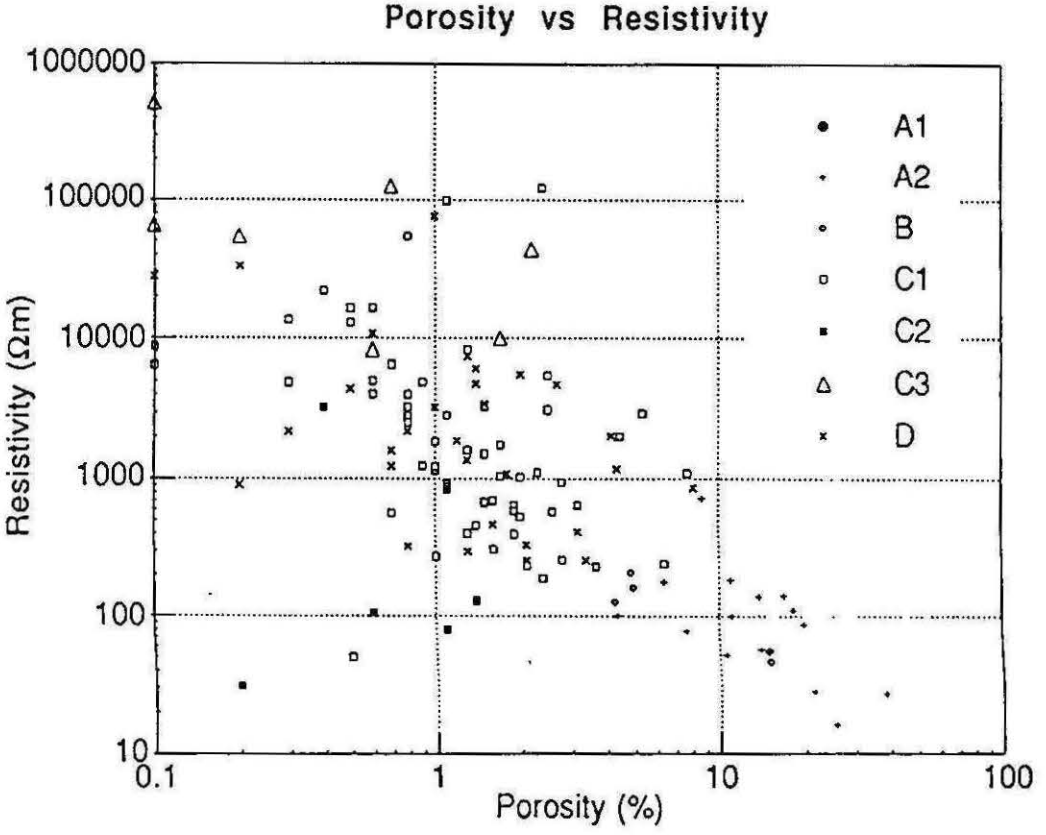

Figure 5.19:

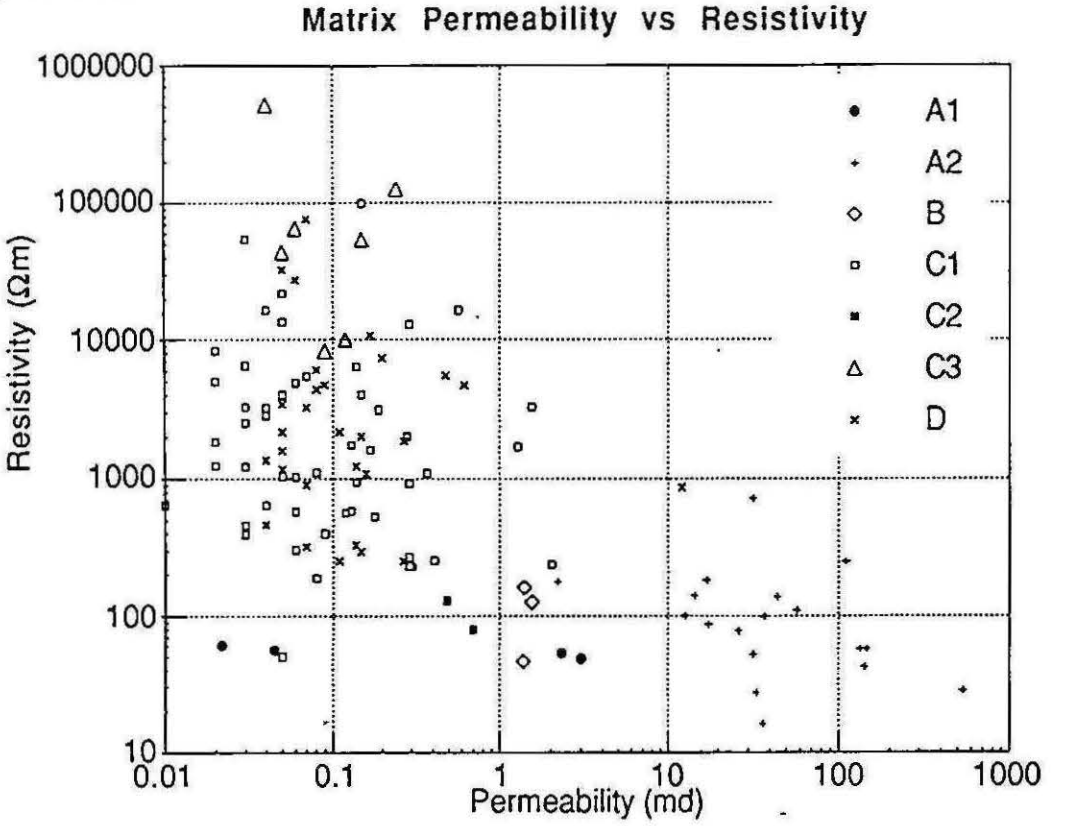

Figure 5.20:

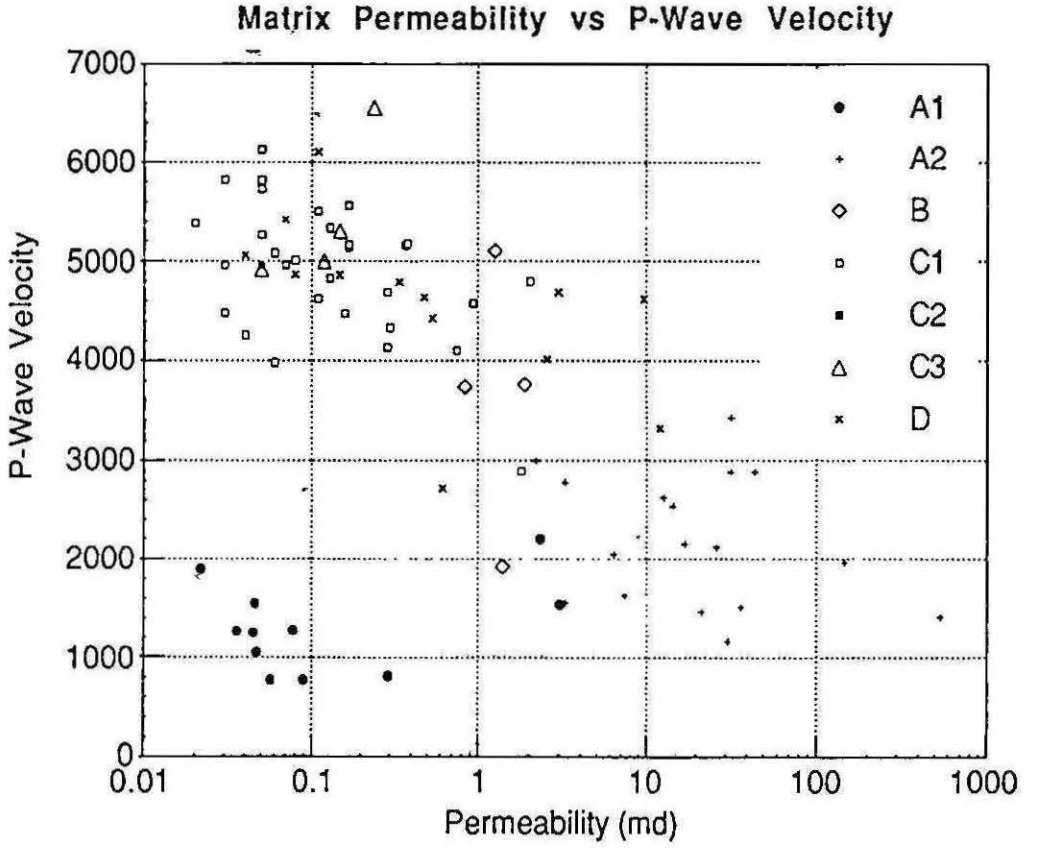

Figure 5.19: Matrix Permeability vs Resistivity:

The correlation between these properties is less distinguishable than some other crossplots, even so, an inverse relationship can be seen. Most notable are Zone A2 samples which exhibit high permeabilities and low resistivities, clearly illustrating the relationship referred to at the beginning of this section. Again the amphibolite samples have the highest resistivities and the lowest permeabilities. The character of the low resistivity and low permeability Zone A1 samples is also clearly illustrated.

Figure 5.20: Permeability vs P-Wave Velocity:

A broad inverse relationship between permeability and P-Wave velocity can be seen. The Zone A1 samples are distinct from the rest of the samples represented due to their very low permeabilities and low P-Wave velocites. It is curious that a more distinct relationship between these properties is not observed, given that a higher degree of fracturing would almost certainly result in lower P-Wave velocities. This may be due to the bias toward cohesive samples in the petrophysical sampling program mentioned earlier.

Figure 5.21: Porosity vs P-Wave Velocity:

A clear inverse relationship can be seen from this crossplot, the weathered zone materials all showing corresponding high porosity and low P-Wave velocity. C1 samples show the broadest spread of results with generally higher P-Wave velocities, excepting a single sample which has a velocity of 2895 m/s.

Figure 5.22: Density vs P-Wave Velocity:

This crossplot shows perhaps the clearest correlation of all the crossplots and reflects virtually the inverse of the porosity vs P-Wave velocity. Since the density reflects the amount of pore space, this crossplot is a strong confirmation of the

earlier mentioned relationship between P-Wave velocity and pore space. Each petrophysical zone is very clearly defined as a distinct zone.

Figure 5.23: DDH 50 and W7 Petrophysical Properties vs Depth

Plots of dry bulk density, apparent porosity, matrix permeability, electrical resistivity, P-Wave velocity and magnetic susceptibility were created of DDH 50 and W7 by this author in order to determine if distinct relationships existed between certain petrophysical properties at different depths, especially permeability, porosity and density in the weathered zone. The plots in fact illustrated the erratic nature of the weathering of rock material at Koongarra, especially at depths less than 20 m. There is a general correlation between the results obtained from DDH 50 and W7 samples, even though the drillholes are not in the same location. The results below the weathered zone reflect similar properties as the crossplots: higher densities, low porosities, low permeabilities and higher resistivities and P-Wave velocities.

Interestingly, the lowest densities and highest porosities occur between about 18 and 15 m depth, after which the density and permeability increase and the porosity decreases. The relationship between depth and degree of weathering is evidently not linear as may have been expected and the erratic and variable nature of petrophysical character in the weathered zone is evident.

Figure 5.21:

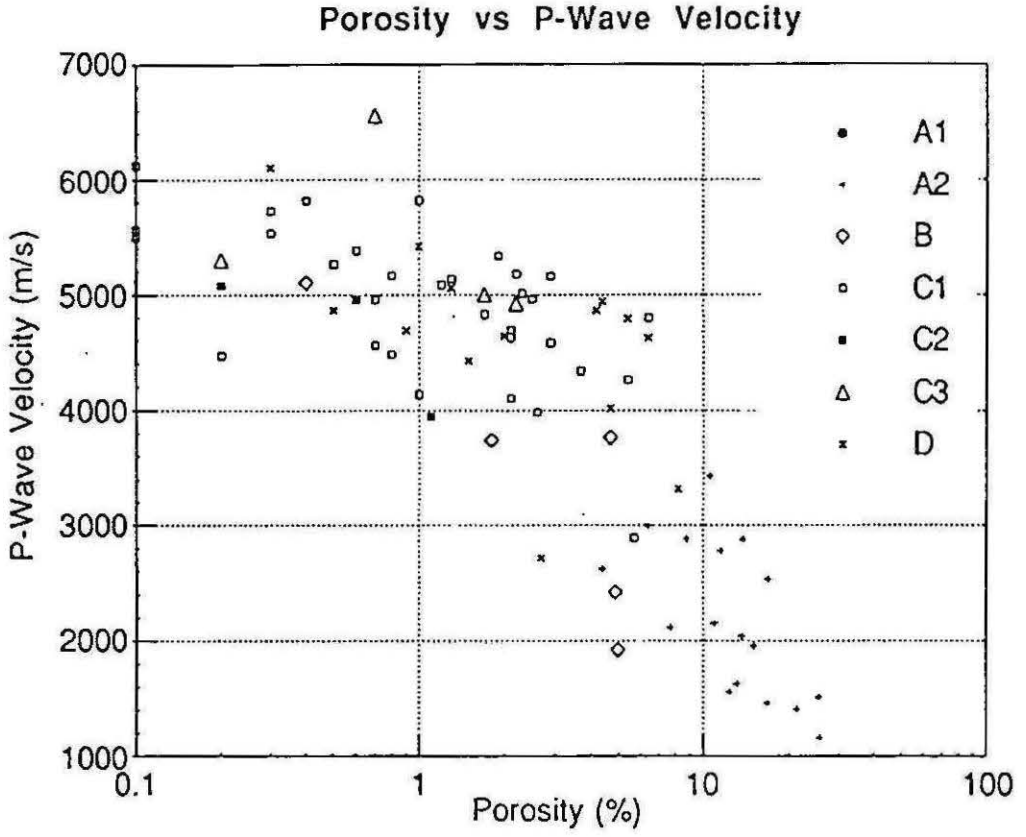

Figure 5.22:

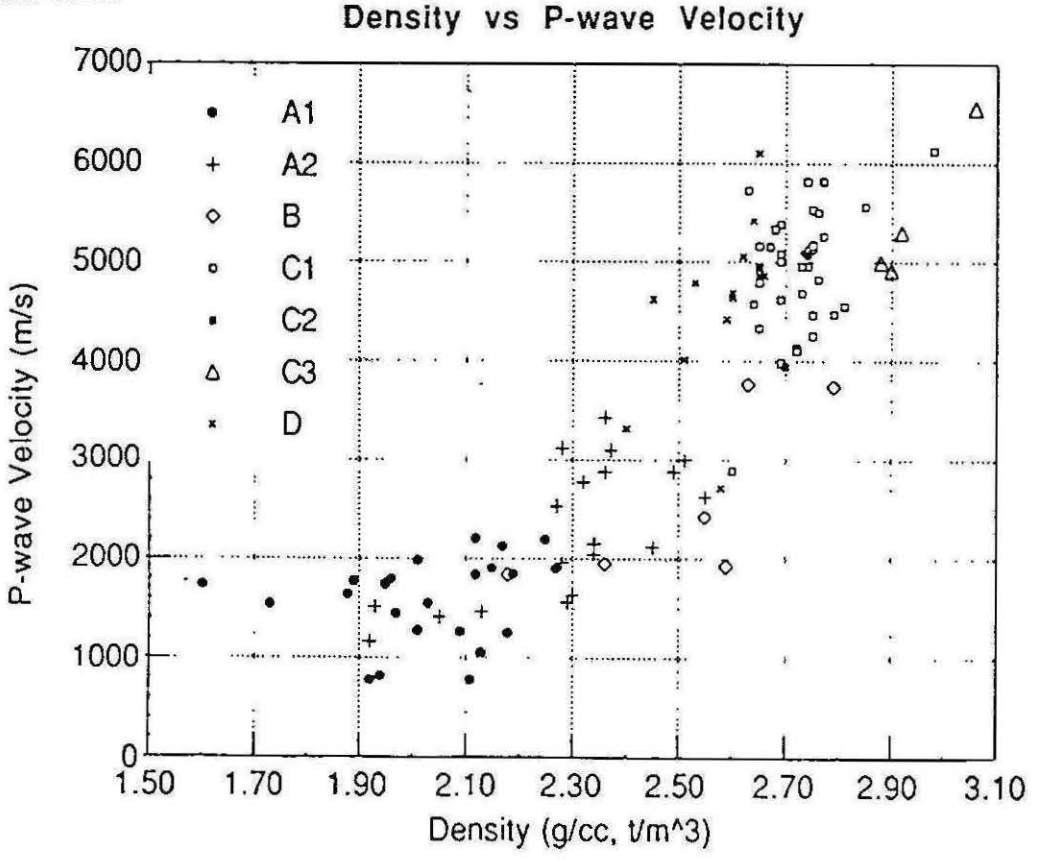

Figure 5.23: A comparison of the physical properties of DDH50 and W7 vs depth.

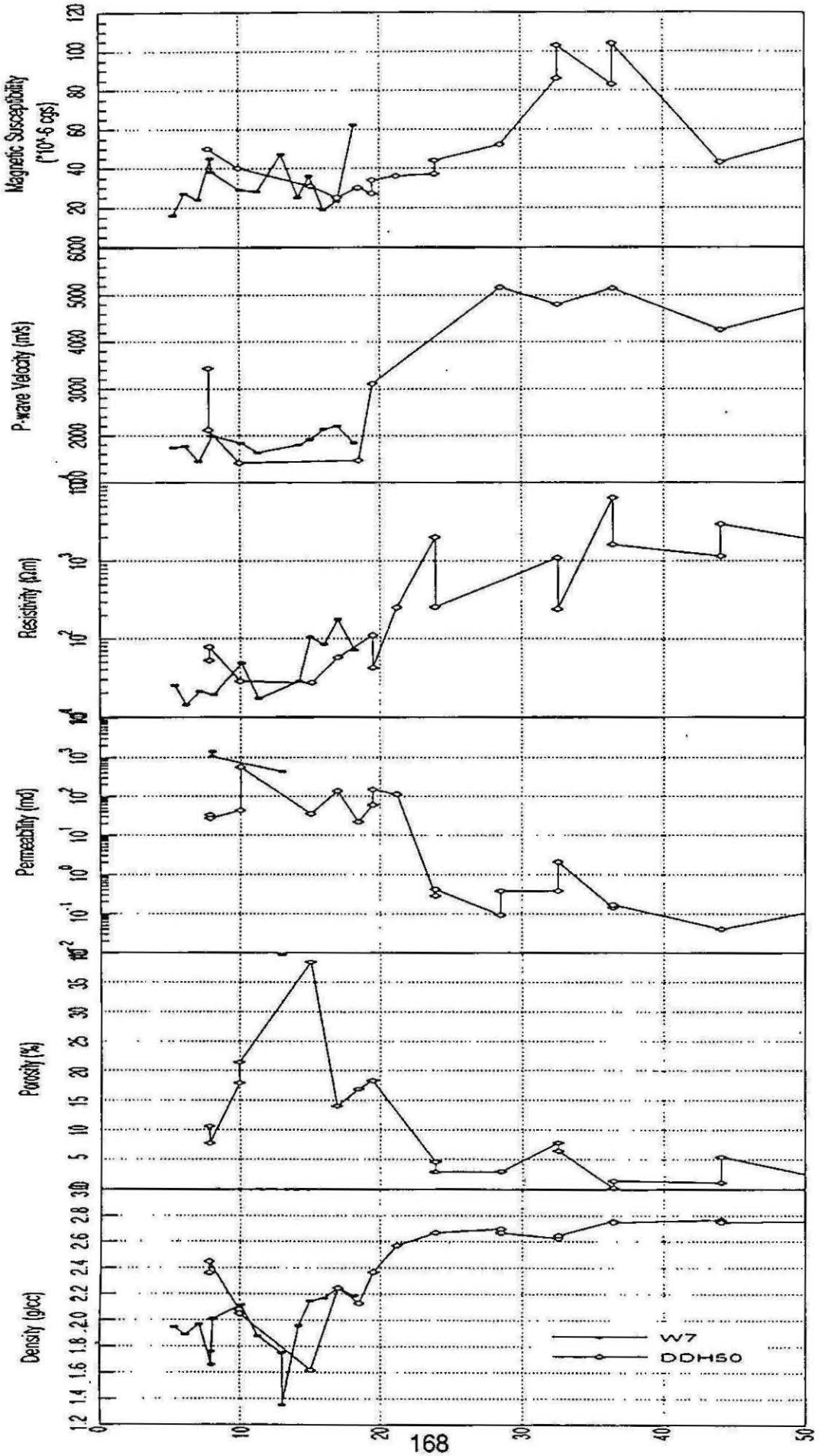

DISCUSSION

The petrophysical data illuminate many features of the lithologies at Koongarra, particularly within the weathered zone. Generally, density increases to a certain point with depth until it is dominated by mineral grain density. Porosity shows a marked decrease with depth, as does matrix permeability. P-Wave velocity reflects the density, porosity and permeability results and increases with depth. Electrical resistivity is seen to be low in the weathered zone, increasing markedly in the unweathered materials. Magnetic susceptibility is relatively low in the weathered Cahill Formation schists, increasing with depth in the unweathered materials. Magnetic susceptibility is extremely low in the Kombolgie Formation and relatively high in the amphibolitic unit. The surficial ferricretes show quite high magnetic susceptibilities, a feature which becomes evident in the geophysical survey results.

Relationships between various petrophysical characteristics have been delineated through the use of depth plots and scatter plots and can be seen in Table 5.4 (in Emerson *et al* 1992, compiled from petrophysical data acquired by this author).

Zone A1 was seen to have high porosity but very low permeability, low density, relatively low magnetic susceptibility and P-Wave velocity and moderate resistivity.

Zone A2 has moderate porosity and (relative to the site) higher permeability, low density, relatively low magnetic susceptibility, low P-Wave velocities and medium resistivity.

Zone B shows a generally low porosity and a moderate permeability, medium density, low velocity and relatively low resistivity.

Zone C1 and C2, comprising the quartz-chlorite-mica and graphitic schists exhibits low porosity and very low permeability, medium density, low magnetic susceptibility, high P-Wave velocities. Resistivities are very high for zone C1 and relatively low for zone C2.

Zone C3, the amphibolitic unit, exhibits low porosity, very low permeability, relatively high density and high magnetic susceptibility for the site, high P-Wave velocity and extremely high resistivity.

Zone D, The Kombolgie Sandstone, exhibits low porosity and permeability, medium density, medium velocity and very high resistivity.

One of the most interesting features to come from the petrophysical studies, especially the permeability studies, is that the highest permeability zone lies within Zone A2, and not in the transitional Zone B. This is a curious feature, not emphasised enough elsewhere and indicates that the zone of greatest fluid flow is not at the base of weathering but rather a few metres above it. This may be a result of the expansion of the weatherable minerals within the rock, which may allow more water movement at a time later than the period of incipient weathering.

TABLE 5.4
PHYSICAL PROPERTY CHARACTERISTICS

ZONE	Lithology	Possible Characteristic Physical Features	Indicative Physical Properties		
			Density (wet bulk) g/cc (approx)	Electrical Resistivity ohm m (approx)	P wave Velocity m/s (approx)
A1	relatively clayey highly weathered Cahill Formation Schists	lowest density, resistivity and velocity	2.0	20 - 50	1600
A2	relatively sandy highly weathered Cahill Formation Schists	low density, resistivity, velocity ; maximum effective voids : relatively high matrix porosity and matrix permeability for the weathered materials	2.2 - 2.5	50 - 150	2300
B	lower weathered 'transitional' schists	intermediate (in properties) between highly weathered and unweathered schists	2.6	100 - 200	3000
C	Cahill Formation Schists				
	C1 quartz-chlorite-mica schists	high resistivity and velocity (but similar to Kombolgie Ss)	2.7	6000	4900
	C2 graphitic schists	low resistivity (compared to other unweathered schists) electrical anisotropy, electrochemical character of complex resistivity response	2.7	700	4600
	C3 amphibolites	highest density, resistivity, velocity, magnetic suscept	3.0	10000	5500
D	Kombolgie Sandstone	very low magnetic susceptibility; high resistivity and velocity (but similar to bulk of Cahill Fm.)	2.6	7000	4500
E	Ferricretes	high resultant magnetisation	magnetic susceptibility and remanence		

CHAPTER 6:

GEOPHYSICAL STUDIES AT KOONGARRA

A number of geophysical surveys were carried out at the Koongarra site by the University of Sydney Department of Geology and Geophysics, as part of the ARAP. The surveys were: magnetic, electromagnetic, self-potential, electrical resistivity and radiometric. This data may be analysed to give auxiliary information relating to the hydrological properties of the site. Additionally, the geophysical responses elicit information about the geology often not evident in surface expression. In certain cases, such as the scintillometer survey, the geophysical results relate directly to the ARAP study, revealing the direction of movement of radionuclides in the upper layers at the site.

Some regional geophysics and other site geophysical studies were available. These included 1:100 000 scale total magnetic intensity contours and total count radiometric profiles as well as a broad 11 km Bouguer gravity grid. Geoterrex Pty Ltd (1990) carried out an airborne magnetic and electromagnetic traverse line across the Koongarra orebody at an elevation of 120 m. Geoterrex Pty Ltd also carried out an EM37, magnetic and gravity survey of 9 lines from 5621 mN to 7023 mN in 1982. Australian Groundwater Consultants carried out electrical resistivity soundings at the Koongarra site which were documented in 1979.

Geophysical Surveys by the University of Sydney

Geophysical surveys by the University of Sydney (including this author) were carried out in a series of trips to the site, the first in August to September 1990, a second from 31 October to 11 November 1990, a third in August 1991 and some additional magnetic traverse lines in November 1991. The surveys were carried out over 13 roughly NW - SE traverse lines and 4 tie-lines, a total of 12 kilometres of data usually at 20 m intervals. The most western line was 5758 mN (8900 ft N), the most easterly, 6560 mE (11000 ft N). Survey size and extent was sometimes limited by geographic features such as topography in the area of the Kombolgie Sandstone. A clear plastic overlay of site geology (at the same scale as the images) is included in a sleeve in the rear of this thesis and is valuable when viewing the geophysical images.

Magnetics

Magnetic data were acquired using a portable proton precession magnetometer. Three images of the Total Magnetic Intensity are presented: Raw data (Figure 6.1); a dataset previously presented in Emerson *et al* (1992) (regridded and imaged by this author, Figure 6.2); and a new magnetic dataset created by this author (Figure 6.3). The latter two of these have been edited to eliminate spikes in the data caused by metallic casings on the boreholes and ferrous refuse in the vicinity of the No.1 orebody. The final dataset was created by this author by editing the ARAP magnetic dataset following the completion of the ARAP Final Report, as it was considered that the data still contained numerous areas influenced by the

presence of metallic borehole casings. Even considering the removal and smoothing of spiky peaks caused by ferrous material, the data still contain areas affected strongly by the borehole casings.

The raw magnetic data provide perhaps the best representation of the magnetic responses of the site, even considering the influence of the boreholes. The image was created using a random gridding procedure of GEOSOFT mapping software, with a grid interval of 5m, approximately 1/4 the spacing of sample points along each survey line. This grid spacing minimises the effects of any large spikes outside a small radius and gives preference to the greater number of datapoints (in this case the background magnetic intensity), over the single point magnetic spikes. Magnetic dipole effects caused by the earth's magnetic field have not been removed. A very minor smoothing algorithm has been applied to the image to eliminate pixel blockiness, and a sunshade from magnetic north has been applied to emphasise strikebound magnetic trends. The sunshade emphasises the irregular nature of the data from line to line. Although diurnal corrections have been made to the data, some effects of survey time differences are evident in the data, especially the tieline at 3352 mE (11000 ft E). A suggestion for further work would be to carry out levelling of the magnetic data from traverse-line to traverse-line and from traverse lines to tie-lines.

Features immediately evident from the raw total magnetic intensity image include the lower magnetic background of the region around the orebodies, north to the Kombolgie Sandstone, and the dominating presence of the magnetic signatures of the metallic boreholes. It is evident that the higher magnetic signature indicated in

the ARAP Final Report Vol. 4 (Emerson *et al* 1992) is mostly due to the effects of borehole casing noise and the grid spacing used to create the Total Magnetic Intensity map. The GEOSOFT gridding procedure utilised by this author better represents the actual distribution of data due to the algorithm and the grid interval used (this author created the magnetic map presented in the ARAP Final Report Vol. 4, so this comment is not surmise).

Emerson *et al* (1992) interpreted some magnetic crosstrends southeast of the No.1 orebody. These can be seen in the raw magnetic data image, continuing to the furthest eastern extent of the survey area (Trend Ai). However, these low lineaments may be merely due to the geometry of the ferrous noise spikes, numerous in this area. Additionally, another north-south trending feature originating at the northernmost corner of the survey area can be distinguished in this image (Trend A ii).

The magnetic background increases gradually from the south of the No.1 orebody and there are some broad magnetic high features centred around 3500 mE, 5800 mN (labelled as Zone B). These features may be due to magnetised surficial laterites developing at the top of the weathered zone.

A long magnetic lineament (Trend C), in the southeast of the survey area running roughly north-northeast to south-southwest is strongly evident. The five separate peaks on this feature are mostly due to the gridding interval and the line spacing rather than discontinuity of the magnetic high band. A magnetic dipole effect can

be seen south of this feature. The position of this feature corresponds approximately to the position of Koongarra Creek.

South of the creek and the magnetic lineament, another broad magnetic high is evident, centred around 6350 mN (Zone D). This feature may be related to surficial ferricretes. No direct correlations can be made between this feature and an interpretation of local lithology and structure interpreted from aerial photography (See Figure 2.2).

Of particular note is a curved magnetic high feature to the west and south of the No.1 orebody, south of 3500 mE and immediately north of the magnetic lineament mentioned in the previous paragraph (Trend E). It is considered that this feature may represent the surficial expression of some magnetic features at depth, for instance a magnetic amphibolitic unit south of Unit C (quartz-chlorite-mica-feldpsar schists - See Figure 3.8), and the curved shape may reflect the fold in the lithologies initially noted from borehole logs studies by this author and the BTV work. The position of this magnetic feature does not correspond to the projected surficial positions of amphibolites from borehole logs (Figure 3.9, this thesis). The distinctly rounded shape of this feature at its most northern point is likely due to the gridding algorithm at the edge of the dataset. It is also interesting to note that this feature is joined to the large magnetic lineament but does not continue south of the lineament. It is considered that the magnetic lineament may therefore represent a magnetic intrusive along a fault, not evident in outcrop, which corresponds to the position of the Koongarra Creek and displaces the Koongarra lithologies.

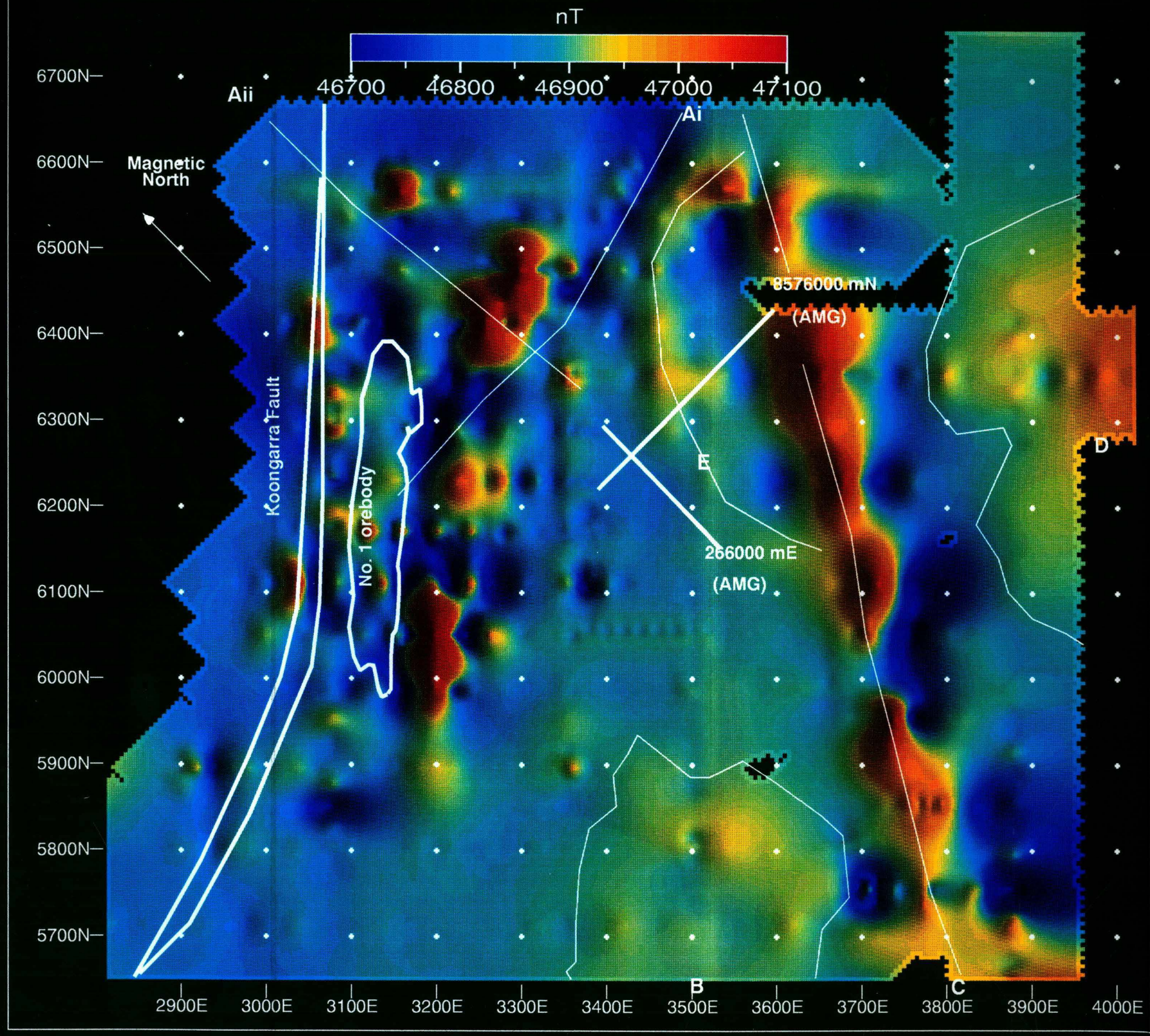

Koongarra Uranium
Deposit
Northern Territory
Australia

Figure 6.1:
Total Magnetic Intensity
Diurnal corrections made

Scale 1 : 5000
AMG Zone 53
Data gathered by the
University of Sydney
1990 and 1991
as part of the
Alligator Rivers
Analogue Project

Images produced by
Michael Hallett
and David Daggar
February 1996.

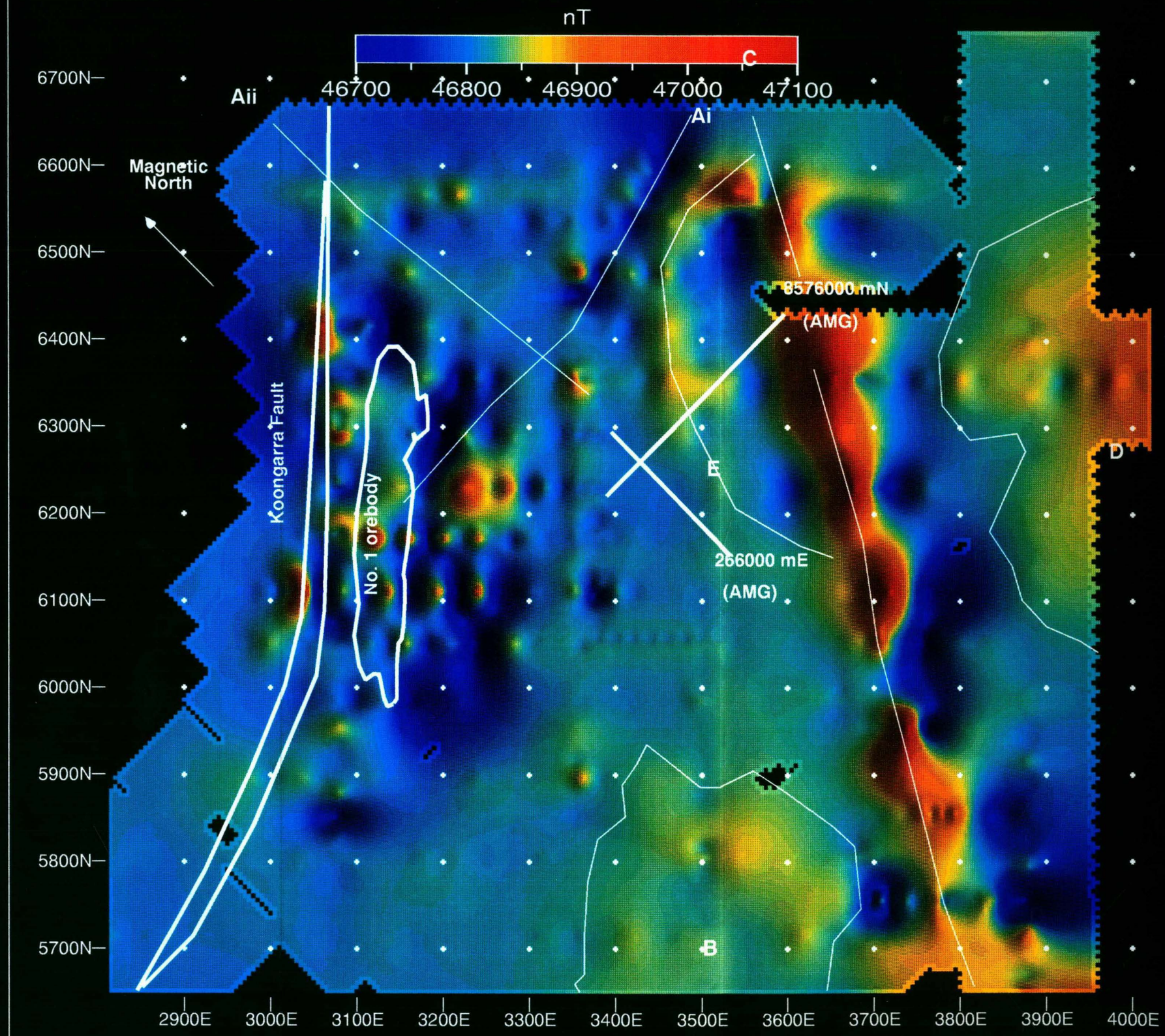

Koongarra Uranium
Deposit
Northern Territory
Australia

Figure 6.2:
Total Magnetic Intensity
Diurnal corrections made,
Borehole spikes removed
Data as presented
in ARAP Final Report

Scale 1 : 5000
AMG Zone 53
Data gathered by the
University of Sydney
1990 and 1991
as part of the
Alligator Rivers
Analogue Project

Images produced by
Michael Hallett
and David Daggar
February 1996.

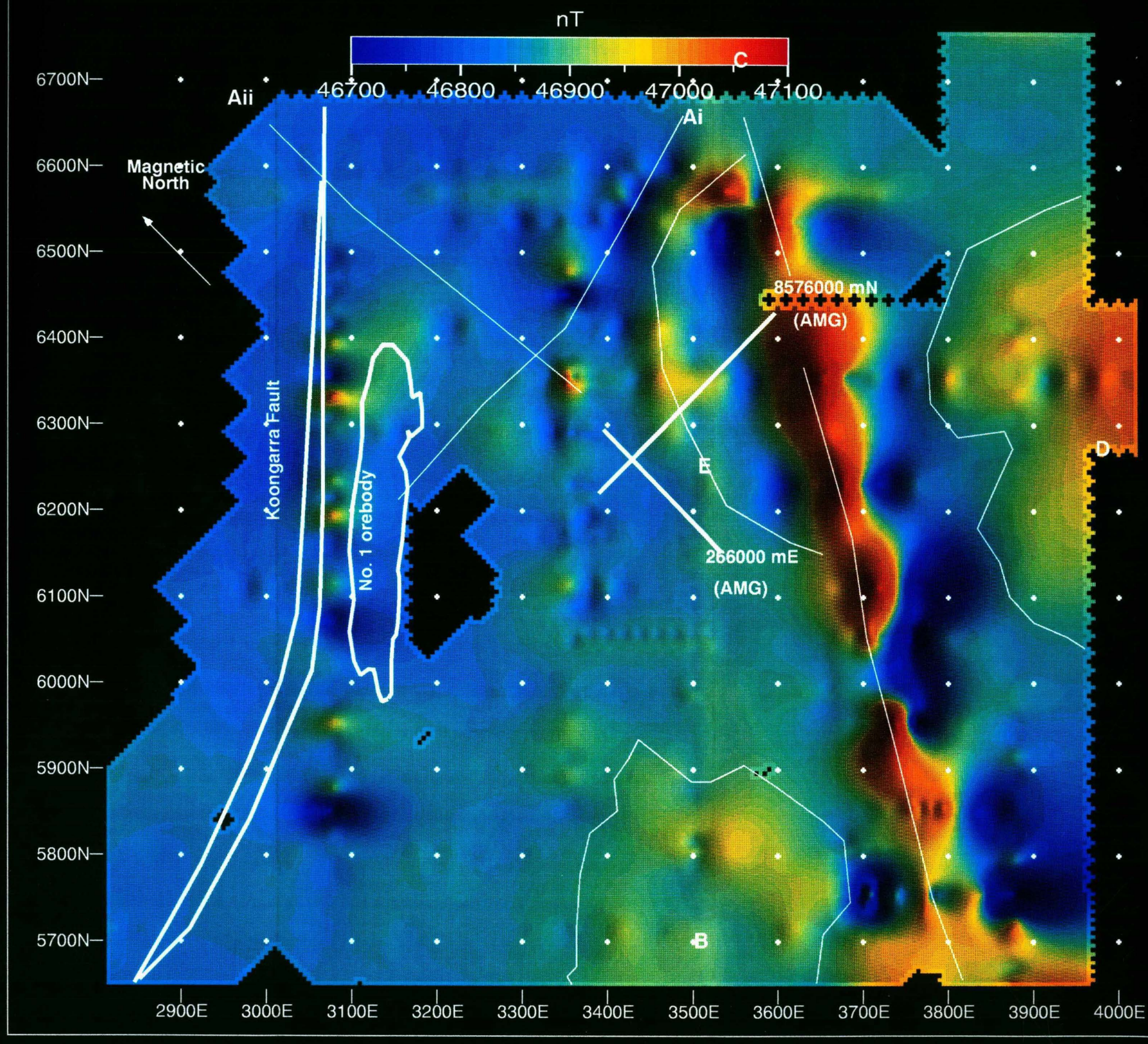

Koongarra Uranium
Deposit
Northern Territory
Australia

Figure 6.3:
Total Magnetic Intensity
Diurnal corrections made,
Additional borehole
spikes removed

Scale 1 : 5000
AMG Zone 53
Data gathered by the
University of Sydney
1990 and 1991
as part of the
Alligator Rivers
Analogue Project

Images produced by
Michael Hallett
and David Daggar
February 1996.

Electromagnetics

A dual coil Geonics EM34-3 electromagnetic system was employed for the electromagnetic survey. This system was operated at 1.6 kHz induction frequency with a 20 m coil separation. Both horizontal dipole and vertical dipole configurations were used to provide apparent resistivities for approximate depths of 15 m (horizontal dipole) and 30 m (vertical dipole). The vertical coil configuration responds better to vertical structures, a useful feature given the almost vertical dip of the units at Koongarra.

The results of the EM34 survey are possibly some of the most useful of the geophysical surveys carried out, as the apparent resistivity data acquired may relate directly to the hydrologic and petrophysical properties of lithologies of the site. The effects of the metallic casings of the diamond drill holes seen in the magnetic data are also evident in the EM34 data.

The most resistive area on the maps is the region north of the orebodies and represents the Kombolgie Sandstone. South of the Kombolgie Sandstone, in the area of the two orebodies, a distinct low resistivity zone can be seen (Zone A), and is most evident on the vertical dipole image. This zone has its origin near the northern end of the No.1 orebody, extending in a southwesterly direction roughly following strike to the southwestern extent of the survey area. This resistivity low may be related to the graphitic hanging wall unit of the mineralised zone, although it is displaced some fifty to a hundred metres from the exact location of the graphitic zone.

The lower resistivity trend continues from the area of the No.1 orebody and extends in a southerly direction from approximately the area of the southern tip of the No.1 orebody (Zone B). This area corresponds to the nose of the fold structure delineated through borehole geological studies by this author and the Borehole Television studies (see Figure 3.8, Geological plan of the site). The implication is that increased fracturing in this zone may have caused increased water saturation of the rock, resulting in lower apparent resistivities. This large trend of lower resistivities is more evident on the vertical dipole configuration image, suggesting that these features are characteristic of the weathered zone at depth, and the more spiky features of the horizontal coil image reflect more laterally limited, surficial features.

Corresponding to the magnetic high lineament southeast of the No.1 orebody are three areas of relatively higher resistivity (Trend C i and Zone C ii). These can be seen on the three "fingers" of the surveys extending south from the main survey area. Trend C I resistivity highs are most likely part of one continuous trend and reflect the electromagnetic features of the magnetic lineament (Trend C from the magnetic image). The location of the southernmost resistive feature of these three corresponds more closely to the broad magnetic high seen to the north of the magnetic high lineament (Zone B in the magnetic images), is slightly less evident in the vertical dipole image and may represent more resistive ferricretes in the shallow subsurface.

Another feature of interest is a trend originating at approximately 6100 mN, extending in a northeasterly direction to the northeasterly extent of the EM34

survey (Trend D). This resistive zone corresponds to the curved magnetic trend mentioned in the previous section and is more evident in the vertical dipole image, suggesting it is a feature at greater depth. It is suggested by this author that the curvature of this feature reflects a curve or fold in some magnetic units not seen in the boreholes and corresponds with the magnetic features seen in this area, suggesting that that the magnetic features are not related to magnetic borehole casing noise nor are simply fortuitous in shape.

Parallel to this structure is another EM lineament (Trend E), which diverges from Trend D in the south. The strongly linear low resistivity area separating the two suggests that these two features are actually one and that the low between the two may be a feature of the gridding. However, the divergence of these two features near the south-east tip of the No.1 orebody is interesting as it persists at depth, in the vertical dipole image.

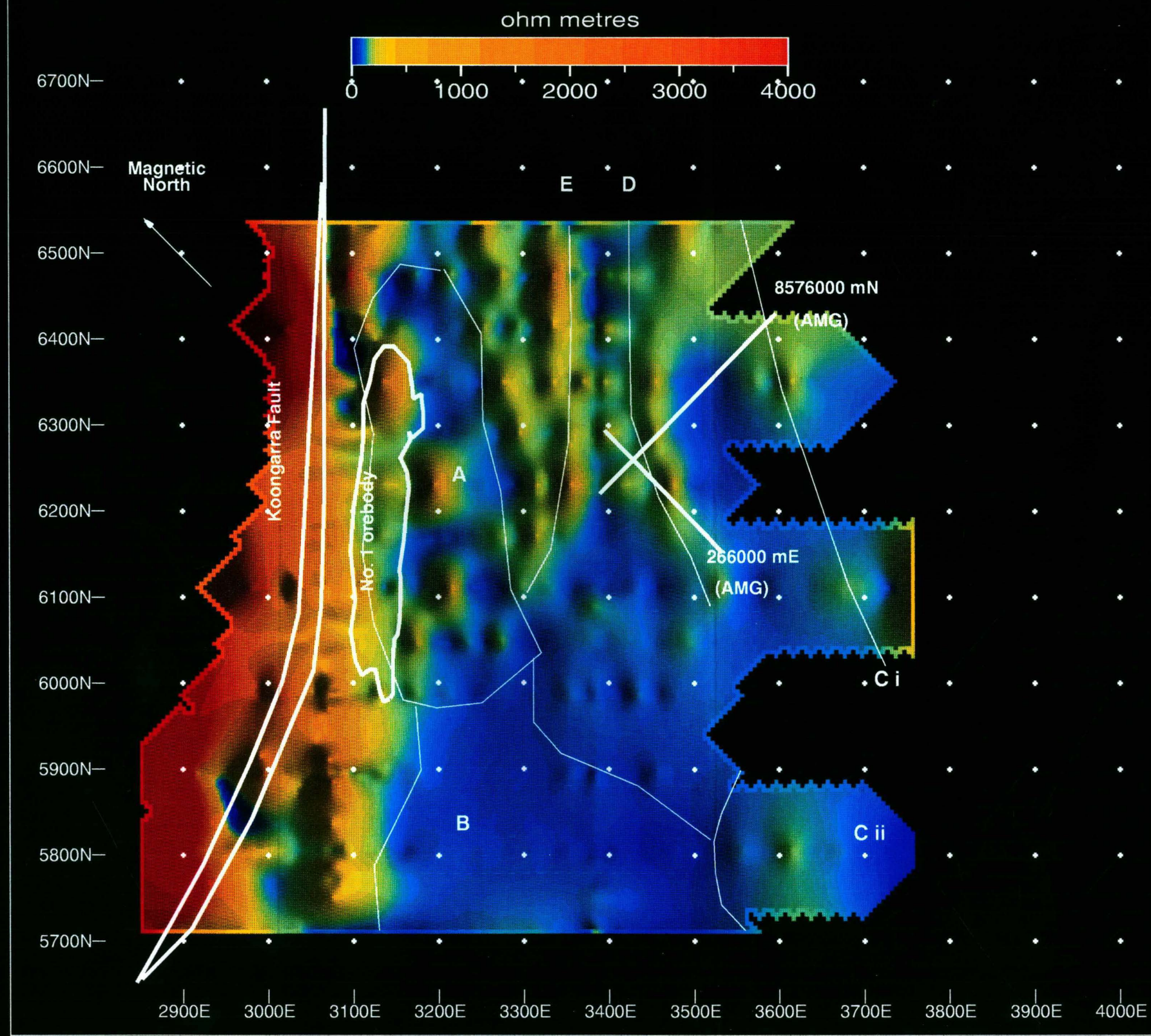

Koongarra Uranium
Deposit
Northern Territory
Australia

Figure 6.4:
Apparent Resistivity
EM34 Horizontal Dipole

Scale 1 : 5000
AMG Zone 53
Data gathered by the
University of Sydney
1990 and 1991
as part of the
Alligator Rivers
Analogue Project

Images produced by
Michael Hallett
and David Daggar
February 1996.

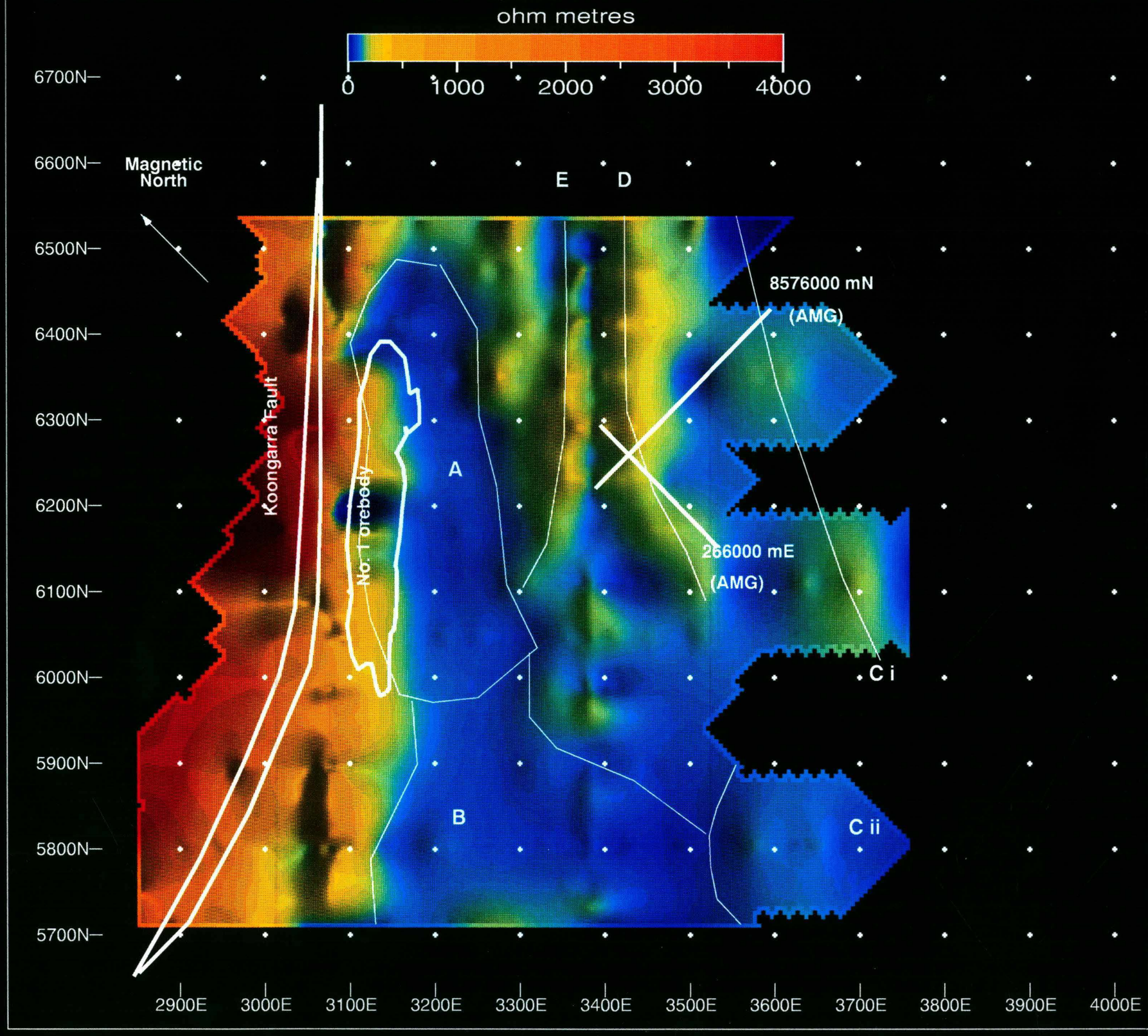

Koongarra Uranium
Deposit
Northern Territory
Australia

Figure 6.5:
Apparent Resistivity
EM34 Vertic al Dipole

Scale 1 : 5000
AMG Zone 53
Data gathered by the
University of Sydney
1990 and 1991
as part of the
Alligator Rivers
Analogue Project

Images produced by
Michael Hallett
and David Daggar
February 1996.

Self-Potential (Spontaneous Polarisation)

The self-potential (SP) method is a relatively little used electrical method in geophysical prospecting. The SP technique gathers data relevant to electrical potential differences in the ground which may be associated with sulfidic or graphitic minerals, or with electrofiltration currents caused by groundwater movement associated with a pressure gradient. Generally, the electric potential difference, thus the electric field and therefore the direction of electrolyte flow is related directly to the direction of the pressure gradient. The SP technique has a depth of investigation of about 15 - 20 m (Corwin 1990) and is thus directly relevant to fluid potential and graphitic units and structure of the weathered zone at Koongarra.

The surveys were carried out by establishing a base station (the potential) and recording potential variations at the site using a moving electrode. The electrode is connected to the base station by wire, through a very high impedance millivoltmeter. Two surveys were carried out, one in November 1990 and the other in August 1991. The survey in November 1990 was the smaller of the two and the survey in August 1991 was carried out to extend the size of the first survey and to create two new easterly cross-lines (3078 mE and 3352 mE), displaced further north and south of the previous crosslines to avoid SP spikes caused by metallic borehole casings in the vicinity of the No.1 orebody which affected the first survey. Thirteen traverse lines were surveyed between 5758 mN (8900 ft N) and 6560 mE (11600 ft N), and four tie-lines between lines 3078 mE and 3352 mE (10100ft E and 11000 ftE) at 20 m intervals.

The results of the two SP surveys are presented separately. The two datasets were merged together and gridded, however, due to the different seasons during which the surveys were carried out, the merged grid was considered to have too many inconsistencies attributable to variations in the water table levels and ground saturation, and was discarded in favour of separate grids of both surveys.

The results from the SP surveys are interesting, reflecting the site geology and structure and correspond well to the EM34 and magnetic data. The SP survey carried out in November 1990 shows different results to the larger survey in August 1991, and most notable is a region of high SP millivolts (Zone A), which is not evident on the later SP survey. This may reflect differences in the groundwater table levels according to the season during which the surveys were carried out. This zone appears to correspond to the position of lithology C (Quartz-chlorite-mica-feldspar schist), however this may be fortuitous. Zone B, a low SP region, corresponds well to the low SP zone on the later survey (Zone G, Figure 6.7).

A negative SP trough which was noted by Emerson *et al* (1992) (perpendicular to the orebody, running approximately along 6270 mN, observed in the SP survey carried out in November 1990, but not in the survey in August 1991), is not strongly apparent in these images.

A large area of negative SP millivolts can be seen on and to the immediate southeast of the No.1 orebody (Zone C). This feature continues to the northern extremity of the survey area and corresponds to the EM34 data. This SP low area may be a response to the hanging wall graphitic unit. However, a narrow SP high

lineament (Trend D) appears to correlate very well to the position of the graphitic unit. The two small peaks on this lineament do not correspond to the positions of any metallic borehole casings.

The Kombolgie Sandstone area north of the reverse fault shows SP high values. Positive anomalies are seen to the southeast of the orebody as small distinct peaks, and there is a large zone of positive millivolts directly east of the northern tip of the No.1 orebody (Zone E). A linear high trend running almost north-south can be seen in the southwest corner of the survey area, joining with the Kombolgie Sandstone highs (Trend F). Directly east of this lineament is a trough of low SP which joins the low SP region around the No.1 orebody (Zone G). This feature is interesting because it is a trend of relatively small magnitude and is interpreted to represent streaming potentials in the shallow subsurface of the site. It is thus relevant to the ARAP study because it is associated with the hydrological properties of the site rather than the mineralogy.

The higher resistivity zones noted in the EM34 survey which correlate to the magnetic high lineament are also evident in the SP data (Trend H) and may represent an area of low fluid flow (an hydrologic barrier).

millivolts

-100 0 100 200 300

6700N
6600N
6500N
6400N
6300N
6200N
6100N
6000N
5900N
5800N
5700N

Magnetic North

8576000 mN (AMG)

266000 mE (AMG)

Koongarra Fault

No. 1 orebody

A

B

2900E 3000E 3100E 3200E 3300E 3400E 3500E 3600E 3700E 3800E 3900E 4000E

Koongarra Uranium Deposit
Northern Territory
Australia

Figure 6.6:
Self Potential
November 1990

Scale 1 : 5000
AMG Zone 53
Data gathered by the
University of Sydney
1990 and 1991
as part of the
Alligator Rivers
Analogue Project

Images produced by
Michael Hallett
and David Daggar
February 1996.

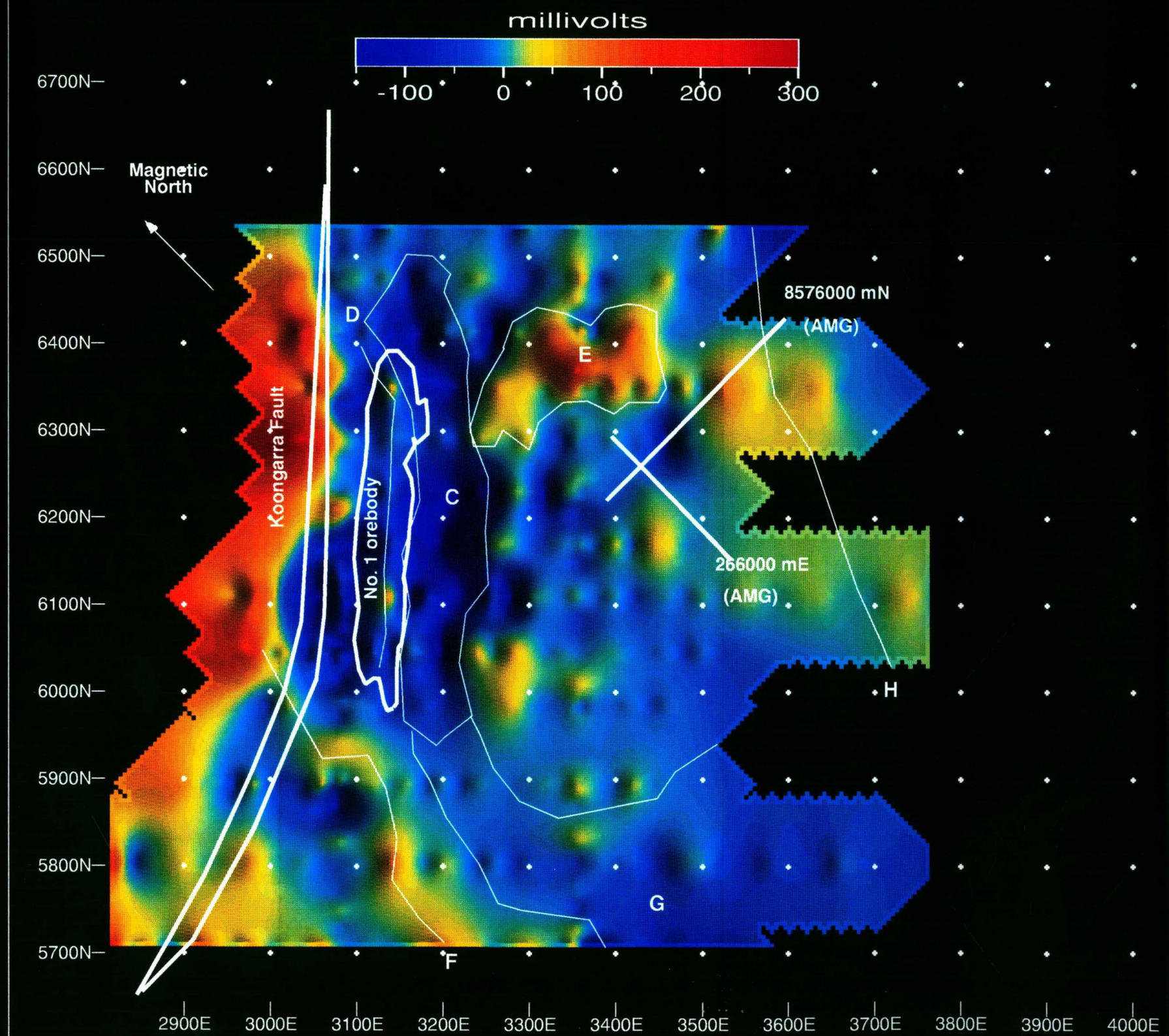

Koongarra Uranium
Deposit
Northern Territory
Australia

Figure 6.7:
Self Potential
August 1991

Scale 1 : 5000
AMG Zone 53
Data gathered by the
University of Sydney
1990 and 1991
as part of the
Alligator Rivers
Analogue Project

Images produced by
Michael Hallett
and David Daggar
February 1996.

Electrical Resistivity

Direct Current (DC) electrical resistivity profile traverses were carried out using the Wenner Array method and the Pole-Dipole method. The resistivity method can delineate the apparent resistivities of the ground and thus reveal information pertaining to the petrophysical database and also to the factors affecting bulk resistivity including conductive mineral content, rock porosity, interconnected porosity and degree of saturation of the rock matrix.

Wenner and pole-dipole array resistivity traverses were carried out along lines 3104 mE and 3200 mE and 6050 mN, 6105 mN, 6107 mN, 6230 mN and 6290 mN. Wenner array traverses were carried out with 20 m, 40 m, and 80 m spacings and pole-dipole arrays with 20 m, 40 m and 60 m spacing.

The section 3200 mE runs directly through the Koongarra No.1 orebody. This section clearly indicates a layering of resistivity characteristics, generally reflecting the petrophysical data. It must be noted that the resistivity psuedosection is only representative of the true resistivity of the rock fabric and due to the scale of investigation, naturally indicates only an average of resistivities for a given x, y, z location. To the southwest end of the 3200 mN pole-dipole array section, lower resistivities extend deeper (80 ohm m deeper than 25 m) and represent deeper weathering in this area. Higher resistivities are seen at the far southwestern end of the 3200 mE section and may represent unsaturated surficial materials such as sands.

The 6170 mN resistivity section traverses the No.1 orebody and clearly shows high resistivity corresponding to the position of the reverse fault and the Kombolgie Sandstone. Further to the southeast, the resistivity becomes lower and begins to reflect the layering seen in the 3200 mE section, indicating the medium resistivities of the Cahill Formation schists.

Figure 6.8:

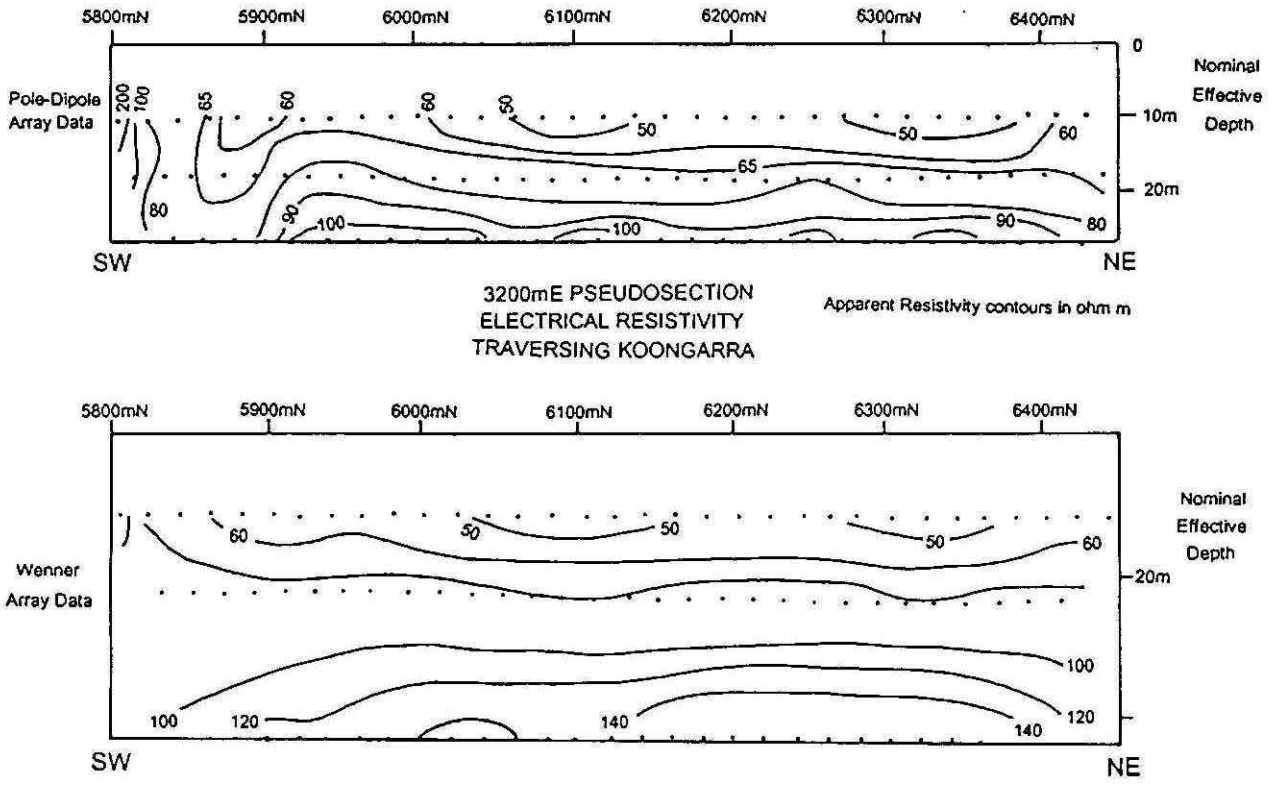

Figure 6.9:

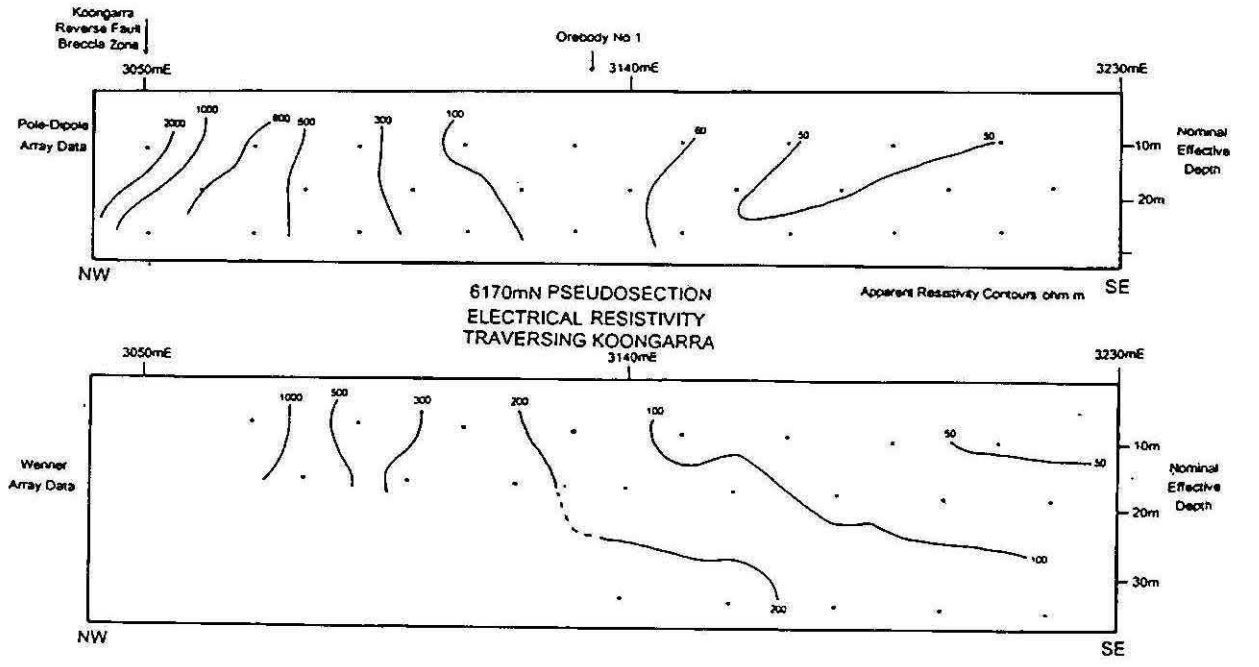

Radiometrics

Two radiometric surveys were carried out, one using a total count scintillometer and the other with a DISA-400 scintillometer (giving K, U and Th counts per second), both with a window setting of 0.5 to 3.0 MeV. The DISA-400 survey was limited to a smaller area around the south and southeast of the No.1 orebody due to the time necessary for the readings (2 minutes). For both methods, the reading reflects radioactive materials from the upper few metres of soil or weathered rock, and does not necessarily represent the motion of radionuclides at greater depth. Cao (1992) presented uranium concentration contour maps at a variety of different depths produced from borehole studies carried out by ANSTO.

The total count scintillometer data indicate a distinct lobe of radioactive material migrating in a southerly direction from the main orebody. Two areas of highest radioactivity are evident, these actually lying approximately 50 m southeast of the main orebody. This suggests that the greatest concentration of radionuclides has migrated approximately 50 m during the time which it has taken from the first mobilisation of the nuclides in the dispersion fan to the present.

The lobe to the south from the southern tip of the No.1 orebody correlates both with the EM34 and SP data, suggesting that the conductive zones in this area, probably caused by increased fracturing around the nose of the fold (delineated by the geological studies of this author and the Borehole Television work), may have been preferential channels of radionuclide migration.

The DISA-400 K-U-Th survey data are presented as cps. These data were previously presented by Cao (1992) but it appears that the calculation from counts per second to percentage potassium or parts per million thorium or uranium are erroneous, as the percentage potassium values are all negative and are actually lowest in the vicinity of the orebody. Given that the potassium counts are sometimes above 7500 counts in two minutes, it may have been that the volume of material used to calculate the percentage potassium (and thus the stripping ratios) may have been too great, or that an accidental inversion of the data occurred.

The K-U-Th data are presented instead as counts per second (cps), and appear not to indicate any particular plumes emanating from the south end of the No.1 orebody, rather just a relatively even spread of data, and the counts per second become gradually less with distance from the orebody. It is interesting to note that the southern end of the orebody does not show high counts of any of potassium, uranium or thorium, the high reading proximal to the orebody does not extend further south than approximately 6100 mN.

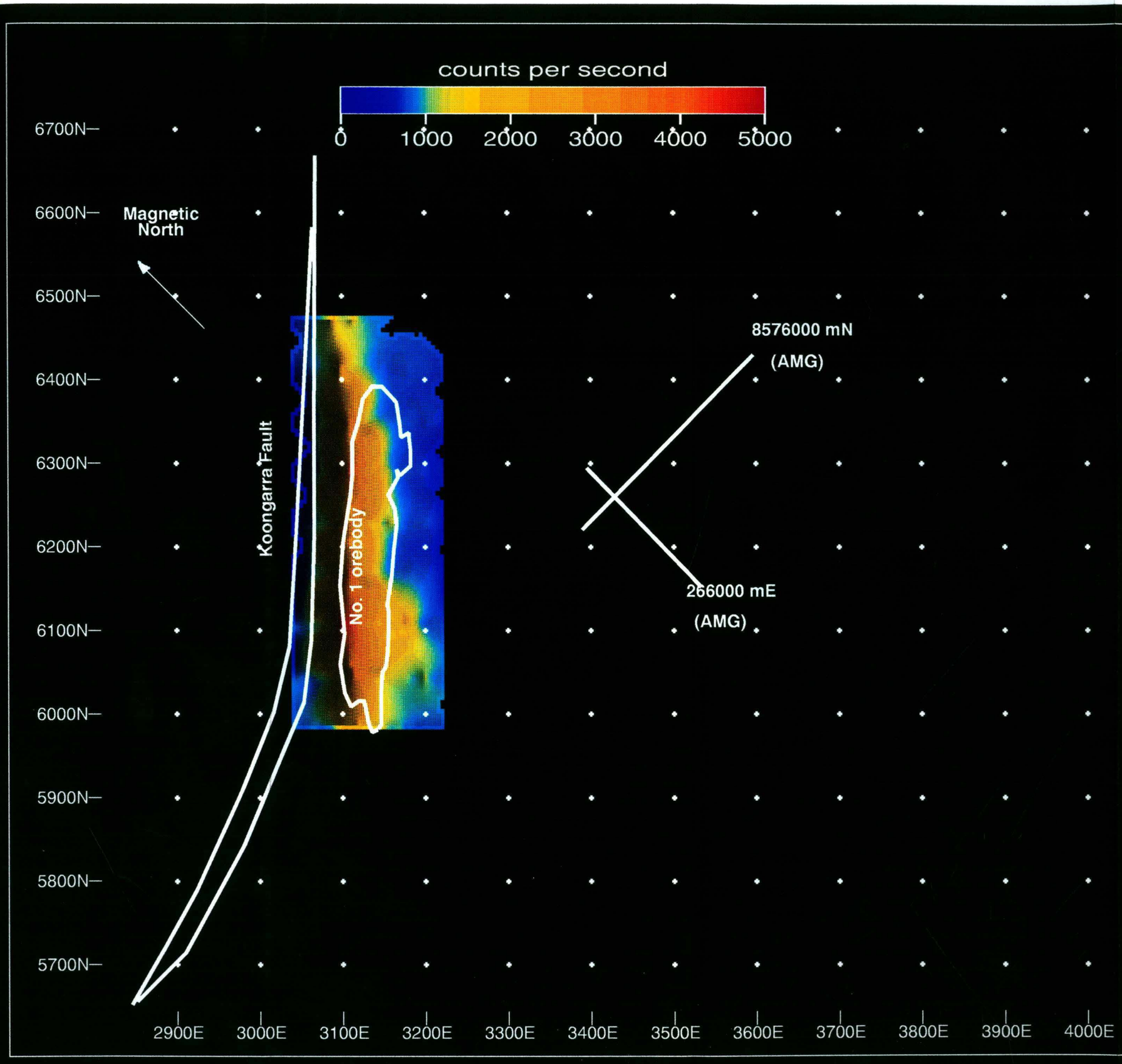

Koongarra Uranium
Deposit
Northern Territory
Australia

Figure 6.10:
Image of Scintillometer
total count

Scale 1 : 5000
AMG Zone 53
Data gathered by the
University of Sydney
1990 and 1991
as part of the
Alligator Rivers
Analogue Project

Images produced by
Michael Hallett
and David Daggar
February 1996.

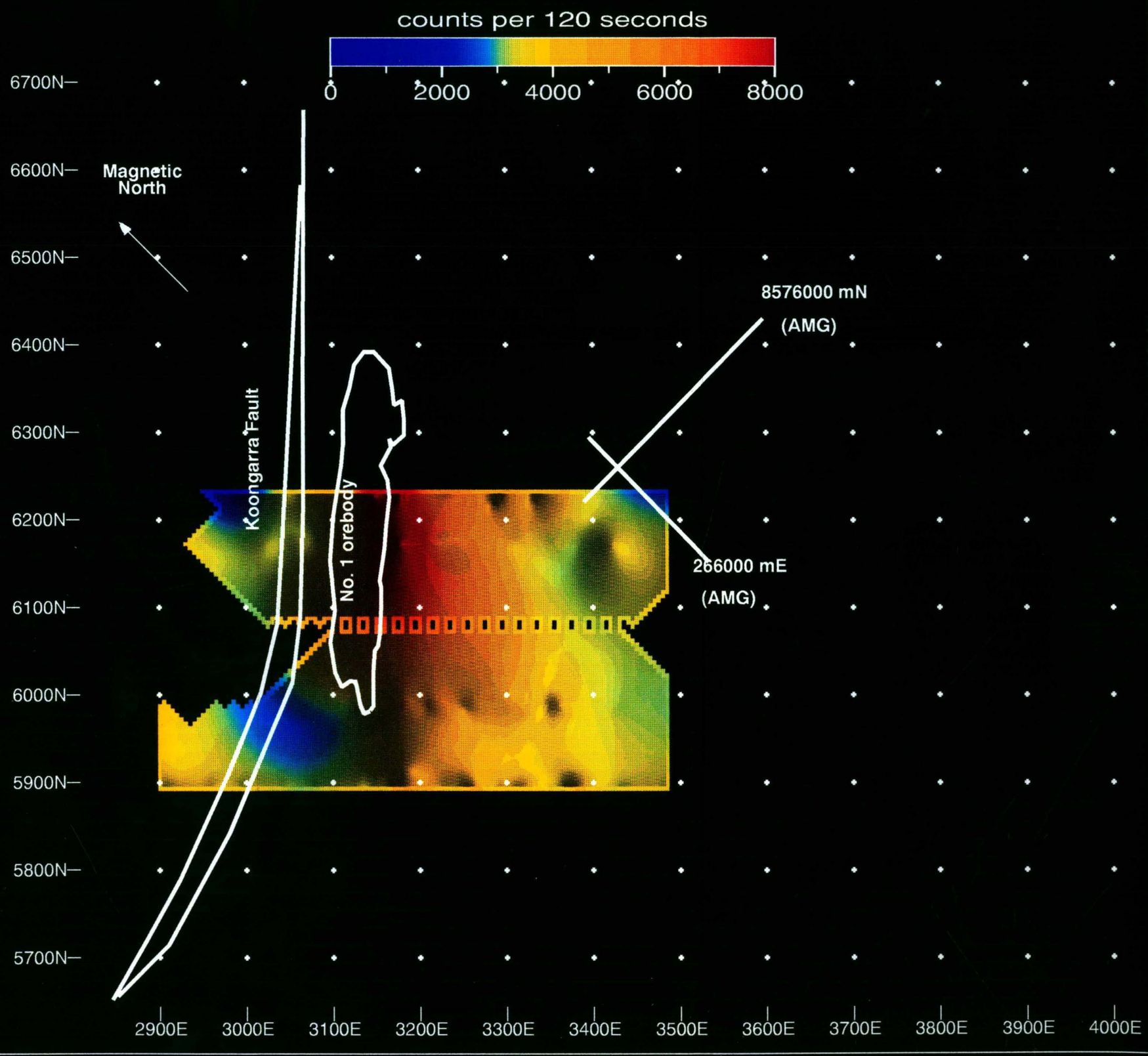

Koongarra Uranium
Deposit
Northern Territory
Australia

Figure 6.11:
Image of Potassium counts

Scale 1 : 5000
AMG Zone 53
Data gathered by the
University of Sydney
1990 and 1991
as part of the
Alligator Rivers
Analogue Project

Images produced by
Michael Hallett
and David Daggar
February 1996.

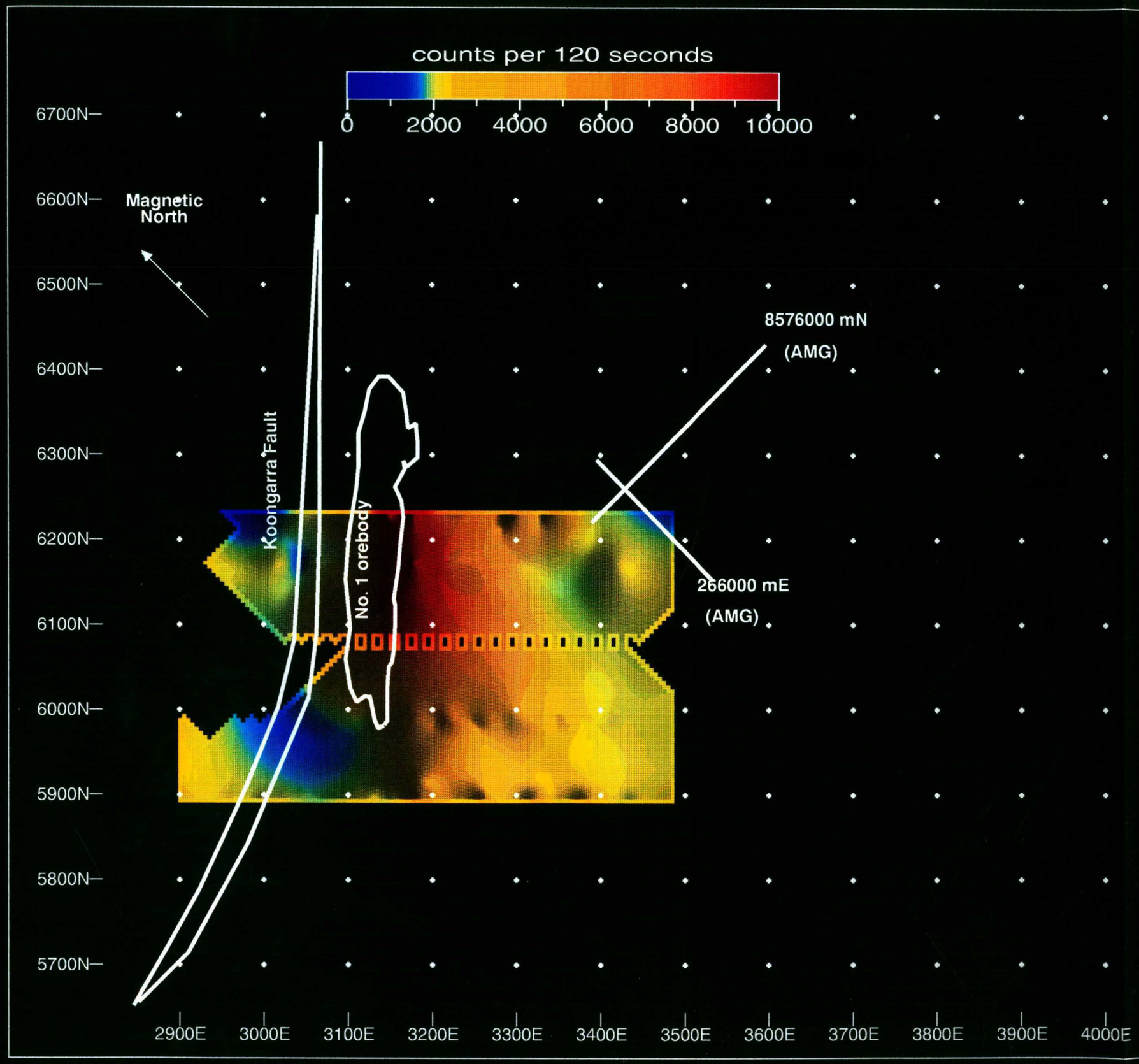

Koongarra Uranium
Deposit
Northern Territory
Australia

Figure 6.12:
Image of Uranium counts

Scale 1 : 5000
AMG Zone 53
Data gathered by the
University of Sydney
1990 and 1991
as part of the
Alligator Rivers
Analogue Project

Images produced by
Michael Hallett
and David Daggar
February 1996.

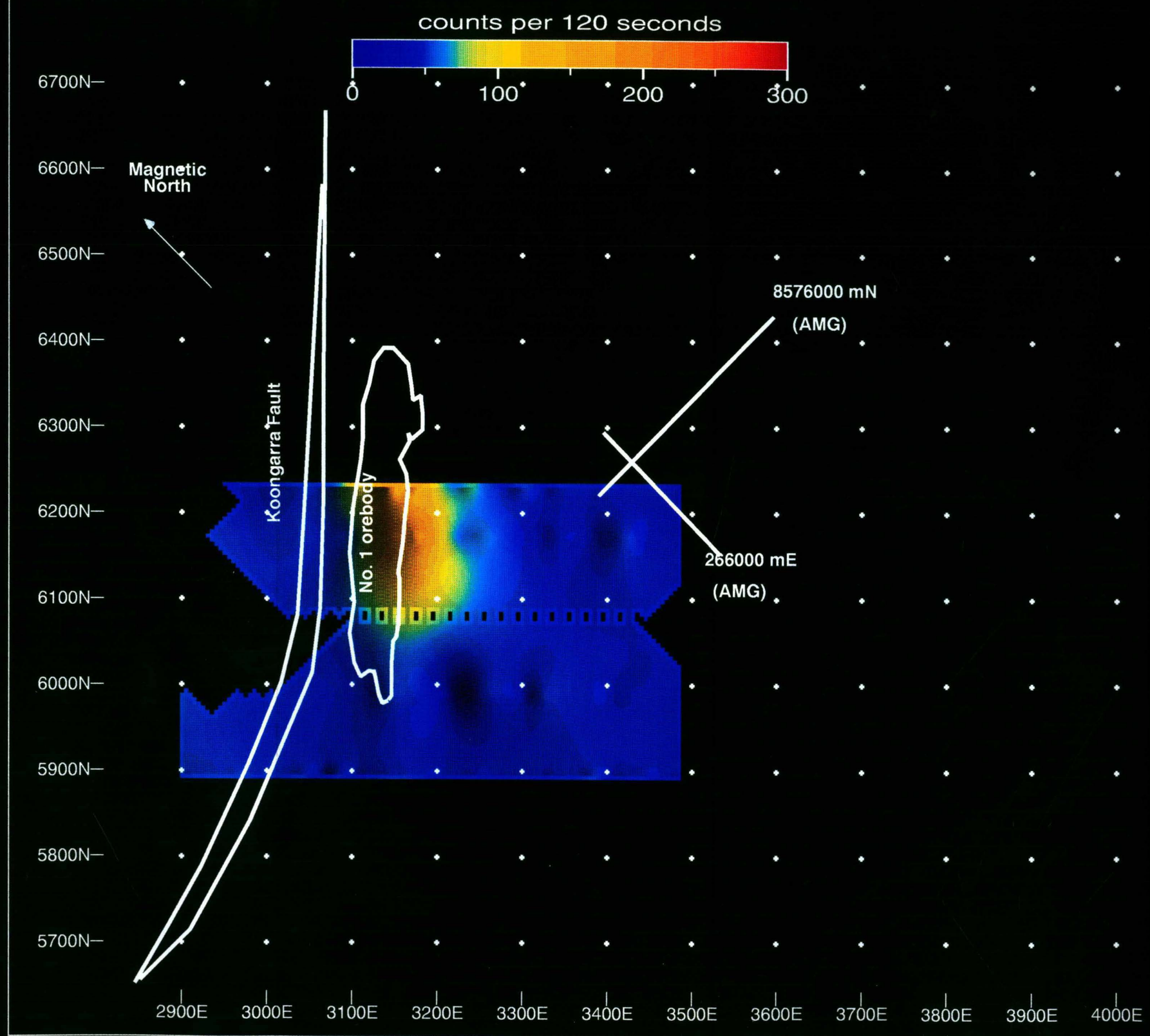

Koongarra Uranium
Deposit
Northern Territory
Australia

Figure 6.13:
Image of Thorium counts

Scale 1 : 5000
AMG Zone 53
Data gathered by the
University of Sydney
1990 and 1991
as part of the
Alligator Rivers
Analogue Project

Images produced by
Michael Hallett
and David Daggar
February 1996.

Gravity

The gravity results show a broad residual high of about 1.6 milligals approximately parallel to the Koongarra Fault. This anomalous region reflects the generally higher density of the schist units of the Cahill Formation and runs in the same direction of the strike of the lithologies in this area. The western side of the image shows an area of negative milligals, representing the lower density Kombolgie Sandstone. The low density region in the east and south of the image may be related to the feldspar hosting schists in this region, which have a lower density than the quartz-chlorite schists nearer to the orebody.

Koongarra Uranium Orebody
Northern Territory
Australia

Figure 6.14
Bouguer Residual gravity Image

Surveyed by Geoterrex Pty Ltd.
1982

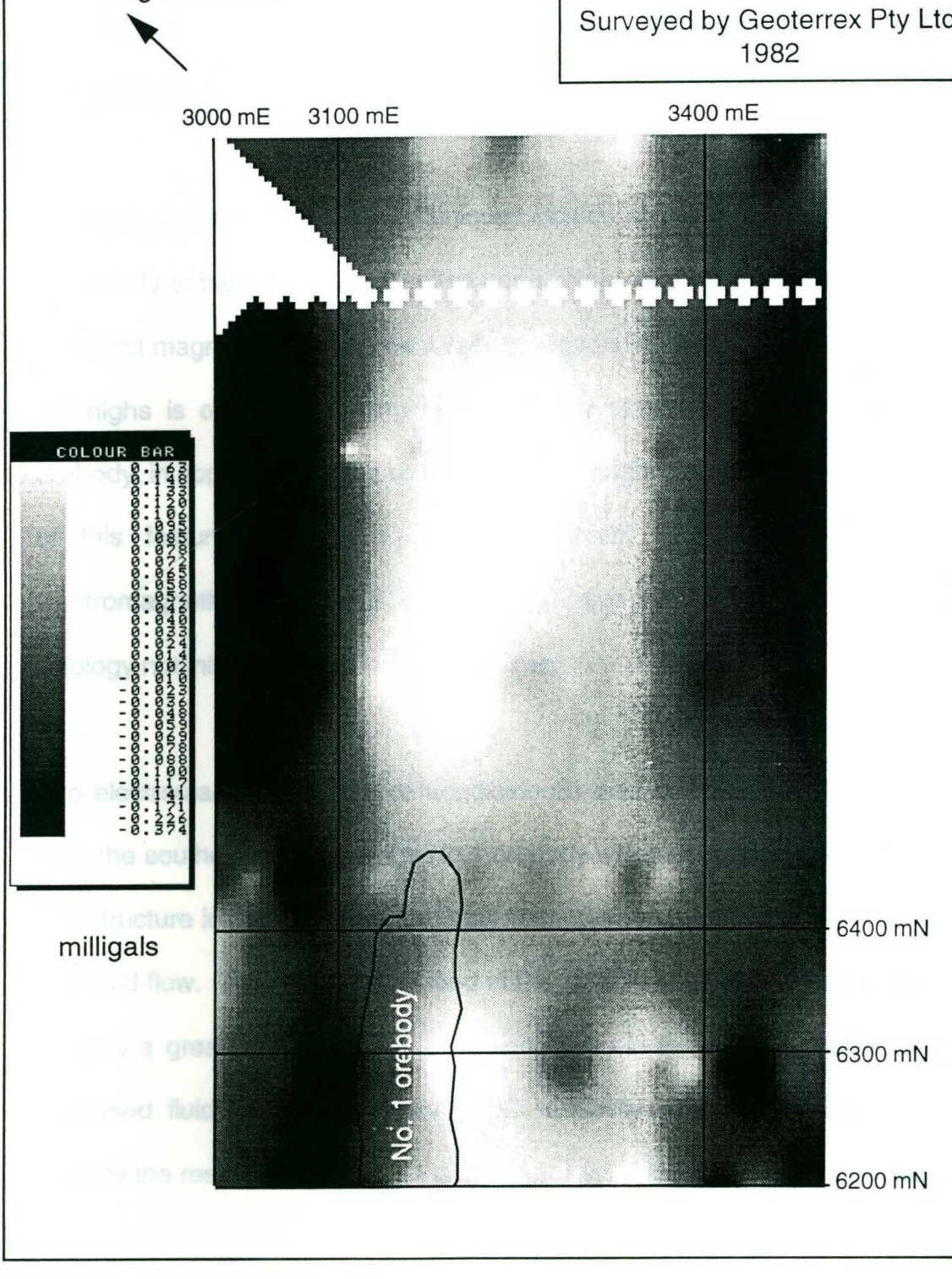

Discussion of The Geophysical Results

The geophysical studies have indicated some interesting features of the weathered zone materials at Koongarra. Strong correlations can be seen using the various techniques, and these correlations are supported by the petrophysical data presented in Chapter 5. Particularly notable are the correlations between magnetic, electromagnetic and SP techniques.

Features delineated by these techniques include a resistive and magnetic low in the vicinity of the No.1 orebody, often obscured by ferrous borehole casing noise. A distinct magnetic high lineament with corresponding high apparent resistivity and SP highs is observed running in a southerly direction, southeast of the No.1 orebody, in approximately the position of the Koongarra Creek. Directly to the west of this feature is a curved structure evident in both the magnetic and electromagnetic data. This is interpreted to represent a magnetic and resistive lithology not intersected in the site boreholes.

The electromagnetic and SP data indicate an area of lower resistivity emanating from the southern extreme of the No.1 orebody which correlates with the nose of a fold structure in the lithologies and may represent an area of increased saturation and fluid flow. This feature is echoed in the scintillometer data which indicate that there is a greater concentration of radionuclides in this area, possibly related to increased fluid flow in this region. DC resistivity data gathered from the site indicate the resistivity layering of the lithologies with depth, the high resistivity of the

Kombolgie Sandstone and a possible increase in the depth of weathering to the south of the No.1 orebody.

CHAPTER 7

DISCUSSION AND CONCLUSIONS

The reasoning behind the study of a natural analogue of a man-made nuclear waste repository has been presented. Consideration needs to be given to the long-term storage of the by-products of nuclear energy generation for both presently existing and future nuclear waste. The likelihood of continued nuclear power generation is high, especially considering other currently used major methods of power generation. The role of the Koongarra site and the Alligator Rivers Analogue Project in the investigations for the solution to the nuclear waste question have been described.

The regional geological structures and lithologies have been reinterpreted in close vicinity to Koongarra because regional structural and lithological components may play significant roles in the mobilisation of radionuclides at the site. A tabled summation of the geological history of the region with respect to the Koongarra site illustrates the factors responsible for the formation of the Koongarra uranium orebody and its subsequent dispersion.

A study of the site geology and structure utilising borehole studies and field observations, delineated significant geological and structural differences to the previously accepted geological and structural framework of the Koongarra site (Snelling 1990). A broad fold structure in the lithologies at Koongarra was delineated and significant fracturing in the nose of the fold was discerned through

the use of the Borehole Television technique. The geological map, geological cross-section and three dimensional depiction of the geology and structure of the site presented in this thesis have significant implications for the interpretation of the hydrology of the site and thus the motion of radionuclides therein.

An examination of the possible role of amphibolitic units in the restriction of groundwater flow in the southeast part of the site determined that the existent amphibolitic units would play no major role in the inhibition of groundwater movement at the site.

A detailed study of the weathered zone / regolith at Koongarra recognises the significance of geomorphological and climatic controls in regolith formation, and hence development of the dispersion fan. Regolith terminology has been applied to the weathered material in order to characterise the Koongarra regolith in context with other recent regolith studies and other regolith models from northern Australia. The saprolite, saprolith (comprising pallid and mottled zones) and the pedolith have been defined. A resume of current regolith terminology and interpretation elicited significant differences in opinion between workers on the importance of various processes in the development of a regolith profile. The physical factors responsible for the development of the regolith at Koongarra indicated that the major mobilisation of radionuclides occurs in the few metres above the base of weathering.

Petrophysical studies of weathered and unweathered material at Koongarra examined the physical constraints on groundwater movement at Koongarra, focusing on the upper 25 - 30 m of weathered materials. Porosity and permeability data have distinguished significant controls in the mobilisation of groundwaters at the site. At meso-scale, the Koongarra Fault material was examined, and not found to be particularly permeable. The role of the Koongarra Fault in the hydrology of the site is still not considered to be adequately defined, however, it is movement of groundwater within the weathered Cahill Formation schists that facilitates migration of radionuclides. Cross plots of the petrophysical data permitted the properties to be viewed in perspective and have defined the relationships between the porosity, permeability, density, electrical resistivity and compressional wave velocity, especially within the weathered zone. Through this study, the region most conducive to the movement of groundwaters was found to be the lower and middle parts of the saprolite, just above, but not within the zone of incipient weathering.

The petrophysical characteristics of the divisions of the weathered zone and unweathered lithologies represented at Koongarra are well demarcated and can be used in defining the various lithologies, especially the magnetic amphibolites and the non-magnetic Kombolgie Sandstone. The weathered zone has been seen to be a heterogeneous region of varying porosity, permeability and fracture characteristics. It is these variable characteristics that have largely determined the spatial arrangement and distribution of the dispersed radionuclides at the Koongarra site.

The geophysical studies correspond well to the new geological site plan, the structure revealed by the Borehole Television studies and the petrophysical database. The magnetic data treatment revealed possible structural information not seen in previous studies. A distinct curvilinear feature east of the No.1 orebody is interpreted to represent a more magnetic lithology not previously seen at the site. Other magnetic features include a strongly magnetised lineament proximal to Koongarra Creek which may be a magnetic intrusive along a fault. The Kombolgie Sandstone was seen to be a region of very low magnetic intensity.

The electromagnetic conductivity data further outlined the structures evident in the magnetic data and indicated a region of low resistivity extending from the southeastern tip of the No.1 orebody in a southerly direction.

Self-Potential surveys confirmed the position of the hanging-wall graphitic schist unit and delineated areas of possible electrofiltration (due to moving groundwaters), which correspond well to the magnetic and electromagnetic data.

Resistivity traverses illustrated the layered nature of the weathered zone and pointed out an area of lower resistivity and possibly increased weathering near the southern end of the No.1 orebody. These macro-scale conclusions corroborate those drawn from the the meso-scale petrophysical studies, suggesting no major zones of macrofracturing.

Radiometric surveys demonstrated the distribution of radionuclides in the shallowest subsurface zones, possibly reflecting the movement of radionuclides at greater depths, and the mobilisation of radionuclides through the weathered rock at earlier times before the present ground surface was exposed.

The correspondence of the geophysical results to the petrophysical data and the geological and regolith studies is considered to be very strong. The implications through resistivity and SP lows, of increased weathering and possibly greater fluid flow in a southerly direction from the southeastern tip of the No.1 orebody are also corroborated by previously published groundwater chemistry studies.

In conclusion: this study has examined the Proterozoic schists enveloping the Koongarra uranium orebody. The structural and geological study has redefined the geological interpretation of the site. Little evidence has been found to support the previously presented geological site plan, the interpreted faults and amphibolitic units within. The Koongarra Fault has been seen as a broad zone of fractured material. There is no physical evidence to establish the Koongarra Fault as a significant conduit for groundwaters, however, field observation and geochemical studies suggest that it does, or did once carry groundwater from the Kombolgie Sandstone into the Cahill Formation schists. If it still behaving in this way presently, it would only be in the weathered zone, not deeper.

The weathered zone has been considered as a pelitic regolith terrain, whch exhibits significant erosion of the surface layers and little development of deep

lateritic profiles or iron-enriched zones. The development of the regolith occurs through downward weathering of rock, concurrent with removal of material from the ground surface. The region of greatest fluid flow is the slightly weathered rock, within a metre or two of the base of weathering, but not **at** the base of weathering.

Petrophysical studies showed the unweathered rock at Koongarra to be impermeable, low in porosity with few open fractures. The unweathered, unfractured rock is unlikely to act as a conduit for the movement of groundwater. The weathered material is heterogeneous in character, showing high porosity but relatively low permeability. Fractures are most probably the regions of most groundwater flow within the weathered zone.

The geophysical images illuminated the site as relatively electrically conductive tract of generally subdued magnetic character. Broad geological divisions can be seen in the geophysical data between the Kombolgie Sandstone and Cahill Formation schists, most notable in the electromagnetic and SP data. The magnetic data delineate some structures not seen previously, which are interpreted as either surficial magnetic ferricretes or possible amphibolitic units within the bedrock. Layering within the weathered zone with depth can be seen in the resistivity data. The electromagnetic and SP data indicated a region of lower resistivity and possible increased groundwater movement to the southeast of the No.1 orebody. This feature is also seen in the scintillometer data.

The geological and geophysical studies have provided valuable information pertaining to the geological and hydologic properties of the site which control the movement of radionuclides within the weathered zone. These conclusions are directly relevant to any future studies of a nuclear waste repository analogue and thus the aims of the Alligator Rivers Analogue Project.

This thesis has endeavoured to contribute to the definition of the parameters of the lithological framework of the Koongarra site. Through a comprehensive site characterisation, the conditions determining the dynamics of the hydrology of the site have been observed.

8. References

* indicates texts referred to but not cited in the text

Anand, R. R., Smith, R. E. and Robertson, I. D. M. 1994. Clasification and Origin of Laterites and Ferruginous Regolith Materials in the Yilgarn Craton, Western Australia. Australian Regolith Conference 1994 (Pain, C. F. and Craig, M. A., Eds).

Airey, P. L., Golian, C. and Lever, D. A. 1986. An approach to the mathematical modelling of the uranium series distribution within orebodies. Australian Atomic Energy Commission, Topical Report AAEC/C49 (NUREG/CR-5060).

Australian Groundwater Consultants Pty Ltd, 1979. Report on investigation of groundwater and the design of the water management and tailings retention system for the Koongarra Project (Noranda Report).

Blix, H. 1987. Nuclear Power and The Environment. The Present and Future Place of Nuclear Power in the World and its Role in Relation to Environmental Risks and Energy Production. Speech at Seminar on Managing Environmental Risks at Schloss Leopoldskron Salzburg Austria, March 1987.

Bockris, J. O'M., 1980. Energy Options. Real Economics and the Solar-Hydrogen System. Australian and New Zealand Book Company, Sydney.

Bourman, R. P. 1994. Towards Distinguishing Transported and *in-situ* ferricretes: Data from Southern Australia. Australian Regolith Conference 1994 (Pain, C. F. and Craig, M. A., Eds).

*Bowen, R., 1979. Geothermal Resources. Applied Science Publishers Ltd, London.

*Breiner, S. 1973. Applications Manual for Portable Magnetometers. GeoMetrics, California.

*Brookins, D.G., 1984. Geochemical Aspects of Radioactive Waste Disposal. Springer-Verlag, New York.

Butt, C. R. M. and Anand, 1994. Terminology of Deeply Weatherd Regoliths. Australian Regolith Conference 1994 (Pain, C. F. and Craig, M. A., Eds).

Butt, C. R. M. and H. Zeegers (Editors), 1992. Regolith Exploration Geochemistry in Tropical and Subtropical Terrains. Handbook of Exploration Geochemistry 4. Elsevier, Ansterdam, 607 pp.

Cao, L. Q. 1992. Investigation of Factors Infleuncing the Uranium Secondary Dispersion Fan, Koongarra Uranium Deposit, Northern Territory. M.Sc. thesis, The University of Sydney.

*Clark, D.A., and Emerson, D.W., 1991. Notes on rock magnetization characteristics in applied geophysical studies. Explor Geophys., 22, 547 - 555.

*Colog Inc. 1991. Borehole Video Surveys: A Geophysical Imaging Device. Colog Inc. Technical Notes, Volume 2, No. 1. Spring 1991.

Corwin, R.F., 1990. The Self-Potential Method for environmental and engineering application. In Geotechnical and Environmental Geophysics. Ward, S. H. (Editor), Vol.1 127-145. Soc Expl. Geophys., Tulsa

*Deer, W. A., Howie, R. A. and Zussman, J. 1983 (14th impression). An Introduction to the Rock Forming Minerals. Commonwealth Printing, Hong Kong.

*Dobrin, Milton, Savit, Carl, 1988. Introduction to Geophysical Prospecting. Fourth Edition. McGraw Hill.

*Duerden, P. and Golian, C., 1991. Koongarra Uranium Deposit general background description, Alligator Rivers Analogue Project, Progress Report: 1 March 1991 - 31 August 1991. 225 - 233.

Emerson, D.W., 1969. Laboratory electrical resistivity measurements of rocks. Proc. Aust. Inst. Min. & Metal., no. 230, 51 - 62.

*Emerson, D. W., 1989. Physical Property measurements on drill core from the Koongarra Uranium Deposit, NT, Alligator Rivers Analogue Project, 1 June - 31 August 1989, 133 - 151.

Emerson, D. W., 1990. Electrical and Acoustic Measurements on rock suite samples from the Koongarra Uranium Deposit, NT, Phase 3 Report, Alligator Rivers Analogue Project Report, 1 December 1989 - 28 February 1990, p 133 - 153.

*Emerson, D. W., 1990. Comments on electrical geophysical results, Koongarra Uranium deposit, NT, Alligator Rivers Analogue Project Progress Report, 1 December 1989 - 28 February 1990, 155 - 164.

*Emerson, D. W., 1990. Geophysical Field Program August 1990: Preliminary Comments. Alligator Rivers Analogue Project Progress Report, 1 June 1990 - 31 August 1990, 91 - 95.

Emerson, D. W., 1991. Notes on mass properties of rocks - density, porosity, permeability. Exploration Geophysics, 21, 209 - 216.

*Emerson, D. W., Cao, L. Q. and Mills, K. J., 1991. A geotechnical study of DDH 53 core: observations on macro and micro-fracturing to the south of the Koongarra Uranium Deposit; Alligator Rivers Analogue Project Progress Report, 1 March 1991 - 31 August 1991, 165 - 216.

*Emerson, D. W., Mills. K. J., Cao, L. Q. and Hallett, M. S. C., 1991. Geophysical and geological site characterisation studies at Koongarra, Alligator Rivers Analogue Project. 3rd Annual Report.

Emerson, D. W., Mills. K. J., Miyakawa, K., Hallett, M. S. C. and Cao, L. Q., 1992. Geophysics, Petrophysics and Structure. Volume 4, Final Report, Alligator Rivers Analogue Project. Australian Nuclear Science and Technology Organisation.

*Emerson, D. W., Mills, K. J. and Hallett. M. S. 1993. Site Characterisation with respect to groundwater flow. Commission of the European Communities, Nuclear Science and Technology. 5th CEC Natural Analogue Working Group Meeting and Alligator Rivers Analogue Project Final Workshop. Toledo, Spain. (Published in the EUR Series).

Ferguson, J. and Needham, R.S., 1978. The Zamu Dolerite: a lower Proterozoic preorogenic continental tholeiitic suite from the Northern Territory, Australia. Jour. Geol. Soc. Aust., 25, 309 - 322.

*Ferguson J., Chappel, B.W., and Goleby A. B., 1980. Granitoids in the Pine Creek Geosyncline. In Ferguson J. and Goleby, A. B. (Editors), Uranium in the Pine Creek Geosyncline. Proceedings Series International Atomic Energy Agency Vienna 91 - 100.

Ferguson, J., Ewers, G. R. amd Donnolley, T. H. 1980. Model for the development of economic mineralisation in the Alligator Rivers Uranium Field. In: Uranium in the Pine Creek Geosyncline, J. Ferguson and A. B. Goleby (Editors), International Atomic Energy Agency, Vienna, pp 563 - 574.

Foy, M. F., and Pederson, C. P., 1975. The Koongarra uranium deposit. In Economic Geology of Australia and Papua New Guinea. Vol. 1, Metals (Knight, C. L., Editor), 317 - 321. The Australian Institute of Mining and Metallurgy, Monograph Series No.5, Melbourne.

GEOTERREX Pty Ltd 1990. Logistics report for an airborne electromagnetic survey Jabiru N.T. for Surtec Geosurveys Pty Ltd. Geoterrex Job No. 2-636. Sydney.

GEOTERREX Pty Ltd. 1982. Logistics report EM-37, gravity, magnetics survey over the Koongarra Uranium Prospect Koongarra N.T. Geoterrex Job No. 85-1449. Sydney.

*Hallett, M. S. C, Mills, K. J. and Emerson, D. W., 1991. Amphibolites in the Koongarra sequence. Aliigator Rivers Analogue Project, Progress Report 1 March - 31 August, 217 - 224.

Hallett, M. S. C., Emerson, D. W. and Duerden, P. 1992. Site Characterisation Studies in the Alligator Rivers Analogue Project. Expl. Geophys. Vol. 23. Nos. 1/2. Conf. Ed.

Hills, J.H. and Richards, J.R. 1976. Pitchblende and galena ages in the Alligator Rivers region, Northern Territory, Australia. Mineralium Deposita 11, 133 - 154.

*Johnston, D. J., 1984. Structural evolution of the Pine Creek Inlier and mineralisation therein, Northern Territory, Australia. Ph,.D. thesis, Monash University (unpublished).

*Keller, G. V. and Frischknecht, F. C. 1966. Electrical Methods in Geophysical Prospecting. Pergamon, London.

Koppi, A., Klessa, J. D. and Conoley, C. 1991. Particle size analysis and mineral weathering in M1, M2 and M3. Alligator Rivers Analogue Project, Progress Report 1 March 1991 - 31 August, 225 - 233.

Krauskopf, K.B., 1988. Radioactive Waste Disposal and Geology. Chapman and Hall, London.

Lawrance, L. M. 1994. Signposts old and New: Prediction of Present and Palaeo-Supergene Geochemical Environments using Iron Redox Chemistry. Australian Regolith Conference 1994 (Pain, C. F. and Craig, M. A., Eds).

Lemons, J., Malone, C. and Piasecki, B. 1989. 'America's High Level Nuclear Waste Repository : A Case Study of Environmental Science and Public Policy', International Journal of Environmental Sciences 34, 25 - 42.

*MacKenzie, W. S. and Guildford, C. 1986 (5th impression). Atlas of rock-forming minerals in thin section. Longman, England.

McMahon, Burgess and Yeates, 1981. Koongarra Project Report on site investigation for water management structures.

Maas, R., 1987. The application of Sm-Nd and Rb-Sr isotope systematics to ore deposits, PhD thesis (unpublished), The Australian National University.

Maas, R., 1989. Nd-Sm isoptope constraints on the age and origin of unconformity-type uranium deposits in the Alligator Rivers Uranium Field, Northern Territory, Australia. Economic Geology 84, 64 - 90.

*Marley, R. D., 1990. Hydrogeologic field study of the Koongarra uranium deposit in the Northern Territory of Australia. M.Sc. thesis, University of Arizona. Australian Nuclear Science and Technology Organisation.

*Mills, K., 1990. Brief preliminary comments on some aspects of the Koongarra area with reference to aerial photography, structure and hydrogeology. Alligator Rivers Analogue Project, Progress Report March - May 1990, 91 - 94.

*Mills, K., 1990. Report on Geological field inspection and investigations in the Koongarra area, 7 - 9 August 1990. Alligator Rivers Analogue Project, Progress Report 1 September - 30 November, 93 - 102.

Milnes, A.G., 1985. Geology and Radwaste. Academic Press, London.

*Murphy, W.M., and Pearcy, E.C. 1992, Source-Term Constraints for the Proposed Repository at Yucca Mountain, Nevada, derived from the Natural Analog at Pena Blanca, Mexico. Mat Res. Soc. Symp. Proc. Vol. 257, 1992.

Needham, R.S., 1982. Cahill, Northern Territory - 1:100000 geological map commentary. Bureau of Mineral Resources, Australia.

*Needham, R.S. and Stuart-Smith, P.G., 1976. The Cahill Formation - a host to uranium deposits in the Alligator Rivers Uranium Field, Australia. BMR Journal of Australian Geology and Geophysics, 1, 321 - 333.

*Needham, R.S. and Stuart-Smith, P.G., 1980. Geology of the Alligator Rivers Uranium Field. In Ferguson, J. and Goleby, A.B., (Eds), Uranium in the Pine Creek Geosyncline. Proceedings Series, International Atomic Energy Agency, Vienna, 233 - 258.

Needham, R.S., 1988. Geology of the Alligator Rivers Uranium Field, Northern Territory. Bulletin 224, Bureau of Mineral Resources, Geology and Geophysics, Australian Government Publishing Service, Canberra. 96pp.

Noranda Australia Ltd. 1987. Koongarra Project Draft Environmental Impact Statement, Noranda Aust. Ltd, Melbourne.

*Norris, J.R., 1989. Preliminary hydraulic characterization of a fractured aquifer at the Koongarra Uranium Deposit, Northern Territory, Australia, Master of Science thesis, The University of Arizona.

*Norris, J. R. and Duerden, P. 1989. Preliminary hydraulic characterisation of the Koongara uranium deposit. Alligator Rivers Analogue Project, 1st Annual Report, 65 - 77.

Ollier, C., 1994. Exploration concepts in laterite terrains. The AusIMM Bulletin, 3, 22-27.

Page, R.W., Compston, W. and Needham, R.S. 1980. Geochronology and evolution of the late Archaean basement and Proterozoic rocks of the Alligator Rivers Uranium Field, Northern Territory, Australia. Uranium of the Pine Creek Geosyncline Proceedings Series, Ferguson, J.A. and Goleby A.B. (editors), International Atomic Energy Agency, Vienna, 39 - 68.

*Paillet, F.L. 1991. Use of Geophysical Well Logs in Evaluating Crystalline Rocks for Siting of Radioactive-Waste Repositories. The Log Analyst, March-April 1991 p 85 - 107.

Pain, C. F. and Ollier, C. D. 1994. Some Misconceptions about Regolith Stratigraphy. Australian Regolith Conference 1994 (Pain, C. F. and Craig, M. A., Eds).

*Parasnis, D. S., 1972. Principles of Applied Geophysics (2nd Edition). Chapman and Hall, London.

Payne, T. E., 1991. Groundwater sampling and analysis. Summary of Progress to August 1991. 1st Annual Report, Alligator Rivers Analogue Project, p119 - 129. Australian Nuclear Science and Technology Organisation.

*Payne, T.E. 1991. A Study of Uranium and Thorium Migration at the Koongarra Uranium Deposit with Application to Actinide Transport from Nuclear Waste Repositories. M.Sc. Thesis, Macquarie University.

Pederson, C.P. 1978. The Geology of the Koongarra Uranium Deposits, including investigations of contained elements. Koongarra Project Draft Environmental Impact Statement, Appendix 5, Noranda Australia Limited, Melbourne.

Prowse, G. 1990. Geological history of the South Alligator Region - retreat of the escarpment. Alligator Rivers Analogue Project, 1st Annual Report, 19 - 25. Australian Nuclear Science and Technology Organisation.

*Read, H. H. 1981 (26th edition). Rutley's Elements of Mineralogy. Allen and Unwin, London.

Ringwood, A.E., 1978. Safe Disposal of High Level Nuclear Waste: A New Strategy, Australian National University Press, Canberra.

*Sandberg, E.V., Olsson, O.L., and Falk, L.R. 1991. Combined Interpretation of Fracture Zones in Crystalline Rock Using Single-Hole, Crosshole Tomography and Directional Borehole-Radar Data. The Log Analyst, March-April 1991, 108 - 119.

*Snelling, A. A., 1990. Koongarra Uranium Deposit. 1st Annual Report, Alligator Rivers Analogue Project, ANSTO. p11-18.

*Snelling, A.A., 1980. A geochemical study of the Koongarra uranium deposit, Northern Territory, Australia. Ph.D. Thesis. University of Sydney (unpublished).

*Snelling, A. A., 1990. Geological development of the Koongarra Uranium Deposit. Alligator Rivers Analogue Project, Progress Report 1 September - 1990 - 30 November 1990, 7 - 44.

Snelling, A. A., 1990. Koongarra Uranium Deposits. In: Geology of the Mineral Deposits of Australia and Papua New Guinea (Ed F.E. Hughes), pp. 807 - 812. Aust. Inst. Min. & Metall. Melbourne.

Snelling, A. A., 1990. Koongarra Uranium Deposit, Alligator Rivers Analogue Project, 1st Annual Report 1988-89, 11 - 18.

Snelling, A. A., 1992. Geologic Setting. Volume 2, Final Report, Alligator Rivers Analogue Project. Australian Nuclear Science and Technology Organisation.

*Tanka, K., Miyakawa, K., Inoue, D., Yoshida, E., Osawa, H., Ogata, N., Yanagisawa, K. and Yanakawa, M. 1990. Fracture System of Granite at the Tono Mine - Evaluation of Fracture Characteristics at #AN - 1 (0 - 270 m) by Borehole Television System. Abiko Research Laboratory Report no. U.88003. Tokyo.

*Telford, W. M., Geldart, L. P. and Sheriff, R. E. 1990. Applied Geophysics, Second Edition. Cambridge University Press.

Trescases, J. J. 1992. Chemical weathering. In: C. R. M. Butt and H. Zeegers (Editors), Regolith Exploration Geochemistry in Tropical and Subtropical Terrains. Handbook of Exploration Geochemistry 4. Elsevier, Ansterdam, 25 - 40.

*Whitten, D.G.A with Brooks, J.R.V. 1979. A Dictionary of Geology. Penguin Books, Middlesex, Great Britain.

Williams, M. A. J. 1969. Geology of the Adelaide-Alligator area. In: Story, R., Williams, M. A. J., Hooper. A. D. L., O'Ferrall, R. E. and McAlpine, J. R. (Editors). Lands of

the Adelaide-Alligator area, Northern Territory. CSIRO Land Research Series No. 25, 56 - 70

*Wylde , A.R., Bloom, M.S. and Wall, V.J. 1988. Transport and Deposition of Gold Uranium and Platinum Group Elements in Unconformity-Related Uranium Deposits. In Keays, R.R., Ramsay, W.R.H. and Groves, D.I. (Editors). The Geology of Gold Deposits: The perspective in 1988. Economic Geology Monograph 6.

Wyroll, K. H., 1992. Geomorphology and Palaeoclimatic History. Volume 3, ARAP Final Report. Australian Nuclear Science and Technology Organisation.

*Zemanek, J., Glenn, E.E., Norton, L.J. and Caldwell, R.L. 1970. Formation Evaluation by Inspection with the Borehole Televiewer. Geophysics, Vol.35, No.2, 254 - 269.

Appendix I: Depth to base of weathering data.

10195	10340	-18.39	DDH1
10194	10384	-21.12	DDH2
10199	10451	-24.52	DDH3
10200	10517	-23.82	DDH4
10411	10344	-24.17	DDH5
10612	10429	-23.12	DDH6
10829	10420	-25.22	DDH7
9804	10277	-23.82	DDH8
10609	10334	-24.05	DDH9
9808	10463	-21.71	DDH10
11201	10429	-17.98	DDH11
10999	10388	-21.95	DDH12
9807	10457	-21.71	DDH13
11203	10353	-17.51	DDH14
11205	10254	-17.28	DDH15
11607	10307	-17.51	DDH16
11397	10299	-19.5	DDH17
10406	10286	-22.18	DDH18
10410	10422	-21.48	DDH19
11605	10210	-14.01	DDH20
10400	10527	-26.15	DDH21
11803	10260	-14.48	DDH22
10837	10331	-25.68	DDH24
31560	16198	-42.5	DDH25
11807	10307	-15.64	DDH26
10600	10281	-26.85	DDH27
11607	10410	-15.41	DDH29
9997	10347	-22.42	DDH30
10840	10282	-26.15	DDH31
11605	10450	-18.68	DDH35
11808	10348	-19.61	DDH37
10838	10212	-32.92	DDH38
10004	10206	-25.68	DDH40
11001	10256	-19.85	DDH41
10594	10175	-45.53	DDH43
11396	10328	-46.49	DDH44
11001	10529	-16.8	DDH46
10000	10459	-24.28	DDH47
12003	10434	-17.32	DDH48
10601	10500	-28.48	DDH49
10001	10598	-23.86	DDH50
10405	10243	-19.73	DDH51
10202	10202	-29.52	DDH52
9802	10585	-22.15	DDH53
9802	10439	-19.38	DDH54
11001	10320	-23.35	DDH55
10814	10130	-31.99	DDH56
10602	10164	-27.79	DDH57
10498	10358	-21.25	DDH58
10701	10328	-24.52	DDH59
10500	10430	-24.05	DDH60
10701	10423	-24.05	DDH61
10496	10267	-30.47	DDH62
10700	10185	-39.69	DDH63
10300	10420	-23.35	DDH64
10300	10299	-29.19	DDH65

Appendix I: Depth to base of weathering data.

10100	10440	-25.68	DDH66
10300	10536	-22.18	DDH67
10100	10347	-21.01	DDH68
10800	10504	-25.92	DDH69
10900	10335	-24.05	DDH70
11801	10535	-21.95	DDH71
10900	10226	-30.35	DDH72
10900	10441	-21.01	DDH73
11100	10437	-22.88	DDH74
11600	10459	-31.52	DDH75
11100	10346	-19.61	DDH76
11701	10400	-17.98	DDH77
11901	10495	-19.85	DDH78
11701	10316	-16.34	DDH79
11500	10312	-18.68	DDH80
9900	10345	-19.85	DDH81
9899	10476	-21.6	DDH82
10100	10590	-22.18	DDH83
10300	10215	-30.35	DDH84
10500	10176	-37.36	DDH85
10300	10648	-26.15	DDH86
10500	10530	-24.75	DDH87
11700	10486	-21.01	DDH89
10101	10242	-28.02	DDH90
10500	10640	-29.19	DDH92
10100	10462	-21.01	DDH93
11800	10651	-24.52	DDH94
11800	10899	-28.02	DDH95
11599	10731	-26.85	DDH96
12000	10853	-28.02	DDH97
10500	11015	-28.02	DDH98
10400	10762	-17.51	DDH99
13200	10086	-21.01	DDH100
11600	11004	-24.52	DDH101
13200	10431	-25.68	DDH102
11701	10473	-29.19	DDH103
10900	10701	-29.19	DDH104
11199	10744	-24.52	DDH105
10699	10709	-25.68	DDH107
11400	10992	-28.49	DDH108
11400	11272	-24.98	DDH109
11200	11011	-21.01	DDH110
11101	10146	-37.36	DDH111
9900	10111	-30.35	DDH114
11400	10551	-29.19	DDH115
11700	10904	-26.85	DDH116
10900	10149	-21.34	DDH118
10500	10390	-24.52	DDH119
14400	11266	-30.35	DDH120
9799.75	10265	-28.79	DDH8
9799.75	10376.8	-23.5	DDH54
9799.75	10456.2	-21.59	DDH13
9799.75	10463.8	-21.21	DDH10
9799.75	10580.6	-24.24	DDH55
9901.45	10068.4	-46.97	DDH114
9901.45	10344.4	-19.7	DDH81

Appendix I: Depth to base of weathering data.

9901.45	10476.3	-21.2	DDH82
9999.88	10130.8	-55.3	DDH40
9999.88	10344.4	-23.48	DDH30
9999.88	10458.9	-25.76	DDH47
9999.88	10600.6	-23.11	DDH50
10098.3	10178	-53.79	DDH90
10098.3	10334.5	-24.24	DDH68
10098.3	10438.8	-26.52	DDH66
10098.3	10588.1	-22.73	DDH83
10200	10155.7	-44.72	DDH52
10200	10310.6	-21.45	DDH1
10200	10379.8	-24.39	DDH2
10200	10449.3	-25.2	DDH3
10200	10514.6	-24.8	DDH4
10298.4	10121.3	-30.87	DDH113
10298.4	10302.4	-29.27	DDH65
10298.4	10410.6	-26.02	DDH64
10298.4	10530.7	-24.39	DDH67
10298.4	10651.8	-24.39	DDH86
10400.1	10182.6	-48.78	DDH51
10400.1	10265.3	-38.21	DDH18
10400.1	10347.6	-26.42	DDH5
10400.1	10428	-24.39	DDH19
10400.1	10527.8	-28.46	DDH21
10600.3	10163.9	-52.85	DDH43
10600.3	10239.7	-43.1	DDH27
10600.3	10328	-26.02	DDH9
10600.3	10422.4	-26.02	DDH6
10600.3	10498.6	-29.27	DDH49
9400	10200	-14.83	PH79
9400	10300	-16.86	PH74
9400	10400	-16.75	PH73
9400	10450	-17.02	PH66
9400	10550	-19.22	PH62
9400	10600	-21.97	PH80
9400	10650	-24.22	PH81
9400	10700	-24.49	PH83
9400	10750	-26.09	PH84
9400	10800	-29.11	PH85
9400	10850	-26.36	PH87
9400	10900	-24.71	PH88
9400	10950	-20.59	PH92
9400	11000	-19.77	PH93
9400	11055	-23.34	PH95
9600	10150	-23.12	PH61
9600	10200	-21.49	PH59
9600	10250	-16.86	PH46
9600	10300	-21.22	PH53
9600	10350	-24.75	PH54
9600	10400	-22.85	PH56
9600	10450	-23.12	PH57
10411	10143	-24.99	DDH5
10612	10425	-25.6	DDH6
9804	10160	-64.92	DDH8
10609	10334	-25.3	DDH9
10609	10313	-31.09	DDH9

X

Appendix I: Depth to base of weathering data.

10609	10295	-37.49	DDH9
9808	10457	-24.38	DDH10
11201	10422	-20.73	DDH11
10999	10387	-22.86	DDH12
9807	10454	-23.17	DDH13
11203	10280	-48.77	DDH14
11203	10335	-24.08	DDH14
11205	10226	-30.48	DDH15
11607	10308	-17.37	DDH16
11397	10300	-26.52	DDH17
10406	10213	-53.34	DDH18
10410	10422	-22.56	DDH19
11605	10192	-19.51	DDH20
10400	10514	-25.91	DDH21
10600	10175	-68.28	DDH27
10600	10275	-29.57	DDH27
11607	10408	-15.85	DDH29
9997	10162	-89.92	DDH30
10004	10138	-54.86	DDH40
11001	10225	-32.31	DDH41
10594	10157	-57.3	DDH43
10594	10188	-43.28	DDH43
11396	10398	-18.59	DDH44
11001	10492	-32	DDH46
10000	10340	-64.01	DDH47
10000	10333	-65.53	DDH47
10000	10293	-81.69	DDH47
10000	10240	-97.54	DDH47
10000	10455	-25.91	DDH47
12003	10432	-19.05	DDH48
10601	10508	-25.3	DDH49
10001	10593	-25.6	DDH50
10405	10195	-41.15	DDH51
9802	10582	-23.77	DDH53
9802	10376	-24.99	DDH54
11001	10316	-24.38	DDH55
10602	10140	-39.62	DDH57
10498	10340	-28.35	DDH58
10701	10320	-28.96	DDH59
10500	10427	-24.38	DDH60
10701	10418	-25.91	DDH61
10496	10262	-34.44	DDH62
10700	10180	-42.67	DDH63
10100	10303	-77.12	DDH66
10100	10440	-26.52	DDH66
10100	10230	-99.06	DDH66
10100	10292	-40.54	DDH68
10100	10345	-21.34	DDH68
10100	10193	-71.63	DDH68
10900	10337	-24.38	DDH70
10900	10228	-32.92	DDH72
10900	10439	-23.17	DDH73
11100	10436	-24.08	DDH74
11600	10495	-19.51	DDH75
11100	10334	-25.6	DDH76
11701	10404	-17.68	DDH77

Appendix I: Depth to base of weathering data.

11901	10497	-18.9	DDH78
11701	10310	-17.68	DDH79
11500	10322	-15.24	DDH80
9900	10345	-20.12	DDH81
9899	10338	-66.45	DDH82
9899	10476	-21.64	DDH82
9899	10295	-79.25	DDH82
10100	10558	-26.52	DDH83
10100	10588	-22.86	DDH83
10100	10578	-34.14	DDH83
10500	10115	-62.48	DDH85
10500	10524	-26.52	DDH87
11700	10496	-17.37	DDH89
10101	10160	-60.96	DDH90
10900	10128	-45.11	DDH91
10500	10639	-29.26	DDH92
10999	10463	-21.64	DDH93
11599	10735	-25.3	DDH96
11600	11005	-24.99	DDH101

Appendix II: Petrophysical database.

ZONE	DRILL HOLE	Vertical Depth (m)		DENSITY WBD (g/cc) (*=DBD)	Total Porosity (%)	Water perm k (μd)	Resistivity 1000Hz (Ωm)	Velocity Vp (m/s) (500kHz)	Mag k (cgs* 10^-6 ≈ SI*10^-5)	CORE CUT (wrt axis)
A1 :	M1	8.0		1.92		78			16	_I_
Weathered	M1	8.3		1.92		57		779		
Zone	M1	8.3		2.13		47		1051		
Cable Tool	M1	14.0		1.94		870			16	_I_
samples :	M1	14.0		2.11		90		778		_I_
M, W holes	M1	14.0		2.01		78		1275		//
	M1	21.0		2.16		30			33	_I_
	M1	21.0		2.18		45	56	1250		//
	M1	21.0		2.09		36		1264		//
	M2	3.0		1.60		1	23	1727		//
	M2	8.0		2.43		98				_I_
	M2	13.0		2.26					28	
	M2	17.0		1.86		2654			29	//
	M2	21.0		2.07		545			28	//
	M2	21.0		2.12		2340	53	2202		//
	M2	25.0		1.77					57	
	M3	8.0		2.00		18			30	_I_
	M3	8.0		1.61*	39.5					
	M3	8.0		1.92		31				_I_
	M3	8.0		1.94		293		814		//
	M3	8.0		1.91		1417				//
	M3	15.0		2.27		22	61	1892	28	//
	W1	8.0		1.79		8708			12	_I_
	W1	8.0		1.86		4032				//
	W1	8.0		1.50*	35.7					
	W1	13.0		1.85		166			22	_I_
	W1	18.0		1.73		3030	48	1540	25	_I_
	W1	18.0		1.63		587				//
	W1	24.0		1.88		1			15	_I_
	W1	24.0		2.03		46		1545		_I_
	W1	24.0		1.74		126				//
	W2	8.0		1.68		307			34	//
	W2	14.0		2.11					16	
	W2	16.0		1.87		102			22	_I_
	W2	16.0		1.85		1695				//
	W2	16.0		1.45*	40.5					
	W4	8.0		1.70		5640			24	_I_
	W4	8.0		1.38*	32.4					
	W4	8.0		1.93		404				//
	W4	8.0		1.73		2263				//
	W4	8.0		1.80		444				//
	W4	12.0		1.69		2614				_I_
	W4	12.0		1.63		1542			26	//
	W4	16.0		2.34					23	
	W5	8.0		1.78		2647			47	//
	W5	8.0		1.62*	16.4					
	W5	13.0		2.37						
	W7	5.3		1.95			25	1740	16	_I_
	W7	6.1		1.89			14	1769	27	_I_
	W7	7.1		1.97			21	1446	24	_I_
	W7	8.0		1.66		1358			45	_I_
	W7	8.0		1.76		1013				//

	DRILL	Vertical		DENSITY	Total	Water	Resistivity	Velocity	Mag k	CORE
ZONE	HOLE	Depth		WBD	Porosity	perm	1000Hz	Vp	(cgs*	CUT
		(m)		(g/cc)	(%)	k (μd)	(Ωm)	(m/s)	10^-6 ≈	(wrt
				(*=DBD)				(500kHz)	SI*10^-5)	axis)
A1 :	W7	8.1		2.01			19	1984	38	_|_
Weathered	W7	10.1		2.12			48	1834	29	_|_
Zone	W7	11.3		1.88			17	1634	28	_|_
Cable Tool	W7	13.0		1.75		414			47	//
samples :	W7	13.0		1.35*	39.5					_|_
M, W holes	W7	14.2		1.96			28	1792	25	_|_
	W7	15.0		2.15			104	1903	36	_|_
	W7	16.0		2.17			84	2125	19	_|_
	W7	17.0		2.25			177	2194	23	_|_
	W7	18.2		2.19			71	1842	62	_|_

ZONE	DRILL HOLE	Vertical Depth (m)	Inclined Depth (ft)	DENSITY DBD (g/cc)	Apparent Porosity (%)	Air perm k (md)	Resistivity 1000Hz (Ωm)	Velocity Vp (m/s) (500kHz)	Mag k (cgs* 10^-6 ≈ SI*10^-5)	CORE CUT
B :	53	13.4	55.0	2.14	15.1	1.38	46			_|_
Transitional	53	13.4	55.0	2.18				1838	44	//
Zone	53	17.3	71.0	2.29	13.1	1.78				_|_
	53	17.3	71.0	2.36				1947	53	//
	53	18.7	77.0	2.40			75		60	
	67	23.7	101.5	2.57	7.2	0.93			60	//
	74	19.5	83.5	2.55	4.9	(fract)	208	2422		_|_
	74	19.5	83.5	2.59	5.0	1.40	162	1923	45	//
	86	23.0	98.5	2.67	4.3	1.55	127		63	//
	86	25.6	109.5	2.26	16.3	1.50			42	_|_
	86	25.6	109.5	2.34	15.0	(fract)	55		50	//
	107	24.8	106.0	2.63	4.7	1.88		3765	23	_|_
	107	24.8	106.0	2.62	4.2	39.86			40	//
	119	23.7	101.5	2.79	1.8	0.84		3742	37	_|_
	119	23.7	101.5	2.74	0.4	1.26		5105		//

ZONE	DRILL HOLE	Vertical Depth (m)	Inclined Depth (ft)	DENSITY DBD (g/cc)	Apparent Porosity (%)	Air perm k (md)	Resistivity 1000Hz (Ωm)	Velocity Vp (m/s) (500kHz)	Mag k (cgs* 10^-6 ≈ SI*10^-5)	CORE CUT
C1 :	50	23.9	98.0	2.67	4.5	0.28	2012		37	_|_
Quartz	50	23.9	98.0	2.67	2.8	0.41	256		44	//
schists	50	28.5	117.0	2.70	2.9	0.09			52	_|_
+/- chlorite	50	28.5	117.0	2.67	2.9	0.37		5162		//
+/- mica	50	32.6	134.0	2.63	7.8	0.37	1096		86	_|_
	50	32.6	134.0	2.65	6.4	2.03	241	4799	103	//
	50	36.5	150.0	2.76	0.1	0.14	6411		83	_|_
	50	36.5	150.0	2.75	1.3	0.17	1602	5139	104	//
	50	44.1	181.0	2.77	1.0		1152		43	_|_
	50	44.1	181.0	2.75	5.4	0.04	2935	4262		//
	50	51.4	211.0	2.76	1.7	0.13	1749	4829	58	_|_
	50	51.4	211.0	2.75	1.9	0.01	642		52	//
	50	58.7	241.0	2.81	0.8	0.05	4001		74	_|_
	50	58.7	241.0	2.77	0.5	0.05	50	5265	45	//
	50	65.7	270.0	2.78	0.7	0.12	564		52	_|_
	50	65.7	270.0	2.77	1.0	0.03	1220	5819	52	//
	50	73.0	300.0	2.74	0.4	0.05	21876	5814	30	_|_
	50	73.0	300.0	2.75	0.6	0.04	16511			//
	50	80.8	332.0	2.76	< 0.1		8817			_|_
	50	80.8	332.0	2.75	0.3		4861	5533		//
	50	95.2	391.0	2.70	0.5	0.57	16391		26	_|_
	50	95.2	391.0	2.69	0.6	0.02	4987	5382	21	//
	50	109.3	449.0	2.65	2.5	0.19	3115		16	_|_
	50	109.3	449.0	2.68	1.6	0.06	306		14	//
	50	116.8	480.0	2.65	2.8	0.14	942		25	_|_
	50	116.8	480.0	2.68	1.9	0.03	399		23	//
	53	21.7	89.0						44	
	53	23.9	98.0	2.67	0.6	0.08			29	_|_
	53	23.9	98.0	2.64	4.6	0.33				//
	53	26.5	109.0	2.60	5.7	1.80	(sheared)	2895	23	_|_
	53	29.2	120.0	2.77	2.9	0.05			73	_|_
	53	34.6	142.0	2.69	5.3	0.66			33	_|_
	53	34.6	142.0	2.62	3.5	0.21				//
	54	24.6	105.5	2.70	1.3	0.56			22	_|_
	54	24.6	105.5	2.65	3.1	0.26				//
	54	29.1	124.5	2.69	1.2	0.06		5083	28	_|_
	54	29.1	124.5	2.73	0.4	1.11				//
	54	32.8	140.5	2.62	3.0	0.33			29	_|_
	54	32.8	140.5	2.68	2.0	(fractured)				//
	64	24.5	105.0	2.72	1.0	0.29	272	4137	40	_|_
	64	24.5	105.0	2.65	3.7	0.30	230	4337		//
	64	27.7	118.5	2.80	< 0.1	0.09			40	_|_
	64	27.7	118.5	2.76	< 0.1	0.07				//
	64	31.4	134.5	2.76	1.1	0.04			50	_|_
	64	31.4	134.5	2.85	< 0.1	0.17		5561		//
	64	35.0	150.0	2.76	< 0.1	0.11		5500	30	_|_
	64	35.0	150.0	2.77	< 0.1	0.15				//

	DRILL	Vertical	Inclined	DENSITY	Apparent	Air	Resistivity	Velocity	Mag k	CORE
ZONE	HOLE	Depth	Depth	DBD	Porosity	perm	1000Hz	Vp	(cgs*	CUT
		(m)	(ft)	(g/cc)	(%)	k (md)	(Ωm)	(m/s)	10^-6 ≈	
								(500kHz)	SI*10^-5)	
C1 :	67	25.2	108.0	2.52		1.67			60	_|_
Quartz	67	25.2	108.0	2.75	2.2	0.38		5176		//
schists	67	25.2	108.0					4853		
+/- chlorite	67	30.4	130.0	2.73	3.5	0.07			61	_|_
+/- mica	67	30.4	130.0	2.77	0.1	0.07				//
	67	34.9	149.5	2.69	4.4	0.14			31	_|_
	67	34.9	149.5	2.77	0.7	0.21				//
	70	51.3	219.5	2.73	1.6		692		36	
	74	21.1	90.5	2.69	2.3	0.08	1112	5011	63	_|_
	74	21.1	90.5	2.68	1.9	0.13	586	5333		//
	74	23.1	99.0	2.65	0.8	0.17		5167	44	//
	75	70.2	300.5	2.76	1.5		1513		57	_|_
	75	70.2	300.5	2.77	2.1	0.04			53	//
	82	23.3	100.0	2.74	2.5	0.07	5447	4962	74	_|_
	82	23.3	100.0	2.73	2.1	0.29	234	4692		//
	82	27.6	118.0	2.77	0.5	0.11			48	_|_
	82	27.6	118.0	2.79	0.4	0.16				//
	82	31.3	134.0	2.69	2.1	0.11		4625	48	_|_
	82	31.3	134.0	2.73	1.3	0.20				//
	82	34.6	148.0						57	
	82	85.5	366.0	2.73	0.5	0.09				_|_
	82	85.5	366.0	2.73	0.8	0.08			64	//
	86	30.2	129.5	2.72	1.5	0.12			45	_|_
	86	30.2	129.5	2.84	1.4	0.26				//
	86	39.7	170.0	2.73	1.7	0.05	1040		46	_|_
	86	39.7	170.0	2.69	2.6	0.06	578	3985	39	//
	86	44.4	190.0	2.07	0.8		2803		47	_|_
	86	44.4	190.0			1.28	1695			//
	86	49.3	211.0	2.67	0.9	0.02				_|_
	86	49.3	211.0	2.76	2.1	0.04				//
	86	79.6	341.0	2.81	1.4	0.03	461		46	_|_
	86	79.6	341.0	2.80	1.3	0.09	402		42	//
	86	82.7	354.0	2.73	1.5		677		32	_|_
	86	82.7	354.0	2.78	2.4	0.08	189		47	//
	86	121.9	522.0	2.70	1.1	0.29	922		77	//
	98	88.5	379.0	2.81	0.9	0.06	4887		25	_|_
	98	88.5	379.0	2.81	0.8	0.03	2515		63	//
	98	92.2	395.0	2.79	0.8	0.03	54385	4482	64	_|_
	98	92.2	395.0	2.77	1.3	0.02	8328		68	//
	98	108.5	464.5	2.97	0.1	0.05			72	_|_
	98	108.5	464.5	2.98	0.1	0.05		6125	65	//
	98	110.0	471.0	2.73	0.7	0.03	6513	4960		_|_
	98	110.0	471.0	2.73	0.7	0.02			69	//
	98	187.4	802.5	2.78	0.8	0.03	3289		62	_|_
	98	187.4	802.5	2.78	0.9	0.02	1231		58	//
	98	187.5	803.0	2.75	1.5	1.55	3268		55	_|_
	98	187.5	803.0	2.76	1.1		874		50	//

	DRILL	Vertical	Inclined	DENSITY	Apparent	Air	Resistivity	Velocity	Mag k	CORE
ZONE	HOLE	Depth	Depth	DBD	Porosity	perm	1000Hz	Vp	(cgs*	CUT
		(m)	(ft)	(g/cc)	(%)	k (md)	(Ωm)	(m/s)	10^-6 ≈	
								(500kHz)	SI*10^-5)	
C1 :	98	189.7	812.5	2.70	2.0	0.18	528			_|_
Quartz	98	189.7	812.5	2.71	3.2	0.04	643		50	//
schists	107	25.6	109.5	2.63	6.9	1.00			39	_|_
+/- chlorite	107	25.6	109.5	2.64	2.9	0.94		4580		//
+/- mica	107	30.4	130.0	2.77		0.12			75	_|_
	107	30.4	130.0	2.75	0.2	0.16		4472		//
	119	26.6	114.0	2.72	2.7	0.43			36	_|_
	119	26.6	114.0	2.72	2.1	0.75		4105		//
	119	32.0	137.0	2.73	3.9	0.22			60	_|_
	119	32.0	137.0	2.81	0.7	(fract)		4561	25	//
	119	43.9	188.0	2.65	1.1	0.04	2840		18	//
	119	48.1	206.0	2.67	0.4	0.04	3232		19	_|_
	119	48.1	206.0	2.66	1.0	0.02	1843			//
	119	68.4	293.0	2.63	2.4		122370		11	_|_
	119	68.4	293.0	2.66	2.0	0.06	1029		16	//
C1a :	50	56.0	230.0	2.60	1.1	0.15	99060		<1	_|_
Siliceous	50	56.0	230.0	2.63	0.3	0.05	13558	5726	1	//
Schists	86	132.9	569.0	2.64	0.5	0.29	12925		6	_|_
	86	132.9	569.0	2.64	0.6	0.15	4020		7	//
C2 :	50	81.5	335.0	2.76	0.4		3230			_|_
Graphitic	50	81.5	335.0	2.74	0.2		31	5079		//
Schists	53	59.5	244.5	2.68	1.4	0.49	130		39	_|_
	53	59.5	244.5	2.68	1.1	0.70	80		33	//
	119	38.5	165.0	2.70	1.1		836	3947		_|_
	119	38.5	165.0	2.65	0.6		106	4955		//
C3 :	67	26.3	112.5	2.88	1.7	0.12	10059	5000	125	_|_
Amphibolite	67	26.3	112.5	2.97	0.6	0.09	8333			//
	86	34.8	149.0	2.90	2.2	0.05	43896	4921	76	_|_
	86	34.8	149.0	3.06	0.7	0.24	126457	6554	100	//
	98	82.9	355.0	3.06	0.1	0.06	65018		121	_|_
	98	82.9	355.0	3.06	0.1	0.04	517503		112	//
	98	105.5	452.0	2.92	0.2	0.15	53941	5300	387	_|_
	98	105.5	452.0	2.92	0.2	0.54			96	//

	DRILL	Vertical	Inclined	DENSITY	Apparent	Air	Resistivity	Velocity	Mag k	CORE
ZONE	HOLE	Depth	Depth	DBD	Porosity	perm	1000Hz	Vp	(cgs*	CUT
		(m)	(ft)	(g/cc)	(%)	k (md)	(Ωm)	(m/s)	10^-6 ≈	n/a
								(500kHz)	SI*10^-5)	sst
D :	47	107.3	459.5	2.64	0.2	0.05	32648		2	_|_
Kombolgie	47	107.3	459.5	2.64	0.1	0.06	27316		2	//
Sandstone	53	143.6	590.0	2.65	0.3	0.11	2164	6105		_|_
and breccia	53	143.6	590.0	2.66	0.5	0.08	4353	4867		//
	53	147.3	605.0	2.64	1.0	0.07	75834	5417		_|_
	53	147.3	605.0	2.62	1.3	0.04	1354	5060		//
	53	148.2	609.0	2.63	1.0	0.07	3245		1	_|_
	53	148.2	609.0	2.64	0.8	0.05	2169		2	//
	53	169.9	698.0	2.65	4.2	0.15	2008	4859		_|_
	53	169.9	698.0	2.65	4.4	0.05	1168	4941		//
	58	78.5	336.0	2.61	1.4	0.08	6061		2	_|_
	58	78.5	336.0	2.61	1.4	0.09	4734		2	//
	64	85.1	364.5	2.61	2.1	0.14	332		4	_|_
	64	85.1	364.5	2.61	2.1	0.27	254		3	//
	87	113.0	484.0	2.64	0.8	0.07	321		2	_|_
	87	113.0	484.0	2.63	1.8	0.16	1080		2	//
	87	117.3	502.5	2.63	1.3	0.15	295		3	_|_
	87	117.3	502.5	2.62	1.6	0.04	466		2	//
	92	137.8	590.0	2.64	0.6	0.17	10819		4	_|_
	92	137.8	590.0	2.64	0.3	0.08				//
	95	297.0	1272.0	2.65	0.2	0.07	894		<1	_|_
	95	297.0	1272.0	2.64	1.3	0.20	7358		2	//
	104	208.3	892.0	2.69	3.2		411		10	_|_
	104	208.3	892.0	2.68	3.4	0.11	252		8	//
	105	218.7	936.5	2.64	0.7	0.05	1584		2	_|_
	105	218.7	936.5	2.64	1.2	0.27	1867		2	//
	105	220.7	945.0	2.64	0.7	0.14	1220		<1	_|_
	105	220.7	945.0	2.64	1.5	0.05	3419		1	//
	117	5.3	6.9m=	2.60	2.0	0.48	5514	4639	7	_|_
	117	5.3	22.6ft	2.58	2.7	0.62	4691	2719		//
	117	12.9	16.9m=	2.59	1.5	0.54		4426	5	_|_
	117	12.9	55.4ft	2.51	4.7	2.55		4014		//
	117	20.6	26.9m,8	2.47	6.6				<1	
	117	30.6	39.9m=	2.45	6.4	9.71		4622	<1	_|_
	117	30.6	130.9ft	2.40	8.2	12.15	857	3321		//
	117	30.6	130.9ft					2516		//
	117	36.0	47m=154.2ft						<1	
	117	38.5	50.3m=	2.53	5.4	0.34		4792		_|_
	117	38.5	165ft	2.51	4.1	1.26			4	//
	117	46.4	60.6m=	2.58	1.8	0.23			12	_|_
	117	46.4	199ft	2.60	0.9	2.98		4688		//

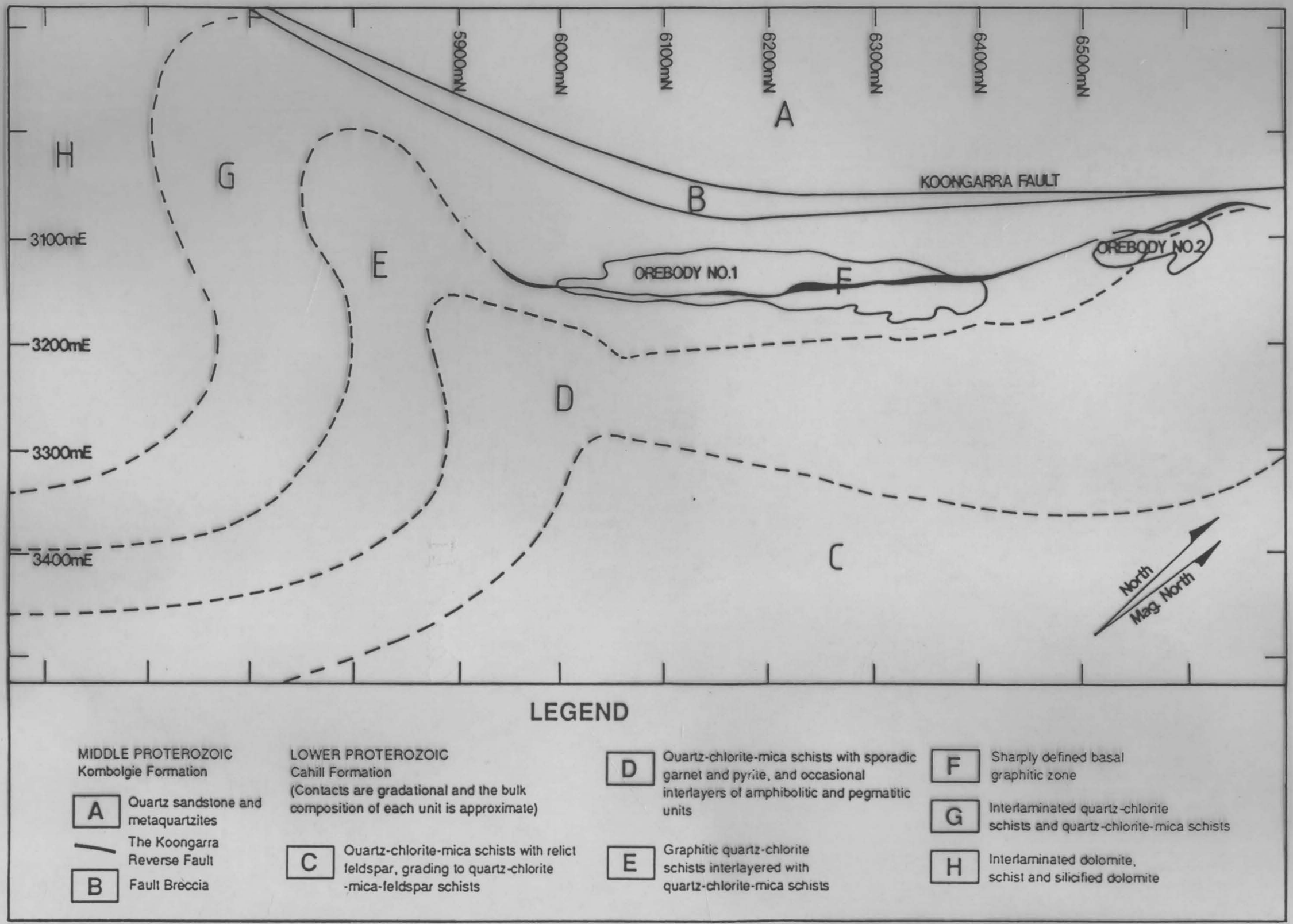

Figure 3.8: Geological Plan of the Site, corresponding to the Geological Cross-Section (Figure 3.6), prepared by this author in conjunction with drillhole and BTV work.